



Steel design and high speed machining aspects in the transition from case hardening to induction hardening of automotive transmissions (MAC D)

EUROPEAN COMMISSION

Directorate-General for Research and Innovation
Directorate D — Key Enabling Technologies
Unit D.4 — Coal and Steel

E-mail: rtd-steel-coal@ec.europa.eu
RTD-PUBLICATIONS@ec.europa.eu

Contact: RFCS Publications

European Commission
B-1049 Brussels

Research Fund for Coal and Steel

Steel design and high speed machining aspects in the transition from case hardening to induction hardening of automotive transmissions (MAC D)

Thomas Björk

Swerea KIMAB

Isafjordsgatan 28 A SE-164 40 Kista, Sweden

Diego Herrero

Sidenor I+D

Barrio Ugarte s/n 48970 Basauri (Vizcaya), Spain

Patrik Holm

Ovako Sweden AB

SE-813 82 Hofors, Sweden

Eva Butano

C.R.F. S. C. p. A.

Strada Torino 50, 100 43 Orbassano (TO), Italy

Kristian Berggren

EFD Induction AB

Kokillgatan 3, S-721 33 Västerås, Sweden

Dieter Lung / Patrik Vogtel / Benjamin Döbbeler / Martin Seimann

Aachen Univ. of Technology (RWTH) WZL

Steinbachstraße 19, 52074 Aachen, Germany

Pedro Arrazola

Mondragon Unibertsitatea – Faculty of Engineering

Loramendi, 4; 20500 Arrasate-Mondragón, Spain

Grant Agreement RFSR-CT-2011-00024

1 July 2011 to 31 December 2014

Final report

Directorate-General for Research and Innovation

LEGAL NOTICE

Neither the European Commission nor any person acting on behalf of the Commission is responsible for the use which might be made of the following information.

The views expressed in this publication are the sole responsibility of the authors and do not necessarily reflect the views of the European Commission.

***Europe Direct is a service to help you find answers
to your questions about the European Union***

**Freephone number (*):
00 800 6 7 8 9 10 11**

(*) Certain mobile telephone operators do not allow access to 00 800 numbers or these calls may be billed.

More information on the European Union is available on the Internet (<http://europa.eu>).

Cataloguing data can be found at the end of this publication.

Luxembourg: Publications Office of the European Union, 2016

Print	ISBN 978-92-79-62620-3	ISSN 1018-5593	doi:10.2777/358146	KI-NA-28-140-EN-C
PDF	ISBN 978-92-79-62621-0	ISSN 1831-9424	doi:10.2777/512149	KI-NA-28-140-EN-N

© European Union, 2016

Reproduction is authorised provided the source is acknowledged.

Printed in Luxembourg

PRINTED ON WHITE CHLORINE-FREE PAPER

TABLE OF CONTENTS

Table of contents	3
FINAL SUMMARY	5
Background	5
Work piece materials and heat treatments	5
Material characterization	7
Rough machining in turning and hob milling	8
Rough soft "green" turning	8
experimental simulation of gear hobbing	9
Fine machining of hardened steels	11
Tool wear and fundamental studies in hard part turning:	11
Fatigue strength	12
Multi-axial fatigue testing	12
Rotating beam fatigue testing.	12
Component testing	13
Demonstrators	14
Induction hardening of the demonstrator gear	14
Comparison of manufacturing costs, carburizing vs induction hardening	14
Machining of the demonstrator gear made of 50CrMo4 trough induction hardening	15
Extended conclusions	16
WP1: Work piece materials and heat treatments	17
AIM of WP1:	17
OBJECTIVES of WP1:	17
Task. 1.1.- Selection and manufacturing of steel grades.	17
Task 1.2.- Heat treatment for the as-delivered condition	17
Task 1.3 Secondary heat treatment (Induction hardening)	18
Task 1.4. Work piece material for pilot component manufacturing in WP6	19
WP2 Material characterization	21
Task 2.1 Test specimens for material characterisation.	21
Task 2.2. Microstructural and chemical characterisation	24
CHEMICAL COMPOSITION	24
INCLUSIONARY STUDY	24
Task 2.3 Testing of hardness, toughness and tensile strength	29
HARDNESS MEASUREMENTS	29
TENSILE TEST	30
TOUGHNESS TEST	31
WP3: Rough machining	33
Task 3.1 Tool life tests in roughing.	33
Tool life tests in roughing turning	33
Tool life tests in experimental simulation of gear hobbing	36
Task 3.2 Tool wear study in roughing	39
Task 3.3 Study of chip removal in roughing	42
Motivation	42
Experimental setup	42
Chip Maps	43
Quick Stop Test	44
Task 3.4. Fundamental cutting tests	47
WP4: Finishing hard machining	55
Task 4.1 Selection of cutting tools and conditions for finishing turning	55
Task 4.2 Tool life tests in finishing turning	57
Task 4.3 Tool wear study in finishing turning	60
Task 4.4 Rim zone analysis of the finish turned induction hardened work piece	62
Task 4.5. Fundamental cutting tests in finishing turning	69
Results of fundamental cutting tests	71
WP5 Fatigue testing	77
Task 5.1 Manufacturing and verification of test samples	77
MULTIAXIAL FATIGUE TEST SAMPLES	77
ROTATING BEAM TEST SAMPLES	78
MANUFACTURING OF SPUR GEARS FOR COMPONENT FATIGUE TESTING	81
Task 5.2 Testing of fatigue strength of test specimens	82
MULTIAXIAL FATIGUE TESTING	82
ROTATING BEAM TESTING	85
Task 5.3 Testing of fatigue strength of actual components	88
WP6 The demonstrator component; manufacturing and comparison, case hardening vs. induction hardening	92
Task 6.1 Decision of demonstrator component	92

Task 6.2 Today's manufacturing route through carburizing	93
Heat treatment cycle	96
Task 6.3 Pilot manufacturing of demonstrator component through the induction hardening route	97
Task 6.4. Comparison of total manufacturing costs and component properties, case hardening vs. induction hardening	103
cost of work piece material and forging process	103
Heat treatment and associated systems	103
machining processes	107
Exploitation and impact of the research results	112
Technical potential of induction hardening of gears	112
Economic potential of induction hardening of gears	113
List of figures	114
List of tables	118
ANNEX WP1	120
ANNEX WP2	120
ANNEX WP3	124
ANNEX WP4	128
ANNEX WP5	131
ANNEX WP6	132

FINAL SUMMARY

Background

Some 21 million vehicles (18 million cars, rest light commercial vehicles, heavy trucks and buses) were manufactured in Europe in 2008 [OICA survey]. A very large business of the European steel industry is devoted to the needs of the automotive industry. That includes foremost the manufacturing of steel sheet for car bodies and long steel products for the manufacturing of drive chains. For transmission components, many specialty steel alloys have been developed to meet the customer's needs of high tensile strength and high fatigue strength, combined with high machinability, among others. Gears are typically manufactured from bar steels, about 0.2%C. They are rough machined in a soft condition, carburizing case hardened, and fine machined or ground in the last machining operations.

Carburizing as heat treatment of gears and transmission components is extremely well established. However, the major drawback is the extended process time due to the inherent diffusion based carburizing. Carburizing is a typical batch process. Gears numbering 50-500 are loaded on palettes and treated for 5-15 hours depending on the specifications of the carburizing case and the furnace capabilities. Significant emissions of CO₂ and other more hazardous gases is associated with carburizing.

Induction hardening is typically a one piece process. Components are treated one at a time in induction hardening systems that include a copper coil with alternating magnetic field at high frequency that enables rapid heating of the part to austenite transformation. Also included is a direct water sprinkling system for immediate quenching. Typically axles and shafts are induction hardened with great success, see Figure 1. Another advantage is the possibility of localized hardening of e.g. bearing positions, cams and splines. Note that there is no external carbon uptake involved. The carbon must be present in the steel. Consequently, quench-and-tempering steels with C=0.3-0.5 wt% are typically used.

Induction hardening is extremely geometry dependent. Sharp edges and three dimensional geometries often mean big challenges in the heat distribution. This means that induction heating can be done in large scale production of e.g. bars and tubes at steel works with great ease and productivity, thanks to the straight and simple geometries of these products. However, induction hardening of components with complex geometries involves extremely short heating cycles and lots of know-how to enable as even heat distribution and phase transformations as possible. Two properties are very important for the success of induction hardening: (1). the hardenability of the steel and (2) the microstructure of the as-delivered component.

The more the carbon atoms are dissolved in the microstructure prior to induction hardening the better the hardness increase gets. This means that a quench-and-tempered structure is much more favorable than e.g. a spheroidized annealed structure. The optimization of microstructure prior to induction hardening actually constitutes a major aspect of the entire MAC D project, with respect to both productivity in machining processes as well as fatigue strength.



Figure 1. Examples of induction hardening of components. (a) A spur gear and (b) a shaft.

Work piece materials and heat treatments

As reference material of the project was chosen a 18CrMo4 steel, hereafter referred to as **C**, see Table 1. It is a very frequent steel for gears in the automotive industry. The as-delivered microstructure was agreed to be isothermally annealed with a ferrite-pearlite microstructure. Its denomination is **IA**. As candidates of the induction hardening of gears and shafts was chosen the 35CrMo4 (QL) and 50CrMo4 (QH). Their denominations came up as quench-and-tempering steel

with low (QL, 0.35% C) and high (QH, 0.5 %C) carbon content. As reference to the hard part machining tasks a frequent ball bearing steel was chosen, 100Cr6, denominated B. It came in a spheroidized annealing condition (SA).

The QL and QH steels came at different quench-and-tempering microstructures, T1 and T2 with different target hardness. The hardest steel was the QH-H1 at 345 HB. The reason of this was the need from induction hardening process of a dissolved carbon structure prior to the induction hardening.

The 18CrMo4 and 35CrMo4 steels were manufactured by Gerdau using continuous casting. The 50CrMo4 and the 100Cr6 were manufactured by Ovako using ingot casting.

Table 1. Steel variants and denominations for the rough soft machining part of the project.

Steel grade	18CrMo4	35CrMo4	50CrMo4	100Cr6
Short name	C	QL	QH	B
Supplier	Gerdau	Gerdau	Ovako	Ovako
Heat treatment				
Quench & tempering I		● QL-T1	■ QH-T1	
Quench & tempering II		● QL-T2	■ QH-T2	
Annealing**	▲ C-IA			◆ B-SA

Steel grade	18CrMo4	35CrMo4	50CrMo4	100Cr6
Short name	18	35	50	100
Supplier	Gerdau	Gerdau	Ovako	Ovako
Heat treatment				
Quench & tempering I		● 35-T1	■ 50-T1	
Quench & tempering II		● 35-T2	■ 50-T2	
Annealing**	▲ 18-IA			◆ 100-SA

Steel bars were hardened for the tests in hard part machining in WP4. The reference was the ball bearing steel (B-H) at 62 HRC, see Table 2. The most interesting hardened steel was the 50CrMo4 hardened to about 58 HRC (QH-H1). This turned out to be the most realistic steel to be used in the future induction hardened gear in the project. The other steels in the hardened condition were included for more of academic interest with respect to the behavior in terms of tool wear and rim zone formation in hard part turning.

Table 2. Steel variants and denominations for the hard fine machining part of the project.

Steel grade	18CrMo4	35CrMo4	50CrMo4	100Cr6
Short name	C	QL	QH	B
Supplier	Gerdau	Gerdau	Ovako	Ovako
Heat treatment				
Induction hardening I	▲ C-H1	● QL-H1	■ QH-H1	
Induction hardening II		● QL-H2	■ QH-H2	
Through hardening				◆ B-H1

Steel grade	18CrMo4	35CrMo4	50CrMo4	100Cr6
Short name	18	35	50	100
Supplier	Gerdau	Gerdau	Ovako	Ovako
Heat treatment				
Induction hardening I	▲ 18-H1	● 35-H1	■ 50-H1	
Induction hardening II		● 35-H2	■ 50-H2	
Through hardening				◆ 100-H1

After the mid-term of the project it was decided to use the 50CrMo4 steel for the demonstrator gear. For that 18 m of Ovako 528E ϕ 70 mm was sent to HotRoll S.r.l. being a major supplier of forgings of Fiat Powertrain.

Material characterization

Samples were made for tensile testing, toughness testing (using a Charpy-V test), microstructural and inclusion characterization. The steels were tested with respect to tensile strength in the as-delivered conditions, cp. Table 1, as well as in the hardened state, cp. Table 2. Samples of the 18CrMo4 steel were carburized and mechanically tested. A dedicated induction coil was made for the tensile test samples and for Charpy-V samples in the induction hardened state. The induction case depth was about 1 mm, relatively similar to that of the carburized 18CrMo4.

The actual composition of the bars is given in Table 3. One can note the relatively high Sulphur content of the 50CrMo4 steel.

Table 3. Chemical composition from the heat in the steel plant. This is a selection of the most important elements.

Steel grade	MAC D name	wt%							ppm	
		C	Mn	Si	S	Cr	Ni	Mo	O	Ca
18CrMo4	C	0,19	0,81	0,29	0,024	1,06	0,12	0,16	10	7
35CrMo4	QL	0,34	0,81	0,31	0,026	1,12	0,11	0,18	12	8
50CrMo4	QH	0,50	0,68	0,23	0,035	0,98	0,21	0,19	8	2
100Cr6	B	0,97	0,31	0,28	0,012	1,41	0,20	0,06	5	3

The steels were characterized with respect to microstructure and inclusion characteristics. The C-IA steel showed a ferrite-pearlite microstructure whereas the QL and QH steels in the T1 and T2 conditions displayed tempered martensitic microstructures.

The hardened steels all displayed martensitic structures following their hardness levels. The B-H steel (reference) was at 62 HRC and the QH-H1 came out at 58 HRC. Note that this steel was induction hardened and subsequently quenched using water spray of the work piece surface. The inclusion characteristics were recorded using LOM on polished sections in the rolling direction and using PDA-OES. Generally the inclusion characteristics followed the expectations from the bulk composition.

The steels were evaluated with respect to mechanical strength, see Table 4. The UTS and YS values followed the hardness numbers. The toughness values are found in Figure 2. One can note that the lowest toughness value was obtained with the reference 18CrMo4 in the carburized condition. The induction hardened samples had significantly higher toughness values. This can be important in an industrial application where the gear is aimed at a hard surface through carburizing and a tough core obtained by the low carbon martensitic transformation underneath the carburized surface layer.

Table 4. Numerical summary of tensile tests. Hardness values included.

Steel grade	Reference	UTS (MPa)	YS (MPa)	EI (%)	RA (%)	Hardness [HB]
18CrMo4	C-IA	538	333	32	72	160
35CrMo4	QL-T1	833	666	20	67	240
35CrMo4	QL-T2	1009	896	17	64	287
50CrMo4	QH-T1	1108	982	16	56	350
50CrMo4	QH-T2	985	855	18	58	315
100Cr6	B-SA	670	396	31	58	240

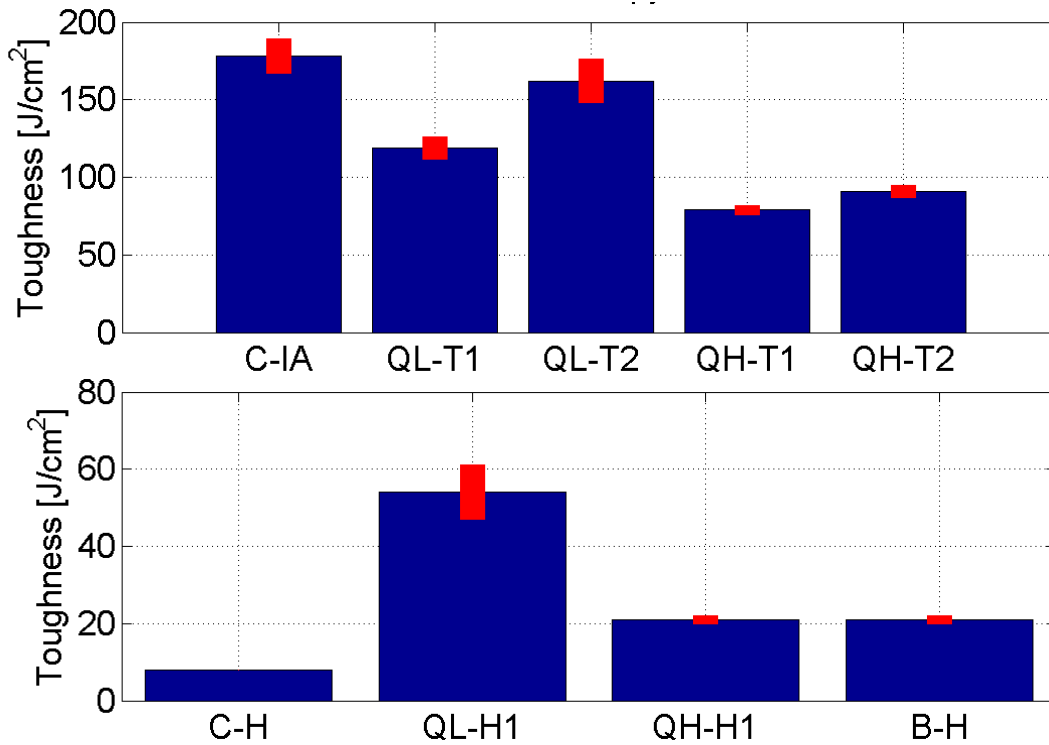


Figure 2. Toughness values recorded with Charpy V testing. NOTE: The C-H was carburized at Fiat. The QL-H1, QH-H1 and B-H were induction treated at EFD Induction.

ROUGH MACHINING IN TURNING AND HOB MILLING

The aim of WP3 was to obtain comparisons of tool life behavior, as well as understanding of the cutting processes of the included steels, with respect to soft “green” turning and hob milling. These two cutting operations were selected as the most important for the production cost of green machining operations of gears.

ROUGH SOFT “GREEN” TURNING

Bars 500 mm and $\Phi 85$ mm were axially turning tested with respect to tool life. The Coromant CNMG120408 PM GC4215 was utilized. The depth of cut $a_p=2$ mm and the feed was $f=0.4$ mm. Cutting speeds in the range 175-550 m min⁻¹ were tested depending on the steel investigated. The aim was to frame the cutting speed that corresponds to a tool life of 15 minutes of engagement (the V15 value), see Figure 3. The reference steel 18CrMo4 (C-IA) is significantly easier to cut, i.e. higher V15 value than the other steels. This is expected given the difference in hardness values. Note however that in an industrial implementation of a steel for induction hardening, much more attention would be spent on finding solutions of productivity. In this case that would mean tests with alternate turning tool geometries and harder carbide grades. That would reduce the difference significantly in productivity. Based on these tests the V15 value of C-IA is 424 m min⁻¹. The steel most likely to be used in an induction hardened gear, QH-H1, had V15=214, i.e. almost 50% of the reference value.

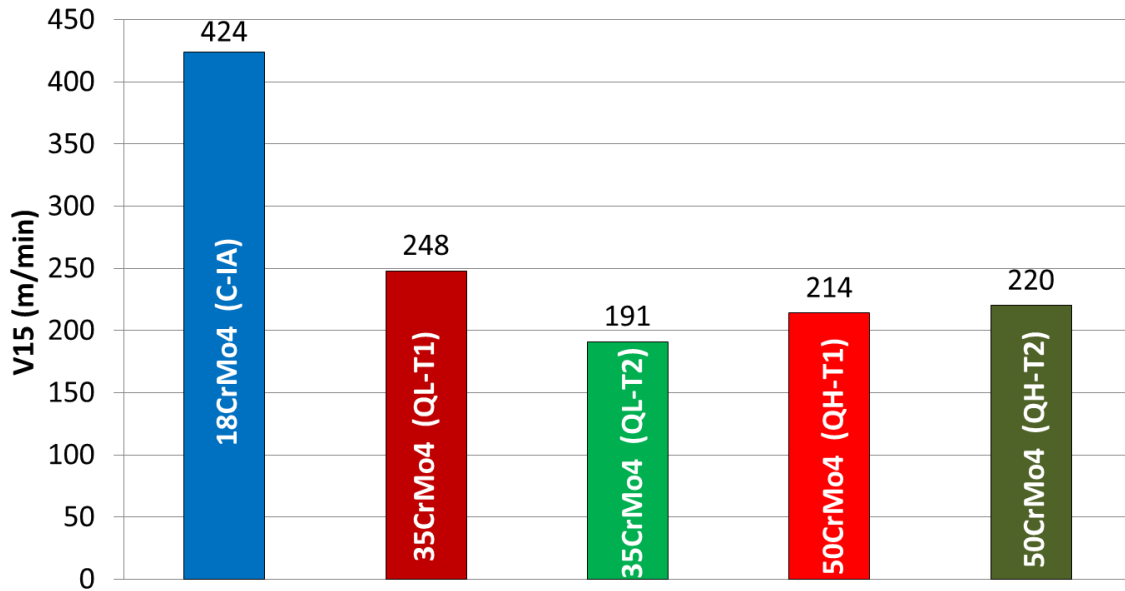


Figure 3. Cutting speed that corresponds to tool life of 15 minutes.

EXPERIMENTAL SIMULATION OF GEAR HOBBIING

An experimental simulation of the hob milling process was undertaken, see Figure 4. It is a development of previous tests using a face milling configuration [ref]. The current tests utilise a commercial tool holder and commercial cutting tools, see Figure 5. The milling cutters and holders were obtained from Alesa AG. The cutter was $\Phi 12$ mm, made of HSS and PVD coated with a multilayered TiAlN coating. Three major facts make the test realistic and interesting:

1. The cutters are made of PVD coated HSS, the same material as conventional hob material.
2. The cutters have a circular geometry. This means that the varying chip thickness of hob milling is replicated.
3. Wear study of used milling inserts show the same wear types and wear mechanisms as those of actual hob edges.

The tool life was plotted with a number of cutting speeds, cp. the turning tests above.

Industrially used solid hobs for gear cutting are said to be reground and coated after about 3 metres of cut gear root length. Given the some 150-200 teeth of each hob, about 200-500 gears are typically cut with a hob in between the service intervals.

The cross section area in between two of the demonstrator gear teeth was measured. Hence the volume of removed chips in the face milling tests could be transformed into numbers of gear tooth metres. It was found that with the C-IA steel the tool life was about 3 gear tooth metres (GTM) at 200 m min⁻¹, see Figure 6. The corresponding too life of the QL and QH steels was considerably lower. Note that these were the first tests made with this configuration. The very low tool life at low cutting speeds was probably due to lacking separation of the chip from the cutting edge so that the subsequent cut resembled of a chip jamming.

Furthermore, the tests gave the impression that the cutting processes was better at higher cutting speeds. Hence the beneficial results of C-IA. Though, with harder steels, e.g. QH-T1 the risk of sudden overheating of the cutting edges became obvious. This overheating generated a rapid tempering of the HSS substrate followed by spallation of the PVD coating and a very rapid end of life of the cutting edge.



Figure 4. Configuration of the cutting tests. Face milling of bars made of the workpiece materials of the project.

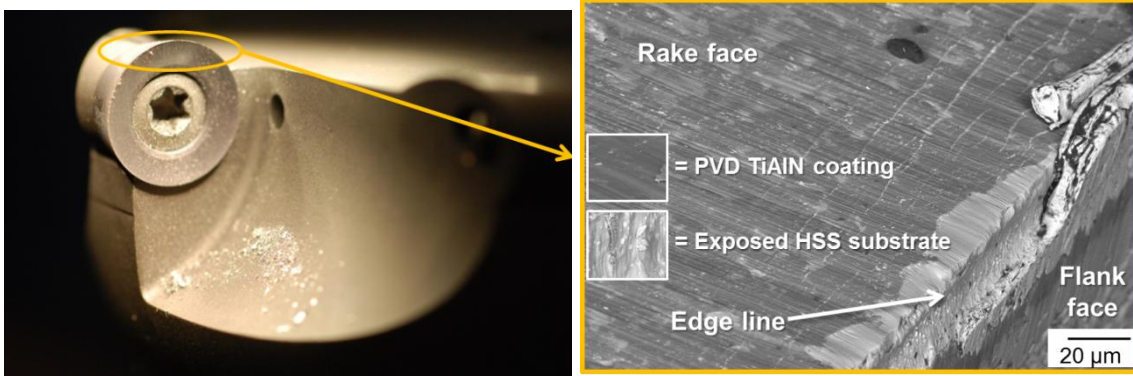


Figure 5. The milling cutter. (a) overview in the tool holder and (b) typical wear of the cutting edge after a cutting test.

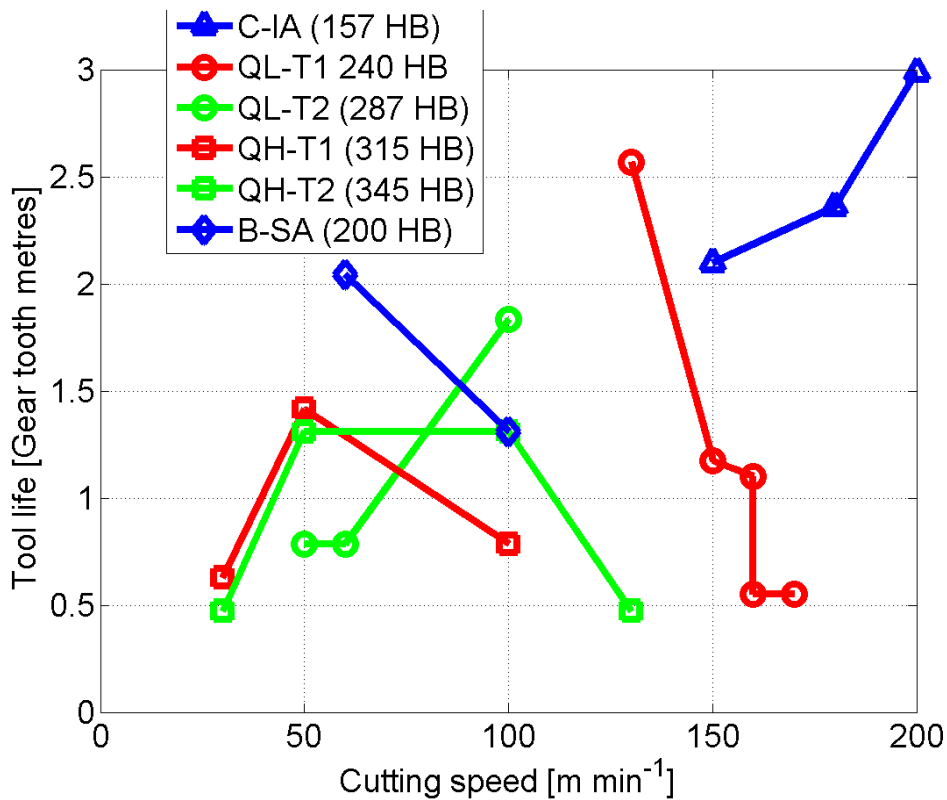


Figure 6. Tool life tests in gear hobbing simulation. The volume of removed chip transformed to corresponding gear tooth metres.

FINE MACHINING OF HARDENED STEELS

The hardness levels ranged from about 25 HRC with the C-H steel through about 45 HRC of the QL_H1 and QL-H2 steels to 58 HRC of the QH-H1 steel. The reference B-H was through hardened to 62 HRC. In fact only the B-H and QH-H1 steels were considered to classify for hard part turning. Typically that limit is defined to above 55 HRC.

It was agreed to test the steels in tool life tests using a polycrystalline cubic boron nitride (PCBN) grade (CNGA 12 04 08 S01030A CB7014) with the B-H, QL-H1, QL-H2, QH-H1 and QH-H2. In addition, a cemented carbide grade aimed at cast iron machining was tested (Coromant CNMG120408 KM GC3205). This is known as a possibility in machining of moderately hard steels. The cutting speed using PCBN is typically 120-200 m min⁻¹ and about 40-70 m min⁻¹ with the carbide alternative, in hardened steels.

The tool life of the hard part turning tests is summarized in Figure 7. The tool life of the CC grade was actually higher than with PCBN when tested with the QL-H1 and QL-H2 steels. The most important condition QH-H1, likely to be used in the demonstrator gear, the PCBN was significantly better than the carbide grade.

The tool life of the reference steel B-H was about 30% below that of QH-H1. Note however, that the actual reference in hard part turning should have been a carburized 18CrMo4 steel, the same as in actual gears. It has been learned from other projects that the tool life of a carburized 18CrMo4 steel is about 30% higher than with a hardened ball bearing steel. The assumption can therefore be that the tool life of QH-H1 is similar to that of a carburized 18CrMo4 steel.

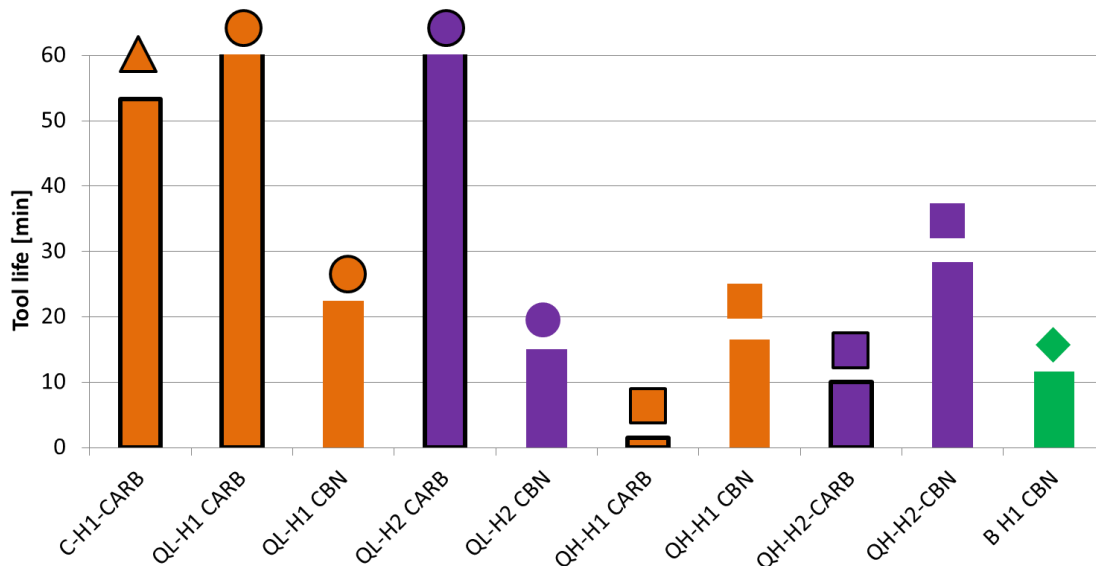


Figure 7. Bar chart of tool life tests in hard part turning. Bars from tests with carbide tools are given with black edges.

TOOL WEAR AND FUNDAMENTAL STUDIES IN HARD PART TURNING:

A tool wear study was undertaken in hard part turning using the CB7014 PCBN grade. All steels were tested at one cutting speed for 3 minutes and 12 minutes, respectively. The steel hardness was found to be the major factor influencing the progression of rake face wear and flank wear. The B-H steel had the highest hardness and consequently the fastest wear propagation. The QH-H1 was second in line. The C-H steel with only about 0.2%C and 28 HRC showed virtually no wear at all on the PCBN cutting edge.

Analyses of the cutting temperatures were made as well as cross section studies of the rim zones of the work piece surfaces. In general, both the cutting edge temperature as well as the rim zone thickness increased with the wear progression of the PCBN cutting edge. Some tests were made to compare the different work piece materials as such, but no significant conclusions could be drawn, aside from the expected link with wear progression of the PCBN edge.

Fatigue strength

The aim of WP5 was to evaluate the extremely important fatigue strength properties of the induction hardened samples and components as compared with the corresponding reference of carburized 18CrMo4 steel. Rotation symmetric samples for fatigue testing were manufactured. The reference of 18CrMo4 was carburized at Fiat Powertrain. A significant effort was made by EFD Induction in the manufacturing of dedicated induction coils and treatments for these samples.

MULTI-AXIAL FATIGUE TESTING

For each steel grade, three different fatigue tests were performed (described below). In all of them the run-out criteria considered was 2.000.000 of cycles and the fatigue limit was determined by the staircase method. (I). Pure tension-compression fatigue test, (II). Pure torsional fatigue test and (III). Biaxial fatigue test. The biaxial fatigue test is developed at Gerdau with the aim to imitate realistic fatigue loads of transmission components.

The sequence was to perform the tension-compression tests, then the torsional tests. The results of these two initial tests were used to define the ratio of T-C and torsion in the biaxial tests. Practically, the test was done as a torsional test but with an overlaid tension-compression load. The test frequency used was 5 Hz and $R=-1$. The reference carburized 18CrMo4 had a fatigue limit of 512 MPa, see Figure 8. The corresponding value of the induction hardened 50CrMo4 with fine machining after the induction hardening was 558 MPa, which is actually 9% better than the reference!

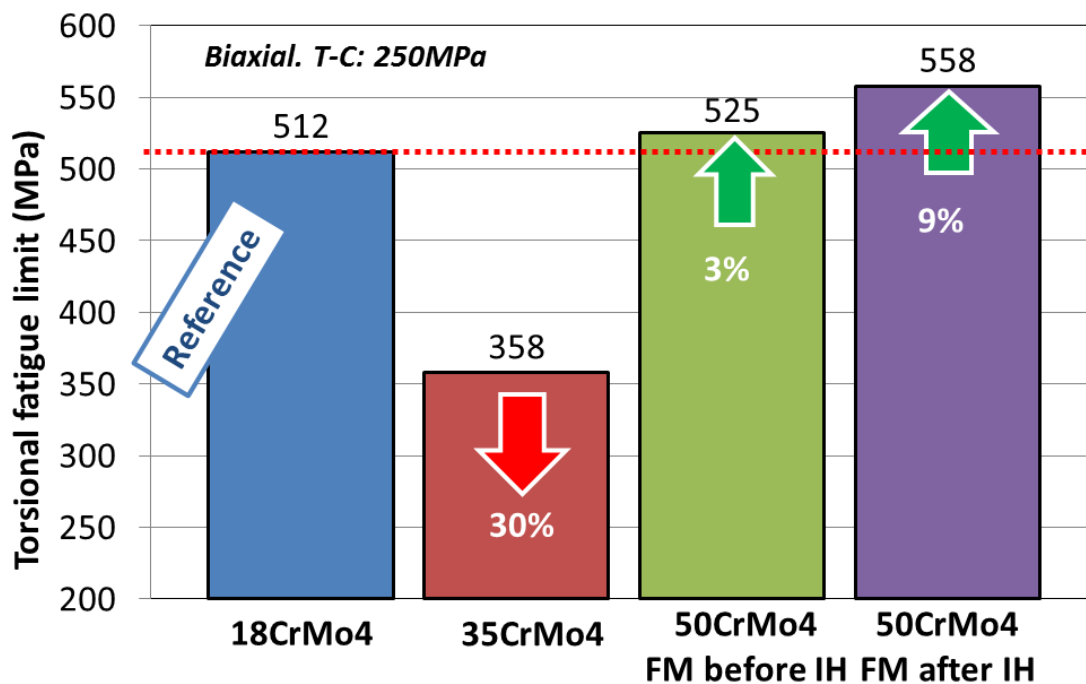


Figure 8. Combined tension-compression and torsional fatigue tests.

ROTATING BEAM FATIGUE TESTING.

Rotating beam samples were produced using an hourglass geometry. Samples were carburized (18CrMo4) and induction hardened (35CrMo4 & 50CrMo4). The fatigue limit is given in Figure 9. The carburized 18CrMo4 and the two variants of 50CrMo4 came out at about 900 MPa. The subsequent study of fractured samples showed that the initiation took place in the transition zone of the samples. The major conclusion from that is that a deeper hardened case would increase the fatigue limits of all the tested samples. The result comes as a result of the sample geometry. A more distinct notch shape would increase the stress concentration and result in more of surface initiations, which is often desired in this kind of testing.

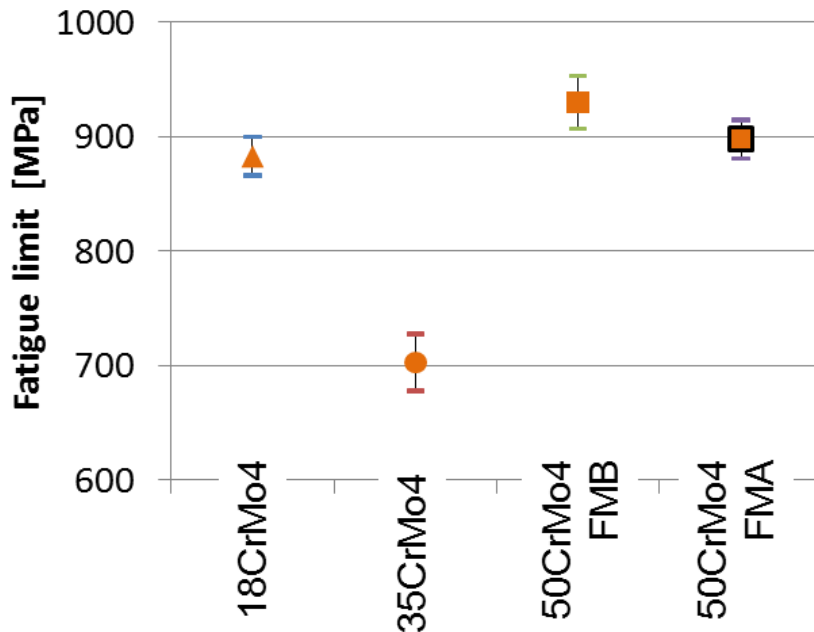


Figure 9. Fatigue limit results with confidence interval of 95%.

COMPONENT TESTING

A spur gear was tested in bending fatigue testing at Gerdau I+D, see Figure 10. The most relevant choice would have been to do tests on the demonstrator gear. However there was no configuration available to test with helical gear geometries.

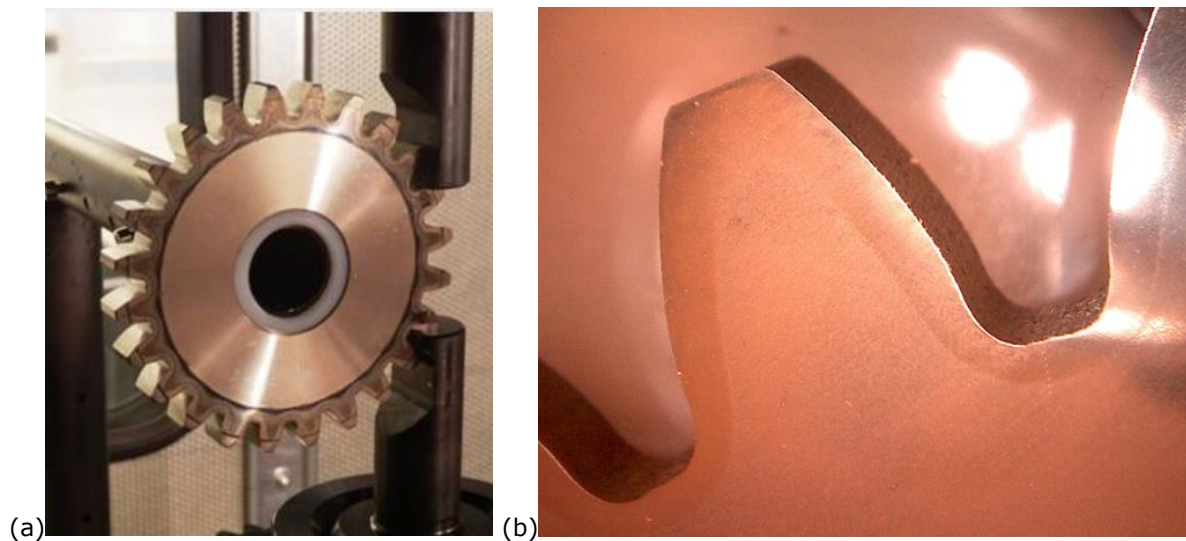


Figure 10. The model gear for component fatigue testing at Gerdau. (a) Mounted in the fatigue testing rig and (b) detail of the gear tooth geometry.

Results: The fatigue limit was determined using load values because of the difficulties to estimate the corresponding tension for the loads applied. The tooth bending fatigue limit are as follows:

- Carburized gears: -23,30kN
- Induction hardened gears: -20,45kN

This means that in this test the induction hardened gears had a fatigue limit about 12% less than that of the carburized gears.

After the tests, the fractures were analysed to determine their origin. All of them initiated at the surface and the origin of most of them (all except one) was related to the presence of MnS inclusions. Note the sulphur content of the 18CrMo4 of S=0.024 wt% while that of the 50CrMo4 is S=0.034 wt%.

Conclusions:

- The fatigue limit obtained for the carburized 18CrMo4 is a 12% higher than the one of the induction hardened 50CrMo4.

- In general, the fractures initiate in the surface and have their origin in MnS inclusions. This was expected because, under the load conditions used in this test, the surface is the zone of the gear tooth where the highest tensions concentration appears.
- As the S content of the 50CrMo4 is clearly higher than the one of the 18CrMo4 and all the fractures initiate in MnS, if the S content of both steel was similar. Besides, if the induction hardened gears were shot peened (as performed for the case hardened ones), their fatigue limit should increase. Taking these two reasons into account, for similar S content and following a similar manufacturing process, the fatigue limit should be similar for both cases (case hardening vs induction hardening).

Demonstrators

The primary demonstrator of the project was a helical gear for a manual gear box of Fiat, see Figure 11. The helix angle is 20° and the peripheral diameter is 168 mm.



Figure 11. The primary demonstrator, a helical gear in a Fiat manual gear box for a small car.

All details of the steel specifications, forging cycle, machining operations and heat treatment cycle were provided to the project. This gear is produced at two plants of Fiat, in Verrone and in Mirafiori. It was agreed to emphasize the production of the Verrone plant, given the fact that this site has a modern line of low pressure carburizing. Hence, up-to-date costs and investment plans have been made and can be used in the comparison with induction hardening.

The complete manufacturing route is as follows: (I). Supply of steel as bar from the steel producer to the forging company, (II). Blank forging & heat treatment, (III). Arrival of gear blank at Fiat Powertrain, (IV). Turning operations. (& dimensional check), (V). Gear cutting, (VI). Chamfering and snagging, (VII). Washing, (VIII). Drilling, (IX). Washing, (X). Carburizing, (XI). Shot blasting of gear roots, (XII). Fine turning of end surfaces, (XIII). Grinding of gear tooth flanks.

INDUCTION HARDENING OF THE DEMONSTRATOR GEAR

The induction hardening of the demonstrator gear was developed at EFD Induction. A single frequency process was utilized. The gear geometry finally chosen required an extremely high peak power in about a second time of heating per gear. The induction hardening of a demonstrator gear is imaged in Figure 12. The cross section of an induction hardened gear tooth displayed a case depth of about 1 mm in the gear root all over the gear width, see Figure 13. However, there was an unbalanced case profile close to the edges. This is expected given the angles of the tooth edges. It can be expected that the root fatigue strength is optimized. However, the flanks may suffer from contact fatigue linked to insufficient surface hardness.

COMPARISON OF MANUFACTURING COSTS, CARBURIZING VS INDUCTION HARDENING

The comparison of heat treatment routes was made by estimation the costs of new investment of low pressure carburizing of the same type as currently used at the Verrone plant, and by estimating the costs of a robotized line of induction hardening. The latter includes one high power station for the hardening sequence and an additional low powered station for induction tempering.

The major difference in heat treatment route is the process time of about 8.5 h using carburizing and about 2 minutes using induction hardening. The actual costs of this difference in terms of space savings, reduced logistics unlocking of values have not been possible to estimate in this work. The direct costs of heat treatment including investment, staff cost, energy consumption, etc. have been estimated. The direct costs are as follows.

- **Carburizing: 2.41€ per gear**
- **Induction hardening: 0.64 € per gear.**

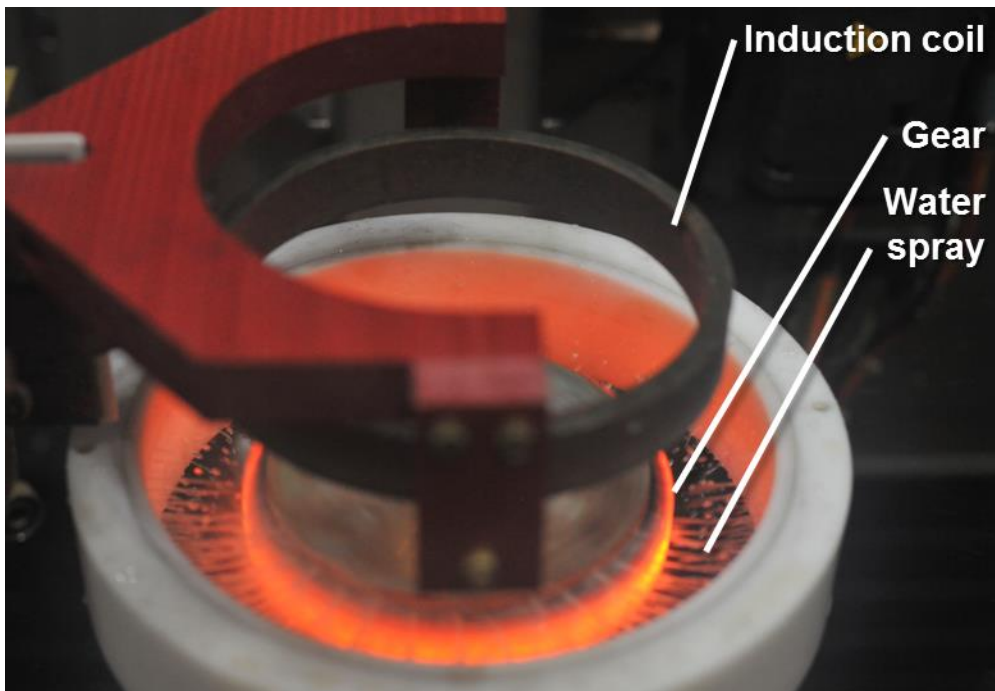


Figure 12. Photo of an ongoing induction hardening cycle of the demonstrator gear.

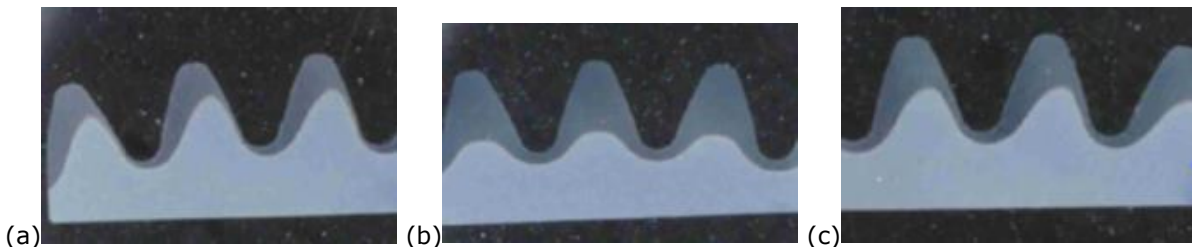


Figure 13. Etched cross sections of the induction hardened gear, positioned (a) 1.5 mm from the left hand edge, (b) middle and (c) 1.5 mm from the right hand edge.

MACHINING OF THE DEMONSTRATOR GEAR MADE OF 50CRMO4 THROUGH INDUCTION HARDENING

A comprehensive list of machining steps was obtained from the production at the Verrone plant of Fiat Powertrain. The machining costs of the C635 gear made of 18CrMo4 and carburized was compared with the corresponding steps in machining of the gear made of 50CrMo4 and induction hardened, see Figure 14. The cost of both green turning and gear hobbing is roughly doubled in case of using the 50CrMo4, resulting of the much higher hardness of 345 HB as compared to the 160 HB 18CrMo4. However, reduced costs are foreseen in hard part turning and tooth grinding.

The estimated costs of the machining processes of the C635 gear are:

Carburizing: 9 € per gear

Induction hardening: 12 € per gear.

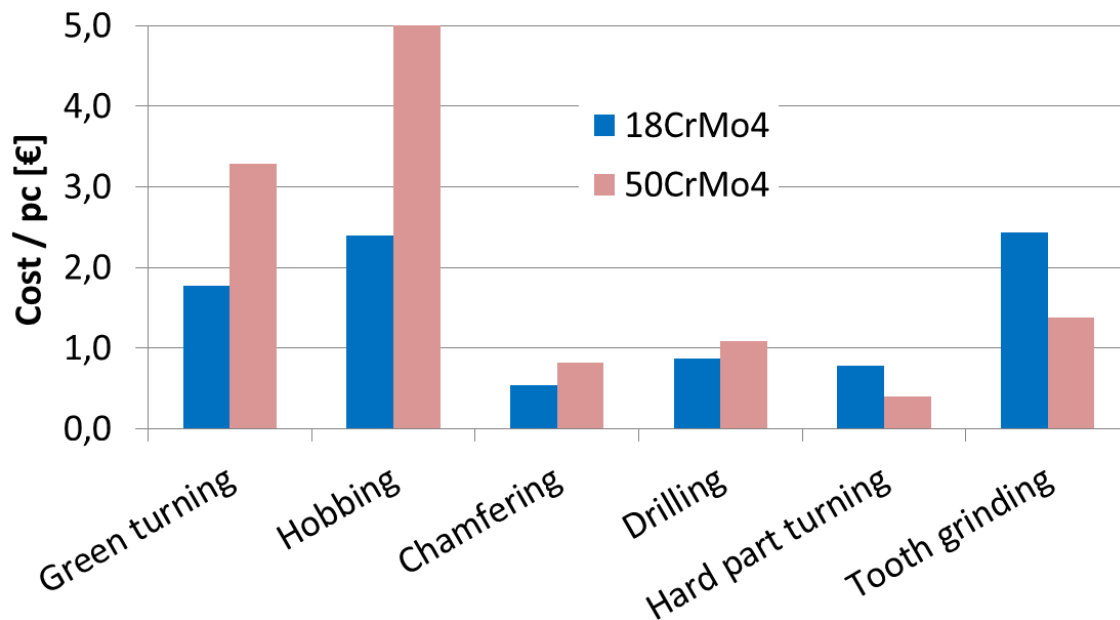


Figure 14. Summary of costs for each machining step of the C635 gear made through 18CrMo4 carburized and 50CrMo4 as induction hardened.

Extended conclusions

The following conclusions can be drawn from this project:

1. The project has shown a realistic potential to replace today's carburizing route in the manufacturing of a helical gear with a induction hardening route. The transition includes evaluation and choice of a new suitable steel and as delivered microstructure from the forging, data of machinability in the vital machining processes, a comparison of fatigue strength and a complete comparison of manufacturing costs.
2. The direct costs of heat treatment were calculated as follows:
 - **Carburizing: 2.41 € per gear**
 - **Induction hardening: 0.64 € per gear.**
 - The comparison includes the direct costs of investment, maintenance and staff.
3. The costs of the entire machining process were obtained from data of the production of the demonstrator gear at Fiat Powertrain. Given the machinability numbers and the manufacturing route through carburizing of the **18CrMo4 steel** of today the total machining cost is **9 € per gear**. The corresponding number of the induction hardened **50CrMo4 steel is 12 €**. The difference is made up of primarily a combination of more difficult green turning and hob milling. On the other hand the costs of hard part turning and the final tooth grinding could be significantly reduced.
4. The process of induction hardening of the helical gear was tailored and realized to enable a desired hardening profile of the gear roots. The hardening profile resembles that of a carburized gear. Yet importantly, the tooth top was not through hardened. The drawback observed is the uneven hardening profile of the tooth edges, resulting from the sharp and blunt edges on each side of the gear edge and the fact that induction hardening is very geometry dependent.
5. The fatigue strength of an induction hardened 50CrMo4 sample and gear component is on the same level as the reference of a carburized 18CrMo4 steel. Sample tests in a component-like load situation of biaxial fatigue tests showed a 13% increase of the induction hardened 50CrMo4. However, bending tests of a spur gear made of induction hardened 50CrMo4 showed about 12% lower fatigue strength than the reference carburized 18CrMo4.
6. Green machining of a 50CrMo4 steel at 345 HB in both rough turning and a simulated hob milling test showed roughly a 50% reduction in performance as compared with the reference 18CrMo4 steel at 160 HB. This is a significant difference in productivity. The primary cost associated with lower performance is the extended machine time and more staff costs. Increased consumption of cutting tools is only a minor part of the increased machining cost. This is also valid in hob milling.

WP1: WORK PIECE MATERIALS AND HEAT TREATMENTS

AIM OF WP1:

- To define and produce all materials of the project.

OBJECTIVES OF WP1:

- To define and execute the manufacturing of the steel alloys to be used in the project.
- To define and execute the heat treatments of the work piece material in the as-delivered, soft condition, for rough machining.
- To define and execute induction hardening sequences of work piece material for finishing hard turning.

Task. 1.1.- Selection and manufacturing of steel grades.

Four steels have been selected to be part of the project, see Table 5. The 18CrMo4 serves as reference material, since it widely used for the transmission components chosen in the project. Most attention will be given the 35CrMo4 and the 50CrMo4-steels, as they are both candidates for induction hardening and the associated applications in automotive transmissions. The 100Cr6 is included as reference for fine hard machining. Though, it is obvious that carburized carburizing steels are as important as reference for fine hard machining. The 18CrMo4 steel is denominated **(C)**. The 35CrMo4 is denominated **(QL)**. The 50CrMo4 is denominated **(QH)**. The ball bearing steel is denominated **(B)**.

Table 5. Steel grades selected in the project.

Steel grade	18CrMo4	35CrMo4	50CrMo4	100Cr6
Short name	C	QL	QH	B
Supplier	Gerdau	Gerdau	Ovako	Ovako

Task 1.2.- Heat treatment for the as-delivered condition

The importance of the as-delivered microstructure of steels for induction hardening comes from the fact that the original microstructure highly influences the hardened microstructure after induction hardening. Note that this is important in induction hardening of components with complex geometry. The heating time is minimized not to overheat parts of the component geometry. The austenite phase transformation depends on both the heating time and the as-delivered microstructure. This is displayed in time-temperature-austenitizing (TTA) diagrams. An example of 50CrMo4 with three starting microstructures is given in [Orlich J., Rose A.: Atlas zur Wärmebehandlung der Stähle, Band 3, ZTA-Schaubilder]

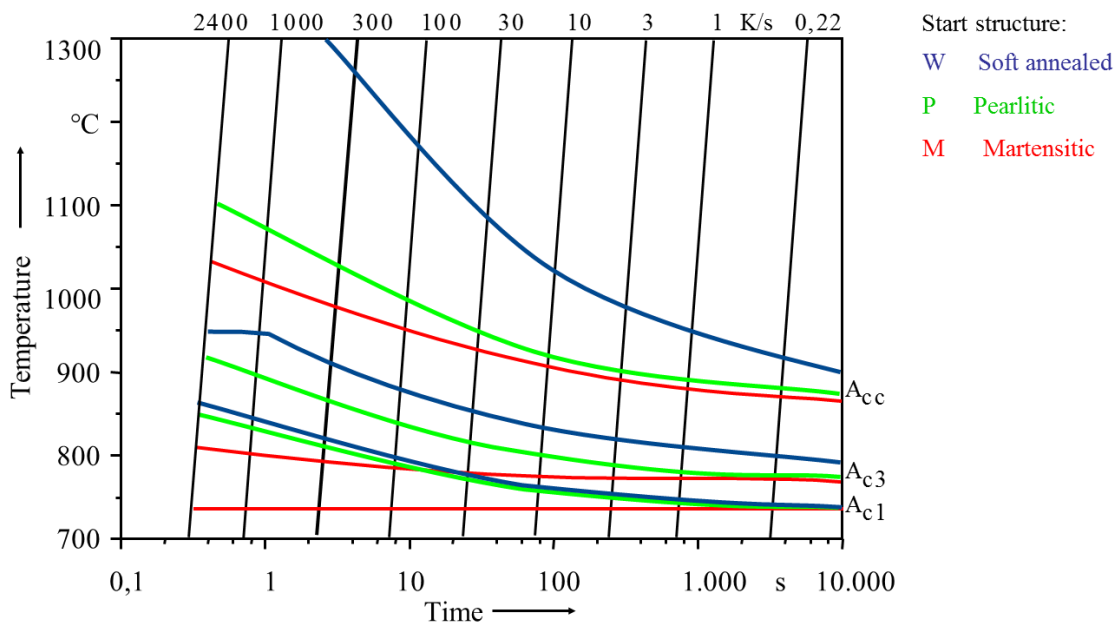


Figure 15. TTA diagram of 50CrMo4 with three realistic starting microstructures.

Two variants of quench and tempering treatments were agreed. They are denominated **(T1)** and **(T2)**. The 18CrMo4 steel comes in isothermally annealed condition **(IA)**. The bearing steel **(B)**

comes as spheroidized annealed (**SA**), see Table 6. The requested target hardness values, and the actually obtained ones, are given in Table 7.

The softest possible condition of carburizing steels is about 160 HB. That is obtained with an isothermal annealing treatment, or with other types of annealing. Isothermal annealing is actually a very frequent specification in the OEM companies for gear hobbing. The hardness values for the QL and QH can be as low as 200 HB in their softest state. However in this project, these steels come in two variants of quench and tempered condition. The reason is that the carbon needs to be relatively even distributed prior to the induction hardening. The induction heating time of a component is very short, some 2-5 s, in order to avoid over heating of edges, gear teeth, etc. With such a short heat treatment time, the carbon must be even diffused in the matrix to achieve a successful hardening.

Table 6. Steel variants and denominations for the rough soft machining part of the project.

Steel grade	18CrMo4	35CrMo4	50CrMo4	100Cr6
Short name	C	QL	QH	B
Supplier	Gerdau-Sidenor	Gerdau-Sidenor	Ovako	Ovako
Heat treatment				
Quench & tempering I		● QL-T1	■ QH-T1	
Quench & tempering II		● QL-T2	■ QH-T2	
Annealing**	▲ C-IA			◆ B-SA

Table 7. Hardness values for the rough soft machining part of the project. The requested numbers are given on top and the actual numbers are given with **bold text** below.

Target hardness & actual hardness				
Quench & tempering I		● 300 HB 240 HB	■ 350 HB 345 HB	
Quench & tempering II		● 250 HB 287 HB	■ 300 HB 315 HB	
Annealing	▲ 160 HB * 157 HB			◆ 240 HB ** 200 HB

Task 1.3 Secondary heat treatment (Induction hardening)

Two hardening treatments, (**H1**) and (**H2**), were agreed for the fine hard machining part of the project, see Table 8. H1 is to achieve as hard material as possible with the given steels and their carbon content. H2 is a somewhat tempered treatment. H1 is of most relevance for this project, while H2 is of more research purpose, for hard machining, and for fatigue testing. Of most industrial importance is probably QH-T1 treatment, in the comparison with a reference carburizing treated work piece, when it comes to both machinability and fatigue strength. **NOTE:** The obtained hardness values were too low according to the desired ones. The QH-H1 condition was re-hardened through induction hardening. The surface hardness of that re-hardened bars was 58 HRC. The requested hardness values and the currently obtained, actual hardness values are given in Table 9.

Bars of the C-H, QL-H1, QL-H2, QH-H1, QH-H2 and B-H qualities have been machined and prepared to fit the turning lathe at CRF for hard turning tests. The length has been reduced to 200 mm, and the clamping diameter has been reduced to 40 mm. Some of these bars are displayed in Figure 16.

Table 8. Steel variants and denominations for the hard fine machining part of the project.

Steel grade	18CrMo4	35CrMo4	50CrMo4	100Cr6
Short name	C	QL	QH	B
Supplier	Gerdau-Sidenor	Gerdau-Sidenor	Ovako	Ovako
Heat treatment				
Induction hardening I	▲ C-H1	● QL-H1	■ QH-H1	
Induction hardening II		● QL-H2	■ QH-H2	
Through hardening				◆ B-H1

Table 9. Requested target hardness values for the fine hard machining part of the project.

Target hardness & actual hardness				
H1	▲ 32 HRC 23 HRC	● 54 HRC 46 HRC	■ 60 HRC 54 HRC	
H2		● 45 HRC 38 HRC	■ 50 HRC 47 HRC	
TH				◆ 62 HRC 62 HRC



Figure 16. Blanks prepared for hard turning in the Hardinge lathe at CRF.

Task 1.4. Work piece material for pilot component manufacturing in WP6

A bar of $\Phi=70$ mm, length 10 m, of the Ovako 528 (50CrMo4) steel was sent to a major supplier of forgings of Fiat Powertrain, Hotroll S.r.l. The bars were sectioned to the desired blank size, and forged to rings using a completely new forging cycle, specially developed for this steel and this component.

The specified hardness of the forged rings was 350 HB. This was based on the fact that the more the carbon constituents are dissolved in the steel structure, the better the hardness uptake is in the subsequent induction hardening. The time at austenitizing temperature of induction hardening of a component is extremely short, only a few seconds. This is linked to the complex geometry, and the risk of overheating certain material volumes, e.g. the gear tooth edges.

The extremely short thermal cycle enables no time for carbon to diffuse, hence the need of an already dissolved carbide structure.

WP2 MATERIAL CHARACTERIZATION

AIM of WP2:

The aim of WP2 was to provide a comprehensive characterization of the materials used in the project.

OBJECTIVES of WP2:

- To verify mechanical properties of work piece bars prior to machining tests in WP3 and WP4.
- To have all necessary characteristics of the work piece materials that is needed to explain results from machining tests, mechanical testing and fatigue tests.

Basic mechanical characterization: hardness, tensile tests and toughness evaluation.

Task 2.1 Test specimens for material characterisation.

Samples for toughness testing according to a Charpy-V geometry have been manufactured. The following sample variants have been manufactured and Charpy tested, of the "soft" conditions: C-IA, QL-T1, QL-T2, QH-T1 and QH-T2, and of the "hard" conditions: C-H (carburized), QL-T1 and QH-T1 (both induction hardened at EFD Induction), and B-H (through hardened in conventional furnace).

A Charpy-V sample geometry for toughness testing is agreed. This geometry is also feasible to treat with induction hardening, which is of importance in the project

An induction coil was specially made for the induction hardening of toughness samples of the 35CrMo4 and 50CrMo4 steels, see Figure 17. A schematic of the induction coil specially designed and manufactured for this task is depicted in Figure 17. A representative longitudinal cross-section of an induction hardened Charpy sample is found given in Figure 18. A few samples, un-treated and carburized, are depicted in Figure 19.

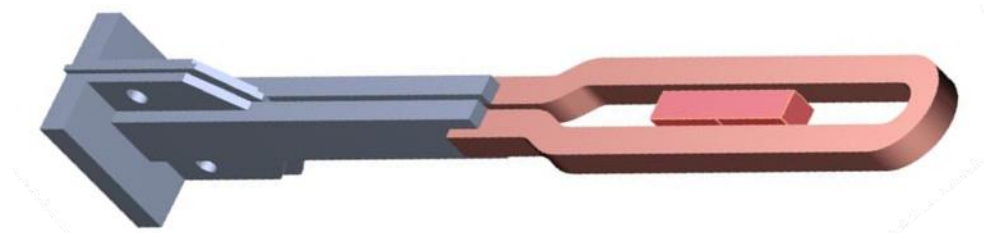


Figure 17. Schematic of the induction designed and manufactured for the toughness tests of 35CrMo4 and 50CrMo4.

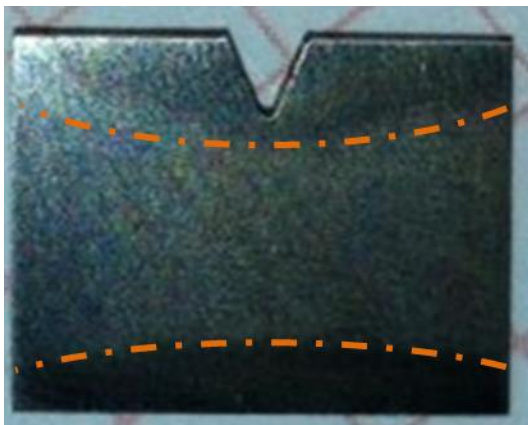


Figure 18. Cross section (etched) of an induction hardened Charpy sample. The approximate zones of hardening are given in orange lines.



Figure 19. Charpy samples prior to test. As-delivered (top), and heat treated (bottom).



Figure 20. (a) Configuration of induction hardening of tensile test samples. (b) The induction coil.

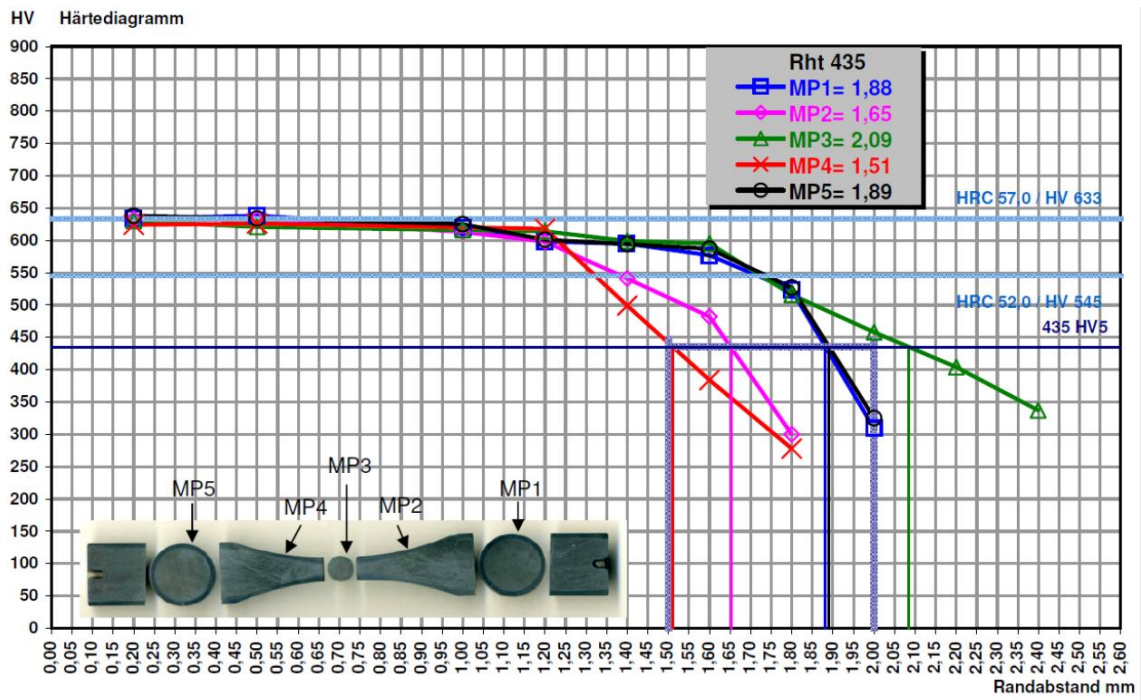


Figure 21. Hardness depth profiles of the induction hardened samples for tensile test made of 35CrMo4.

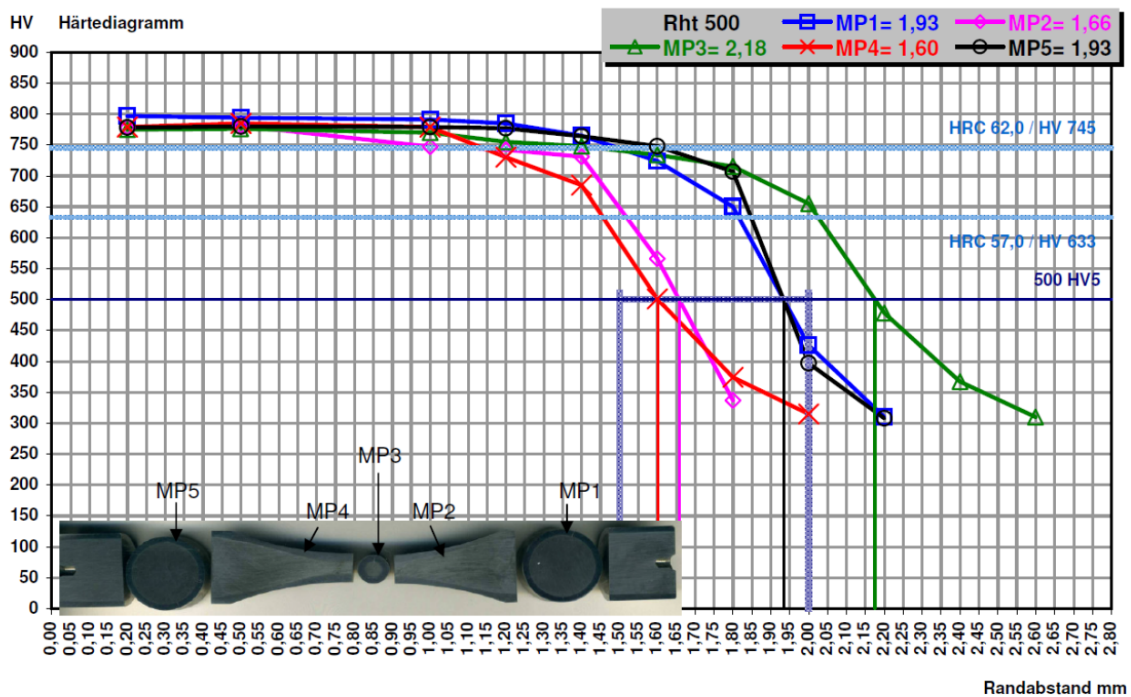


Figure 22. Hardness depth profiles of the induction hardened samples for tensile test made of 50CrMo4.

Task 2.2. Microstructural and chemical characterisation

CHEMICAL COMPOSITION

Aim: To provide useful information regarding chemical composition to understand the results obtained in machining and fatigue tests.

Experimental description: Chemical composition analyses have been performed on final products by spectrometry and CHN analyser (O and N) at each steelmaker's facilities. The chemical composition from the heat of the C, QL, QH, and B batches is given in Table 10.

Table 10. Chemical composition from the heat in the steel plant.

Steel grade	Manu-facturer	MAC D Denomi-nation	Batch/ charge no.	Weight %					
				C	Mn	Si	P	S	Cr
18CrMo4	GERDAU	C	58293	0,19	0,81	0,29	0,011	0,024	1,06
35CrMo4	GERDAU	QL	59788	0,34	0,81	0,31	0,008	0,026	1,12
50CrMo4	OVAKO	QH	V5437	0,50	0,68	0,23	0,018	0,035	0,98
100Cr6	OVAKO	B	V3529	0,97	0,31	0,28	0,019	0,012	1,41

Steel grade	MAC D Denomination	Weight %						Weight ppm			
		Ni	Mo	V	Cu	Al	Sn	Ti	O	N	Ca
18CrMo4	C	0,12	0,16	0,004	0,14	0,017	0,010	20	10	117	7
35CrMo4	QL	0,11	0,18	0,004	0,07	0,023	0,008	20	12	61	8
50CrMo4	QH	0,21	0,19	-	0,17	0,02	0,01	5	8	78	2
100Cr6	B	0,20	0,06	-	0,18	0,041	0,01	7	5	83	3

INCLUSIONARY STUDY

Aim: The main goal of this study is to determine the main inclusions (oxides and sulphides) content of each steel grade. This information will be very helpful to analyse the results obtained in the machining and fatigue tests.

Experimental description: A basic inclusion analysis of oxides and sulphides was made by GERDAU I+D using an automatic analyser by LOM (see Figure 23). The analysed sample size was $100\mu\text{m}^2$, using a detection limit of $15\mu\text{m}$. The inclusions were counted and then sorted out by their Equivalent Circular Diameter (ECD)¹



Figure 23. Automatic measure analyzer by LOM at GERDAU I+D laboratory.

¹ **ECD** is used as a size measure parameter of the inclusions. ECD is the diameter of the circle that would have the equivalent area as the element (inclusion) considered.

The size distribution of oxides is given in Figure 24. The oxide content distribution was similar for the grades studied, except from the ball bearing grade (100Cr6), as expected due to its specific manufacturing process used to assure the high cleanliness required for this kind of application. The oxide content was quite homogeneous throughout the same heat. Different bars from the same heat were analysed obtaining similar oxide levels.

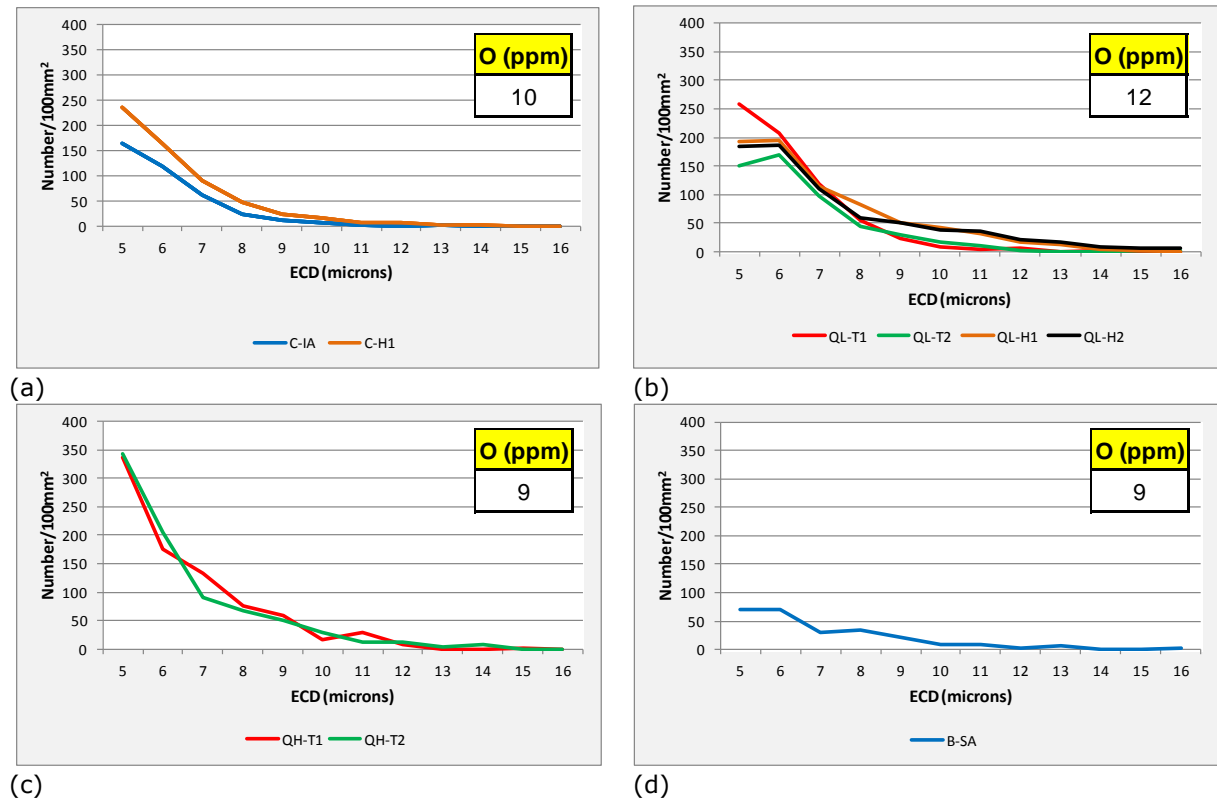
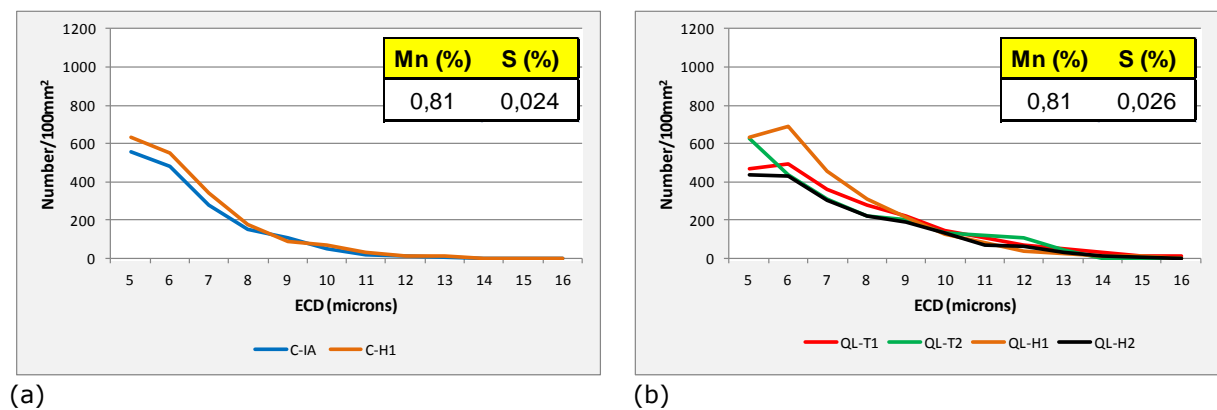
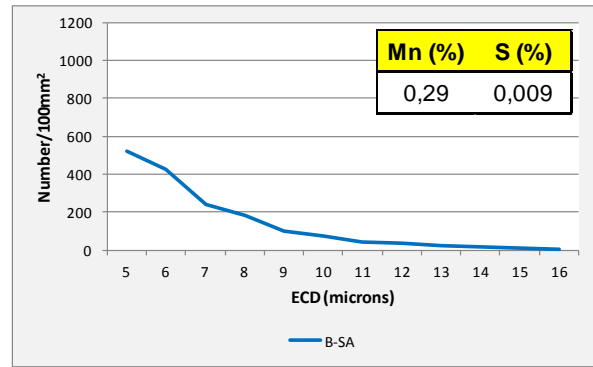
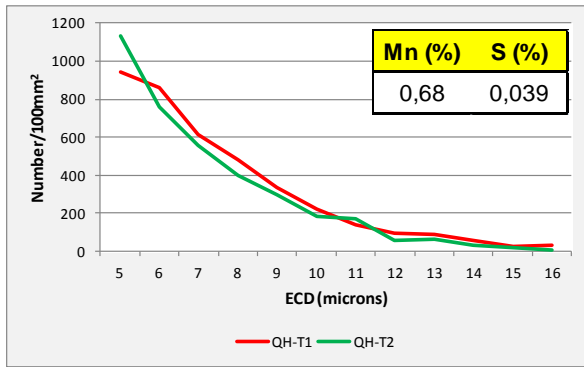


Figure 24. Results of oxide analysis for (a) 18CrMo4 (C-IA), (b) 35CrMo4 (QL-T1, QL-T2) (c) 50CrMo4 (QH-T1 & QH-T2) and (d) 100Cr6 (B-SA).

The differences in the S content detected in the chemical analyses among the 50CrMo4 and the other grades were confirmed in the inclusionary study, see Figure 25. The amount of MnS in both 50CrMo4 was almost the double than in the 18CrMo4 and 35CrMo4. This difference in the MnS content may be critical in their machining and fatigue behaviours. As in the oxides analyses, the sulphides content was quite homogeneous throughout the same heat. Different bars from the same heat were analysed obtaining similar levels.





(c)

(d)

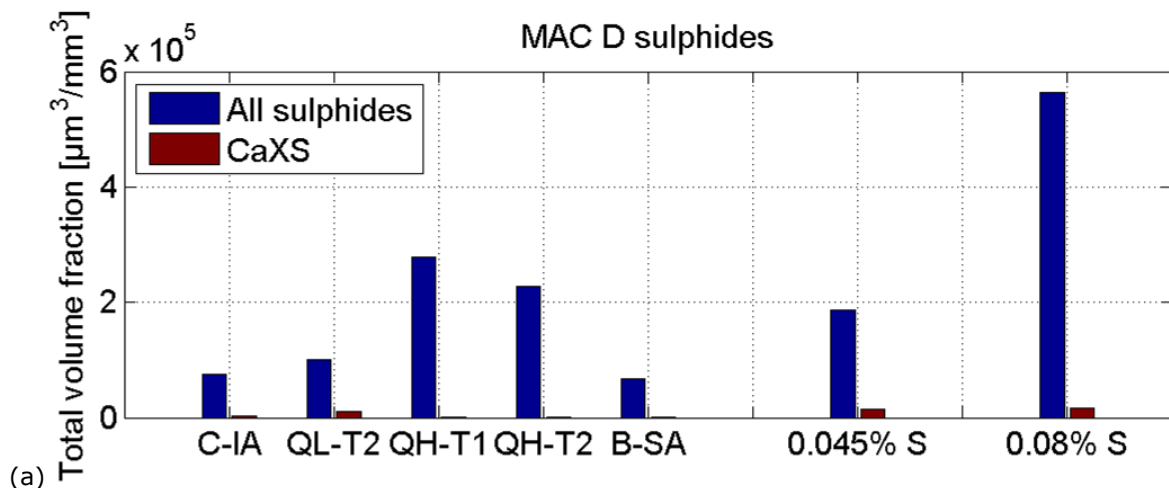
Figure 25. Results of sulphide analysis for (a) 18CrMo4 (C-IA), (b) 35CrMo4 (QL-T1, QL-T2) (c) 50CrMo4 (QH-T1 & QH-T2) and (d) 100Cr6 (B-SA).

Conclusions:

- As expected, different oxides measurements carried out among different bars of the same heat (i.e. samples C-IA and C-H1 are both 18CrMo4 of the same heat but with different heat treatments) show similar results. Similar behaviour for sulphides.
- Comparing the results obtained in both cases (for oxides and sulphides), the 100Cr6 is the steel with the lowest inclusions content, expected because this is a ball bearing steel grade (it follows a specific manufacturing process to ensure its cleanliness).
- Among the other grades, 18CrMo4 and 35CrMo4 have similar sulphides content (they also have similar %S) while 50CrMo4 has a clearly higher sulphides concentration (its sulphur content is almost the double than the other two grades). This S% difference is foreseen to have influence on the machining and fatigue results.

INCLUSION CHARACTERISTICS USING PDA-OES

The inclusionary characteristics of steels of the project were assessed by PDA-OES. PDA-OES is based on spark spectrometry. The elemental composition of each single spark is recorded. Most sparks hit the steel matrix. Occasional sparks goes in inclusions, resulting in elemental spikes of e.g. S, Ca and Al. The corresponding inclusion compound and their size distribution can be obtained through sum normalisation and the link between the inclusion OES spikes and a corresponding average inclusion size. The total volume fraction of sulphides, oxides and complex inclusions are given in Figure 26. In addition, the sub-classes Ca-containing sulphides (CaXS), Ca-containing oxides (Ca-ox) and the oxy-sulphide sub-class are given. As reference a few other well-characterized carbon steels are added. The first one being a Ca-treated steel with 42 ppm Ca-0.045 wt% S, among others. The other one being a high sulphur – high Pb-Bi steel.



(a)

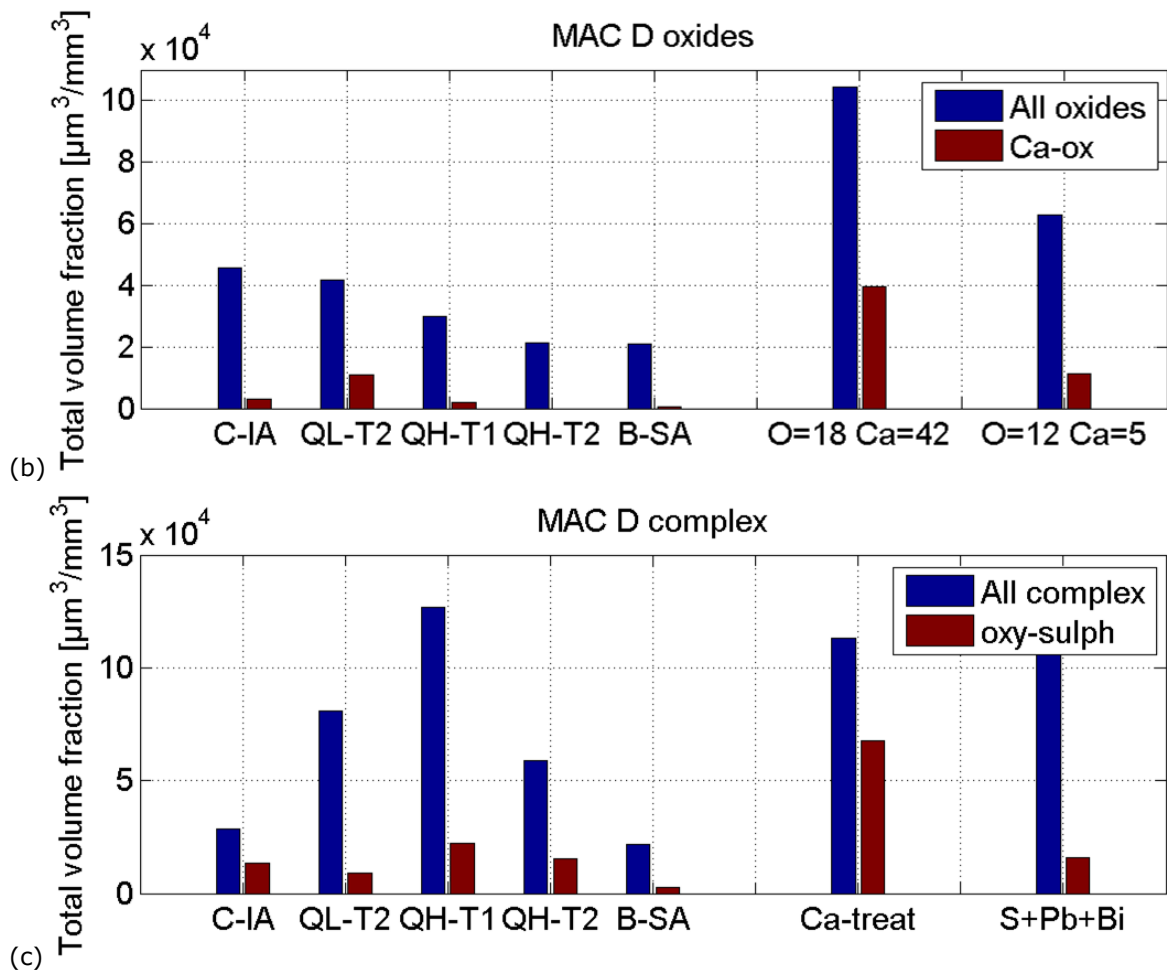


Figure 26. Bar charts of inclusionary characteristics recorded with PDA-OES. (a) Sulphides, (b) oxides and (c) complex inclusions.

MICROSTRUCTURES EVALUATION

Aim: The goal of this study is to provide all the necessary information regarding microstructure to explain the results obtained in machining, mechanical and fatigue tests.

Experimental description: The microstructures obtained through the different heat treatments described in Task 1.2 and 1.3 were evaluated by LOM (Light Optical Microscopy).

Results: A summary of the microstructures obtained is given in Table 11, where:

- Q&T: Quench & Temper heat treatment.
- F: Ferrite; P: Pearlite; B: Bainite; M: Martensite.

Table 11. Microstructure study summary.

Grade	Reference	Manufacturer	As-delivered heat treatment	Secondary heat treatment	Microstr. surface	Microstr. 1/2R	Microstr. core
18CrMo4	C-IA	GERDAU	Isoth. annealing	Non	F-P	F-P	F-P
	C-H1	GERDAU	Isoth. annealing	Q&T	B	B-F	B-F
35CrMo4	QL-T1	GERDAU	Q&T	Non	M	M-B	M-B
	QL-T2	GERDAU	Q&T	Non	M-B	M-B	M-B
	QL-H1	GERDAU	Q&T	Q&T	M-B	M-B	M-B
	QL-H2	GERDAU	Q&T	Q&T	M-B	M-B	M-B

The pictures obtained in this study are shown in [Annex XX](#)

Optical micrographs of the steels can be found in ANNEX 2. In general, the microstructures are homogeneous through the cross-sections. Only minor tendencies of banding are observed.

An example of such micrographs is from the reference steel C-IA, see Figure 27.

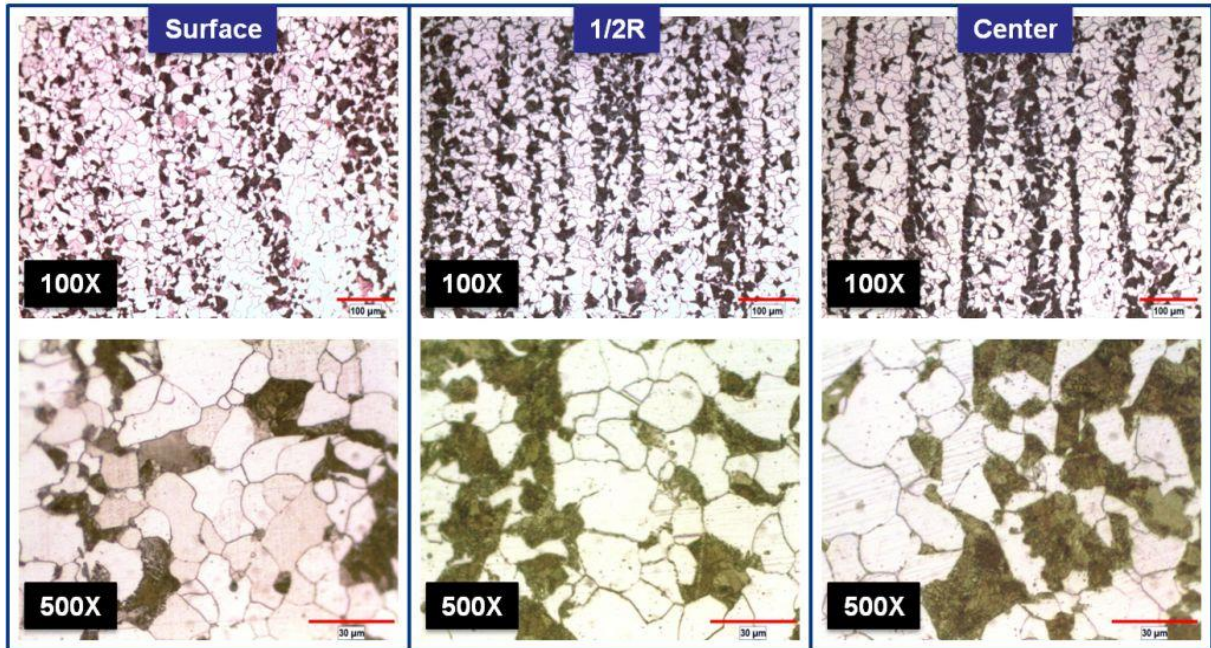


Figure 27. Representative optical micrographs of the C-IA steel. (LOM)

Micrographs of the QL-T1, QL-T2, QH-T1, QH-T2, B-SA, C-H1, QL-H1, QL-H2, QH-H1, QH-H2 and B-H steels are found in ANNEX 2 Figure 127 through Figure 135. The microstructure of the tempered conditions (T1 & T2) is relatively homogeneous through the cross-section. The H1 and H2 conditions show evidence of not transformed martensite. Some lack of hardness in the centre of these materials can be expected.

Conclusions:

- The microstructures obtained in all the cases correspond to the performed heat treatment.

Task 2.3 Testing of hardness, toughness and tensile strength

Aim: To determine the main mechanical properties in order to check if the heat treatments are well performed and to make easier the interpretation of the results obtained in machining and fatigue tests.

HARDNESS MEASUREMENTS

Experimental description: Hardness was measured in Brinell for the as-delivered materials and in Rockwell C for the heat treated materials. Different hardness measurements were performed (one each 5mm) from the surface to the core of the bar.

Results: The results obtained from the assessments of the as-delivered work piece bars from the steel works are shown in Figure 28. The hardness values were relatively expected. The hardness of about 350 HB of the QH-T1 was considered most important and relevant for the further induction hardening of this steel and the resulting martensite transformation during induction hardening.

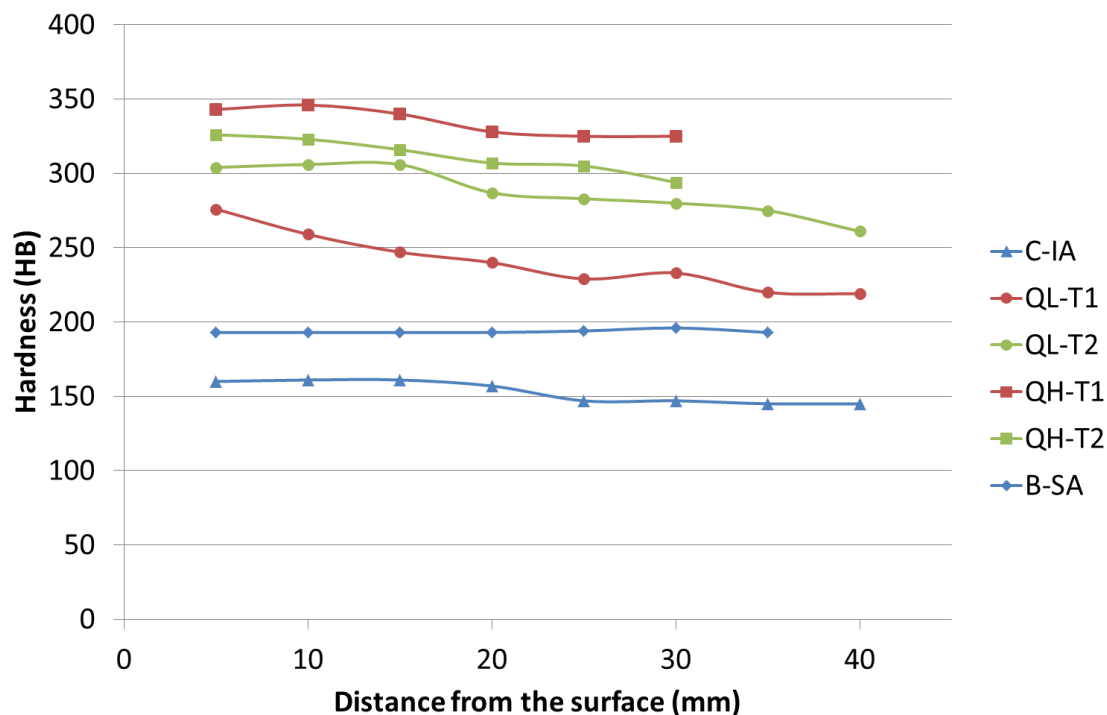


Figure 28. Hardness depth profiles of the work piece materials delivered from the steel manufacturing.

The hardness depth profiles of the steel bars after secondary heat treatment is given in Figure 29. The hardening of these bars was sub-contracted by the steel manufacturers. In general the resulting hardness values were considered too low for a relevant investigation of hard part machining of the project. The reason of the low hardness values probably lies in a combination of the massive geometry and a not sufficient quenching capacity of the quenching processes. The steel of most likelihood for the demonstrator manufacturing was at that time decided to be the QH-H1 (50CrMo4). To enable a fully relevant hardness of this steel, considered to be 58-60 HRC), bars were sent for induction hardening. The important difference from furnace hardening was in fact the water spraying of the bars after austenitizing through induction hardening. The hardness depth profile of those bars is given as QH-H2 IH.

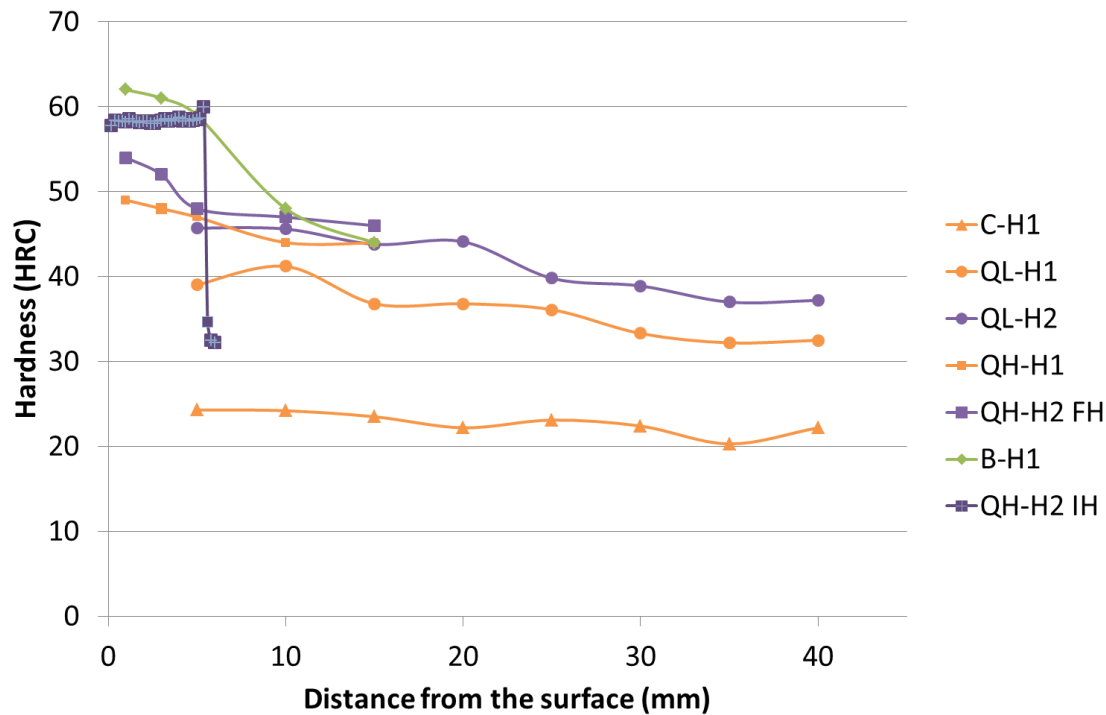


Figure 29. Hardness depth profiles of the work piece materials after secondary heat treatment.

Conclusions:

- The hardness in the cross section of the isothermal annealed 18CrMo4 is very homogeneous.
- As expected, in the case of the Q&T grades, the hardness is clearly higher in the surface than in the core (its cooling speed is faster).
- The hardness values obtained after the secondary heat treatment with the 35CrMo4 are very low to be considered as a possibility to manufacture the real component (the teeth hardness would be lower than the required one). This point was also expected because of its low carbon content.

TENSILE TEST

Experimental description: The tensile tests were performed according to the standard ISO 6892. Three specimens of each grade were tested, these specimens were machined from 1/2 radius.

Results: The average values of strength, yield strength, elongation and reduction of area are given in Table 12.

Table 12. Numerical summary of tensile tests.

Steel grade	Reference	UTS (MPa)	YS (MPa)	EI (%)	RA (%)
18CrMo4	C-IA	538	333	32	72
35CrMo4	QL-T1	833	666	20	67
35CrMo4	QL-T2	1009	896	17	64
50CrMo4	QH-T1	1108	982	16	56
50CrMo4	QH-T2	985	855	18	58
100Cr6	B-SA	670	396	31	58

Conclusions:

- The results obtained in this test are coherent with the hardness values shown before.

- For QL-T2 and QH-T2 similar strength values (about 1.000MPa) were obtained. This fact may allow determining the influence of C and S content on machinability.
- The YS/UTS ratio of the Q&T grades (more than 0,8) shows that the transformation occurred in the Q&T was correct.

TOUGHNESS TEST

The toughness tests assessed with Charpy-V testing. The samples were manufactured externally by a mechanical workshop. The results of the toughness tests of the as-delivered steels is given in Figure 30(a).

However, the most relevant data of toughness is the result of the case hardened samples. The importance comes from the component loading that occasionally includes mechanical shocks. To fulfill these demands the steel and heat treatment of gears are typically designed to have a hard surface and a high toughness of the core. Reference samples for toughness test were made of 18CrMo4 that were carburized in a furnace of Fiat powertrain in the Mirafiori plant using a carburizing cycle as close as possible to that of the demonstrator gear.

The Charpy-V numbers are given in Figure 30(b). The toughness values can also be considered to be expected. Perhaps the higher toughness of the 35CrMo4 steels as compared to the ones of 50CrMo4 could be noted, given their similar hardness values.

The Charpy values of the hardened samples are not fully analyzed. They reflect very much the hardening of the samples. The C-H sample was carburized at CRF. The QL-T1, QH-T2 and B-H1 were induction hardened at EFD Induction.

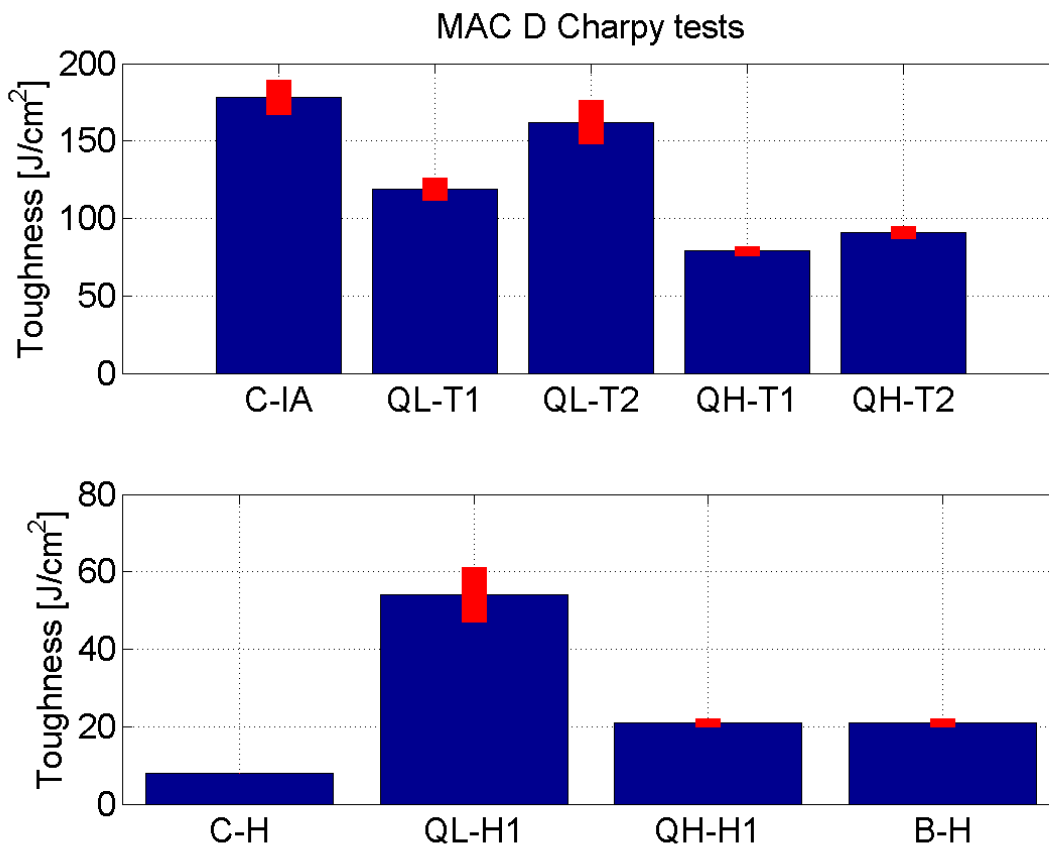


Figure 30. Toughness values recorded with Charpy V testing. **NOTE:** The C-H was carburized at Fiat. The QL-H1, QH-H1 and B-H were induction treated at EFD Induction.

WP3: ROUGH MACHINING

AIM of WP3:

The aim of WP3 was to provide knowledge of tool life in rough turning and in an experimental hob milling test of the steels included in the project. That would provide data for the comparison of manufacturing cost in WP6. Furthermore the life limiting tool wear mechanisms, as well as fundamental understanding of the roughing cutting processes were to be clarified.

OBJECTIVES of WP3:

- To have cutting tools defined for rough machining. **Turning and gear hobbing are addressed.**
- To perform tool life tests for rough turning and gear hobbing operations.
- To generate knowledge about machinability properties of the work piece materials defined in Table 1.

To generate explanatory understanding of tool wear mechanisms and chip formation, in order to explain the machinability data generated. Most attention is given the understanding of machinability difference between the 0.2%C steel and the QT-steels.

BACKGROUND

Tool life tests are performed in rough turning typically according to the standard ISO 3685:1993 or as a derivative of this standard. Frequently the depth of cut and the feed are fixed and the cutting speed is varied from low to high cutting speeds. The flank wear of the cutting tool is recorded repeatedly throughout a test and the tool life is typically reached at a flank wear of $v_b=0.3$ mm. The tool life is monitored to the cutting speed to generate tool life diagrams (VT-diagrams). Often the axes are logarithmic. The Taylor equation tells that that is to generate a relatively straight line.

Task 3.1 Tool life tests in roughing.

TOOL LIFE TESTS IN ROUGHING TURNING

Experimental description: The turning test in roughing was carried out in dry conditions. The employed cutting conditions were:

- Cutting depth (a_p) = 2mm.
- Feed (f) = 0,4mm/rev.
- Maximum flank wear ($VB_{max} = 300\mu\text{m}$).

The used tool holder was the model PCBNL (2525M). This holder engages the blunt nose of the cutting tool. The cutting insert was a CNMG 120408 GC4215, both of them (tool holder and insert) were manufactured by SANDVIK.

The test was performed in a CNC lathe at the GERDAU I+D laboratory, following the ISO 3685:1993 standard indications.

All the materials were tested in the as-delivered conditions. The 100Cr6 was not tested because it was manufactured to be Q&T and then to be used as reference in the hard machining tests.

Results:

The tool life results are summarized in Figure 31. The tool life vs. cutting speed is plotted to form so called Taylor curves. Note that the machining results obtained with the isothermal annealed 18CrMo4 were used as reference because nowadays this is the steel used by FIAT to manufacture the considered component.

To facilitate the interpretation of the tool life tests the cutting speed corresponding to tool life of 15 minutes is displayed in Figure 32. This value is hereafter referred to as the V15 number.

The C-IA that can be considered as a reference has a V15 value of about 425 m min^{-1} . The steels for induction hardening have V15 values from about $200\text{-}250 \text{ m min}^{-1}$. This can be considered a significantly reduced tool life in the rough turning operation.

However, the ranking of the QL and QH steels are somewhat expected, given their corresponding ranking of hardness. Though, there is an exception, the 35CrMo4 (QL-T2) has worse machinability than the 50CrMo4 (QH-T1) when the first one is slightly softer. This may be explained due to the considerably lower S content of the QL-T2 steel.

The machinability of the reference steel (C-IA) is clearly better (V15 more than two times higher) than the one of the 50CrMo4 (QH-T2) that will be the steel chosen to manufacture the demonstrator component by the induction hardening route.

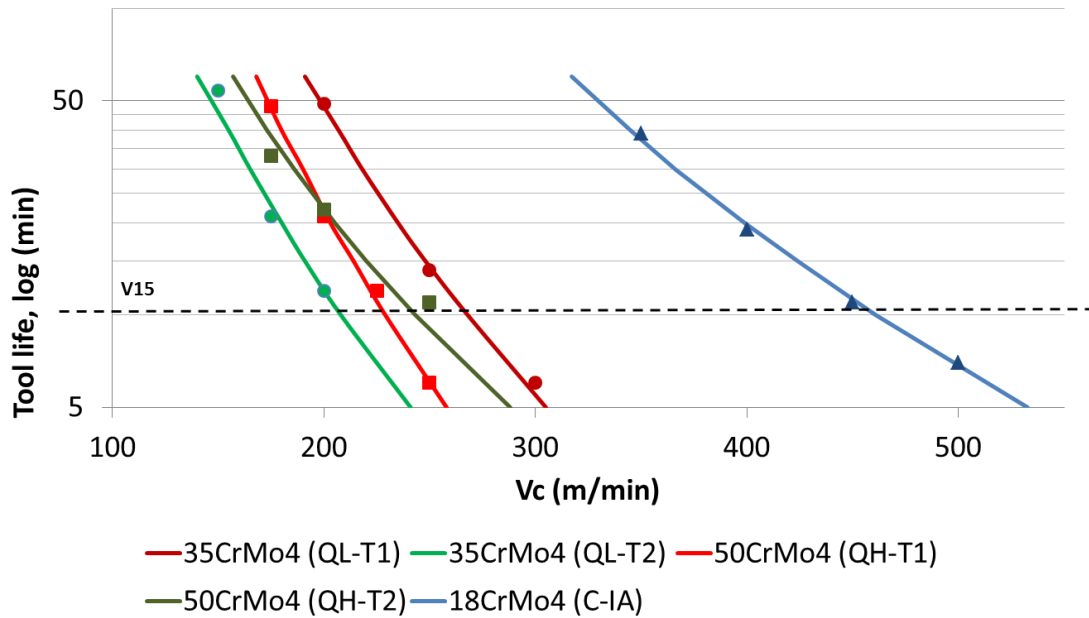


Figure 31. Taylor curves for the tested materials. $a_p=2$ mm and $f=0.4$ mm.

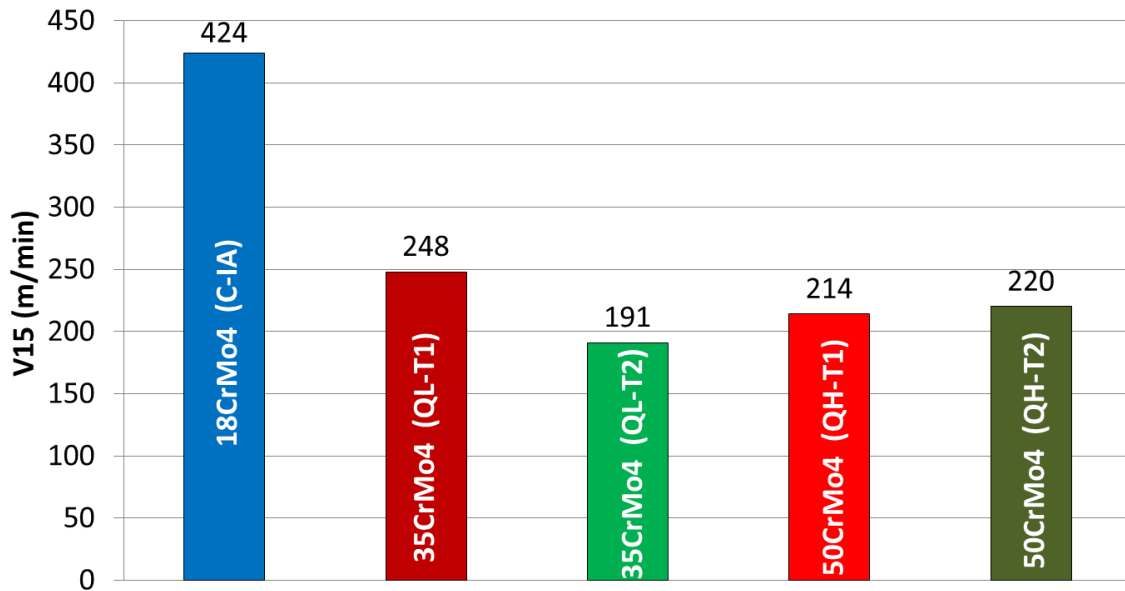


Figure 32. Cutting speed that corresponds to tool life of 15 minutes.

A preliminary comparison of cutting speed at tool life of 15 minutes (V_{15}) vs. ultimate strength shows an established and expected relationship, see Figure 33. The tool performance is reduced with higher ultimate strength of the tested material. The C-IA steel has the lowest UTS of 538 MPa of the tested steels. Consequently it has the highest V_{15} number of 424 m/min. Increased thermomechanical load on the cutting edge that generates plastic deformation of the flank face is the primary reason of the UTS vs. V_{15} relationship.

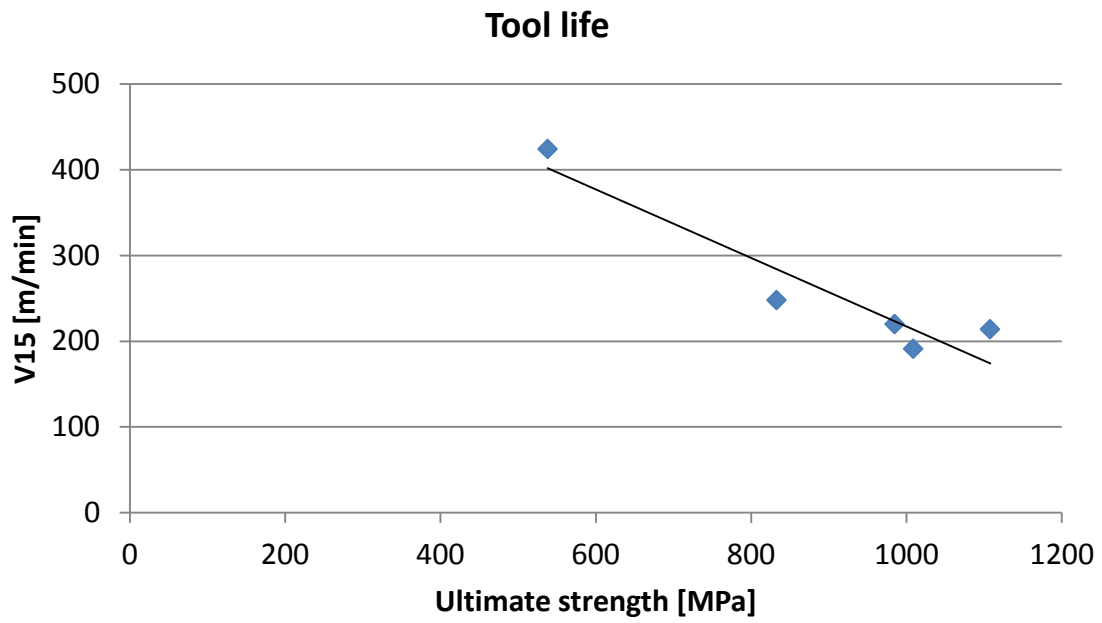


Figure 33. Preliminary comparison of ultimate strength and cutting speed at tool life 15 minutes (V15) of the tested steels.

TOOL LIFE TESTS IN EXPERIMENTAL SIMULATION OF GEAR HOBGING

An experimental simulation of the hob milling process was undertaken, see Figure 34. It is a development of previous tests using a face milling configuration [ref]. The current tests utilise a commercial tool holder and commercial cutting tools, see Figure 35. Two major facts make the test realistic and interesting:

4. The cutters are made of PVD coated HSS, the same material as conventional hob material.
5. The cutters have a circular geometry. This means that the varying chip thickness of hob milling is replicated.
6. Wear study of used milling inserts show the same wear types and wear mechanisms as those of actual hob edges.

Some observations and comments:

- The tool life in terms of number of passages, i. e. removed chip volume, is roughly half with the quench and tempered steels, QL-T2, QH-T1 and QH-T2, as compared to the reference C-IA.
- The solution to successive hob milling of the hard steels is to reduce the cutting speed, to about 80-100 m/min.
- The tool life of the reference steel is about 55 passages at 200 m/min.
- The tool life frequently increased with higher cutting speeds. However, at $vc > 100$ m/min with the QL-T2, QH-T1 and QH-T2 steels, the risk of unexpected edge failure increased. That means that one test can last for 15 passages. The next test may last for only 0.5 passages when the cutting edge is completely worn out.



Figure 34. Configuration of the cutting tests. Face milling of bars made of the workpiece materials of the project.

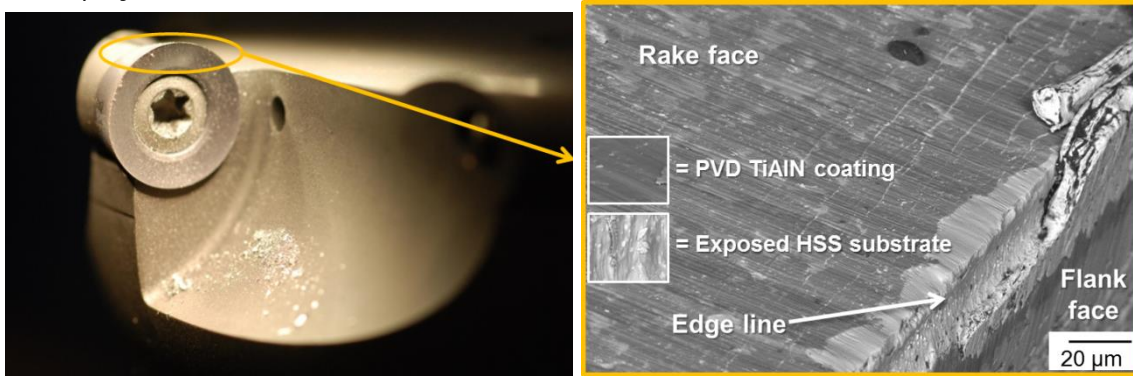


Figure 35. The milling cutter. (a) overview in the tool holder and (b) typical wear of the cutting edge after a cutting test.

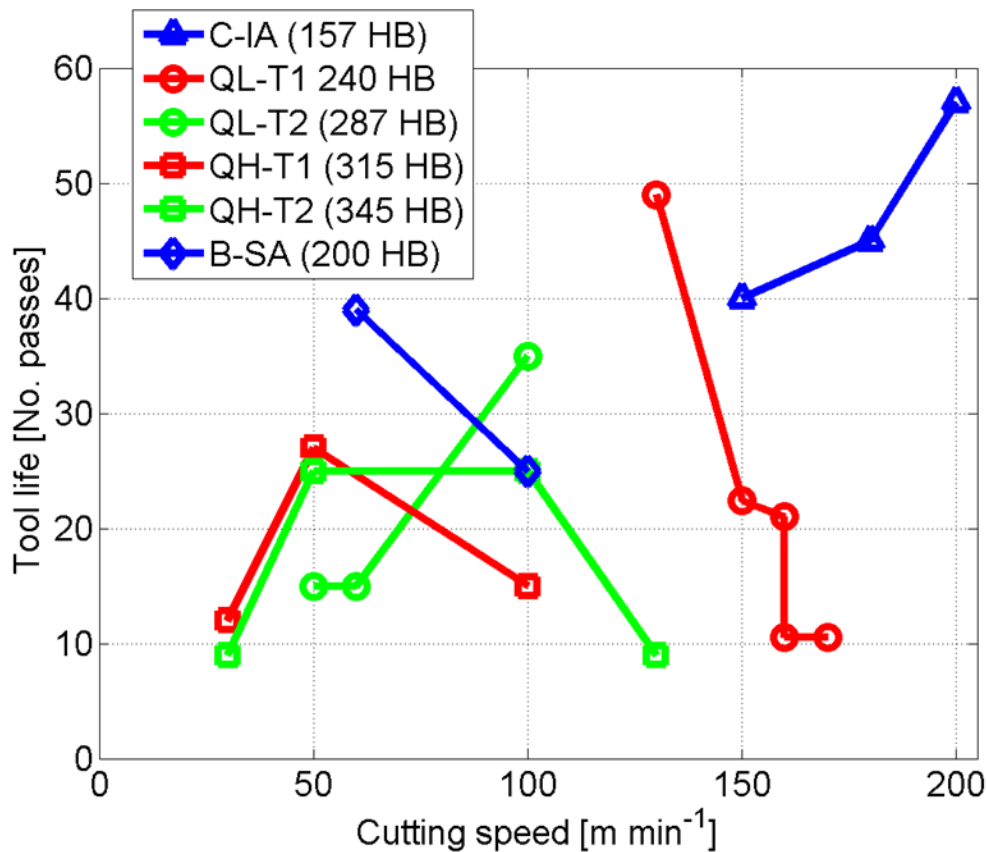


Figure 36. Tool life tests in gear hobbing simulation. No. of passes vs. cutting speed.

A comparison of the volume of removed chips in the utilized milling test was made with the service intervals of actual hob milling tools. The volume of removed chips in this test is given in $V(\text{single tooth test (C-IA) @ 55 passes} = 10\text{mm} \times 500\text{mm} \times 1\text{mm} \times 40 = 27 \times 1\text{e}4 \text{ mm}^3$ (1).

It was told in oral communication that the service interval of gear hobbing tools corresponds to 5 metres of gear tooth length, for each hob tooth of the hob. Assume gear root as rhombohedra, see Figure 37. Then the corresponding volume of that gear tooth is given in Eq. (2).

$$V(\text{single tooth test (C-IA) @ 55 passes} = 10\text{mm} \times 500\text{mm} \times 1\text{mm} \times 40 = 27 \times 1\text{e}4 \text{ mm}^3 \quad (1)$$

$$V(\text{gear tooth}) = (11+2)/2 \times 9 \times 5000 = 29.2 \times 1\text{e}4 \text{ mm}^3 \quad (2)$$

The comparison of actual gear teeth tool life and the current milling concept can then be made. Note, however, that in this comparison, the typical service interval of about 5 gear tooth metres (GTM), as well as the geometry of the gear tooth are relatively rough. It is still extremely interesting that the tool life of the experimental simulation gets very close to actual gear cutting conditions in terms of tool life. Two differences are noted: (I). These tests were done dry, while most gear cutting uses oil lubrication. (II). In actual gear hobbing, the gear translates slowly back and forth during the cutting. The translation cycle may be one minute. Each tooth is then engaged at maximum only a few seconds during that cycle. It then gets time to cool off between each load peak. The milling cutter is engaged each rotation, with no time to chill off.

Given the concept of gear tooth metres, the rhombohedra gear tooth, the tool life diagram can be transformed to the one in Figure 38.

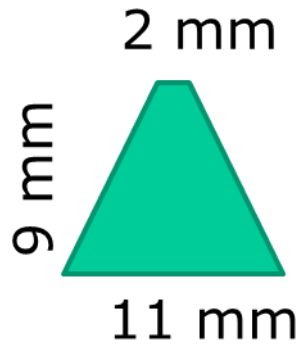
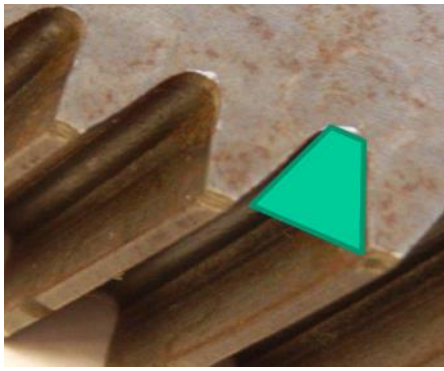


Figure 37. Schematic of the gear tooth volume calculation for the concept of gear tooth meters comparison in tool life tests.

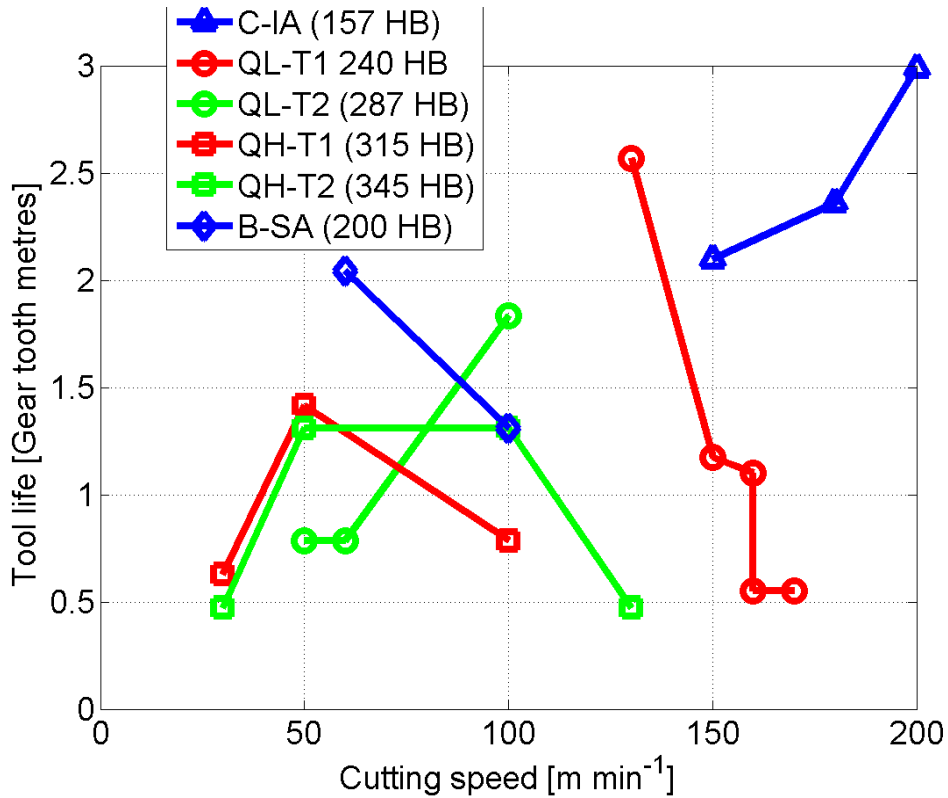


Figure 38. Tool life tests in gear hobbing simulation. The volume of removed chip transformed to corresponding gear tooth metres.

Task 3.2 Tool wear study in roughing

TOOL WEAR STUDY IN TURNING

The tool life tested cutting tools were investigated with respect to life limiting wear type using SEM. The used cutting edges from the tests with 18CrMo4 (C-IA) are found in Figure 41. The corresponding micrographs of 35CrMo4 (QL-T2) are found in Figure 42. The micrographs of 35CrMo4 (QL-T1) and 50CrMo4 (QH-T1 and QH-T2) are found in ANNEX 3, Figure 136 to Figure 138.

The two major components of steel characteristics in terms of tool wear are addressed:

- The steel's abrasiveness
- The chip load, which reflects the chip removal energy.

The abrasion test is a low feed test at intermediate cutting speed. The abrasion of the ceramic coatings is studied. An example of a cutting tool from this test is found in Figure 39. The MAC D materials were abrasion tested for 2 and 6 minutes, respectively. The abrasion width was recorded as shown in Figure 40. The flank faces of the secondary edges of tested inserts are shown in Figure 43. The progression of flank wear with different number of cuts will be re-assessed in short.

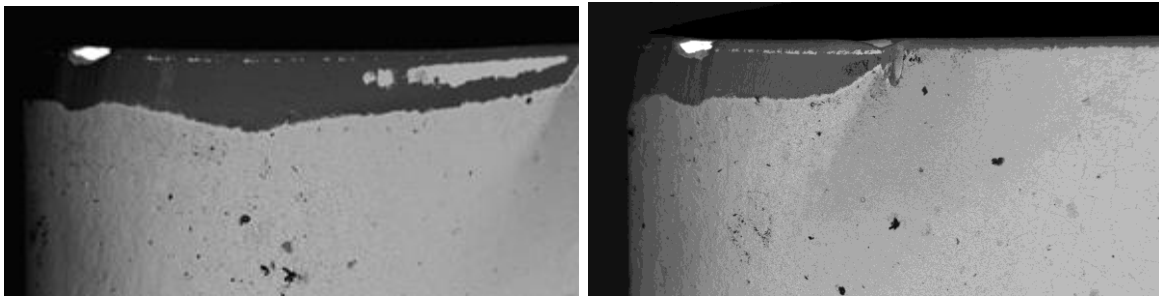


Figure 39. Side views of the (a) primary cutting edge and (b) the secondary cutting edge of the turning cutting tool CNMG120408 PM GC2015. (SEM-BS)

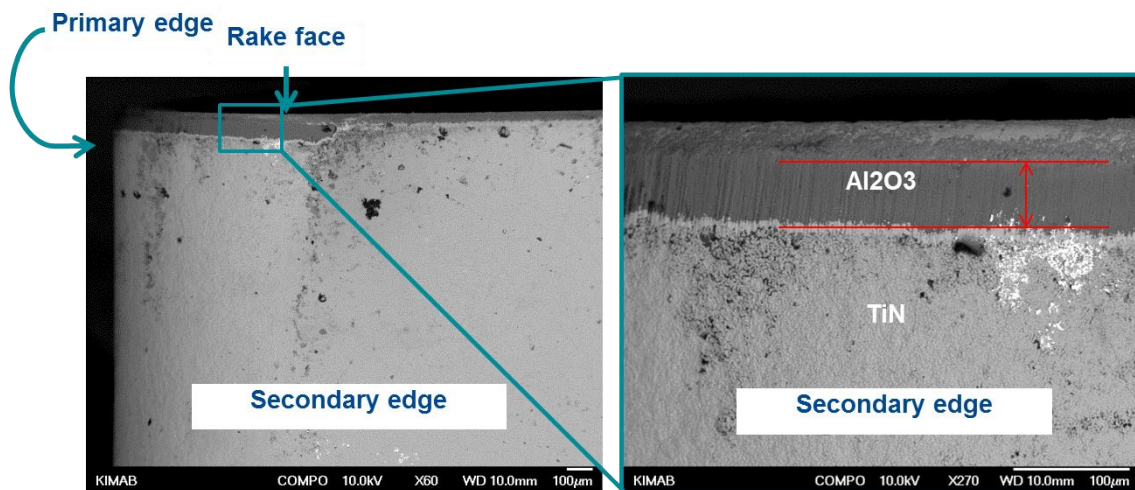


Figure 40. Method of flank wear measurement.

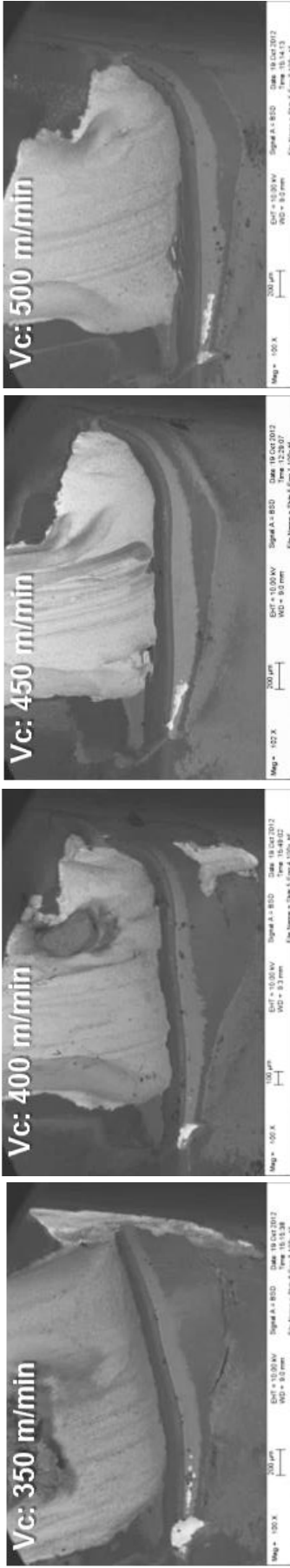


Figure 41. Micrographs from tool life tests with 18CrMo4 (C-IA) at (a) 350 m min⁻¹, (b) 400 m min⁻¹, (c) 450 m min⁻¹ and (d) 500 m min⁻¹. $a_p=2$ mm, $f=0.4$ mm/rev. (SEM-BS)

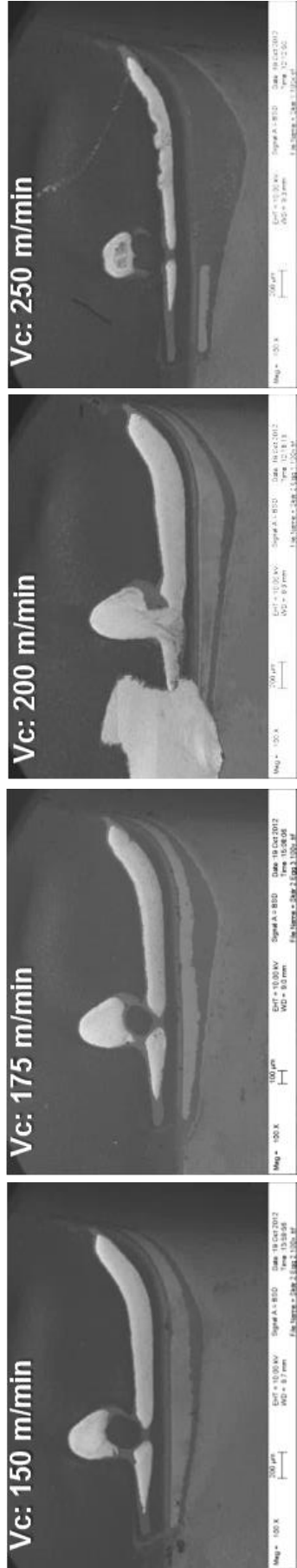
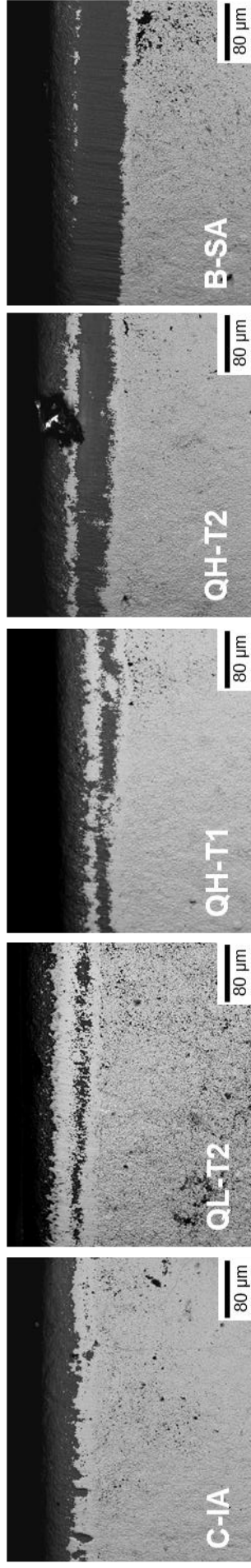


Figure 42. Micrographs from tool life tests with 35CrMo4 (QL-T2) at (a) 150 m min⁻¹, (b) 175 m min⁻¹, (c) 200 m min⁻¹ and (d) 250 m min⁻¹. $a_p=2$ mm, $f=0.4$ mm/rev. (SEM-BS)

Detail of secondary edge, 2 min @ 225 m/min



Detail of secondary edge, 6 min @ 225 m/min

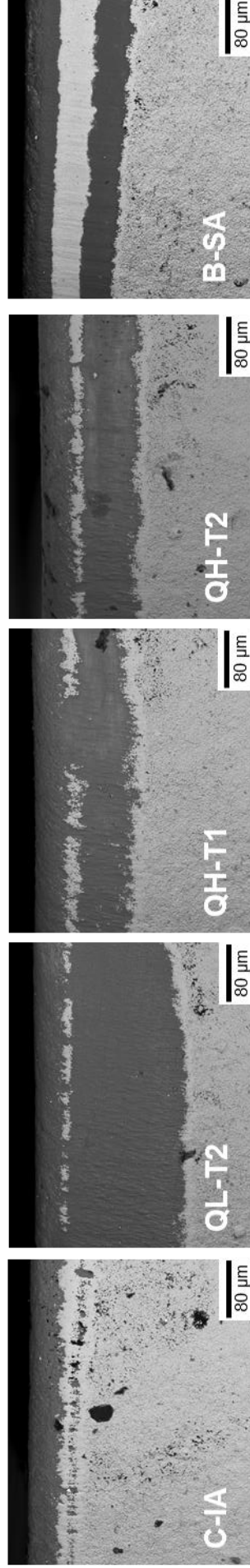


Figure 43. Flank wear after **2 minutes** and after **6 minutes** @ 225 m/min with tested steels.

Task 3.3 Study of chip removal in roughing

Motivation

AIM: (I) To identify the limits of acceptable chip formation in both turning and hob milling and (II) to learn about the steel alloy and microstructural effects on chip removal process.

Experimental setup

The tests were conducted to investigate the machinability criteria cutting force F , surface roughness and chip form. Taking a broad range of depth of cut a_p , feed rate f and two cutting speeds v_c into account, it allows the definition of a process window for external turning operations. External dry turning tests were conducted on a MONFORTS RNC 400 plus lathe. Coated carbide tools were used for a wide range of feeds f and depth of cuts a_p with two cutting speeds v_c , see Table 13. The tests were performed in two steps. In the first step for each steel grade a matrix of feed f and depth of cut a_p was designed, see Table 14. Based on this matrix tests were conducted for the two cutting speeds $v_c = 225$ m/min and 350 m/min.

Table 13. Test conditions used for the screening test

Cutting data	Value
Cutting tool	CNMG120408-PM
Grade	Coated carbide (Coromant GC4215)
Depth of cut	$a_p = 1 - 3$ mm
Feed	$f = 0.1 - 0.6$ mm
Cutting speed	$v_c = 225$ m/min and 350 m/min
Lubrication	Dry

Table 14. Testing matrix of the screening parameters

Material	Feed f / mm					
		0.1	0.2	0.3	0.4	0.6
Depth of cut	1	X	X	X	X	X
	2	X	X	X	X	X
a_p / mm	3	X	X	X	X	X

Cutting forces, surface roughness and chip forms were measured and documented for each point of the matrix. The process forces were measured using a Kistler three component force dynamometer. Surface roughness was assessed by a MarSurf Perthometer M2. The chip forms were classified by ISO3685.

Figure 44 shows the test setup on the lathe. First the bars were pre-turned to a diameter of 78 mm to assure the run out and remove the outer surface. In order to avoid an influence of inhomogeneity over the work piece diameter all tests were conducted on a constant diameter range of the bars. For cutting speed $v_c = 225$ m/min the diameter range was $D = 70 - 74$ mm depending on the depth of cut and for the cutting speed $v_c = 350$ m/min the diameter range was $D = 67$ to 71 mm. In these diameter ranges all materials showed a constant hardness. In order to avoid an influence of inhomogeneity over different work pieces cutting tests for both cutting speeds were conducted on one work piece. The matrix provides testing results over a wide range of parameters. All materials were tested.

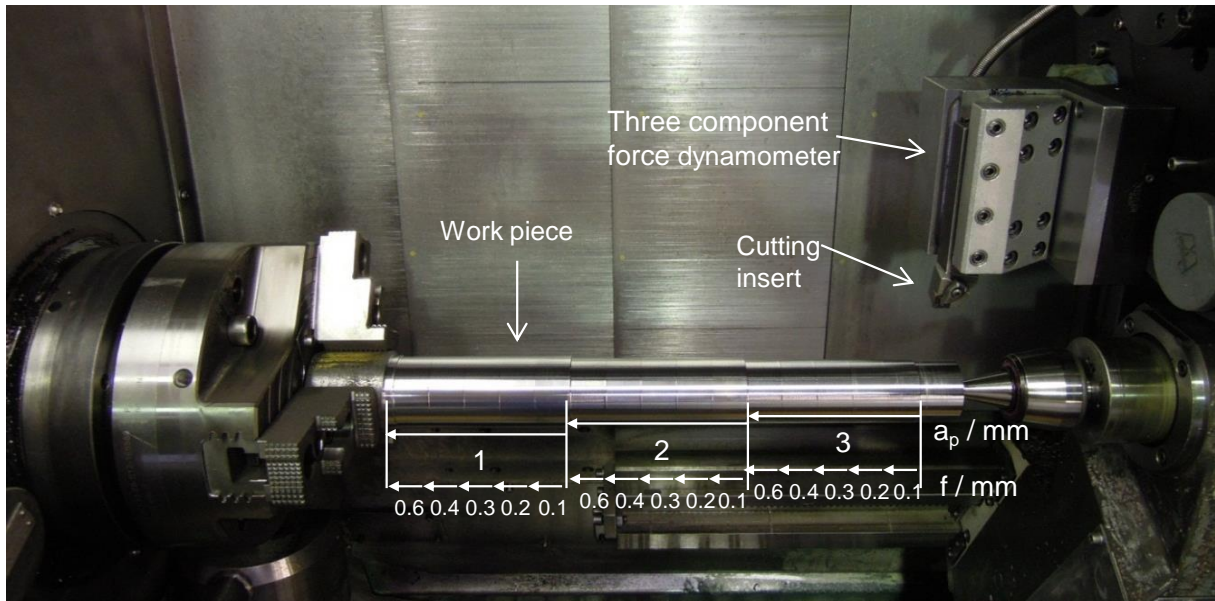


Figure 44. Test setup of the chip map tests.

In a second step a test procedure was conducted to identify a zone of controlled chip breakage. Therefore depth of cut was held constant at $a_p = 2$ and 3 mm and the feed rate was varied. Then the feed rate was held constant at $f = 0.2, 0.4$ and 0.6 mm and the depth of cut was varied. The procedure is pointed out in Figure 45. The setting provides more accurate limits of controlled chip breakage than the previous matrix did. This enables a better direct comparison between the different alloys. The influence of tool wear was neglected as the cutting tools were replaced before tool wear could disturb the results.

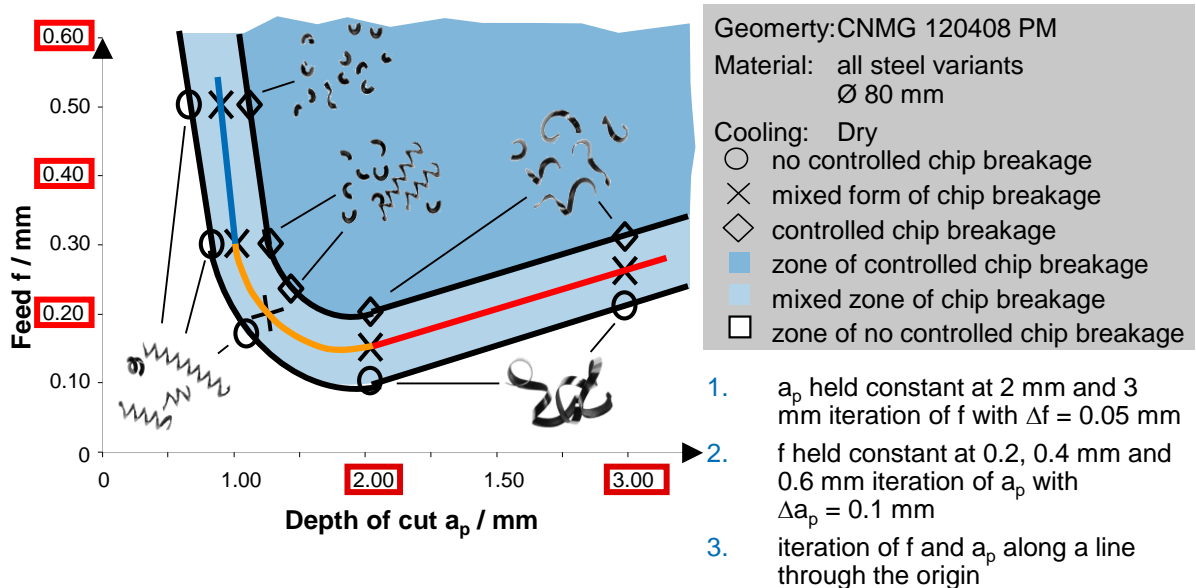


Figure 45. Test procedure to identify zones of controlled chip breakage

CHIP MAPS

In the following chip maps for all tested materials are documented. The chip maps include the limits of controlled chip breakage. Figure 46 shows a chip map for QH-T1 (50CrMo4, head treatment 1) at a cutting speed of $v_c = 225$ m/min. Figure 47 shows a summary of all chip maps recorded at $v_c = 225$ m/min. The two heat treatments T1 and T2 of the two steels 35CrMo4 and 50CrMo4 did not show any significance on the chip breakage. Most significant differences in chip breakage were observed at a depth of cut of $a_p = 2$ mm with the following ranking:

- 100Cr6 = 18CrMo4 > 35CrMo4 (T1 = T2) > 50CrMo4 (T1 = T2)
- B-SA = C-IA > QL-(T1 = T2) > QH-(T1 = T2)

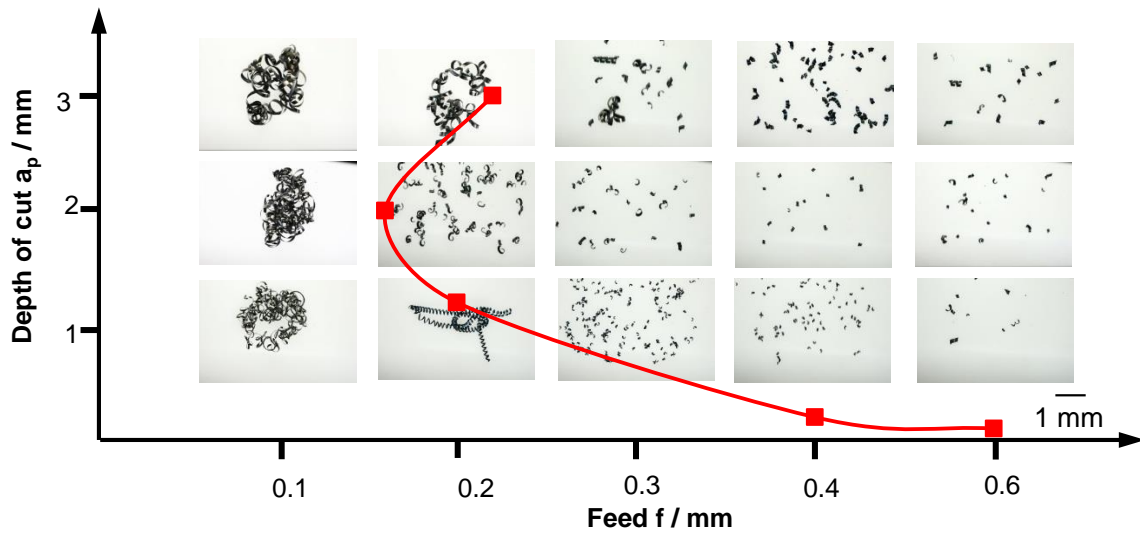


Figure 46. Chip map for QH-T1 at a cutting speed of $v_c = 225$ m/min

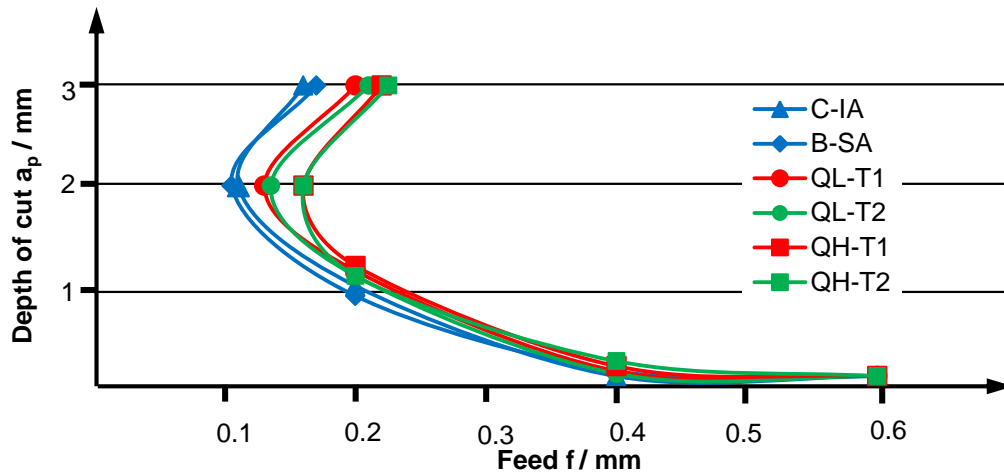


Figure 47. Limits for controlled chip breakage at a cutting speed of $v_c = 225$ m/min

QUICK STOP TEST

The examination of chips gives hints about the chip formation process. In order to understand the mechanism of chip formation, analysis of chip roots are very common. Chip roots are manufactured by interrupting the process. This technique is called a quick stop test. The chip roots were etched and the geometrical dimensions of the shear zone were examined. The quick stop test was conducted according to the method of Buda. Figure 48 shows the material preparation. The geometry creates a predetermined breaking point. In order to manufacture a series of chip roots, several breaking points can be implemented. The moment of chip formation was captured by the stop of the machine. It is advantageous that the chip root is separated from the work piece, and thus the shear zone may be protected from damage during the subsequent metallographic preparation of the samples. The chip roots thus obtained were embedded, polished and etched. The specimens prepared allowed to measure and analyse the geometrical dimensions of the shear zone such as shear angle, chip thickness ratio und segmentation ratio. Triangular flat inserts of type TPUN 160308 were used in an orthogonal cut. The insert was flat and had no chip breaking

geometry. This ensures that the chip forming mechanism was not influenced by a chip breaking geometry and can be traced back to the material properties. Thus machined and prepared chip roots are shown in Figure 139.

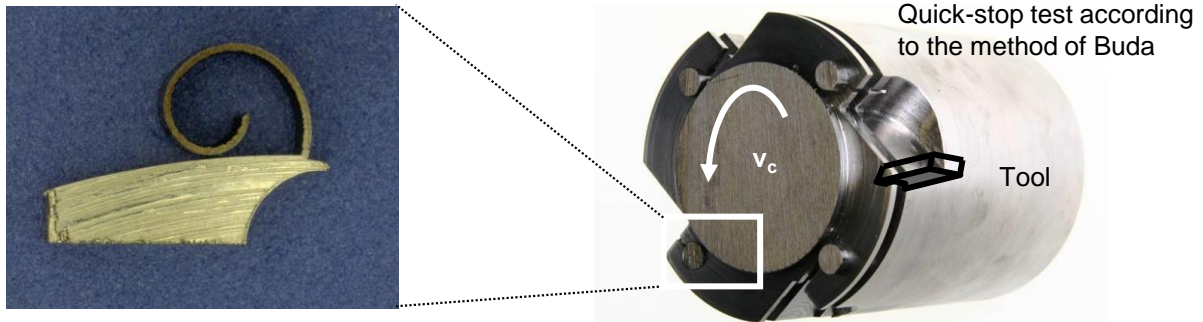


Figure 48. Example of a work piece and a chip root of a quick stop test according to the method of Buda [BUDA68]

The generated chip roots are shown in APPENDIX 3 Figure 139. The un-deformed chip thickness h , chip thickness h_{ch} were measured by digital microscopy, see APPENDIX 3 **Figure 140**. The chip thickness ratio λ_h was calculated by the ration of un-deformed chip thickness h to chip thickness h_{ch} and is documented in **Fel! Hittar inte referenskölla**, as well as the measured shear angle Φ . The shear angle varies in a range of 8% and the chip thickness ratio within a range of 14%. The very low differences confirm similarity of the chip maps for of all steels. The result a that in the tested parameter field, which is relevant for industry, the chip formation shows no significant difference.

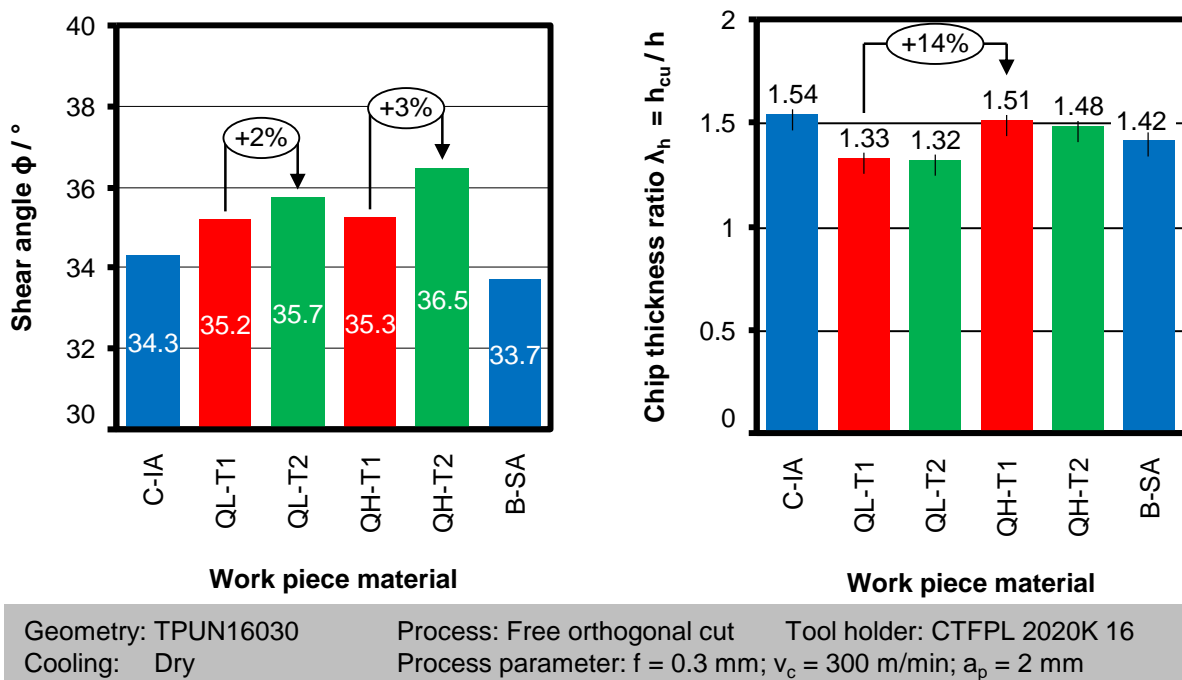


Figure 49. Shear angle Φ and chip thickness ratio λ_h

Results:

- QH (50CrMo4) shows slightly a smaller area of chip breakage than the other steels.
- Cutting forces show more or less the same levels for all steels. A lower cutting speed results in slightly lower process forces.
- The results of the quick stop tests show a continuous chip formation for the steels B-SA, C-IA, QL-T1, QL-T2 and segmented chip formation for the steels QH-T1 and QH-T2.
- Shear angle measured in Buda specimens varies in a range of $34^\circ - 36^\circ$ for all steels.
- The chip thickness ratio is about 14% lower for the QL (35CrMo4) steel compared with the QH (50CrMo4) steel. This can be explained by the smaller hardness of QL steels.

Conclusion:

Concerning the chip breakage and chip formation, machinability can be ensured for all steels. Therefore, all steels can be classified as suitable based on these criteria.

References:

[BUDA68] Buda, J.: Neue Methode der Spanwurzelgewinnung zur Untersuchung des Schneidvorganges. Industrie-Anzeiger Jg. 90 H. 5, pp. 78-81, 1968

Task 3.4. Fundamental cutting tests

AIM:The aim of this task was to provide fundamental understanding of the chip cutting process of conventional hob milling using PVD coated solid hobs made of HSS. Two things were targeted in the similarity of the hob milling, (1). Coating and substrate and (2). The interrupted cutting process. The technical approach was to study the cutting forces and the actual tool temperature in interrupted orthogonal turning.

Experimental Plan:

Tests have been carried out for different working conditions. The workpiece materials, feed rate and cutting speed have been evaluated in order to analyze their influence on cutting forces, temperatures, chip thickness, tool chip contact length, chip morphology during roughing in interrupted cutting in steels without heat treatment.

Experimental Set-Up:

During the machining tests, tool's temperature, and cutting and feed forces were measured. To measure forces, a 3-component dynamometer (Kistler 9121) was placed under the tool holder to record the dynamic changes in the cutting forces throughout the testing. In order to ensure edge sharpness, a new tool insert has been used in each test.

As it is shown in Figure 50, a micro thermal imaging system comprising of a FLIR Titanium 550 M infrared camera and a microscopic lens offering a resolution of 10 μm were used to measure tool's temperatures during the orthogonal cutting of all alloys on the cutting edge.

Finally, a high-speed, high-resolution digital filming system, PHOTRON FASTCAM-ULTIMA APX-RS 250K MONOCHROME, was also employed to analyze the chip shape (segmented or serrated, continuous) and chip formation.



Figure 50. Experimental setup of fundamental cutting test in finishing turning.

The test samples were made of circular steel bars. Tubes were made in one end with a wall thickness of 2 mm and different angles of circumference, see Figure 51. Considering the case study defined by CRF (gear hobbing), interrupted cutting with radial depth of cut of 10% in a 2 mm wall thickness tubes (34° of circumferential length of cutting) has been defined as the reference test. Additional test with different cutting lengths have been machined in order to analyze the influence of this parameter on temperatures.

All tests have been carried out 3 times to estimate the uncertainty and ascertain the repeatability of the test.



Figure 51. Workpiece specimen for interrupted orthogonal cutting in steel without heat treatment and cutting tool inserts.

The cutting tools APFT1604P from Alesa were used throughout the tests. These tools are made of PVD HSS, same as the tools for the experimental hob milling. The motivation of using these tools is to replicate both the material composite of gear hobs with respect to the tool material and the characteristics of the cutting edges. The cutting speeds investigated were 50, 75 and 100 m/min. The circumference angles tested were 10, 34, 45, 90 and 360, i.e. continuous cutting.

The following variables were recorded during the tests:

- Tool's temperature
- Cutting and Feed forces
- Chip thickness
- Tool -Chip contact length.

Major difficulties and comments:

Temperature: When the tool is cutting the temperature increases rapidly, and when it is cutting the air cools (see Figure 52). The camera records the radiation coming from the tool during the whole process, however, in order to have good lectures of temperature during the cutting, and integration time of 200 μ s was been selected, and this implies an underexposure in the frames during cooling, being very difficult to have an accurate measurement of the temperature jump. By increasing the integration time during data acquisition it will be possible to measure correctly the temperature during the cooling, but it will imply a decrease of the rate frame acquisition, and therefore of the number of IR pictures during the cutting. It means that the measured quantitative increase in temperature when passing from cutting in the air to cut in the material has an error.

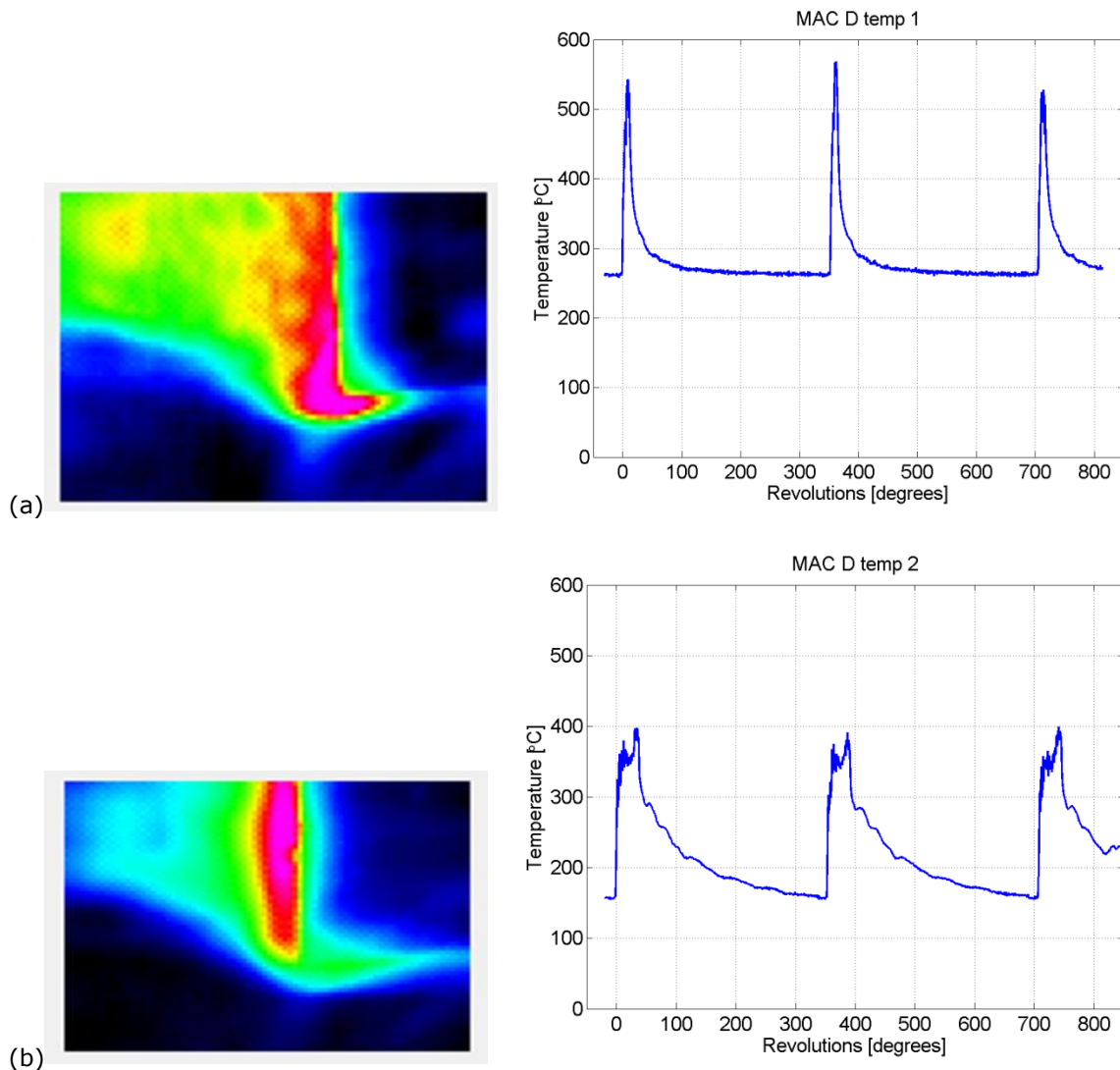


Figure 52. Temperature measurement for two of performed test. (a) 10° and 75 m min^{-1} and (b) 34° and 100 m min^{-1} .

Results:

Temperature:

The true temperature T , can be estimated from Radiation Temperature (RT) using emissivity, ϵ , of the tool. The emissivity ϵ , of the tool was measured in vacuum using a FTIR for the HSS tool, at different wavelengths between 3.96 and $4.01 \mu\text{m}$ at the corresponding radiance temperature. For the range of values of RT obtained in the experimental tests, the emissivity has been estimated to be 0.20 - 0.21 .

In all figures, plotted temperature is the maximum temperature reached in the rake face of the tool during the cutting; the error bar corresponds to the double of the standard deviation obtained for these values taking into account the three repetition test.

Blue squares in Figure 53 shows the tool temperature depending on the angle of material that is cut. As it was expected, it is observed that when angle of material cut increases the temperature increases as well. The steel is C-IA, the Cutting Speed is 75 m/min and the feed rate is 0.2 mm/rev .

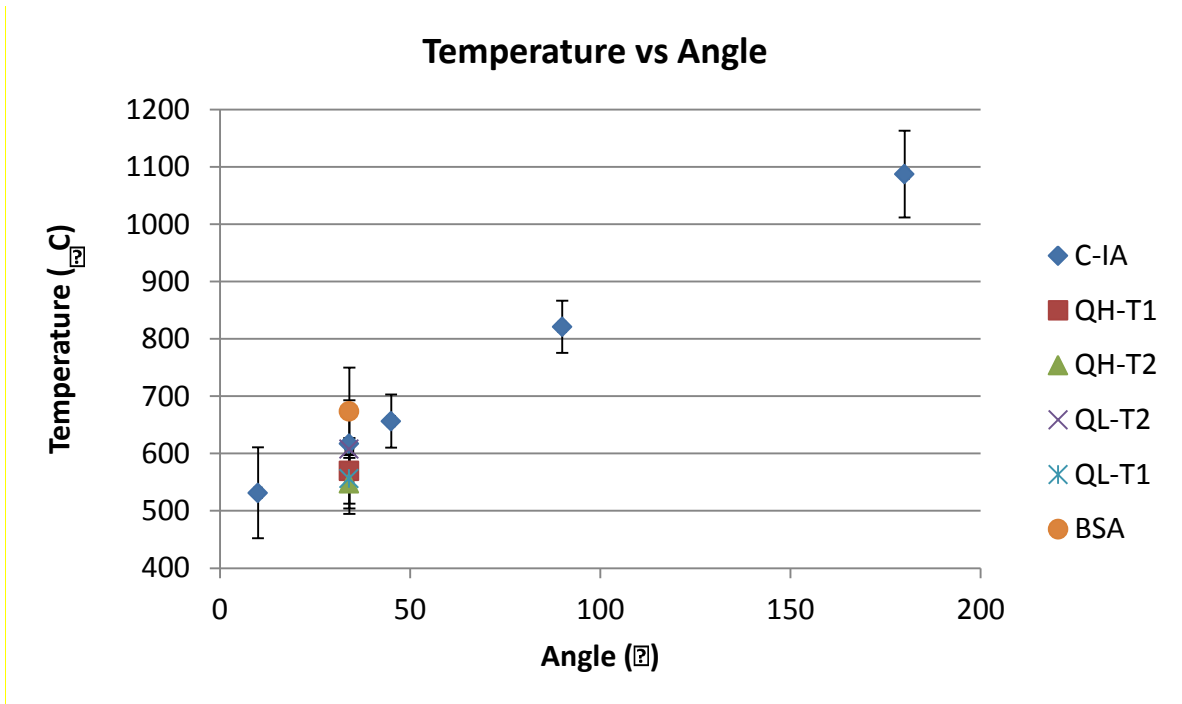


Figure 53. Radiation Temperature depending on the angle of material cut (for C-IA steel) and the Temperature depending on the steel for a given angle for material cut (34°). Cutting Speed: 75 m/min; $f = 0.2$ mm/rev

Figure 53 shows as well the Temperature depending on the steel for a given angle for material cut (34°) (Cutting Speed is 75 m/min and the feed rate is 0.2 mm/rev). However, in order to analyze temperature vs. material, Figure 54 shows tool Temperature when (angle = 34°, $v_c = 75$ m/min and $f = 0.2$ mm).

Surprisingly there is not direct relationship between the hardness and the temperature, and it is observed that as the hardness increases the temperature doesn't follow this trend. For instance, C-IA steel is the softest but has not the lowest temperature, neither the highest. QH-T1 steel is the hardest and has not the smallest temperature. Other parameters will be more significant than hardness.

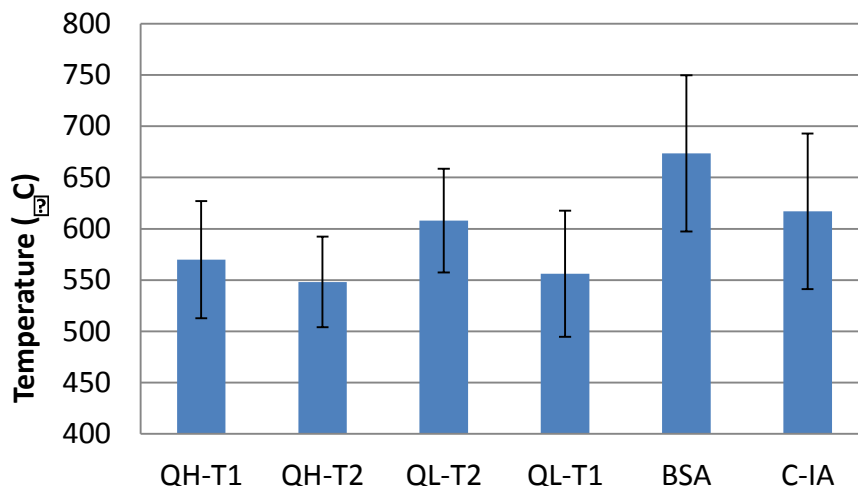


Figure 54. RT vs Material in hardness decreasing order.

Figure 55 shows Temperature depending on the cutting speed for two steels C-IA and QH-T1 for a given angle of material (34°) (the feed rate is 0.2 mm/rev). Again it is observed that there is not direct relationship between the hardness and the temperature: Temperatures in C-IA steels are not lower than in QH-T1 steel.

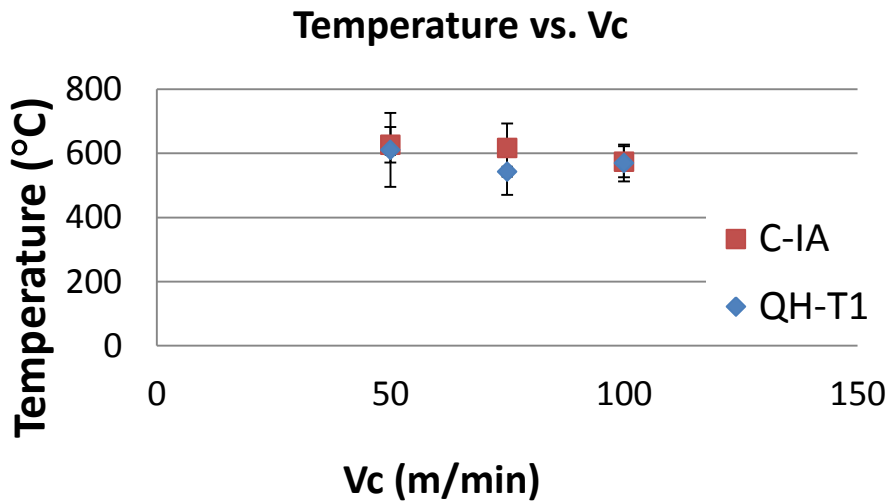


Figure 55. T vs V_c for two different materials C-IA and QH-T1

Figure 56 show the specific forces vs. interrupted angle for these working conditions:

- $v_c = 75$ m/min
- Material : C-IA

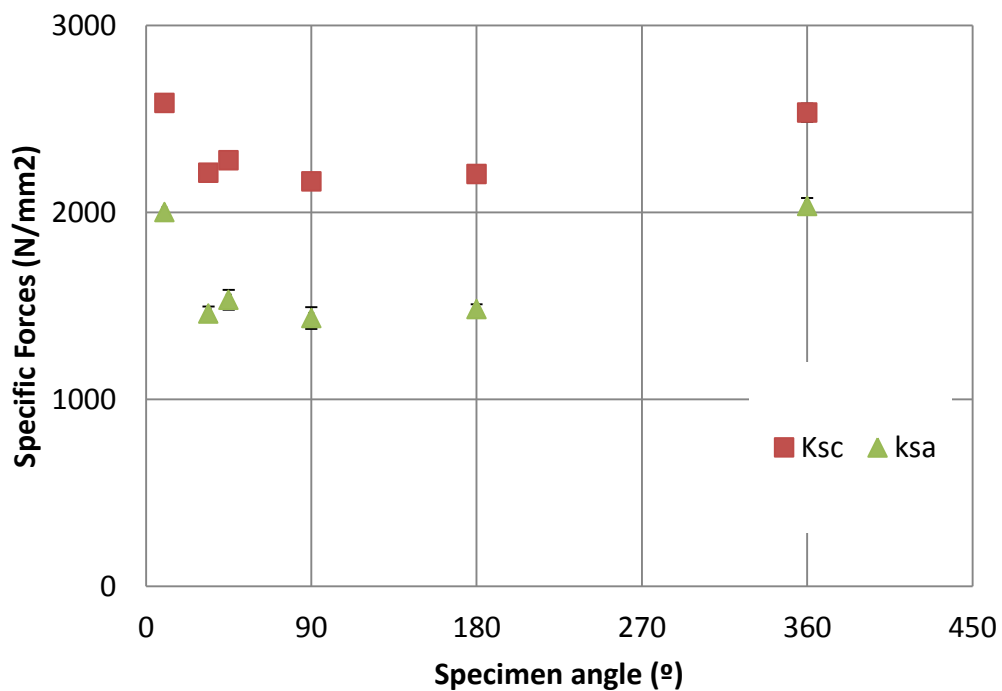


Figure 56. Specific Forces vs interrupted angle.

Figure 57 show the specific forces depending on cutting speed, for an engagement angle of 34° and tow materials (C-IA & QH-T1). It is observed that when cutting speed increases the specific forces decreases.

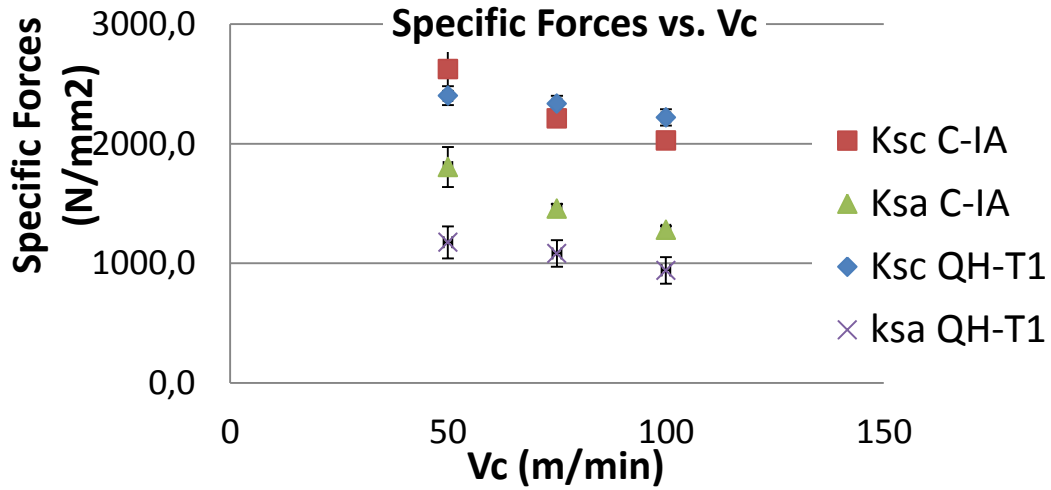


Figure 57. Specific Forces vs cutting speed.

Figure 58 show the specific forces depending on the workpiece material for an engagement angle of 34° and a cutting speed of 75m/min.

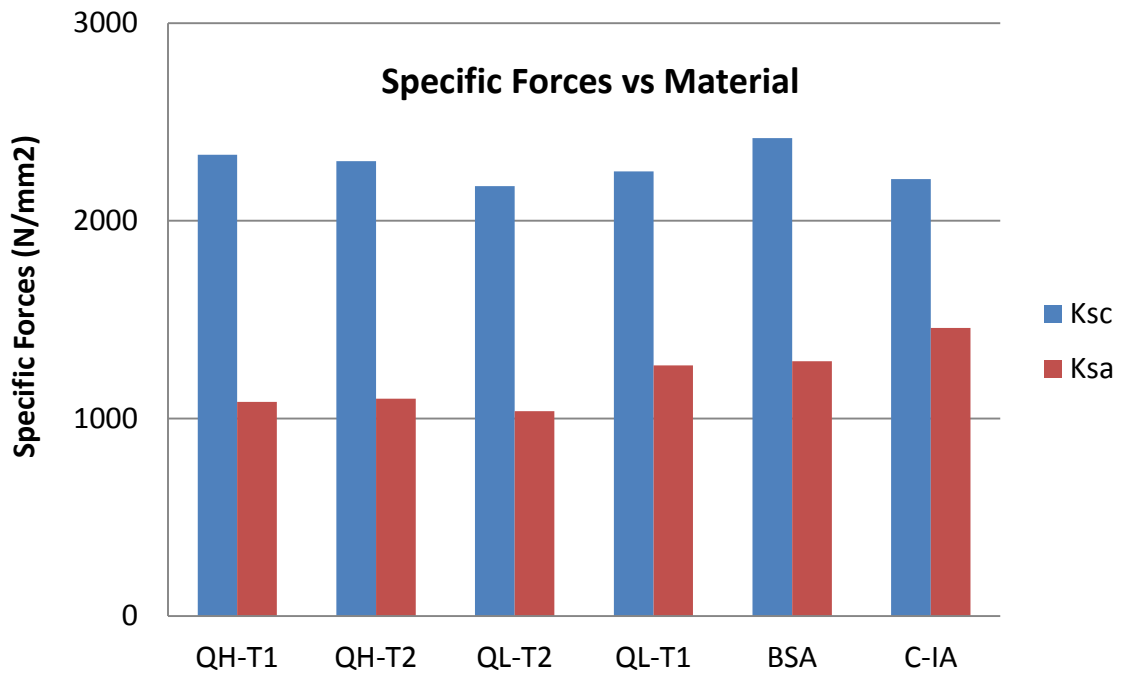


Figure 58. Specific Forces vs material.

Table 15 : Summary of more relevant results (engagement angle 34 °, Cutting speed of 75 m/min, feed rate of 0.2 mm).

Material (Hardness)	Tool-life Ranking v15	Hard. HB	Kc N/mm ²	Kf N/mm ²	Temp. (°C)	Contact Length (mm)	Chip Thickness (%)
C-IA	425.0	157	211.3	557.5	617.0	0.68	246.0
QL-T1	250.0	240	249.6	368.2	556.2	0.60	184.0
QH-T2	225.0	287	301.6	199.5	548.1	0.41	138.0
QH-T1	220.0	345	334.4	183.3	557.4	0.43	153.0
QL-T2	190.0	350	175.4	136.3	608.0	0.62	153.0
BSA	-	200	211.3	557.5	617.0	0.67	246.0

Discussion

Forces and Temperature values are affected by: Working conditions, Material hardness and as well tool-chip contact length. All data obtained in the fundamental cutting tests is summarized in Figure 59.

- The results show a relatively good correlation between tool life (V15) and specific feed force (Ksa). Except for the BSA (200Hb) steel, where tool life data is not provided,.
- Except for the BSA (200Hb) steel, there is a good correlation between the specific cutting force and the material hardness.

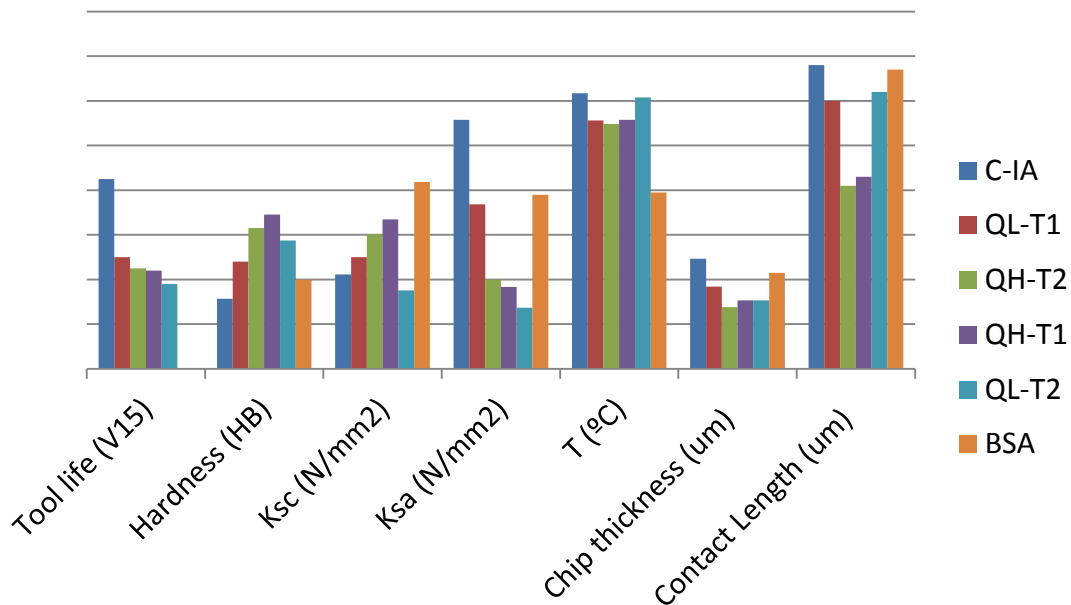


Figure 59. Qualitative comparison of results between the tested steels in the fundamental cutting tests.

- Although BSA (200Hb) steel is one of the softest ones, the remarkable higher chip thickness compared to other ones, generates the second value in the ranking of cutting force.
- In the same way, although C-IA (160Hb) and BSA (200Hb) steels are the softest ones, they generate the higher and the second higher feed forces respectively. This can be due to the higher chip thickness and tool-chip contact length.
- The higher temperature values of the two softer materials can be linked as well to the higher tool-chip contact length.
- The higher cutting force and feed force of the QH-T1 steels compared to the QH-T2 steel, is due to the higher value of the hardness. Both steels have a similar chip thickness value.
- The higher cutting force and feed force of the QL-T1 steels compared to the QL-T2 steel, is due to the higher value of the chip thickness which counterbalance the higher hardness of the later.

Conclusions:

The main conclusions obtained after the experimental tests are the following:

- When the cutting speed increase the specific cutting and feed force decrease, and the tool temperature increases.
- When the feed rate increase the specific cutting and feed force decrease, and the tool temperature increases.
- The softer materials generate the highest feed force, chip thickness and tool chip contact length.
- Except for the BSA (200Hb) steel, where tool life data is not provided, there is a good correlation between tool life and specific feed force, and thus to the chip thickness and tool chip contact length as well. This can be linked to the higher friction energy generated.
- Perhaps, the main conclusion of all this research is that the hardness value or even the material data, it's not enough to predict the temperature and cutting forces, and of course tool life, and thus these considered key out parameters are not sufficient to differentiate two steels.

WP4: FINISHING HARD MACHINING

The objectives of WP4 are:

- Selection of cutting tools for finishing hard turning.
- Elucidation of white layer formation, in connection to the work piece materials tested, cp. Table 2.
- Elucidation of residual stress generation.
- Elucidation of the robustness of residual stress profile, connected to the progression of tool wear.

Task 4.1 Selection of cutting tools and conditions for finishing turning

The cutting tools of the tool life tests in WP4 are shown in Figure 60. The original idea of the project was to evaluate only CBN tools in hard part turning. However, since the actual hardness of the 35CrMo4 and 50CrMo4 steels was in the range 40-62 HRC, a carbide cutting tool was added. This is very useful, and adds lots of industrial relevance to the project.

SANDVIK
CNMG 12 04 08-KM 3215
Coated
Called CARBIDE

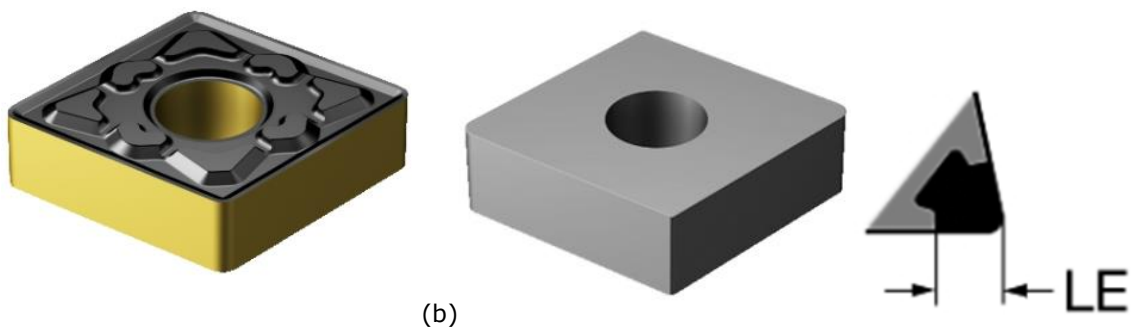
Typical and recommended cutting data:

$v_c=200-400$ m/min
 $f=0.15$ m/rev.
 $a_p=0.2$ mm

SANDVIK
CNGA 12 04 08 S01030A 7014
Uncoated
Called CBN

Typical and recommended cutting data:

$v_c=160-180$ m/min
 $f=0.15$ m/rev.
 $a_p=0.2$ mm



(a)

(b)

Figure 60. Cutting tools of tool life tests in WP4. (a) Cemented carbide GC3205 grade and (b) PCBN tool of grade CB7014 with mechanically locked edge of PCBN.

In order to perform the turning tests, the cutting parameters were suggested from a representative of Sandvik Coromant. For the finishing turning tests the tool life criteria were defined as follows:

- The surface finishing quality and the roughness limit of **0,8-1 micron**
- The limit of the insert flank wear accepted in production, representative of the insert tool life before the change during the manufacturing process, **$vb=250$ μm** .

In order to monitor the depth of the hardening treatment and the quality of the machining the following relieves with portable systems were executed in each sequence of cuts:

- the **roughness** is monitored in three points of the machinable length of the work piece.
- the **hardness** is monitored in three points of the machinable length of the work piece.

The supplied work pieces (80 mm x 500 mm) were prepared and cut in order to be appropriate to the gripping and the working length of the Hardinge lathe. They reached a workable length of 200 mm, see Figure 61. Three assessments of surface roughness were obtained on the work pieces.

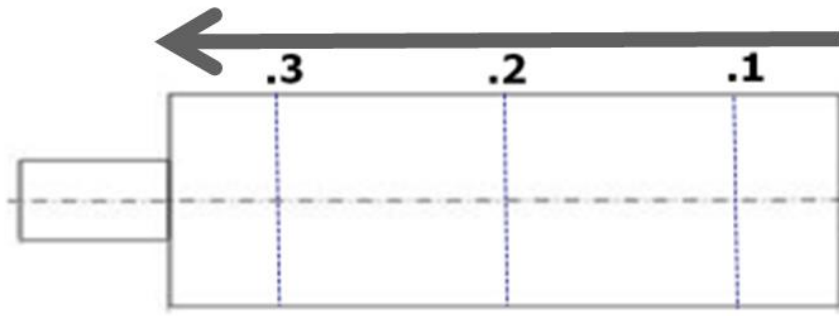


Figure 61. Representation of the machinable length of the billet and the positions of the point of the reliefs.

Task 4.2 Tool life tests in finishing turning

A summary of the tool life tests in hard part turning is given in Table 16. A photo of an ongoing tool life test in the Hardinge lathe is found in Figure 62. The cutting tools were frequently monitored during the tool life tests, to record the flank wear evolution, or other damages. An example of such LOM micrographs is found in Figure 63.

Table 16. Summary of the tool life tests in hard part turning at CRF.

Grade		Lathe	Insert type			N. cuts and repetitions	
			CC/ CBN	Vc	ap		F
C-H1	▲	HARDINGE	CC	240	0,2	0,15	40
QL-H1	●	COLCHESTER	CC	200	0,1	0,1	50; 50
QL-H1	●	COLCHESTER	CBN	240	0,1	0,1	15; 15; 15
QL-H2	●	HARDINGE	CC	200	0,2	0,1	18; 28;10; 35
QL-H2	●	HARDINGE	CBN	180	0,2	0,1	25;5;5;20;15
QL-H2	●	COLCHESTER	CC	200	0,1	0,1	35;40;55
QL-H2	●	COLCHESTER	CBN	180	0,2	0,15	10;10;10
QH-H1	■	COLCHESTER	CC	160	0,1	0,1	1 (fractured)
QH-H1	■	COLCHESTER	CC	240	0,15	0,2	1 (fractured) 1 (fractured)
QH-H1	■	COLCHESTER	CBN	240	0,15	0,2	9; 13; 10
QH-H2	■	HARDINGE	CC	240	0,2	0,15	5; 15
QH-H2	■	HARDINGE	CBN	240	0,2	0,15	17; 17
QH-H2	■	COLCHESTER	CBN	240	0,2	0,15	17
B-H1	◆	HARDINGE	CBN	200	0,1	0,15	7; 7; 7
B-H1	◆	COLCHESTER	CBN	200	0,1	0,15	16



Figure 62. Photo from tool life test in hard part turning with CBN cutting tool in the Hardinge lathe.

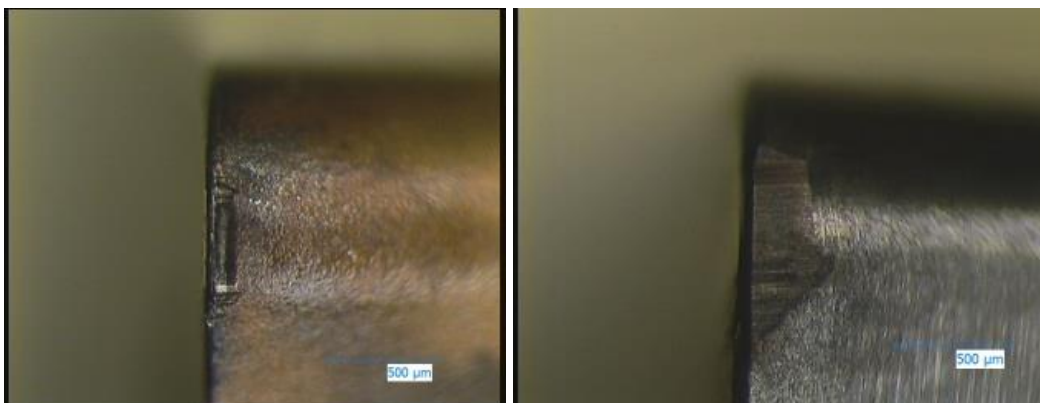


Figure 63. Micrographs of the flank side of used cutting tools from tool life tests of the QL-H1 steel. (a) CC cutting tool and (b) CBN cutting tool. (LOM)

The tool life tests in hard part turning are summarized in Figure 64.

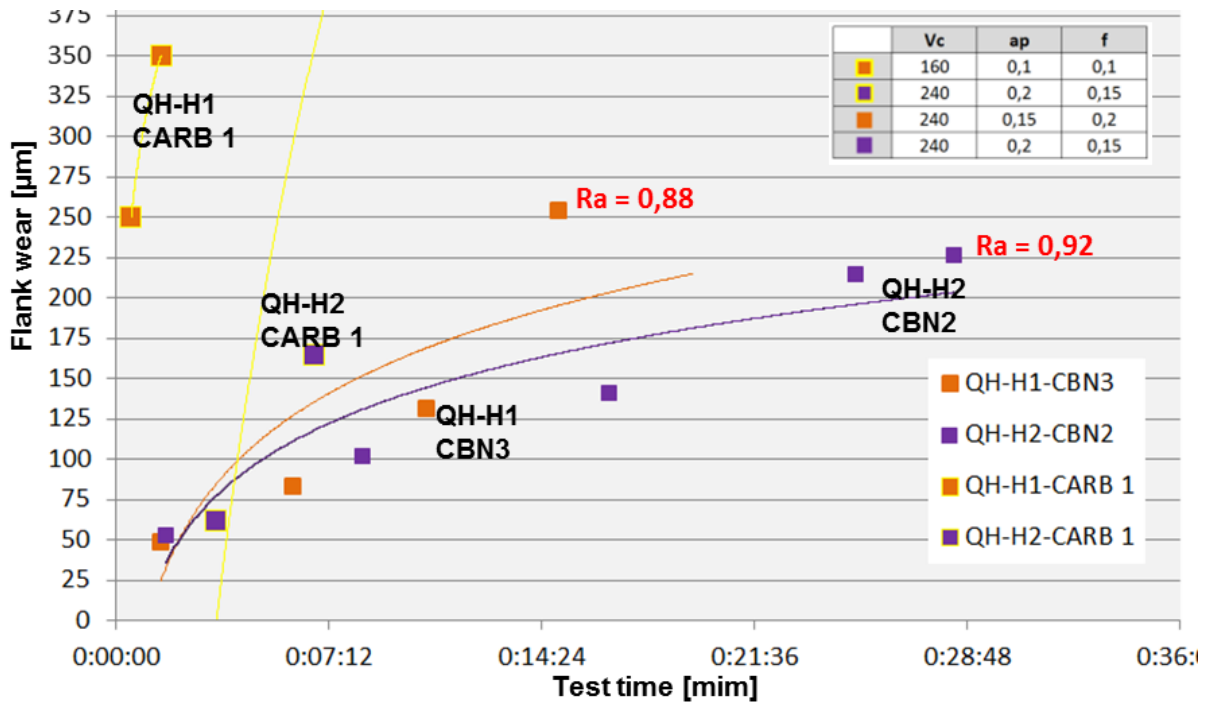


Figure 64. Summary of the tool life tests in hard part turning of the QH-H1 and QH-H2 materials.

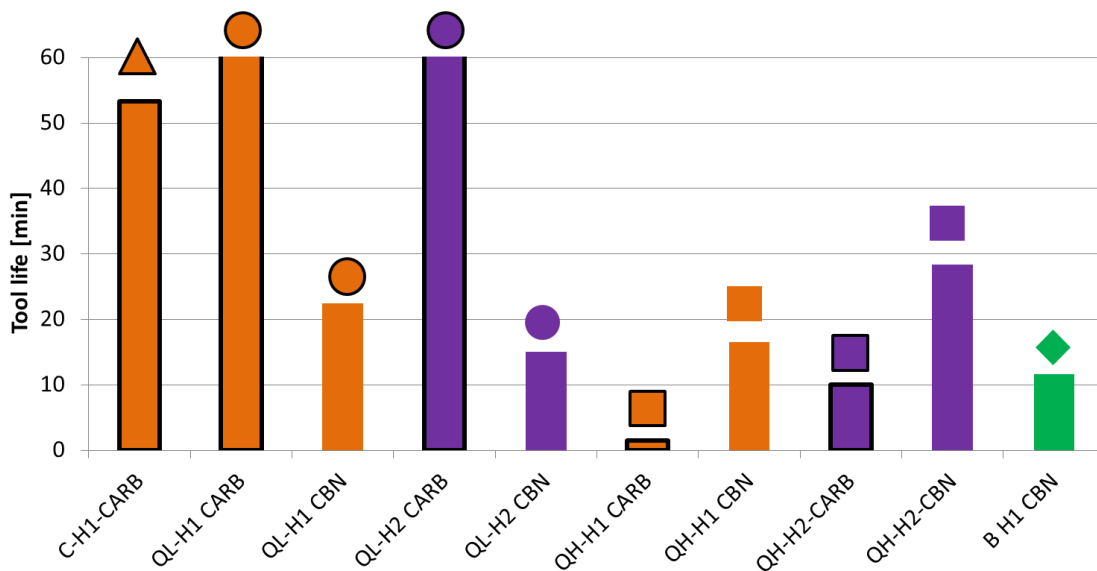


Figure 65. Bar chart of tool life tests in hard part turning. Bars from tests with carbide tools are given with black edges.

Preliminary conclusions from the tool life tests

- The carbide insert is the preferred one for finishing 35CrM04 in each treatment. The CBN insert, instead, causes a temperature increase on the material with consequent roughness increase.

- CBN insert is preferred for machining 50CrMo4 and 100Cr6, while the carbide insert reaches high wear very quickly, due also to the high hardness. For the QH-H1 speed and feed were decreased, obtaining the same results.
- 50CrMo4 in the H2 treatment had longer tool life than the H1 treatment. This is probably linked to the lower hardness of the H2 treatment.
- Focusing on QH, it can be observed that CBN has a longer life compared to the CARBIDE performances. Though, the actual hardness is very important for the tool life of both CC and PCBN cutting tools, as well as for the ranges of possible cutting speeds.
- Comparing the workability for the C-H1 and the QH, the C-H1 hardness facilitates the machining with CARBIDE. On the other hand the CARBIDE shows a limited performance on QH in both H1 and H2, although it is coated. Despite the high wear the roughness is according to the roughness limits.
- The CBN behaves better machining the QH-H2 than the QH-H1 (the QH-H1 billet were treated by induction hardening reaching 58HRC). The material conditions are very challenging in terms of hardness.
- At last, at the same cutting conditions, comparing C-H1 and QH, the life of the CBN insert is halved for the H2. Due to the high level of hardness, the CBN insert life for the H1 is reduced to 28%.

Task 4.3 Tool wear study in finishing turning

The tool wear study followed the original idea of the project, to evaluate the productivity of PCBN cutting tools in hard part turning. The cutting tools used were the Coromant CNGA 120408 CB7014, S010030, same batch as other hard part turning tests in MAC D. The cutting data followed the tool life tests:

- ⇒ $a_p=0.2$ mm
- ⇒ $f=0.15$ mm
- ⇒ $v_c=160$ m/min

Two the test times were used, 180 s (3 min) and 720 s (12 min). The aim was to have the same cut chip length in a comparison between the materials tested. All six hardened steels of the project were tested. The industrial interest of the tests was foremost the comparison of B-H (62 HRC) and the QH-H1 (58 HRC). The B-H was included in the project as reference in hard part turning. However, in fact the actual reference should be the carburized 18CrMo4 steel. However, this was not tested in the tool wear study. A chart of all twelve PCBN cutting inserts tested is given in Figure 66. The 180 s tests are given in the two columns on the left. The 720 s tests are shown in the two columns to the right. The fastest progression of both flank and crater wear of the PCBN cutting tool was obtained with the B-H steel (ball bearing steel). This is expected, given previous experience. At 720 s (12 min) early edge chipping could be found, and the cutting edge has in fact reached its tool life. Some wear progression could be found also with the QH-H1 (58 HRC) at 720 s. The other steels showed only minor wear after the performed tool wear tests. Very minor wear was found after tests with the QL-H1 and QL-H2, and the C-H steels. They are the softest of the tested steels. However, there have been an old "truth" that low carbon steels, e.g. the C-H, would diffuse boron nitride in to the chips, deteriorating the PCBN cutting tool. This was not observed in these tests.

Preliminary conclusions:

- When it comes to rake face wear, hardness matters. It is clear that hardness of the steel is extremely important in the progression of wear on the rake face, i.e. crater wear, and for tool life in hard part turning using PCBN cutting tools.
- When it comes to flank wear, the same ranking as above still holds. Though also with the C-H (23 HRC), a flank wear of 30-50 μm was found. This is probably a limitation in the actual performance of a CBN cutting tool in machining of a relatively soft work piece material, and the region of cutting data where the CC cutting tools have a better production economy.
- The ranking of the materials is relatively expected.
- No effect of the current experience of soft (or low carbon) steels " eating" the PCBN structure, i.e. chemical dissolution of PCBN in soft /low carbon steels).

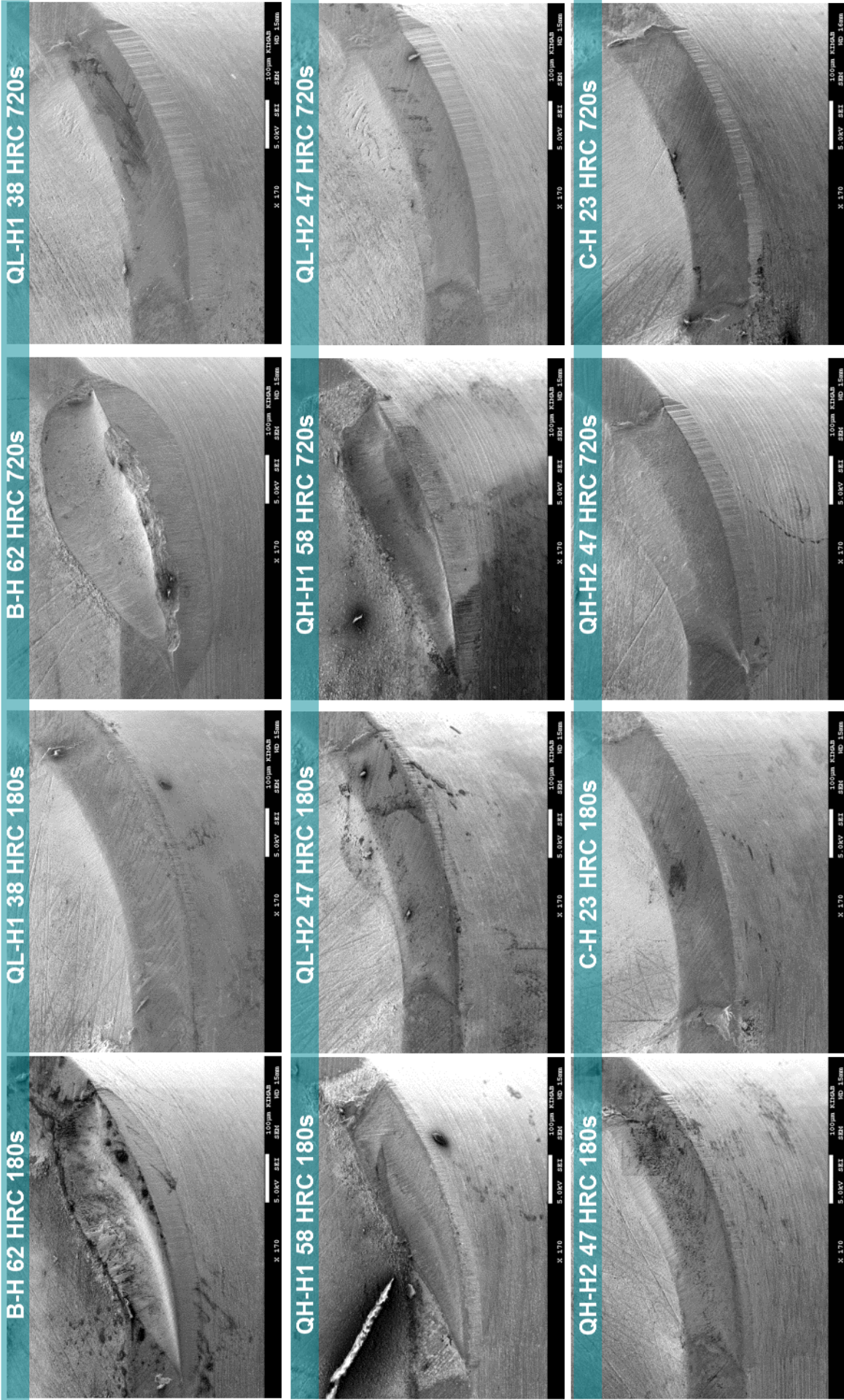


Figure 66. Chart of SEM micrographs of the used CBN cutting tools in the tool wear study.

Task 4.4 Rim zone analysis of the finish turned induction hardened work piece

Motivation

AIM: To understand how the rim zone of induction hardened steels is influenced by varying the cutting parameters, e.g. cutting edge geometry, cutting data and tool wear.

Experimental Setup

External dry turning tests were conducted on a MONFORTS RNC 400 plus lathe. PCBN is the most suitable tool grade for turning high quality surfaces of case hardened steels (58-65 HRC). For the rim zone analysis the uncoated CBN Grade CB7014 from Sandvik was used. The insert has two solid CBN corners mechanically interlocked and brazed to the base body. In addition, tool life tests with cemented carbide were conducted.

For the PCBN tool life tests were conducted with a cutting speed of $v_c = 160$ m/min, a feed of $f = 0.08$ mm and a depth of cut of $a_p = 0.2$ mm. These are typical process parameters for fine machining of case hardened steels as they are used at CRF, the research center of Fiat Powertrain and recommended by Sandvik. For the carbide tools tool life tests were conducted as well with a reduced cutting speed of $v_c = 40$ m/min and $v_c = 80$ m/min. The investigated steel bars were split into two parts. One part was used to wear the insert and the second part was used to manufacture samples for cross sections, as illustrated in Figure 67. During the tool wear tests at predefined stages samples of the rim zone were prepared. In this way the tool wear was evaluated with respect on the influence to peripheral rim zone. In addition cutting force, surface roughness and temperatures were measured to evaluate the machinability of the different steel grades.

For a selected set of materials the rim zone was analyzed in detail:

- Cross-sections of the rim zone to detect white layer formation were created.
- Micro-hardness measurements for all steel grades were conducted.
- Residual stress analyses for the induction hardened steel grade were carried out.
- Surface roughness during the tool life tests was measured and rated.

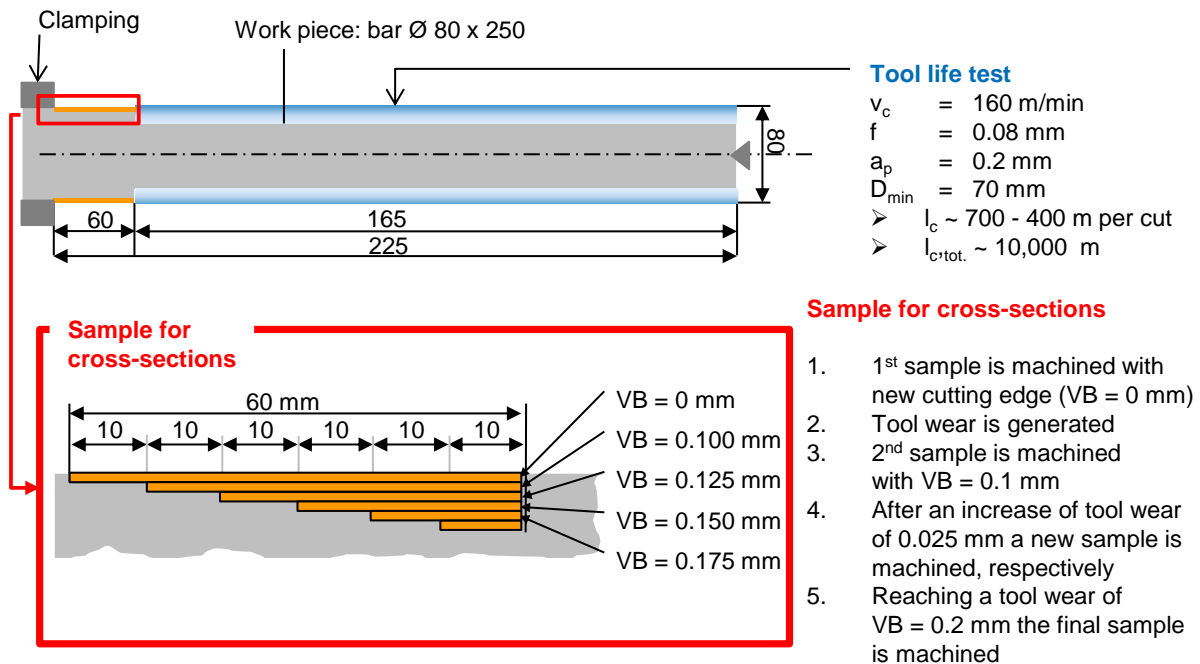


Figure 67. Test setup for rime zone analysis

Figure 68 shows the tool life graphs for machining QH-H1 (50CrMo4) with CBN and cemented carbide. The maximum tool wear is plotted over path length due to primary motion. Best performance was shown by the CBN tools, which enabled a path length due to primary motion of $l_c = 10,000$ m. Only a path length due to primary motion of $l_c = 1,320$ m was achieved with the carbide tool by using the same cutting condition like the CBN tool. A reduction of the cutting speed to $v_c = 40$ m/min leads to an increase of tool life to $l_c = 8,351$ m. Note however, that this reduction of the cutting speed results in a four times higher processing time.

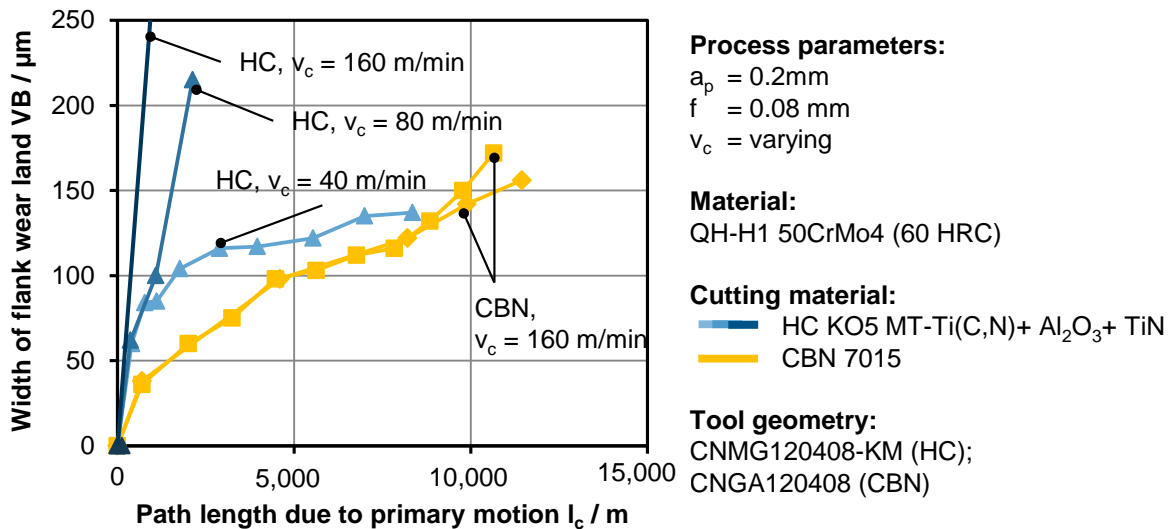


Figure 68. Tool life graph for QH-H1 (50CrMo4) 58 HRC.

The roughness value R_z was in the required tolerances for both carbide and CBN tools. Herein the CBN tool showed better roughness values at high cutting path length than the carbide tool did. This can be attributed to the slower and more uniform tool wear development of the CBN tool.

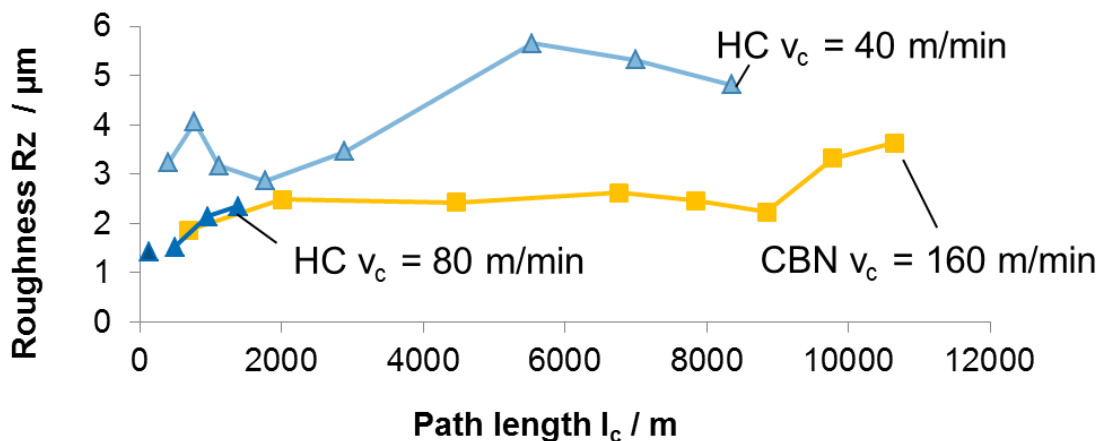


Figure 69. Roughness (R_z) after fine machining QH-H1 (50CrMo4) @ 58 HRC.

Temperature and Force measurements

For temperature measurement in turning processes a two-colour pyrometer of type Fire II was used. Two-colour pyrometers are used to measure a temperature of a surface by emitted infrared radiation. The infrared radiation is received by a non-contacting flexible quartz fiber and is guided to photodiodes. By measuring the intensity of radiation in two discrete, closely adjacent wavelength bands $\Delta\lambda_1$ and $\Delta\lambda_2$, which are in relation to each other, the measurement is independent of the emissivity of the emitting surface. Compared to other measurement methods, the 2-color pyrometer is also characterized by its very high temporal resolution of about 2 μ s, its large temperature measuring range of 250°C to 1200°C and its insensitivity to external influences. Due to the flexible application possibilities and the high thermal stability of only about 0.2 - 0.5 mm thick quartz fiber this method has been successfully used in machining to measure temperatures close to the zone of chip formation. Holes were EDMed in the cutting tools. One was a blind hole just underneath the rake face (P1). Another was an open hole on the flank face (P2) The principle of the two color pyrometer is illustrated in Figure 70. The advantage of a blind hole is the long term use. The drawback is the somewhat slow temperature response. An open hole frequently clogs after a short time.

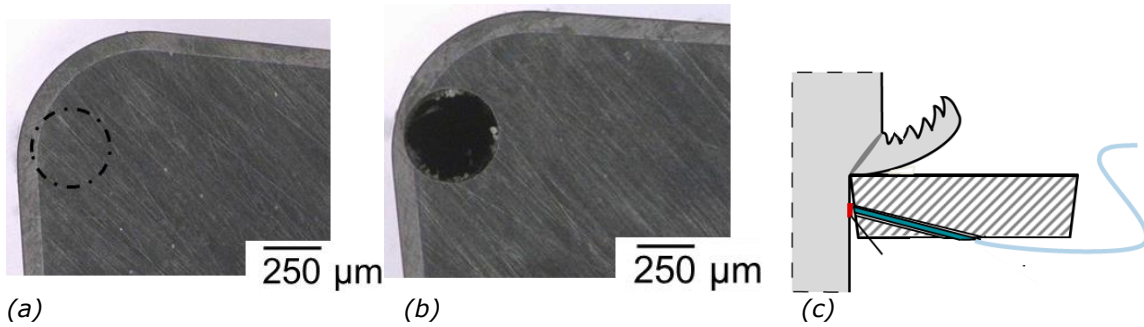


Figure 70. Fundamental investigations in tailored machining tests. The PCBN cutting tool rake face (a) as-received and (b) with EDM machined hole for optical fibre passage.

The measurements were done parallel to the tool wear test. In the lower left part of Figure 70 the position of through hole for temperature measurement under the chip is shown. Figure 71 shows the recorded temperature signal. A clear signal with low scattering was measured on the rake face. The waviness observed in (b) is believed to be linked to chip curling. The temperature on the work piece surface was $T = \sim 420\text{ }^{\circ}\text{C}$. All signals show scattering, because of the rays reflection, which can be explained by the impact of passing chips.

Figure 72 shows the development of the temperature and the cutting forces plotted against the tool path length. The temperature measured in the CBN tool increases from $T = 550^{\circ}\text{C}$ up to $T = 750^{\circ}\text{C}$. At the same time the cutting forces increase from $F_c = 130\text{ N}$ up to $\sim 200\text{ N}$. The feed force F_f increase less than $\Delta F_f = 20\text{ N}$ and the passive forces show no increase at all.

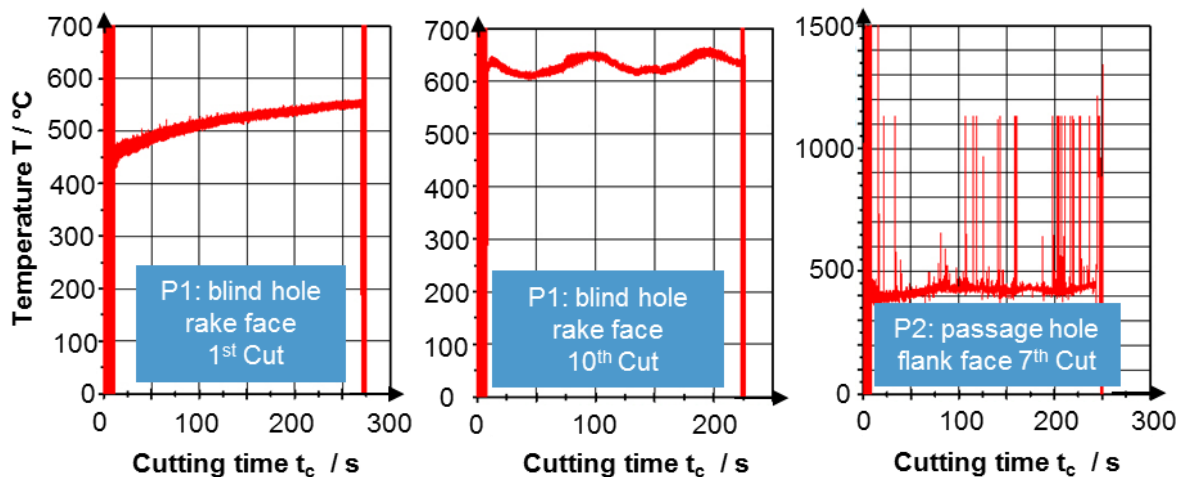


Figure 71. Temperature measurement signals

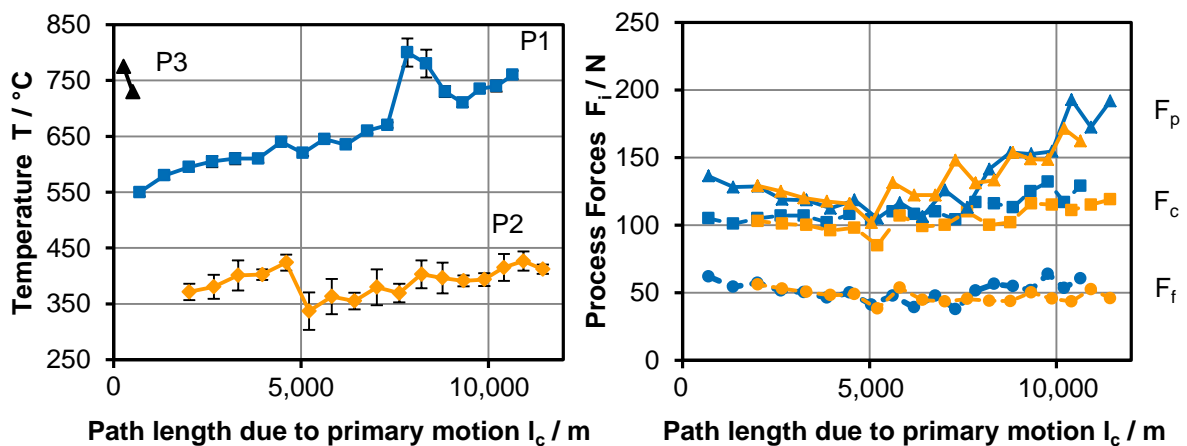


Figure 72. Temperature measurement signals.

Figure 73 shows the tool temperature. The corresponding (see ANNEX 4 **Figure 141** the cutting forces for all materials at the beginning of the test and at the tool life end. QL-H2 (35CrMo4) was

turned with a cutting speed of $v_c = 240$ m/min because of the better surface quality, even if this leads to a deterioration in the tool life. In all experiments increase of the temperature over the life time can be observed. The highest temperature increase is shown for QH-H1 (50CrMo4) and QH-H2 (50CrMo4). This can be explained with the longest tool life time in the tests. Nearly the same effect is shown for the forces in Figure 141. With increasing tool wear mainly the passive force F_p increased significantly. The increase in the feed force F_f and the cutting force F_c is relatively low.

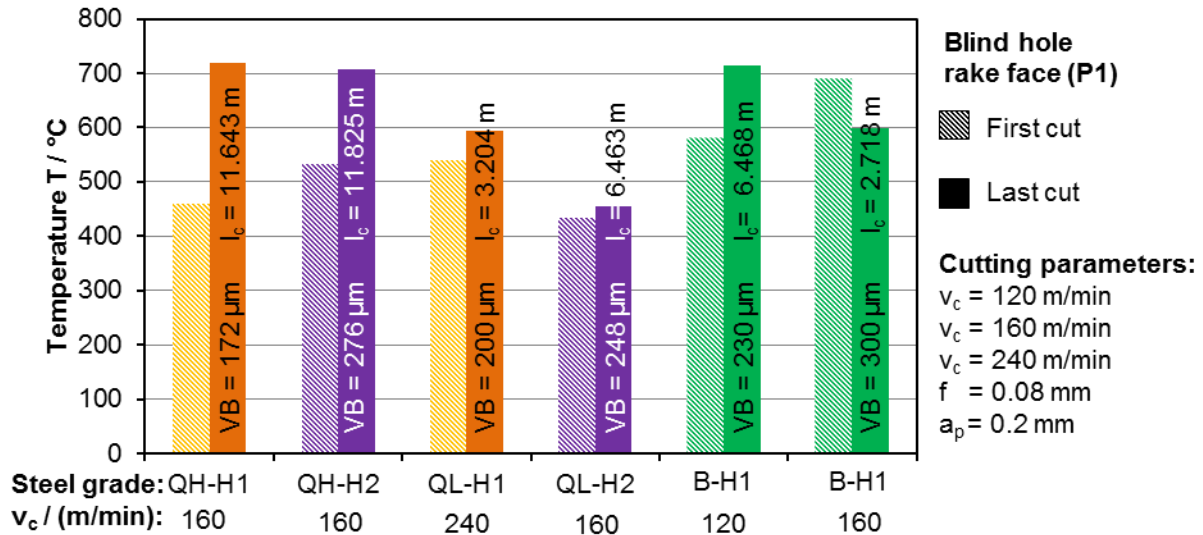


Figure 73. Temperature measurement signals at position P1 (Blind hole rake face)

Analysis of the Rim Zone

The metallographic sample preparation was carried out only for a selection of steels. Sections were made for the materials QH-H1, QH-H2 (both 50CrMo4), QL-H2 (35CrMo4), and B-H1 (100Cr6). No further investigations of the material QL-H1 were done in this study because of the low hardness (25 - 30 HRC). The thickness of the white layers was measured with a light microscope.

Longitudinal and transversal cross sections at pre-defined tool wear stages were done of the 50CrMo4 (QH-H1) steel machined with the CBN tool, shown in Figure 74. With increasing tool wear a white layer was observed. At the beginning of processing, after a cutting path of $l_c = 692$ m ($t_c = 4$ min) and a tool wear of $36 \mu\text{m}$, in the transverse section, a continuous white layer with a thickness of $d_l = 0.95 \mu\text{m}$ was already visible, compare Figure 75. At the end of the experiment, with a tool life $l_c = 10,643$ m ($t_c = 67$ min), the layer thickness in the longitudinal cut is about $d_l = 2.45 \mu\text{m}$, with a pronounced heat-affected zone in the transition to the prospective structure. In the transverse section, a closed white layer with a maximum thickness of $d_l = 3.6 \mu\text{m}$ was observed.

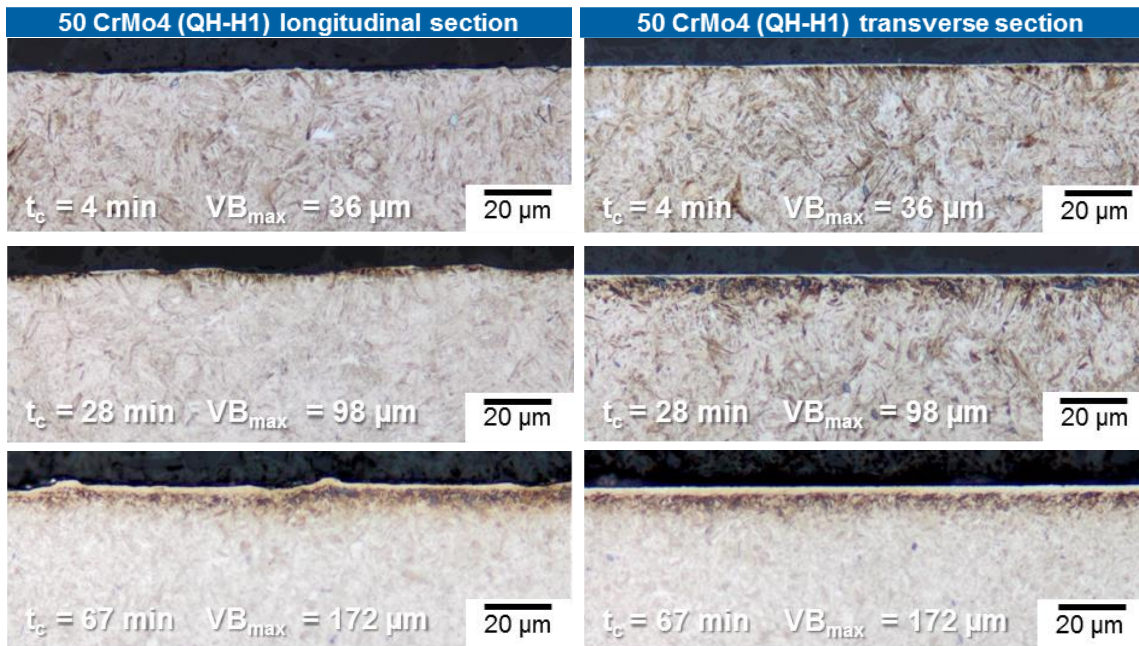


Figure 74. Development of white layer formation, QH-H1 (50CrMo4)

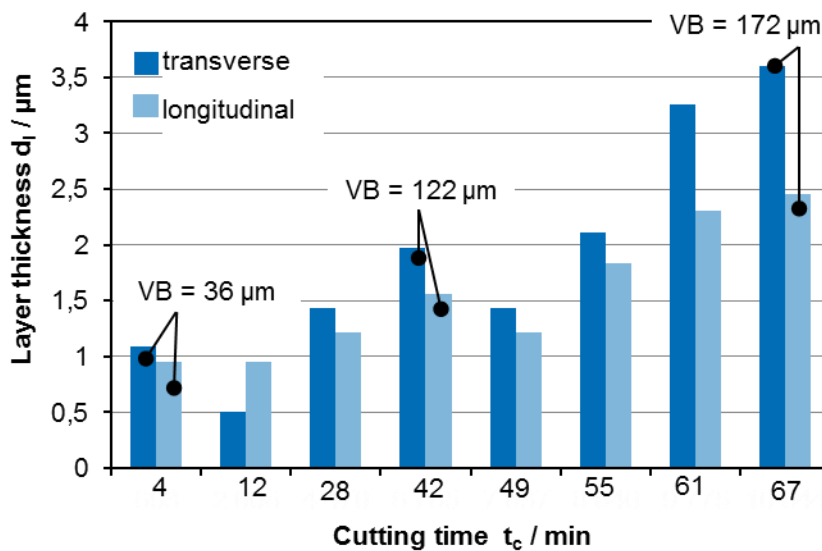


Figure 75. Development of white layer formation, QH-H1 (50CrMo4).

Comparing the cross sections of B-H1 (100Cr6) with the cross sections of QH-H1 less white layer thickness was observed, although B-H1 has a hardness of 55 HRC. One reason for this was the lower cutting speed of $v_c = 120$ m/min. A lower cutting speed is associated with a lower surface temperature, Figure 73. Metallographic cross sections of the steel B-H1 are shown in **Figure 146**. Cross sections and white layer developments of the steels QH-H2 and QL-L2 are documented in the appendix.

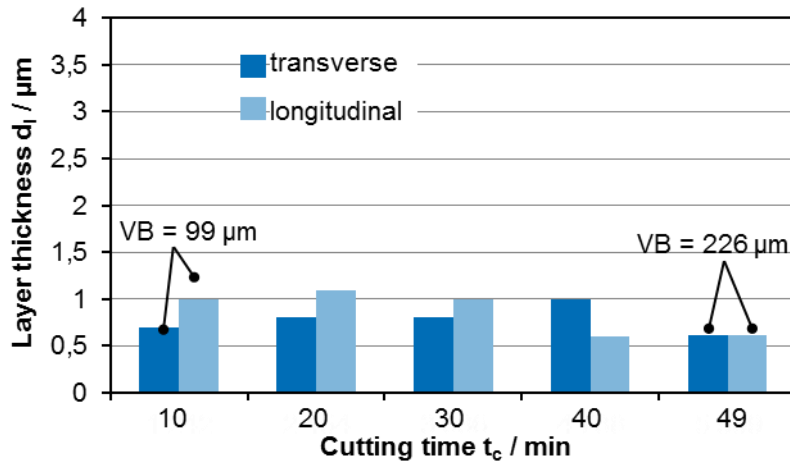
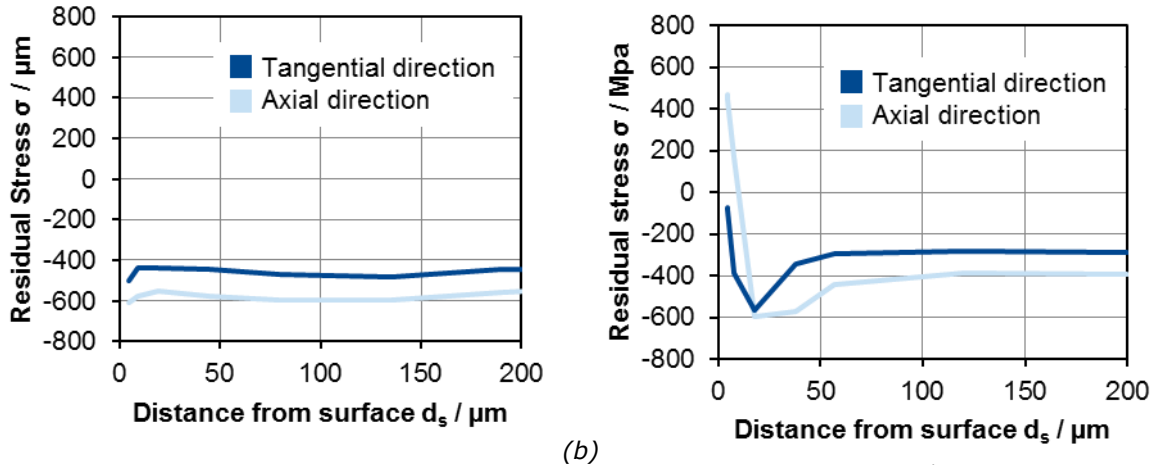


Figure 76. Development of white layer formation, B-H1 (100Cr6)

In addition to the cross sections the residual stresses of the induction hardened 50CrMo4 (QH-H1) was measured by the method of X-Ray diffraction on crystalline lattice. Figure 77 shows the residual stresses measured at an unprocessed work piece. This results in a state of compressive stresses of up to $\sigma = -600$ MPa over the entire measurement depth. This compressive stresses profile is a result of the inductive hardening process. For hardening sufficient temperatures exist only in the rim zone. Because of the temperature distribution at the surface region, a martensitic hardening zone results. The core region of the work piece is not hardened. Due to the volume difference between martensite and austenite the martensite is after quenching under compressive stresses, the austenite under tensile stresses.



(a) (b)
Figure 77. Residual stress profile, QH-H1 (50CrMo4, HRC59). (a) after the 16th cut and (b) stress on the surface.

The right side of Figure 77 shows the residual stresses measured after the first cut and after the last cut (Figure 78). After the first cut tensile stresses were measured from the surface to a depth of 18 μm in axial direction and low pressure stress in tangential direction. From a depth of 18 μm , the tensile stress in axial direction ($\varphi = 0^\circ$) turns into compressive stress. The resulting principal stresses (σ_1, σ_2) are also shown in Figure 78. The residual stress profile is also shown on the right side of Figure 78. Five measurements were made on work piece surface up to a depth of $d_s = 4.7$ μm . The residual stresses at the surface increases from the first to the last cut.

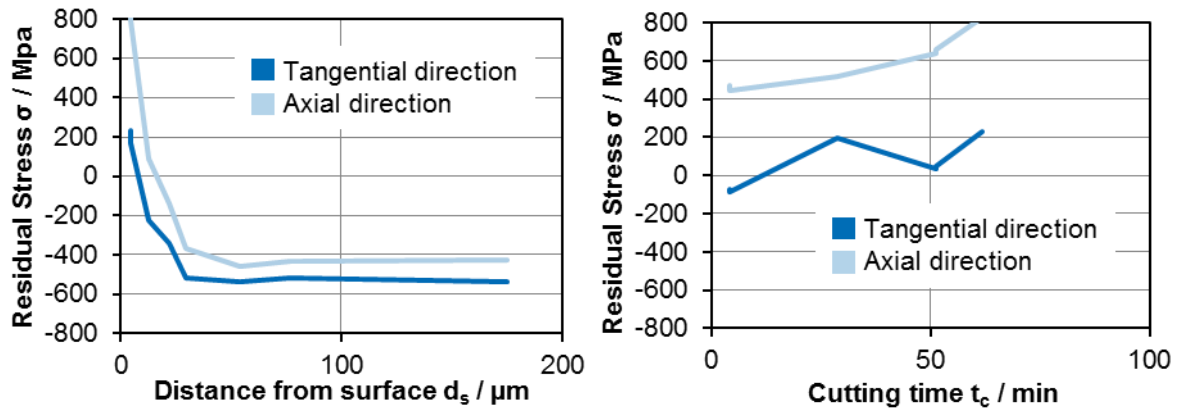


Figure 78. Residual stress profiles, QH-H1 (50CrMo4, HRC59). (a) after the 16th cut and (b) stress on the surface.

Results

- The induction hardened steel QH-H1 (HRC 59) show white layer formation after a tool wear of $VB = 116 \mu\text{m}$. The white layer increases continuously with the tool wear.
- Temperature measured under the rake face increases continuously from first cut to last cut from $T = 450 \text{ }^\circ\text{C}$ to $750 \text{ }^\circ\text{C}$. Cutting forces increase as well with the tool wear from $F_c = 140 \text{ N}$ to 200 N .
- The work piece surface shows residual stresses in cutting direction which increases continuously with the tool wear.
- In automotive industries case hardening can be substituted by induction hardening taking account to the machinability.
- With increasing tool wear a thicker white layer is detectable for all steels.
- The residual stress profile is nearly constant during complete tool life.

Conclusions

Hard machining operations with CBN-Tools and high cutting speeds result in white layer formation for all steels because of the thermos-mechanical load during the machining operation.

Task 4.5. Fundamental cutting tests in finishing turning

Tests have been carried out for different working conditions: work-piece materials, feed rate and cutting speed in order to analyze their influence on cutting forces, temperatures, chip shape and chip formation during finishing in continuous cutting in hardened steel. Specimens have been prepared in a multitask machine tool (Lathe). Considering the case study defined by CRF, continuous cutting in a 2 mm wall thickness tubes have been carried out, see Figure 79. The heat treatment of specimens has been subcontracted. Tests have been repeated 3 times to estimate uncertainty, see Figure 80.



Figure 79. Workpiece specimen for continuous orthogonal cutting of hardened steels and cutting tool inserts.



Figure 80. Workpiece specimens already prepared for different hardened steels.

Cutting conditions:

- Machining tool: CNGA120408 S010 CBN 7025 (Sandvik Coromant)
- Hardness of machined material: 24, 37, 46, 47, 54 and 62 HRC
- Cutting speed conditions, v_c : 100, 150, 200 m/min
- Feed: 0.06 and 0.15 mm/rev
- Thickness: not specified (2mm or less)

The complete test planning is given in Figure 81.

Task 4.5	Continuous (1,5 mm wall thickness) / Only one condition for Heat Treatment	Heat treatment (in MGEP)	Dry	VC	f	Rake angle	Insert tools	Tool Holder	Tool insert
18CrMo4+HT (Gerdau)	C-H1 (24HRC)	CIA + HT: T ^{aus} =900°C-4h+Q in oil and T ^{temper} =500°C-5h cooled in air	Finishing	100	0,06	Constant value	CBN Sandvik	STGCL 1616 H11	TGCW110204 S01020F7025
				150	0,06				
				200	0,06				
				100	0,1				
				150	0,1				
200	0,1								
QL-T1: 35CrMo4+HT (Gerdau)	QL-H2 (46HRC)	QL-T1 + HT1: T ^{aus} =900°C-4h+Q in oil and T ^{temper} =460°C-5h cooled in air	Finishing	150	0,1	Constant value	CBN Sandvik	STGCL 1616 H12	TGCW110204 S01020F7025
QL-T1: 35CrMo4+HT (Gerdau)	QL-H1 (37HRC)	QL-T1 + HT2: T ^{aus} =900°C-4h+Q in oil and T ^{temper} =180°C-5h cooled in air	Finishing	150	0,1	Constant value	CBN Sandvik	STGCL 1616 H13	TGCW110204 S01020F7025
QH-T2:50CrMo4+HT (Ovako)	QH-H1 (54 HRC) (Key case study)	QL-T2 + HT1: T ^{aus} =850°C-100min+Q in oil and T ^{temper} =180°C-180min cooled in air	Finishing	100	0,06	Constant value	CBN Sandvik	STGCL 1616 H14	TGCW110204 S01020F7025
				150	0,06				
				200	0,06				
				100	0,1				
				150	0,1				
200	0,1								
QH-T2:50CrMo4+HT (Ovako)	QH-H2 (47HRC)	QL-T2 + HT2: T ^{aus} =850°C-100min+Q in oil and T ^{temper} =400°C-180min cooled in air	Finishing	150	0,1	Constant value	CBN Sandvik	STGCL 1616 H15	TGCW110204 S01020F7025
100Cr6+HT(through hardened) (Ovako)	TH(62 HRC).	BSA + HT: T ^{aus} =860°C-100min+Q in oil and T ^{temper} =180°C-180min cooled in air	Finishing	100	0,06	Constant value	CBN Sandvik	STGCL 1616 H16	TGCW110204 S01020F7025
				150	0,06				
				200	0,06				
				100	0,1				
				150	0,1				
200	0,1								

Figure 81. Test planning of the fundamental cutting tests in finishing.

Preliminary results and comments:

The tool geometry:



Figure 82. Cutting edge geometry

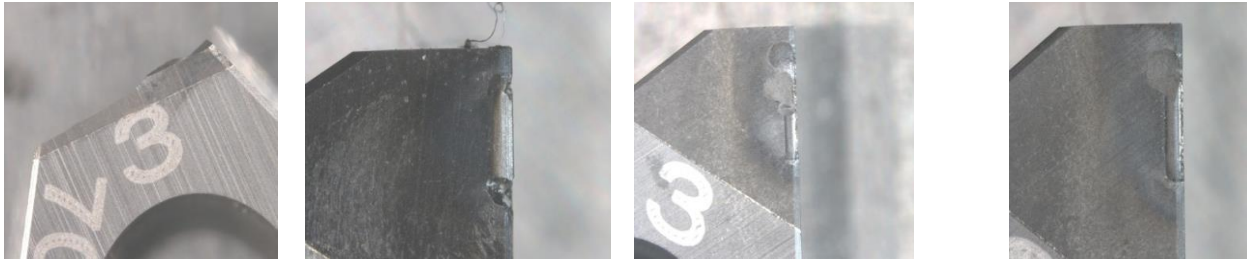
Edge chamfer → cutting mechanics: feed rate < 0.1 mm feed rate > 0.1mm

If thickness > 1mm → depth cut > 50% cutting edge length

If thickness < 1mm → risk of vibrations

Industrial conditions: Vc = 150,200 m/min; f=0.1, 0.15, thickness 0.2mm

Vcm/min	100			150			200		
f mm/vuelta	0,06	0,1	0,15	0,06	0,1	0,15	0,06	0,1	0,15
espesor de tubo									
2	ok		KO	ok			ok		
1,5		ok foto 2	KO					ok	KO
1			KO: Chot			KO			KO



Vc=100 f= 0.15

Vc=150 f= 0.15

Vc=200 f= 0.15

Figure 83. Failed of the cutting edge at feedrate of 0.15mm

Definitive Cutting conditions:

- Machining tool: CBN 7025 (Sandvik)
- Hardness of machined material: 24, 37, 46, 47, 54 and 62 HRc
- Vc conditions: 100, 150, 200 m/min
- Feed: 0.06 and 0.1 mm/rev
- Thickness: not specified (2mm or less)

RESULTS OF FUNDAMENTAL CUTTING TESTS

- When the cutting speed increases the Radiation Temperature increases
- When the feed rate increases the Radiation Temperature increases

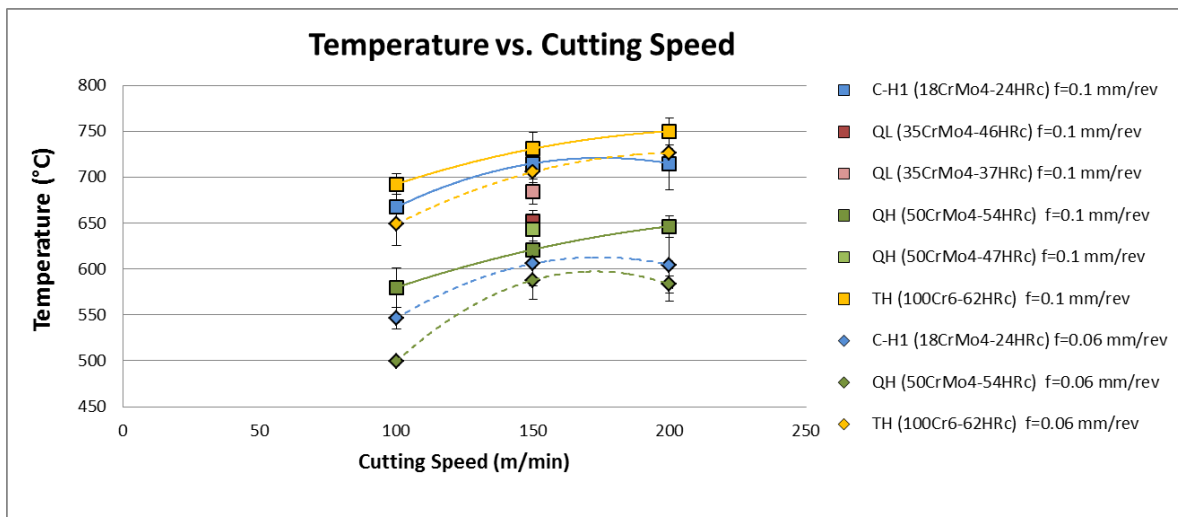


Figure 84. RT vs Cutting speed for different materials and feed rate

- Not always when hardness increases the Radiation Temperature decreases

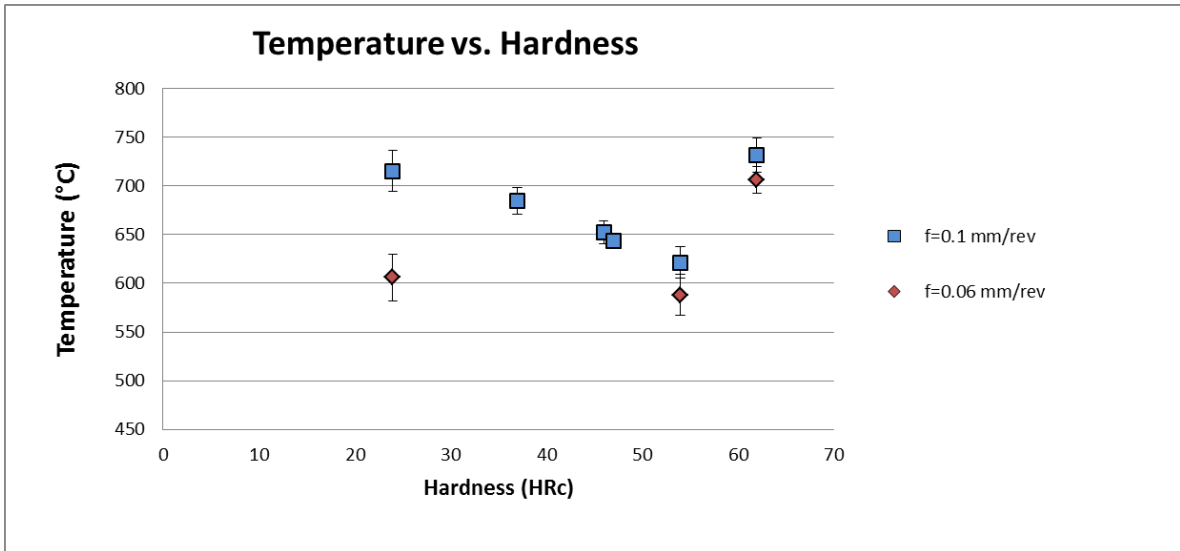


Figure 85. RT vs hardness for two different feed-rates

- When the cutting speed increases the cutting forces decreases
- When the federate increases the cutting forces increases.

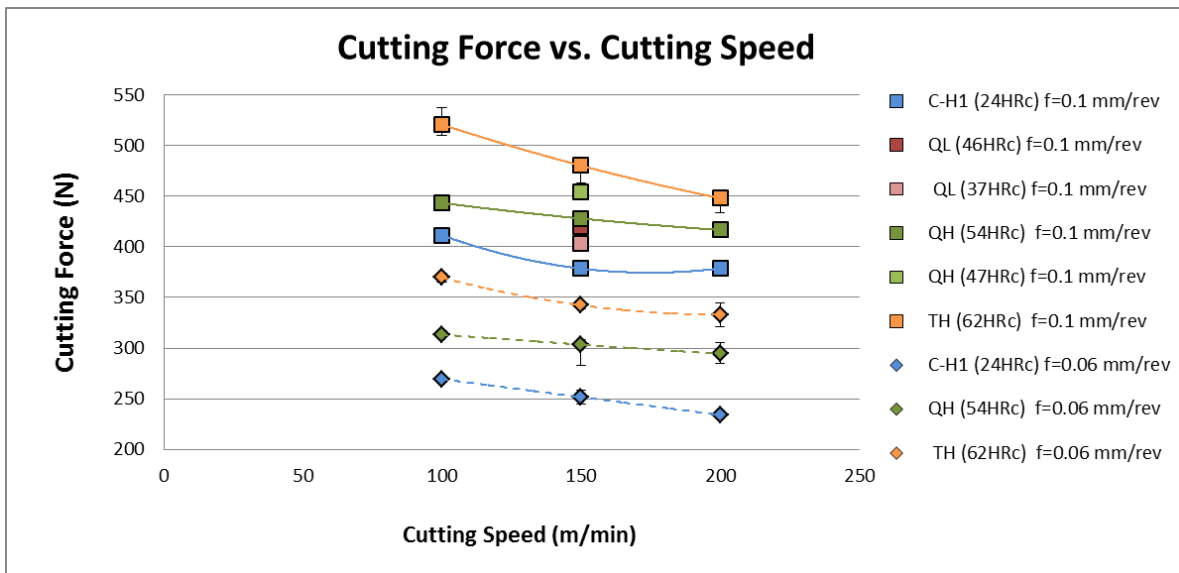


Figure 86. Cutting force vs Cutting speed

- When the cutting speed increases the specific cutting forces decreases
- When the federate increases the specific cutting forces decreases.

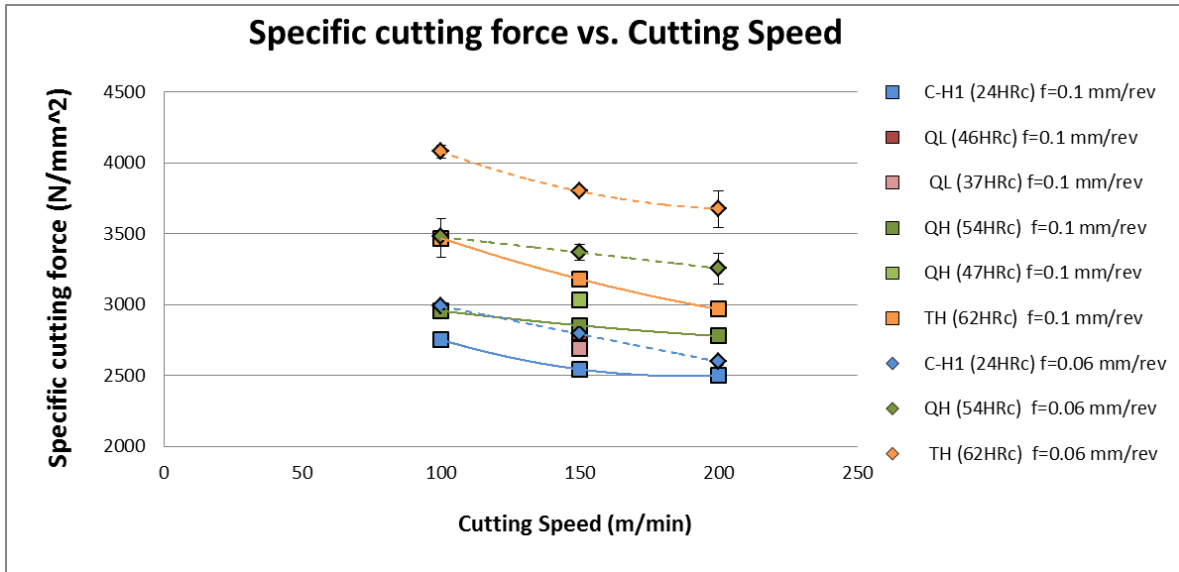


Figure 87. Specific cutting force vs Cutting speed

- When the cutting speed increases the feed forces decreases
- When the feed rate increases the feed forces increases
- In general as the hardness increases the feed force increases

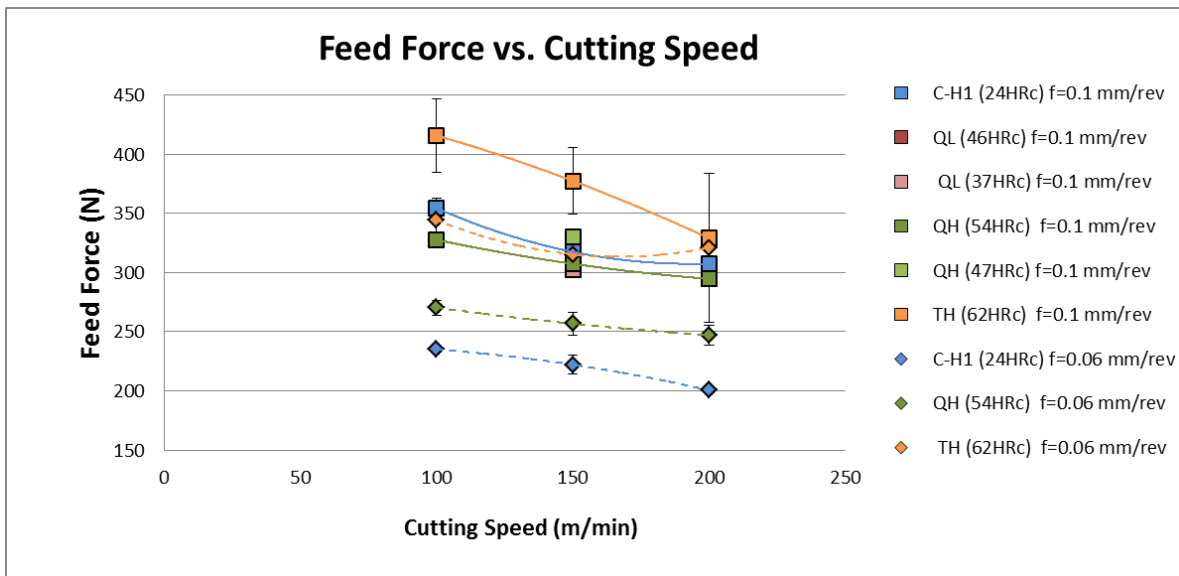


Figure 88. Feed force vs Cutting speed

- When the cutting speed increases the specific feed force decreases
- When the feed rate increases the specific feed force decreases

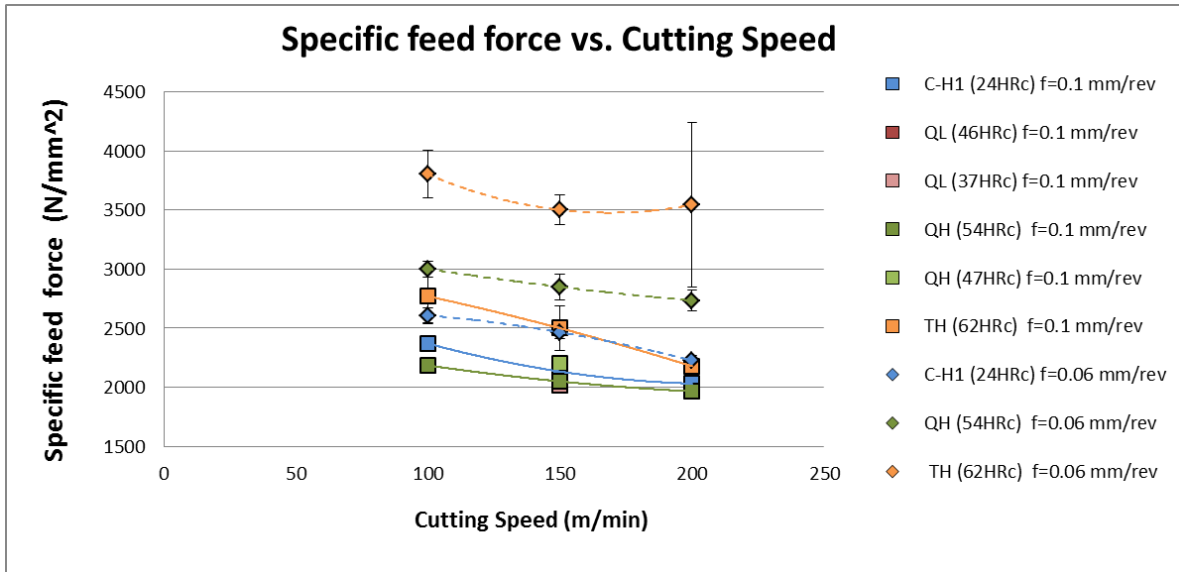


Figure 89. Specific Feed force vs Cutting speed

- Specific tangential cutting force and feed cutting force evolution for different materials at 150 m/min cutting speed and 0.1mm feed
- No direct relationship between hardness and specific cutting forces

Material	Steel Hardness	Kst	Ksf	Kst sigma	Ksf sigma
1	C-H1 (24HRc)	2543	2133	48	34
2	QL-H2 (46HRc)	2801	2050	26	28
3	QL-H1 (37HRc)	2687	2015	9	16
4	QH-H1 (54HRc)	2853	2049	30	41
5	QH-H2 (47HRc)	3031	2200	17	30
6	TH (62HRc)	3180	2500	50	189

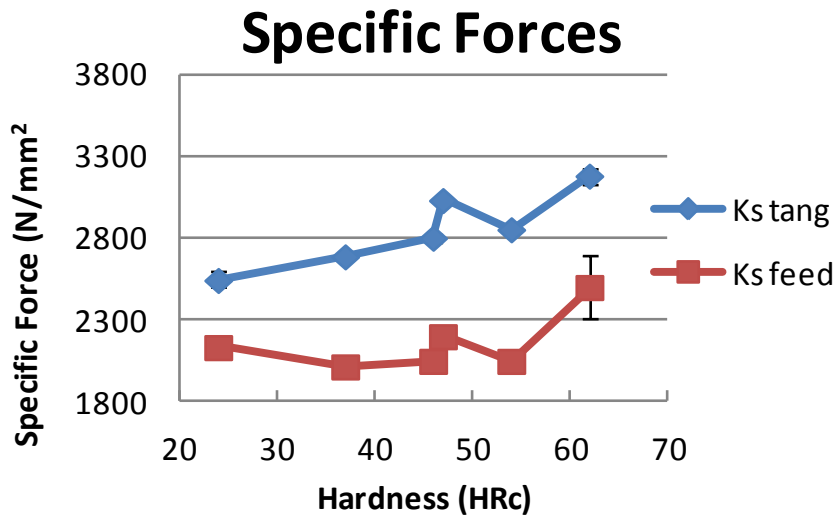


Figure 90. Specific forces vs Material's hardness

WP5 FATIGUE TESTING

The objectives of WP5 are:

- To have all necessary data of mechanical strength and fatigue strength of work piece materials described in Table 1.
- To have an accurate comparison of strength and fatigue strength of the actual production case hardened gear shafts, with the test production induction hardened ones. The comparison includes the associated differences in case depth, etc.
- To obtain fatigue behaviour of materials by testing of fatigue specimens.
- Fatigue evaluation by testing of real components.

Task 5.1 Manufacturing and verification of test samples

Aim: The main goals of this task are:

- To manufacture the specimens to be tested in the fatigue tests.
- To be sure that the specimens fulfil all the mechanical and geometrical requirements to be tested with guarantee.

MULTIAXIAL FATIGUE TEST SAMPLES

Manufacturing process: The reference samples of C-H (18CrMo4) were conventionally carburized and stress relieved, i.e. tempered (180°C 1h), see Figure 91. The samples used in the multiaxial fatigue testing were manufactured following different processes. The main difference among the induction hardened samples is the moment when the samples were fine machined, before or after the surface hardening treatment, see Figure 92 and Figure 93.



Figure 91. C-H (18CrMo4) samples manufacturing process.



Figure 92. QH-H2 (50CrMo4) fine machined after the induction hardening manufacturing process.



Figure 93. Manufacturing process for the QL-H1 (35CrMo4) and QH-H2 (50CrMo4) specimens fine machined before the induction hardening.

The test sample is of diameter $\Phi 25$ mm and length $L=210$ mm, see Figure 94.

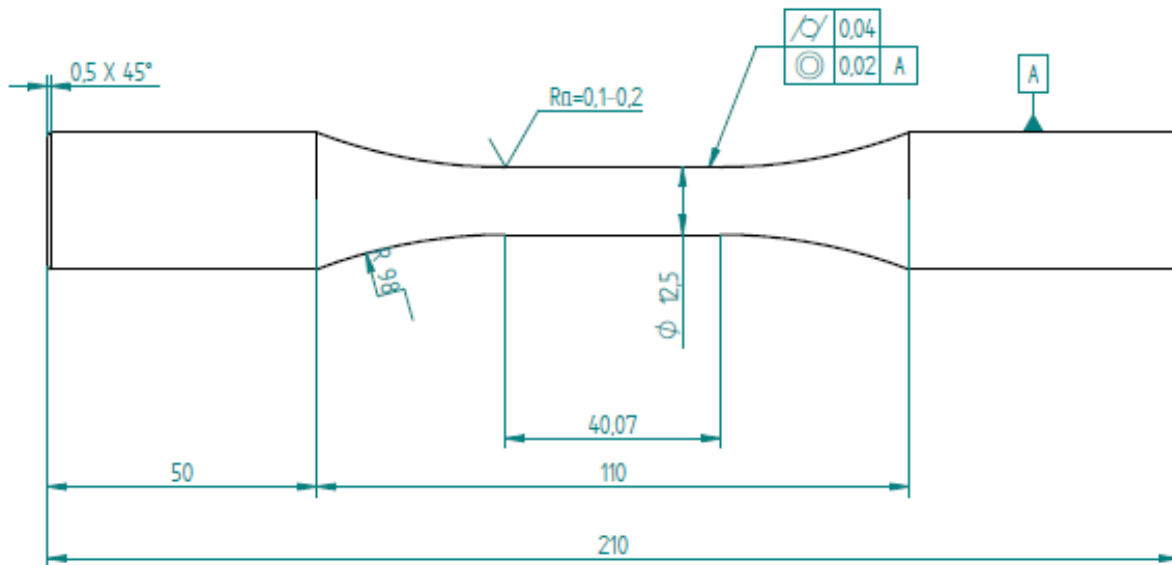


Figure 94. Drawing of multi-axial test sample.

Test specimens verification: After the manufacturing process, some properties of the specimens such as the surface roughness, the hardened layer depth (zone where the hardness is higher than 550HV for case hardened steels and 450HV for induction hardened ones) or the hardness at different depths from the surface were measured. A summary of all of these properties is shown in Table 17.

Table 17. Properties summary of the **multi-axial fatigue test samples**.

		C-H (carburized) (18CrMo4)	QL-H1 (35CrMo4)	QH-H2 (50CrMo4 ⁽¹⁾)	QH-H2 (50CrMo4) ⁽²⁾
Roughness, Ra (µm)		0,05-0,15	0,25-0,40	0,25-0,40	0,10-0,15
Hardened depth (mm)		0,5	3,0	3,5	2,5
Hardness at different distances from the surface (mm)	0	785	660	773	725
	0,5	606	620	707	734
	1	450	577	708	709
	2	412	553	645	648
	3	412	444	626	347
	4	408	302	369	333
	5	390	283	314	303

(1) Fine machining before the induction hardening

(2) Fine machining after the induction hardening

ROTATING BEAM TEST SAMPLES

The sample geometry is of hour glass type, see Figure 95. The diameter of the neck is $\Phi 10$ mm. This is typical with through hardened samples. It can be argued however, as a lesson learned at the end of the project, that a more suitable geometry should have been preferred in testing of case hardened samples. The area ratio of the core and the hardened case should be >2 for a realistic test. This is difficult with a carburized sample and very difficult if the sample is induction hardened. A neck diameter of about 20 mm would actually be recommended for future tests aimed at induction hardening.

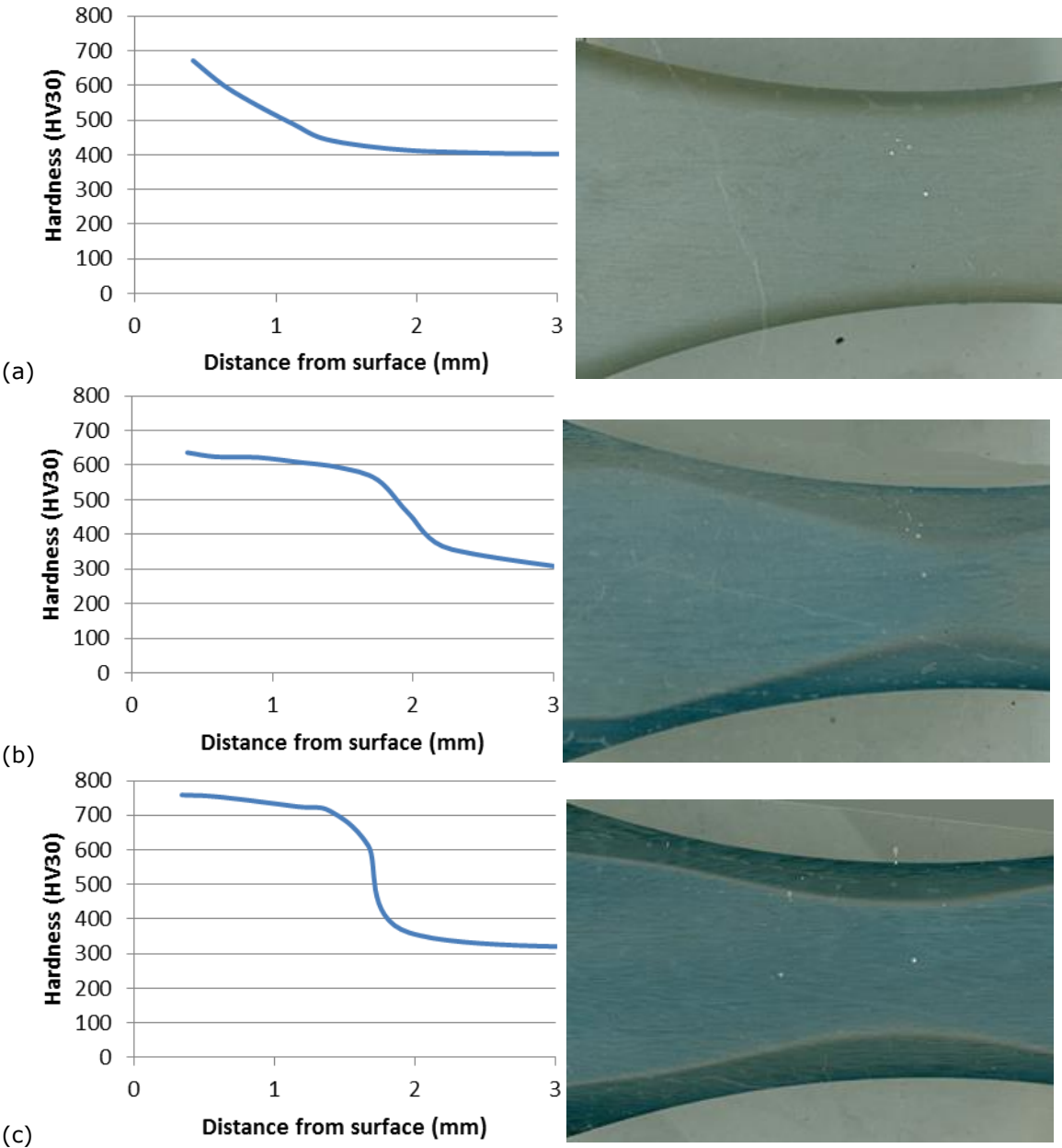
Figure 95. Drawing of the rotating beam test samples.

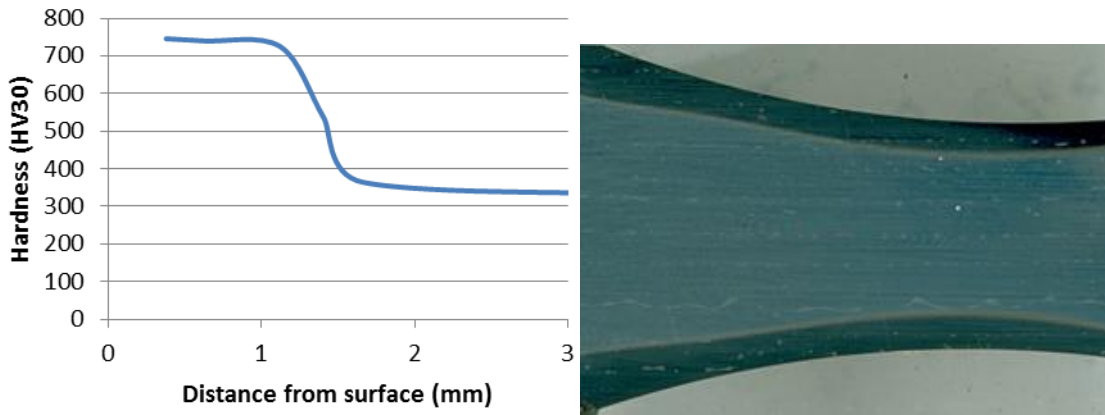
A summary of all the test material and their different heat treatments is shown in Table 18. The steel grade C-H carburized (18CrMo4) was used for the case hardening samples. Two different steel grades were used for the induction hardening samples, QL-H1 (35CrMo4) and QH-H2 (50CrMo4). The QH-H2 samples were tested in two different conditions, fine machined before and

fine machined after induction hardening. The reason was a difference in possible manufacturing route. Fine machining is always made after carburizing due to surface oxidation and distortion. With induction hardening the surface oxidation is extremely small, so is the distortion. Figure 96 shows the hardness depth of the samples after each different hardening and finishing operation.

Table 18. Summary of the different fatigue samples heat treatments and test conditions.

#	1.	2.	3.	4.
Grade	C-H (18CrMo4)	QL-H1 (35CrMo4)	QH-H2 (50CrMo4)	QH-H2 (50CrMo4)
Heat treatment	Carburizing	Induction hardening	Induction hardening	Induction hardening
Surface preparation	Fine machined after hardening	Fine machined before hardening	Fine machined before hardening (FMB)	Fine machined after hardening (FMA)
No. of samples	30	30	30	30





(d)

Figure 96. Hardness profiles and etched cross sections of .(a) C-H carburized, (b) QL-H1(35CrMo4) IH, (c) QH-H2 (50CrMo4) IF FMB and (d) QH-H2 (50CrMo4) IH FMA **of the rotating beam test samples.**

Residual stress measurements of test samples.

The residual stresses of samples for rotating beam tests and multiaxial fatigue tests was assessed using a Stresstech XStress X3000 G2R device. A Cr-K α X-ray tube at 30 kV was used. A pure iron sample was used as calibration sample prior to the analysis of the MAC D samples. The hour glass bottom of the samples was analyzed, see Figure 97. The analyzed area of the samples was electrolytically etched to remove 20 μ m of the surface layer prior to analysis. This was done to align different surface effects, e.g. scale oxides from the carburizing. The residual stress results are given in Table 19. The carburized 18CrMo4 displayed residual stresses of -250 to -400 MPa in both directions. This is relatively high, yet expected. The induction hardened samples show even higher residual stresses, typically of 500-600 MPa in both the axial and transversal directions. It is known that induction hardening generates more compressive stresses than does carburizing. The residual stress results are expected and thus make the heat treatment and comparison of heat treatment process relevant.

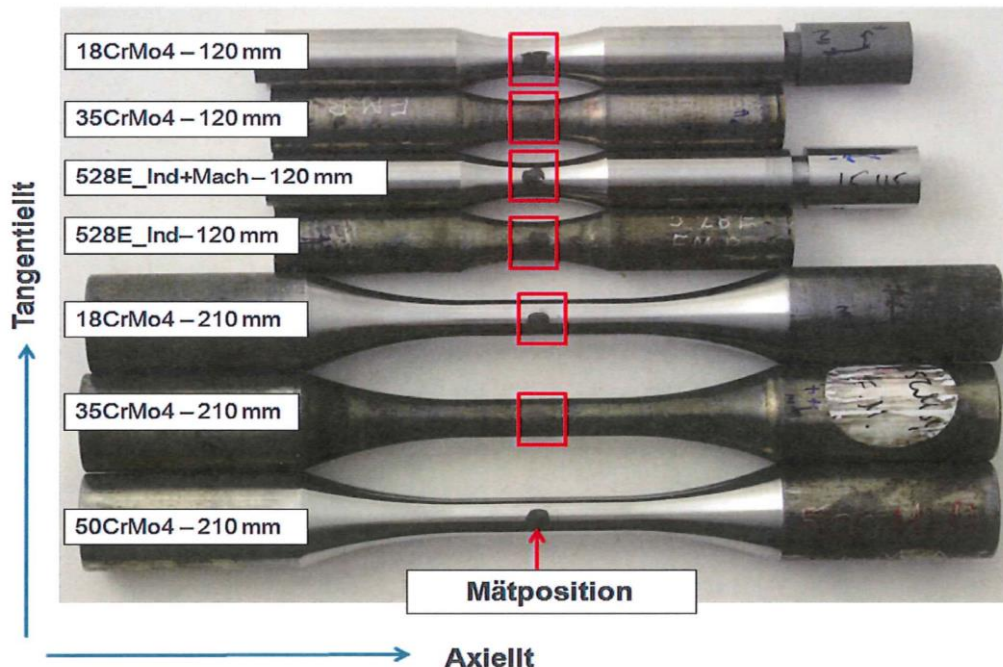


Figure 97. Display of the position of X-ray analysis of the actual samples.

Table 19. Residual stress measurements of samples for fatigue tests.

Steel	Rotating beam sample		Multiaxial fatigue sample	
	Tangential	Axial	Tangential	Axial
C-H carburized	-430 \pm 20	-360 \pm 20	-250 \pm 10	-250 \pm 15

QL-H1	-600±10	-610±10	-480±10	-430±15
QH-H2 FMB	-520±15	-610±10	-390±10	-510±10
QH-H2 FMA	-530±10	-660±10	-	-

MANUFACTURING OF SPUR GEARS FOR COMPONENT FATIGUE TESTING

A model gear with spur geometry is used in internal testing at Gerdau, see Figure 98. Its manufacturing procedure is established in cooperation with a sub-contracted work shop, e.g. for machining operations. The C-IA steel was used for the test gear of this project.

The following details of the gear geometry are given:

Parameter	Value
Peripheral diameter	118
Thickness at the gear roots	14
Gear module	4.5
Condition of the gear roots	Shot blasting ⁽¹⁾

(1): The shot blasting was subcontracted on a routine basis. The objectives of the shot blasting is **A)** to remove the outermost layer of the carburizing that is often weakened by elemental depletion and oxidation and **B)** introduce compressive stresses in the surface. However, shot blasting details are not provided by the supplier.

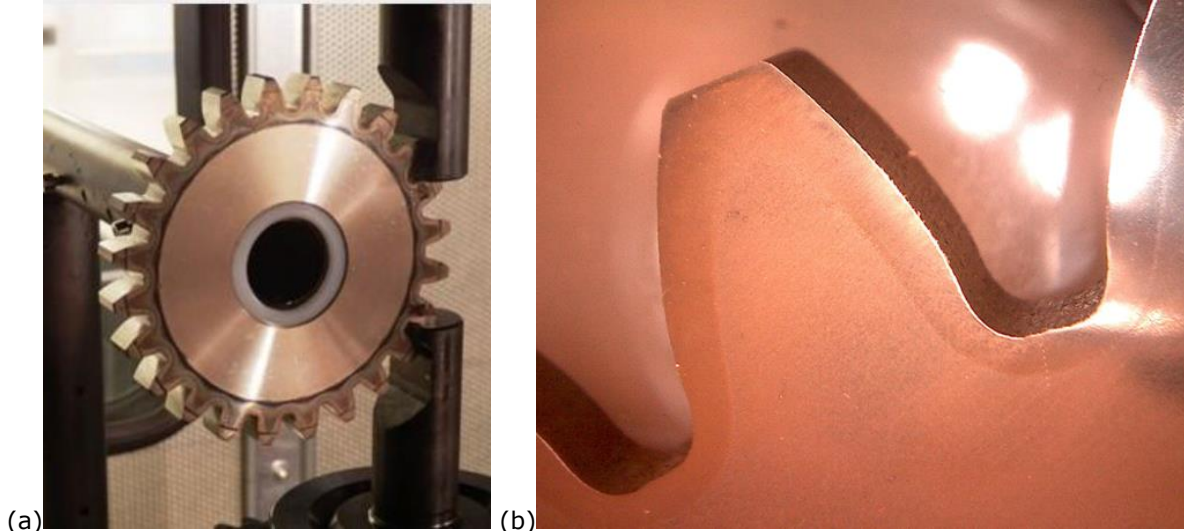


Figure 98. The model gear for component fatigue testing at Gerdau. (a) Mounted in the fatigue testing rig and (b) detail of the gear tooth geometry.

A few tenths of the same model gear were manufactured out of bar material of the QH-H2 (50CrMo4). They were gear cut in a soft condition at the external work shop, quench and tempered at Gerdau to 350 HB and finally sent to EFD for induction hardening.

The resulting hardness as quenched after induction hardening was 800 HV (62.5 HRC). Subsequently the gears were tempered at 180°C for 1h. One of the induction hardened spur gears is depicted in Figure 98(a).

Task 5.2 Testing of fatigue strength of test specimens

MULTIAXIAL FATIGUE TESTING

Aim: The main goals of this task are:

- To evaluate the fatigue strength, considering different loads: axial, torsional and biaxial, of the different steels.
- To determine if any of the induction hardened steels may reach similar fatigue strength than the case hardened steel.

Experimental description: For each steel grade, three different fatigue tests were performed (described below). In all of them the run-out criteria considered was 2.000.000 of cycles and the fatigue limit was determined by the staircase method.

1. Pure tension-compression fatigue test: Only tension-compression (T-C) loads were applied. Through this test pure T-C fatigue limit was determined. The tests were carried out in a MTS 370.10 Landmark hydraulic machine using a frequency of 20Hz and $R=-1$.
2. Pure torsional fatigue test: Only torsional loads were applied to calculate the pure torsional fatigue limit. The tests were carried out in a MTS Biaxial 809-10 hydraulic machine using a frequency of 5Hz and $R=-1$.
3. Biaxial fatigue test: T-C and torsional loads were applied at the same time. A fixed T-C load was used (250MPa), while the torsional load was modified following the staircase method in order to determine the torsional fatigue limit. The tests were performed in a MTS Biaxial 809-10 hydraulic machine. The test frequency used was 5 Hz and $R=-1$.

Results of tension-compression (T-C) tests: The results obtained in the T-C fatigue tests are shown in Figure 99. The material with the highest fatigue limit is the C-H (carburized 18CrMo4). The corresponding level of QH-H2 is about 30% lower and that of QL-H1 is about 40% lower in comparison.

After the test, the fractures were analyzed to determine the fracture initiation. In these tests all the fractures initiated in an inclusion or due to the grain breakage.

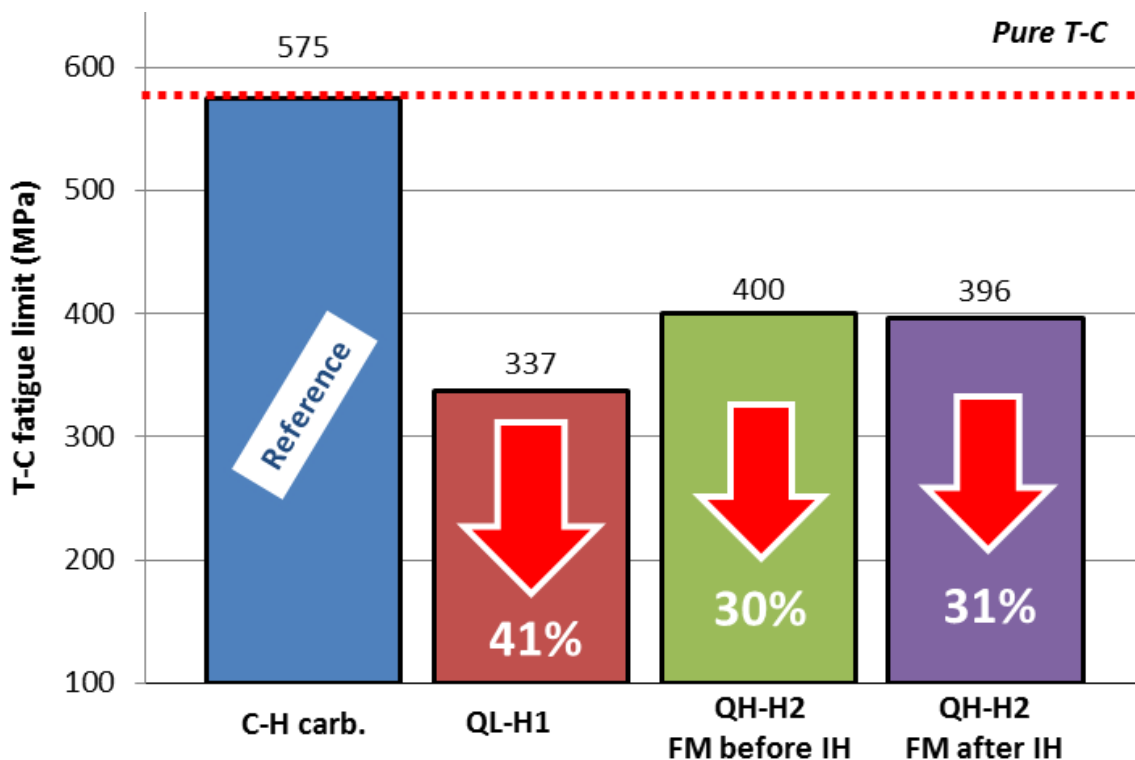


Figure 99. Summary of fatigue limit results in T-C tests.

As the in-service gears do not support pure T-C loads, the results obtained in these fatigue tests are not the most concluding ones in order to decide the feasibility of replacing the carburized C-H (18CrMo4) by a QH-H1 (50CrMo4) induction hardened.

Results of pure torsional tests: The highest torsional fatigue limit was obtained with the QH-H2 (50CrMo4) fine machined before the induction hardening, Figure 100, the one with the deepest hardened layer, see Table 20. For the other induction hardened steels, the fatigue limit in pure torsional conditions is the same (575MPa) than the one of the reference C-H (18CrMo4) carburized and an 8% lower than the highest one.

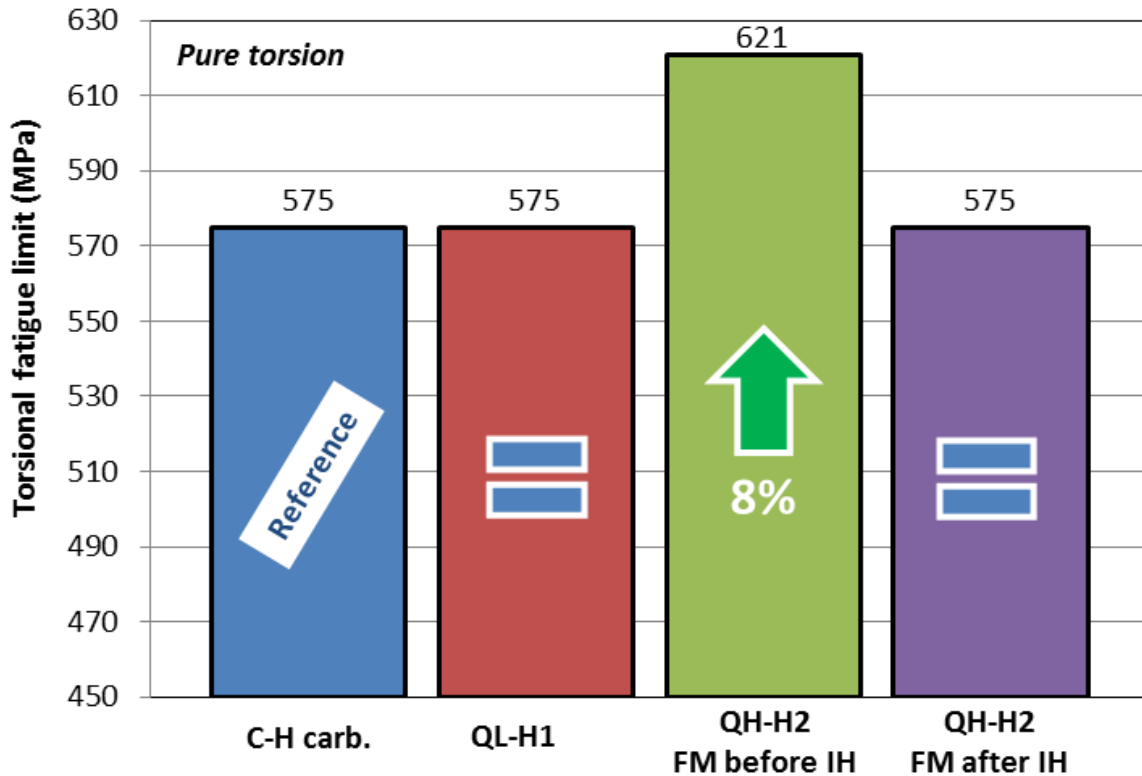


Figure 100. Summary of fatigue limit results in torsional tests.

Table 20. Hardened layer properties.

	C-H carb. (18CrMo4)	QL-H1 (35CrMo4)	QH-H2 (50CrMo4) FM before IH	QH-H2 (50CrMo4) FM after IH
Hardened layer depth (mm)	0,5	3,0	3,5	2,5
Layer average hardness (HV_{1kg})	800	600	700	700

As in the case of the tension-compression test, the fractures were analyzed to determine their origin, in this case the fractures initiated in an inclusion or because of a machining line. A more detailed study may be found in Annex 5. A similar study as in the T-C fatigue test was performed to predict the fracture origin point.

Results of biaxial tests: The biaxial fatigue test combines axial and torsional loads. To simplify the test, the axial load is fixed (at 250MPa) and then, the torsional fatigue limit is determined for this axial load.

The fatigue limits of both 50CrMo4 are higher than the reference C-H carburized (18CrMo4). In this case, performing the fine machining after the induction hardening gives better fatigue results than making it before the induction treatment (torsional fatigue limit increase with respect to the C-H

carburized of a 9% and 3% respectively. The worst results are obtained for the QL-H1, roughly 30% lower than the reference, see Figure 101.

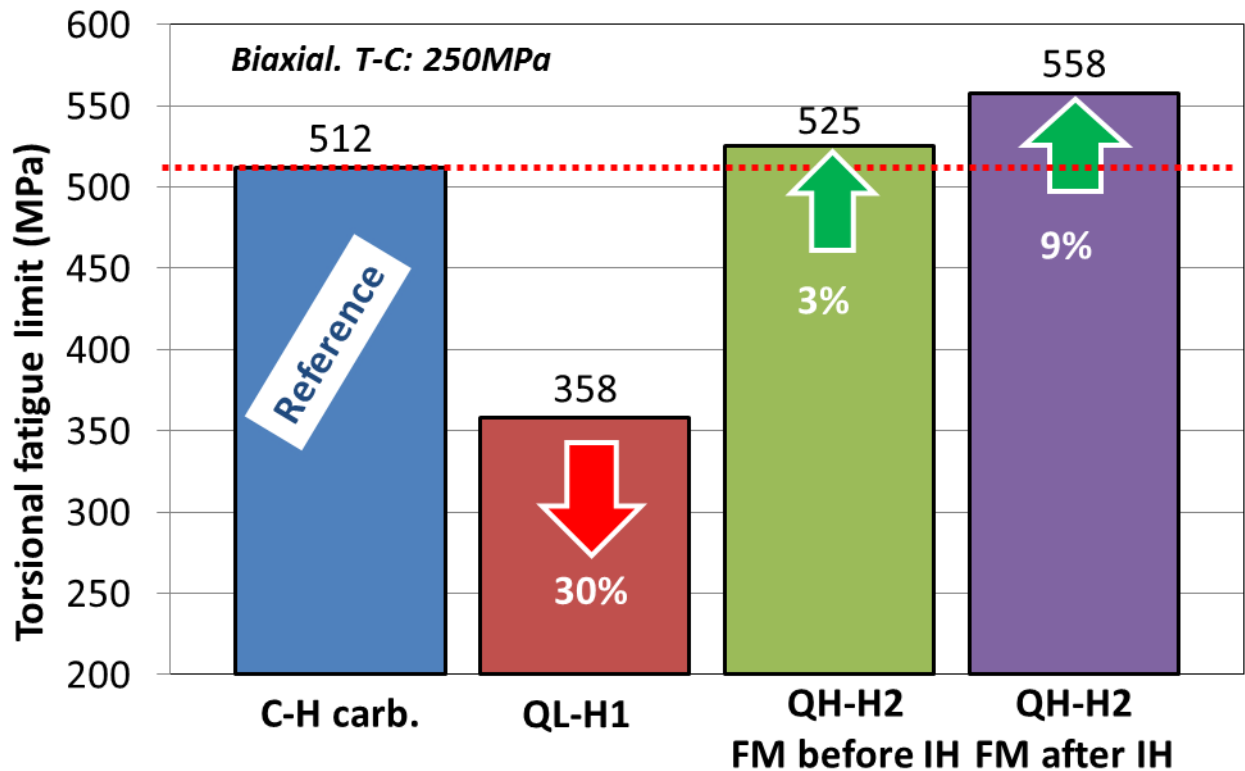


Figure 101. Summary of fatigue limit results in biaxial tests.

As in the other two cases, the fractures were analyzed to determine their origin, in this case the fractures initiated in an inclusion, due to grain breakage or at the surface. The inclusion initiated fractures makes this bi-axial load fatigue test most relevant in the comparison of steels and heat treatments in this project. A theoretical approach of fatigue load distribution of bi-axial (T-C and torsional load) tests is given in Figure 147 (ANNEX WP5). Representative hardness depth profiles are included to demonstrate how the test conditions can be modified to suit the tested heat treatment characteristics.

Conclusions: The following conclusions can be drawn from this work:

- The use of the induction hardened QL-H1 (35CrMo4) is not recommended. The low hardness of the induction hardened case directly affects the fatigue strength.
- The fatigue limits of both variants of QH-H2 (50CrMo4) are quite similar. In the pure torsional test, the fatigue limit of the 50CrMo4 fine machined before the induction hardening is considerably higher, explained by the deeper case depth. Hence, the surface finishing does not seem to have a great influence on the fatigue limit, at least, in the tests performed in this WP.
- Comparing the carburized C-H (18CrMo4) with the QH-H2 (50CrMo4), it is observed that the fatigue limit in pure T-C conditions of the QH-H2 is notably lower than the one for the carburized steel. For the other two fatigue configurations, the behaviour is relatively similar.
- Taken into account the results obtained in this WP, and considering that in-service gears do not work under pure T-C conditions, it could be said that the results obtained for the QH-H2 should not be a problem for its potential use in the gears manufacturing.

ROTATING BEAM TESTING

Aim: The main goals of this task are:

- To evaluate the fatigue strength in a conventional rotating bending fatigue configuration with $R=-1$. The advantage is foremost the straightforward test method and the fact that the samples are easy to mass-produce with high repeatability.
- To determine if any of the induction hardened steels may reach similar fatigue strength than the case hardened steel.

Experimental description:

The Fatigue testing was conducted in AMSLER UBM200 four point bending test machines operated at 5000 rpm, see Figure 102. The stress ratio was specified to $R=-1$, i.e. fully reversed loading. The fatigue limit tests were conducted according to the stair case method with a step size of 25 MPa and survival criteria of 10 million cycles. The fatigue strength tests were performed with a step size of 50 MPa at higher loads until failure.



Figure 102. AMSLER four point bending test machine.

Results of rotating beam tests:

Fatigue limit for the different steel grades are given in Figure 103. The steel C-H carburized (18CrMo4) displayed a fatigue limit of $\sigma_m=883 \pm 17$ MPa, that of QL-H1 (35CrMo4) was $\sigma_m=703 \pm 25$ MPa. The QH-H2 FMB (50CrMo4) displayed a fatigue limit of $\sigma_m=930 \pm 23$ MPa and the same steel with fine machining after induction hardening (IH FMA) had $\sigma_m=898 \pm 17$ MPa. The relationship between applied stress and fatigue life is given in Figure 104.

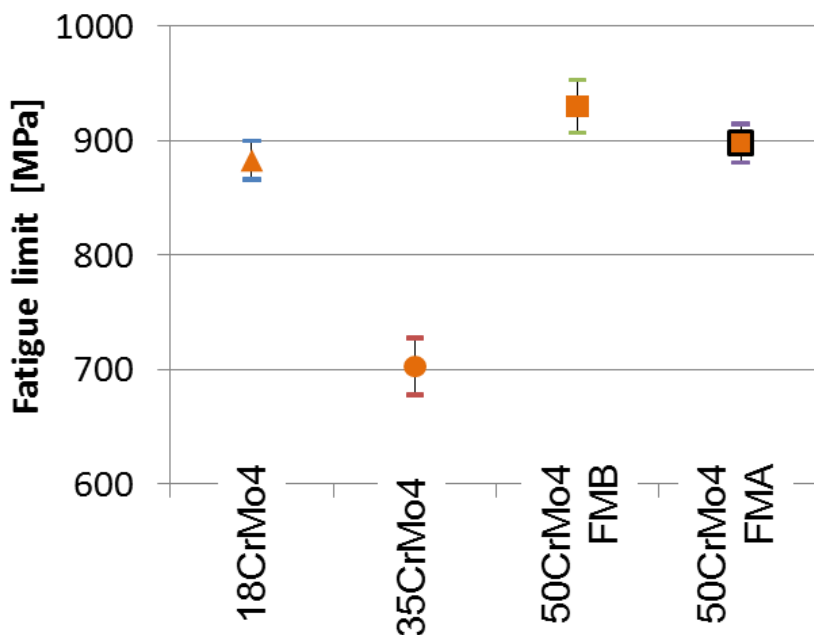
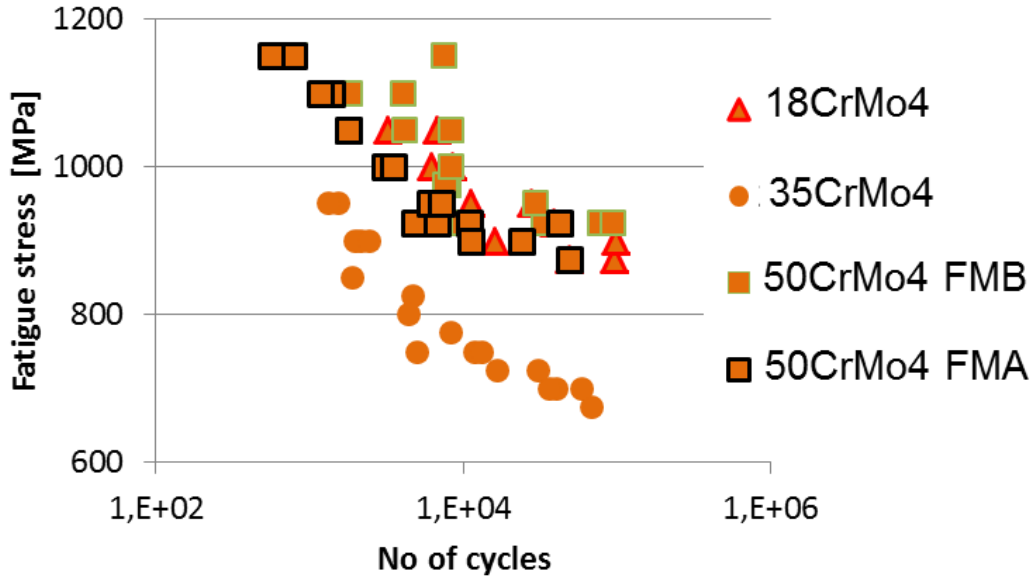


Figure 103. Fatigue limit results with confidence interval of 95%.



OVAKO

Figure 104. S-N diagram for the different test series.

Fractured specimens surfaces were examined using Scanning Electron Microscope. All samples had their point of fracture initiation in the transition zone from hardening case to the core, see Figure 105. The hardness depth profiles of the samples are given in Figure 106, including the fracture initiation point of each steel.

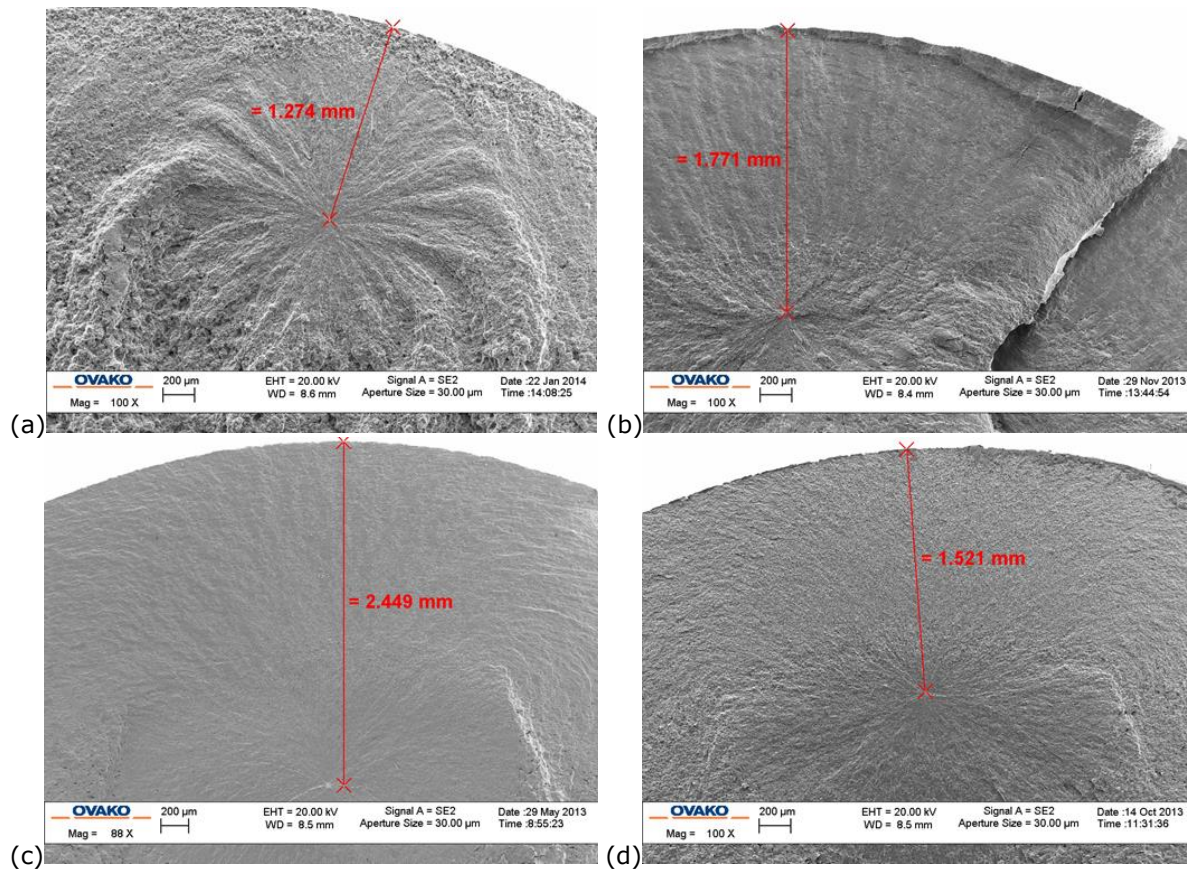


Figure 105. SEM-micrographs of fracture surfaces (a) C-H carburized, (b) QL-H1, (c) QH-H2 FMB, (d) QH-H2 FMA.

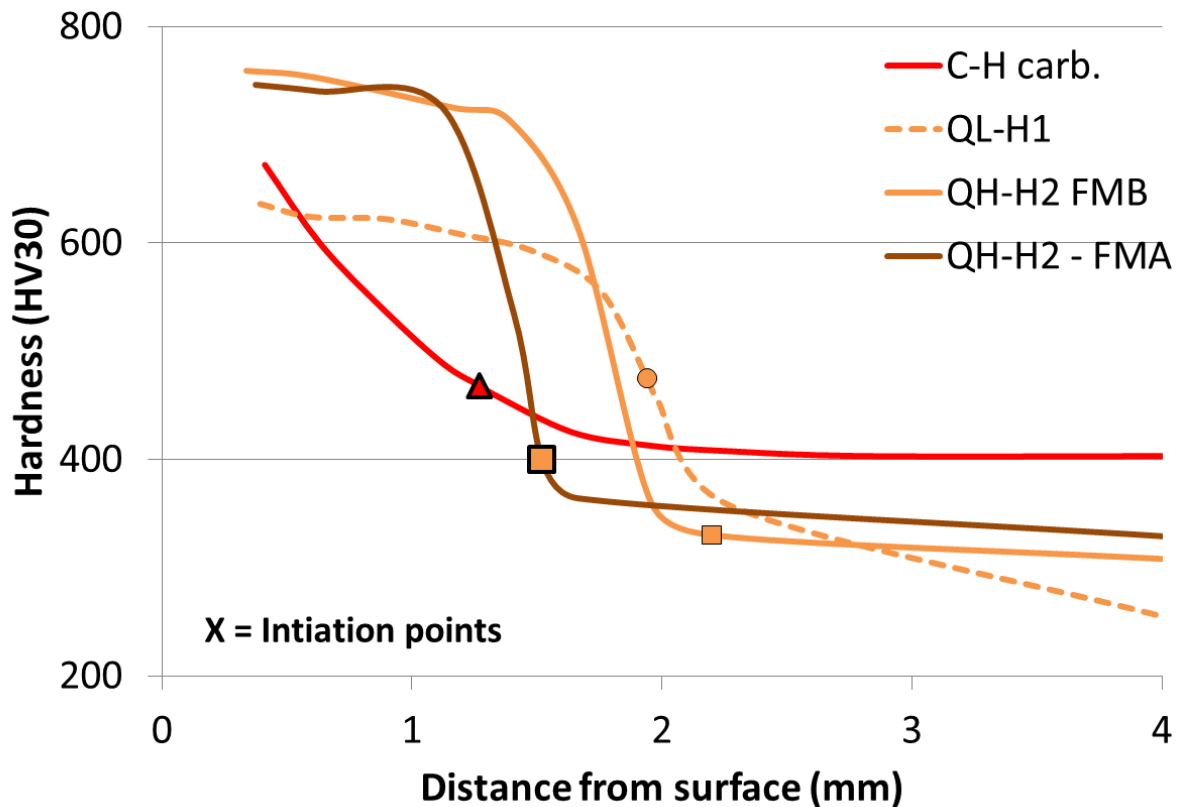


Figure 106. Hardness depth and typical positions, marked with ●, ■ and ▲, of fracture initiation for the fatigue tested samples.

Discussion of rotating beam fatigue tests

The fracture initiation was typically in the steel matrix, i.e. the tests were not in the mode of inclusion induced fracture. The initiation depth was typically in or below the transition zone of the tested samples, cp. Figure 106. Consequently, the results primarily show the effect of the hardened case depth of these samples. As such the comparison of carburizing and induction hardening is relevant. However, it is preferred to have fracture initiation in inclusions in this kind of tests.

A general means to increase the near-surface stress in fatigue tests is to apply a more sharp notch in the middle of the sample. The added stress concentration factor typically generates surface induced fracture initiations. The adopted hour glass test sample geometry was originally developed for through-hardened ball bearing steels.

Conclusions of the rotating beam fatigue tests

The following conclusions can be drawn from the current investigation:

1. The fatigue strength was approximately the same for C-H carburized and QH-H2. The higher fatigue limit value for QH-H2 FMB was probably linked to its deeper case depth.
2. QL-H1 was the steel grade with the lowest fatigue value. This is most likely linked to its lower hardness of the induction hardened case.
3. The results of this investigation primarily shows that the case depth is the most important feature of the hardening process. This conclusion is based on the fact that the depth of fracture initiation was in or below the transition zone for all the samples.
4. An alternate sample geometry incorporating a notch in the middle of the test sample is recommended in future rotating beam fatigue tests to increase the stress in the hardened case and thereby better evaluate the hardened zone properties and to guarantee inclusion initiated fractures.

Task 5.3 Testing of fatigue strength of actual components

Aim: The main goals of this task are:

- To evaluate the fatigue strength in relevant load condition of the actual selected transmission component.
- To determine the influence of the surface treatment on the fatigue behaviour of the actual component (case hardening vs induction hardening).

Manufacturing of components: The main differences in the gears manufacturing processes followed with the C-H carburized, see Figure 107 and the QH-H2, see Figure 108 were the hardening step (case hardening vs induction hardening) and the shot peening, only performed over the carburized gears.

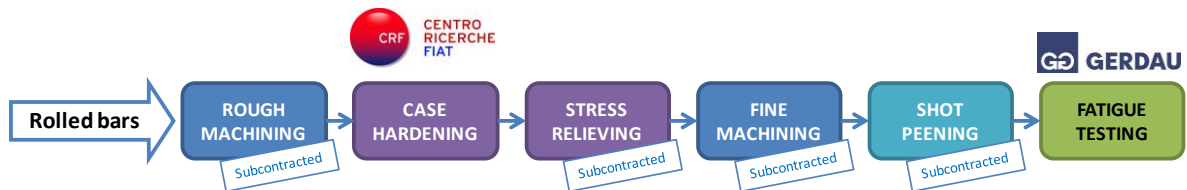


Figure 107. Manufacturing process followed with the 18CrMo4 case hardened gears.

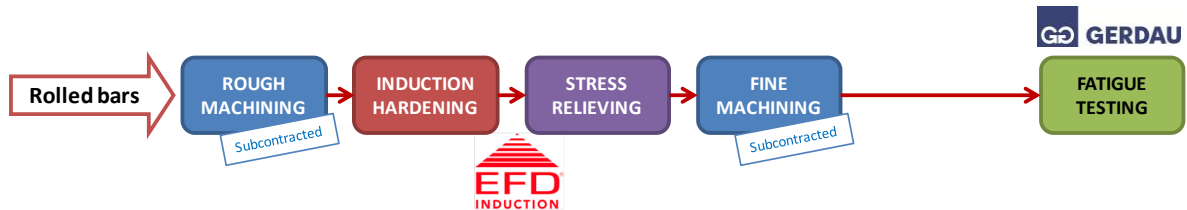


Figure 108. Manufacturing process followed with the QH-H2 treated gears.

Verification of mechanical properties of components prior to fatigue testing: Once the gears were manufactured, some main characteristics (such as geometrical dimensions and the hardness profile in different points of the gears, determining the hardened layer depth) were checked. The points where the hardness was measured are indicated in Figure 109. The results of these hardness measurements are shown in Table 21.

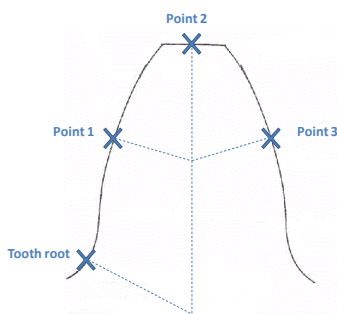


Figure 109. Points of the gear tooth where the hardness was measured at different depths transversally to the surface (following the discontinuous lines).

Table 21. Hardness profiles on different points of a gear tooth.

Dist. to surface (mm)	18CrMo4 Case Hardened				QH-H2 (50CrMo4) Ind. Hardened			
	Point 1	Point 2	Point 3	Tooth root	Point 1	Point 2	Point 3	Tooth root
0,25	769	730	769	805	666	624	621	658
0,50	606	789	587	593	652	625	615	650
0,75	513	470	481	488	630	660	651	606
1,00	446	441	421	406	667	660	668	591
1,50	426	430	414	410	361	544	568	302
2,00	421	413	394	418	294	373	289	320
3,00	405	409	399	411	310	324	287	292

The results of Table 21 show that the carburized layer in the C-H treated gear is relatively homogeneous around the whole tooth. The average hardened layer depth obtained is around 0,75mm. For the induction hardened gear, the hardened layer is not as homogeneous as in the case of the carburized gear. The depth on the tooth root is lower than in the rest of the measured points, 1 mm and 1,5 mm respectively.

Experimental description: The tooth bending fatigue tests were performed in a RUMUL resonant fatigue machine. The tests were carried out in compression-compression conditions ($R=0,1$)², under the resonant frequency of the gear for each load applied (it varied between 90 and 95Hz). The run-out criteria considered was 10.000.000 cycles. The fatigue limit was determined following the staircase method.

The set-up of the tests performed in the GERDAU I+D laboratory is shown in Figure 110.

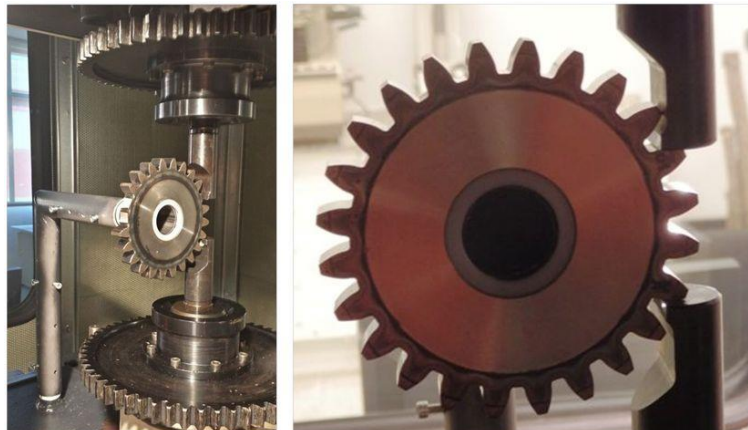


Figure 110. Fatigue test performed over gears in the RUMUL machine.

Results: The fatigue limit was determined using load values because of the difficulties to estimate the corresponding tension for the loads applied.

The tooth bending fatigue limit for the carburized gears is -23,30kN, while for the QH-H2 treated gears it is around a 12% lower than that value (-20,45kN).

After the tests, the fractures were analysed to determine their origin. All of them initiated at the surface and the origin of most of them (all except one) was related to the presence of MnS inclusions.

Conclusions: The main conclusions that can be obtained from the tooth bending fatigue tests are the following ones:

² R is the relationship between the minimum and the maximum load applied.

- The fatigue limit obtained for the C-H carburized is a 12% higher than the one of the QH-H2.
- In general, the fractures initiate in the surface and have their origin in MnS inclusions. This was expected because, under the load conditions used in this test, the surface is the zone of the gear tooth where the highest tensions concentration appears.
- As the S content of the QH-H2 is clearly higher than the one of the C-H and all the fractures initiate in MnS, if the S content of both steel was similar. Besides, if the induction hardened gears were shot peened (as performed for the case hardened ones), their fatigue limit should increase. Taking these two reasons into account, for similar S content and following a similar manufacturing process, the fatigue limit should be similar for both cases (case hardening vs induction hardening).

WP6 THE DEMONSTRATOR COMPONENT; MANUFACTURING AND COMPARISON, CASE HARDENING VS. INDUCTION HARDENING

The objectives of WP6 are:

- To have direct comparison in the manufacturing procedure of the chosen demonstrator component, with respect to:
- Cost of rough and finishing machining
- Cost of heat treatment (carburizing case hardening vs. induction hardening)
- Fatigue strength and other relevant mechanical properties.

Task 6.1 Decision of demonstrator component

Two demonstrator components are agreed in the project:

(I). A HELICAL GEAR, see Figure 111. The gear is part of a Fiat manual gear box. The gear is subjected to medium high cyclic loads during running. Today the gear is made of 18CrMo4 steel, and carburized. The helical gear is a relatively high risk demonstrator, since the induction hardening of helical gears is considered very difficult or impossible. The reason is the risk of overheating of the tooth edges. This particular component was subject to a previous study with not satisfactory results.

EFD Induction believes that it is feasible to succeed with induction hardening treatment through a clever design of the induction heating configuration. The treatment requires extremely high power. Such a unit is available at EFD facilities in Germany, which will be used for the work.

NOTE: The helical gear is considered as primary demonstrator in the project. It is connected to very advanced induction hardening technique. It also connects with gear hobbing and fatigue strength.



Figure 111. The primary demonstrator, a helical gear in a Fiat manual gear box for a small car.

(II). A SECONDARY GEAR SHAFT, see Figure 112. The secondary gear shaft is considered only with respect to the bearing positions, and their machining operations. Consequently, the gear at the end is not considered.



Figure 112. The secondary demonstrator, a secondary gear shaft in a Fiat manual gear box for a small car.

Task 6.2 Today's manufacturing route through carburizing

For this particular gear the company HotRoll S.r.l., part of the Fomas group is the primary supplier of forgings. The preferred bar diameter from the steel plant is $D=70$ mm. The forging process is depicted in ANNEX 6 Figure 150. The following steps are included: (I). Punching, (II). Piercing and (III). Orbital lamination (ring rolling). The current specification of microstructure is pearlite-ferrite in the as-delivered condition to Fiat Powertrain.

The manufacturing route of the gear is as follows:

No.	Sequence	Operation
1	Supply of steel as bar from the steel producer to the forging company.	
2	Blank forging & heat treatment	
3	Arrival of gear blank at Fiat Powertrain.	
4	Turning operations. (& dimensional check)	OP10
5	Gear cutting.	OP30
6	Chamfering and snagging.	OP40
7	Washing.	OP50
8	Drilling.	OP60
9	Washing.	OP70
10	Carburizing.	OP80
11	Shot blasting of gear roots.	OP80
12	Fine turning of end surfaces.	OP100
13	Grinding of gear tooth flanks.	OP110

All parts of the gear ring are machined in the soft condition to have the specified rotational geometry. The operations include facing and peripheral turning in both roughing and finishing. In terms of machinability in soft machining in the comparisons of steels of the project all these operations are considered. Though, the model machining is closest to a peripheral turning operation.

The hob milling tool has 19 teeth around its periphery, see Figure 113. The feed per tooth is $f_z=0.11$ mm. The feed per revolution is consequently $f_r=2.1$ mm. The hob mill cutter and the gear ring rotate simultaneously and the gear translates axially to machine the gear teeth from the top to the bottom of the gear. The steps from forging blank through turning to the hob milled gear are depicted in Figure 114. Note that the milled gear in (c) is chamfered on the tooth edges. The following manufacturing steps of the production gears are (not shown) drilling, carburizing shot blasting of gear roots and grinding of gear flanks.



(a)

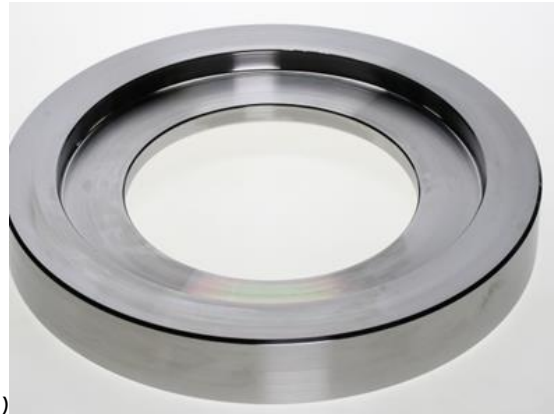


(b)

Figure 113 (a) The machine set up and (b) the hob milling tool.



(a)



(b)



(c)

Figure 114. Soft machining of the demonstrator part. (a) As-forged, (b) turned and (c) gear hobbled.

The machining processes of most attention of the project are the OP10 and OP20. Two factories of Fiat Powertrain have the helical gear in their production, the Mirafiori plant and the Verrone plant. The Mirafiori Plant uses old carburizing furnaces and represents the traditional manufacturing process: the heat treatments lasts up to 20-22hours. The Verrone Plant, according also to the WCM challenges, represents a modern production line. For instance a large installation of low pressure ("vacuum") carburizing furnaces is installed. Thereby the heat treatment time is reduced to 6-8 hours.

Given the status of the two production plants the experience in large scale investment is good in the Verrone plant. This will be used as a bench-mark to the possible investment of a new induction hardening line in Task 6.4.

The part drawing including measures and tolerances after machining operations is found in APPENDIX 6 Figure 148. All relevant details of the machining processes are given in APPENDIX 6 Figure 149. The column called Working time represents the engagement time of each operation in parts per minute, referred to as centiseconds). Consequently the turning operations duration range

from 8 to about 23 seconds. The hob milling operation of each gear takes almost two minutes to complete (194 centsec => 114 seconds of cutting).

From the previous schemes, major turning and hob milling operations are summarized in terms of cutting data. Those of the helical gear are summarized in Table 22. Two roughing operations of the 2nd gear shaft are found in Table 23.

Table 22. Machining parameters of the helical gear. Rough facing, finishing facing and gear hobbing are given.

Facing lathe and turning parameters	Finishing facing lathe parameters	Gear Hobbing parameters
Vc = 250 m/min	Vc = 300 m/min	Vc = 110 m/min
f = 0,40 mm/rev	f = 0,25 mm/rev	f = 2,20 mm/rev
Vf = 280mm/min	Vf = 150 mm/min	Fz = 0,116mm
n = 700rev/min	n = 610 rev/min	n = 350 rev/min
		n. cutting edges = 19

Table 23. Machining parameters of the 2nd gear shaft. Two roughing operations are given.

Roughening 1 Turning parameters	Roughening 2 Turning parameters
Vc = 230 m/min	Vc = 270m/min
f = 0,400 mm/rev	f = 0,250 mm/rev
Fz = 0,400mm	Fz = 0,250mm
Vf = 800mm/min	Vf = 750mm/min
n = 2000rev/min	n = 3000rev/min

HEAT TREATMENT CYCLE

The heat treatment of the components is carried out by carburising furnaces Holcroft 60's. The gears are placed in suitable containers made of high temperature resistant NiCr alloy.

The Holcroft furnace system consists of:

- Carburizing furnace with controlled atmosphere (Endogas) for carburizing step at 880°C (carbon enrichment of 0.6 mm average)
- Oil bath equipped with a lifter for the quenching operation in order to obtain the target surface and root tooth hardness
- Washing machine to remove oil residues from the hardened components.
- Tempering furnace (working temperature, 180°C) for standardizing the material structure after heat treatment.
- Series of internal pushers and external carriers to move the containers along the process.

The particular atmosphere (Endogas, or process/carrier gas) is raised by a chemical reaction with catalyzers at 1030 ° C by special burners. A typical endogas is composed by 20% CO, 40% H₂ and 40% N₂. In an hour time the furnace is fed with a gas volume several times higher than the furnace volume in order to maintain a constant pressure and uniform results. The overall time of the process for each component lasts 20-22 on average. The container can carry about 80 gears each. **NOTE** that the helical gear requires a lot of space in the carburizing furnace, since it is difficult to fixture. For comparison, one container in the carburizing furnace can take 80 gear at a time, while the same container can carry 800 cylinder heads.

The specification of today's carburizing response in the demonstrator gear is shown in Figure 115. The specification includes a contour case around the tooth profile with a surface hardness of 58-62 HRC. The goals to reach through the new induction route are similar to the conventional. In fact **it is very important to obtain the surface hardness condition after the induction treatment both on the flank and on the root of the tooth.** The **hardness range of 58-62HRC indicated in FIAT Standards** on the contour of the tooth surface guarantees the fatigue resistance of the tooth during the transmission exercise.

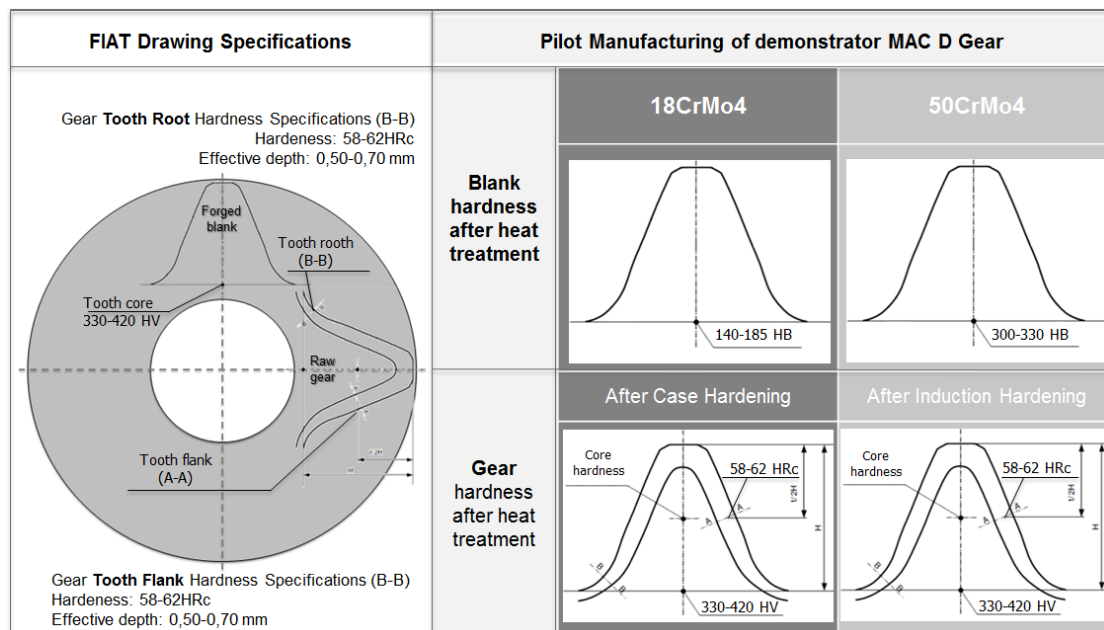


Figure 115. Fiat hardness specification and gear manufacturing piloting.

SUMMARY: The project has all data of machining and heat treatment necessary to make a cost analysis of the demonstrator manufacturing. That actual cost calculation will be made in short in a chart.

Task 6.3 Pilot manufacturing of demonstrator component through the induction hardening route

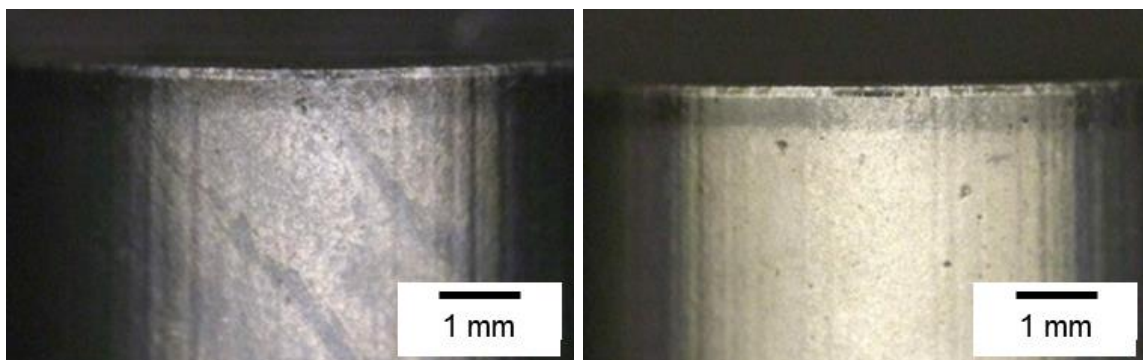
It is the aim to replicate the final geometry of the (case hardened) demonstrator component chosen in the project, through the induction hardening route of manufacturing. As a demonstrator component a helical gear was chosen by CRF.

Steel supply and forging process: Ovako supplied with steel bars of the Ovako 528E steel (50CrMo4) in bars of D=70 mm. 70 rings were forged by HotRoll S.r.l. and supplied to the WZL. For this particular batch of forgings new forging moulds had to be manufactured. In addition, a new temperature cycle had to be defined. The reason was primarily the change of carbon content from the reference 18CrMo4 steel, which changes the hot forging properties as well as the phase transformation to austenite. In addition, a subsequent quench-and-tempering sequence was specified to enable gear rings of hardness 350 HB. The reason of this very high hardness is explained by Figure 15 and the extremely short time of austenite transformation associated with induction hardening of components. The much harder work piece compared to the 160 HB blank made of 18CrMo4 represents the major change and challenge

The forging process was composed of the following steps: (I). Punching, (II). Piercing and (III). Orbital lamination (rolling), cp. Figure 150. The specified hardness of the rings after forging was 350 HB. This is much higher than typical hardness. It is based on the need of an as dissolved carbide structure as possible for a successful induction hardening.

Machining operations: A standard hob milling tool out of production of the actual demonstrator gear was supplied and shipped from CRF to the WZL for the hob-milling operation. The soft machining operation turning and hob milling were done by WZL. In total 34 demonstrator gears were machined through turning and hob milling, cp. Figure 113 and Figure 114. A field study of the used cutting edges of the hob milling tool after the 34 gears cut showed significant chipping of the cutting edges.

The machined gears were shipped to CRF for chamfering in-line of the production at Fiat Powertrain and subsequently shipped to EFD Induction in Freiburg Germany. Note: The original plan was to do the induction hardening at EFD in Sweden. However, given the requirement of maximum power of the induction hardening process for this particular gear, the EFD site in Freiburg turned out to be the best equipped.



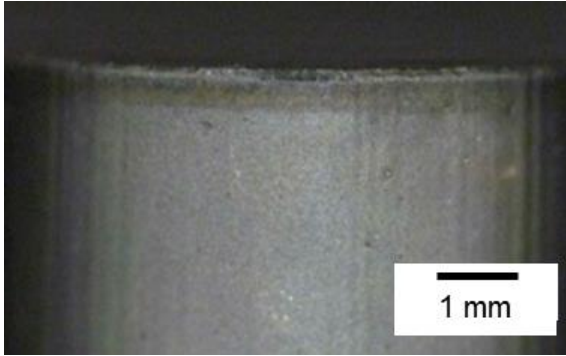


Figure 116. Micrographs of used cutting edges of the gear hob (a) as new, (b) after 4 gears and (c) after 34 gears.

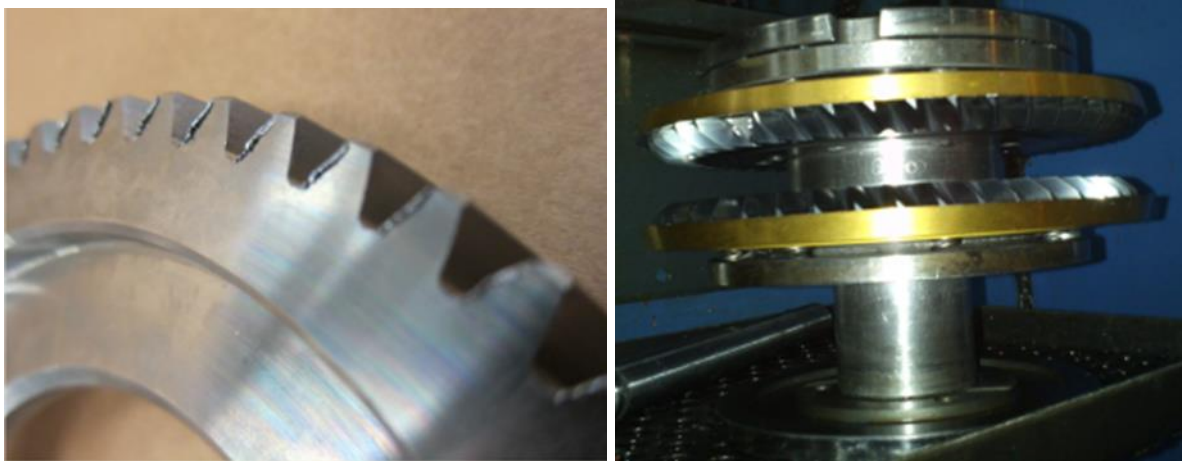
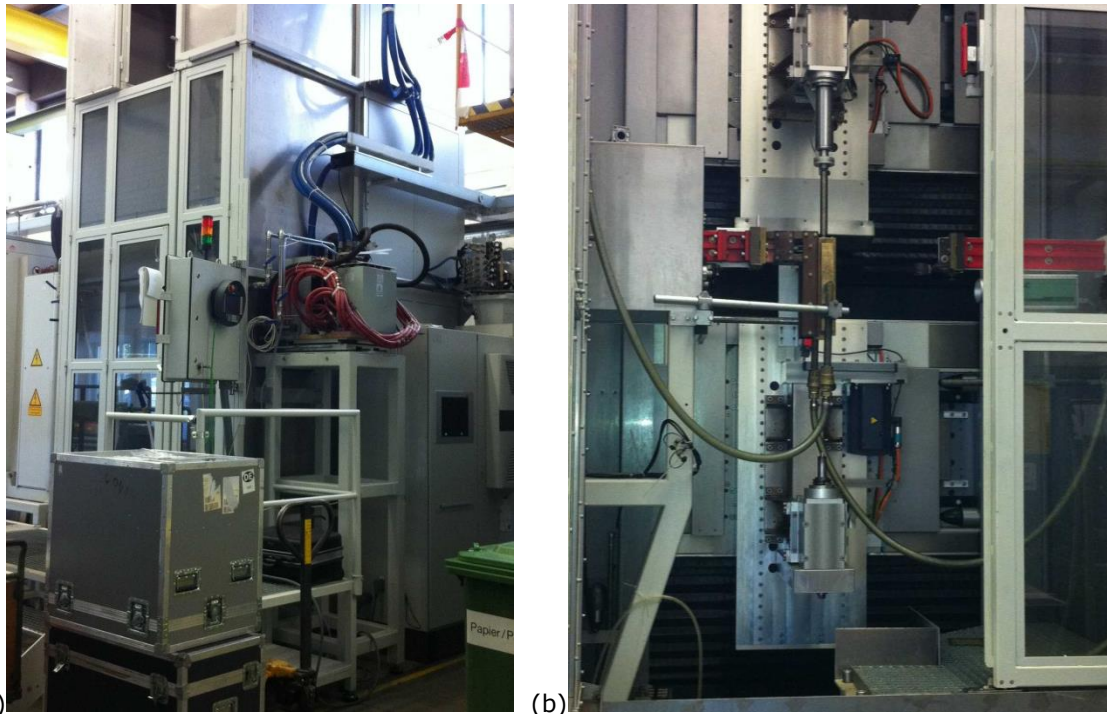


Figure 117. (a) As-hobbed gear teeth and (b) the chamfering tool at Fiat Powertrain.

Induction hardening: The induction hardening was undertaken at EFD Induction in Freiburg in Germany. The power supply is capable of an instant power of 2 MW, which is required for the extremely short heating cycle, see Figure 118.

A single frequency cycle was utilized. In general, significant know-how in the frequency and small details of the heating cycle are of utmost importance for the actual result of the induction hardening. In some similar applications a two frequency technique have been used. Put simply, the lower frequency have been used to heat the gear toots and the high frequency have been used to heat the gear teeth. However, with the demonstrator of this project the major challenge was considered the helical tooth shape, which typically generates uneven heat and martensite transformation of the different parts of the gear tooth. Consequently, most attention was given that challenge. A single induction frequency was utilized throughout the tests.

The induction heating cycle was made up of about 10 seconds of preheating up to about 650°C, followed by about one second of peak power for the transformation to austenite phase, see Figure 119. The gear was then quenched through water sprinkling. A proud project group can be seen in front of the induction hardening machine in Figure 120!



(a) (b)
Figure 118. The induction hardening machine at EFD Induction in Germany. (a) Overview and (b) detail of the induction coil and the water spray devices for quenching.

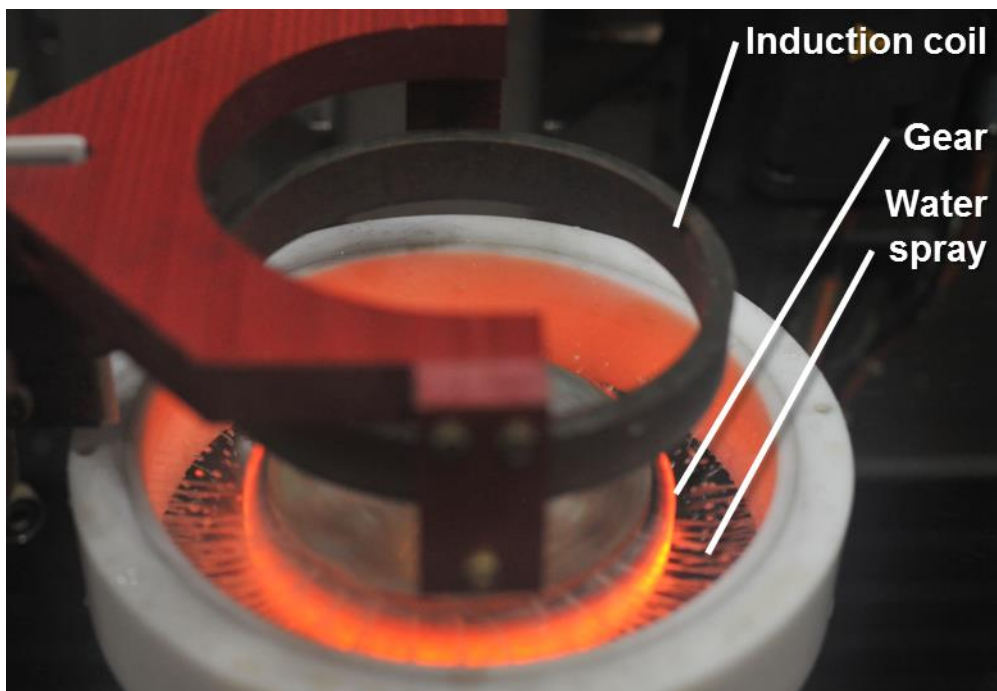


Figure 119. Photo of an ongoing induction hardening cycle of the demonstrator gear.

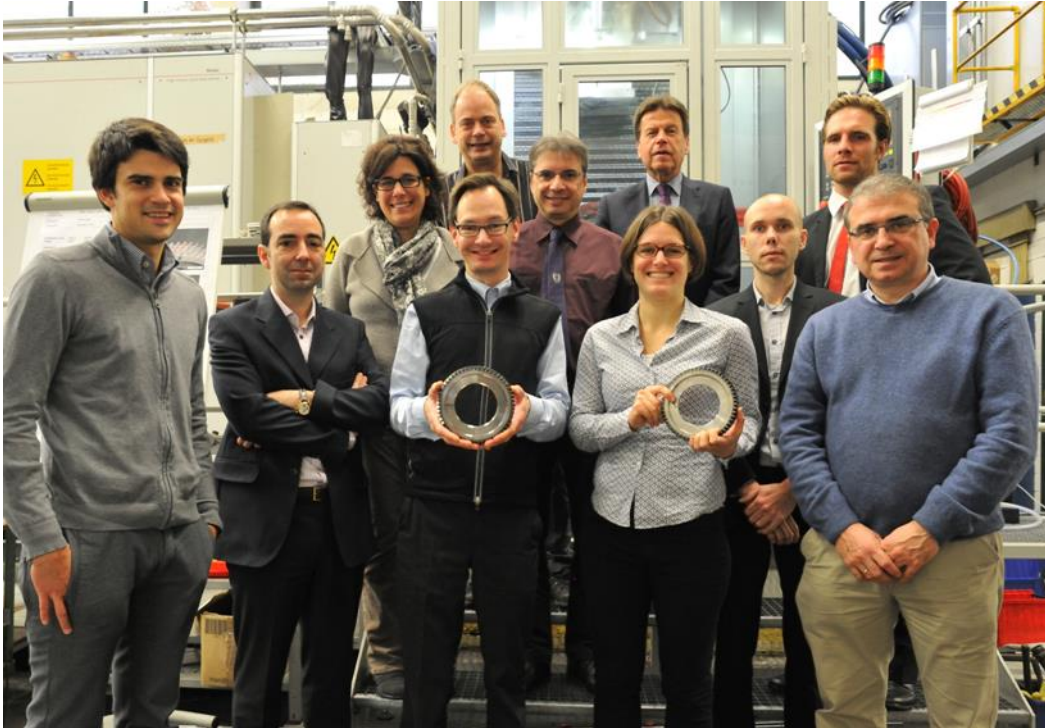


Figure 120. The project consortium in front of the induction hardening device at EFD Induction.

Development steps of the induction hardening process: Significant work and effort was spent on optimizing the hardening case of the gear tooth. The root was to have a sufficient case depth whereas the gear tooth top was to not be overheated. A preferred hardening profile is shown in Figure 121.

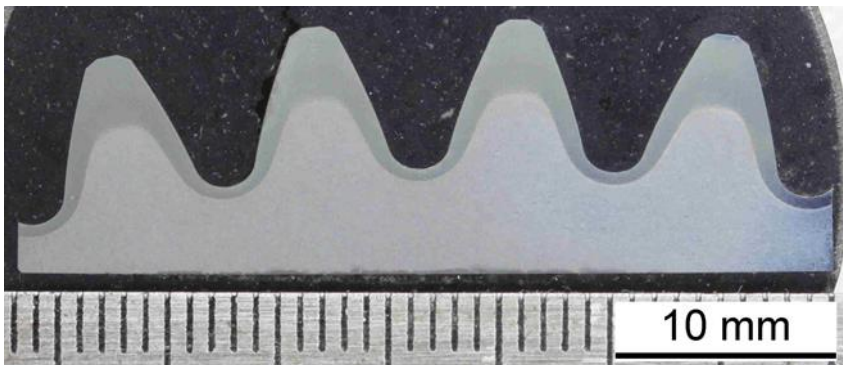


Figure 121. Cross section from the middle of a gear after a successful induction hardening treatment.

However, cracking of tooth edges was the major challenge in this work, see Figure 122(a). The gear delivered to the tests were chamfered on the tooth tip, cp. Figure 114(c). However, the current chamfering process does not machine the tooth flanks. Several tests were made to modify the induction hardening sequence to avoid cracking of the tooth edges. Then it was agreed to test an additional chamfering of the entire tooth flank, see Figure 123. This turned out to solve the cracking problem, cp. Figure 122(b).

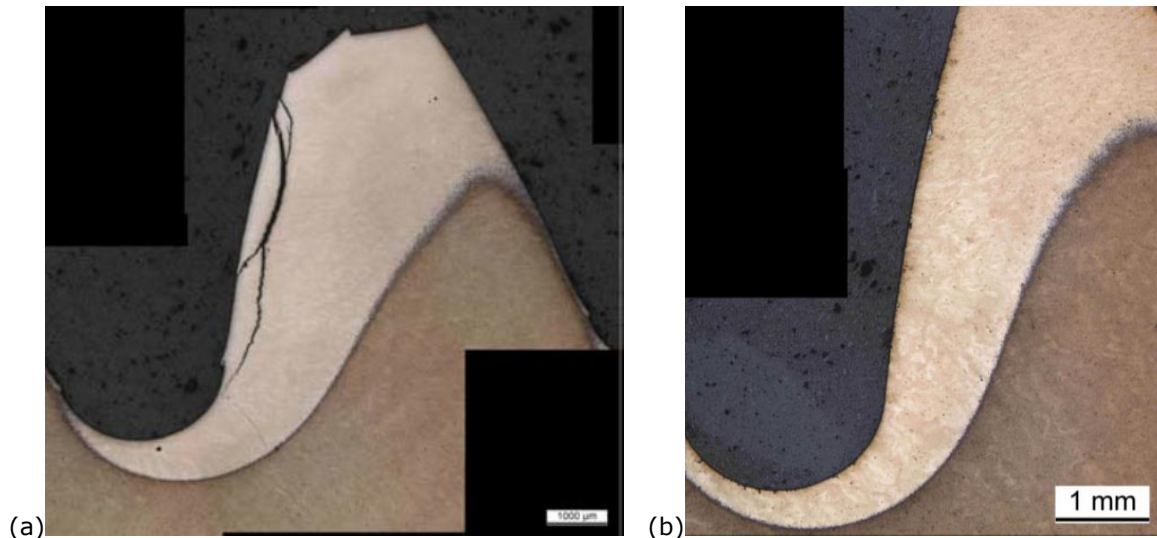


Figure 122. Cross sections of gear teeth. 8a) A tooth with the conventional chamfering process and (b) a gear tooth with a 1.5 mm chamfer manually ground at EFD.

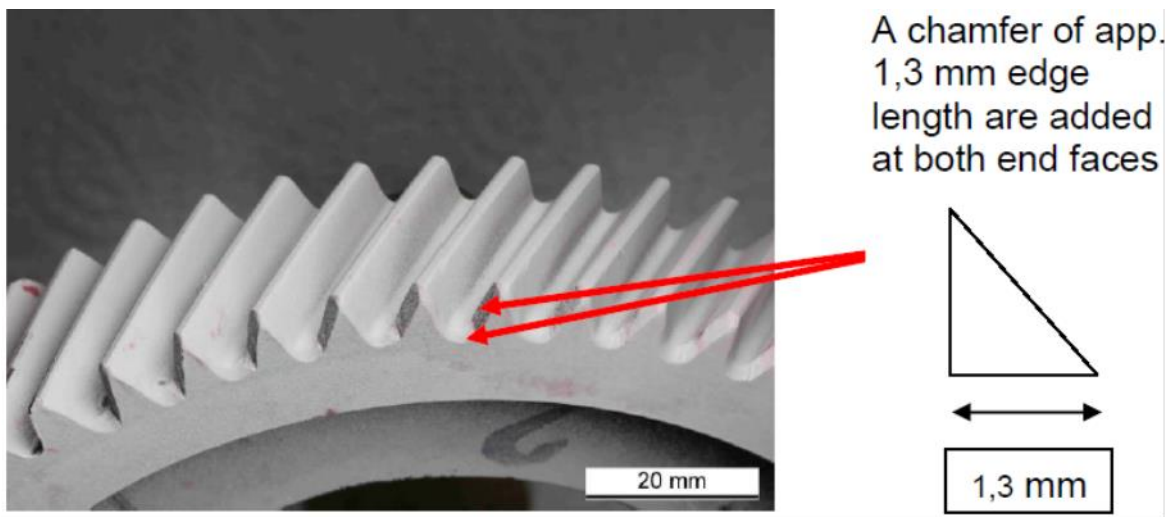


Figure 123. Schematic of a gear with chamfering of the entire tooth profiles.

After having optimized the induction hardening process and after having introduced the chamfering of the entire tooth profile the induction hardening process of this particular gear was fixed. The hardened cases of cross sections at the two edges and in the middle of the gear are found in Figure 124.

It is clear that there is an uneven hardening profile at the tooth edges. However, the optimization has been made so to ascertain a sufficient case depth of the gear root also at the edge positions, to guarantee the bending fatigue strength of the gear root. It should be noted that the uneven case depths of the tooth flanks is extremely difficult to avoid the given the helical angle of the teeth.

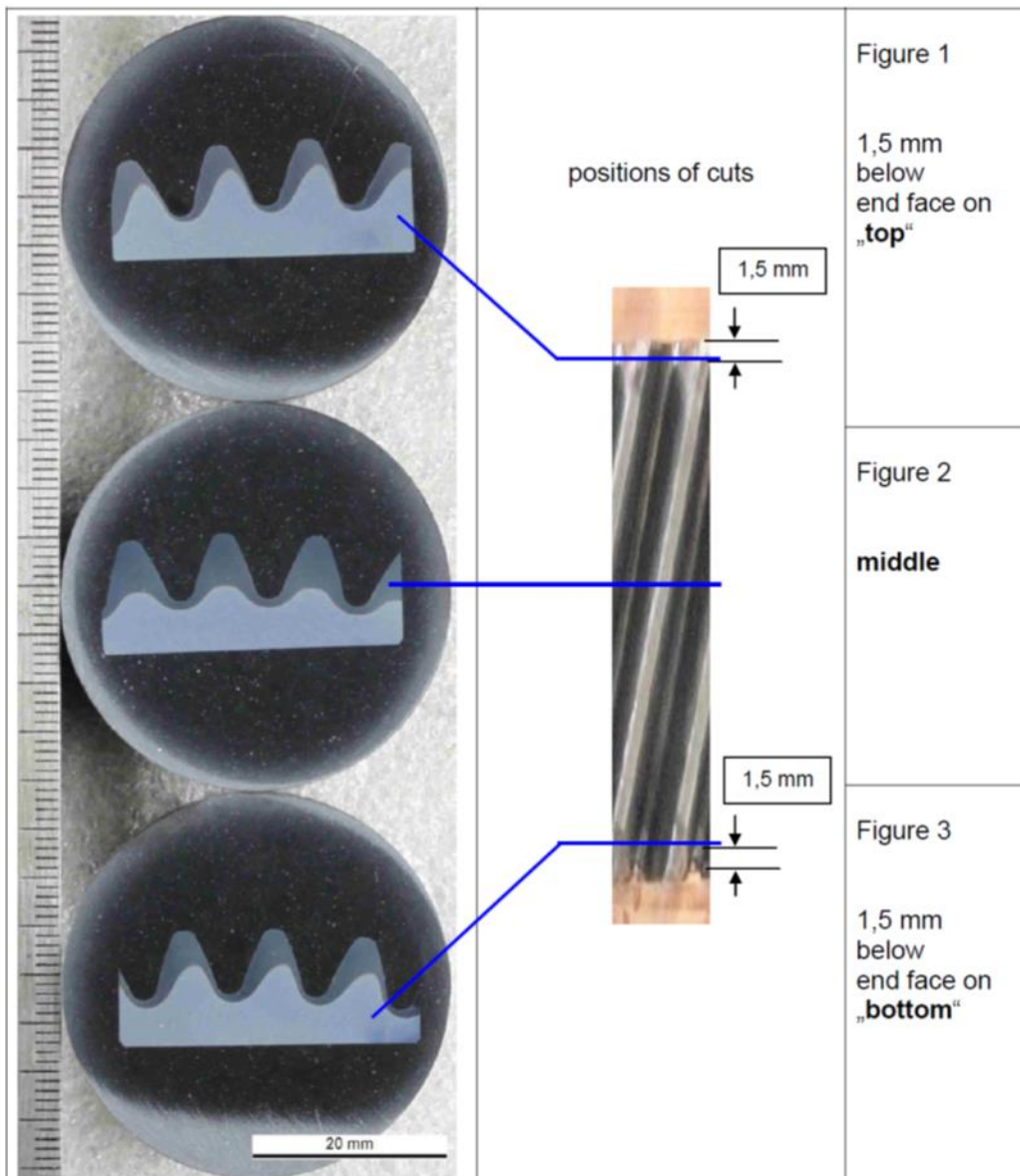


Figure 124. Cross sections of the optimized hardened gear tooth obtained.

Task 6.4. Comparison of total manufacturing costs and component properties, case hardening vs. induction hardening

COST OF WORK PIECE MATERIAL AND FORGING PROCESS

The following aspects are dealt with:

- The cost of steel: The cost of steel is more linked to e.g. the casting process of the steel plant, be it ingot casting or continuous casting, than any difference in price linked to the change of carbon content. The conclusion is that the difference in price between a 18CrMo4 and a 50CrMo4 steel both manufactured with the same casting method is negligible.
- The forging process is the same as well. Small differences in austenitizing temperature are foreseen. However, when introduced in large scale production this should not in principle introduce any extra cost in the forging process.

HEAT TREATMENT AND ASSOCIATED SYSTEMS

It was agreed that a comparison of investment should be made between either a new modern line for batch carburizing process and a corresponding line for induction hardening. Realistic data of investment of a new carburizing line was obtained from the Verrone plant of Fiat Powertrain. The specifications of a line of induction hardening of this particular demonstrator gear was obtained from EFD.

The calculation is based on a yearly production of 550 000 parts of the demonstrator gear. This is considered by any means in the automotive industry a mass production. As such this particular gear is very useful and realistic for the actual possibility of induction hardening. The working time of a furnace system per year is said to be 6300 hours. Furthermore, the cost of electricity is assumed to be 0.11 € per kWh.

Some important aspects of the comparison are summarized below.

1. Tempering of the gears after induction hardening. There is still a debate whether there is an actual need of tempering after induction hardening. Some studies have shown that the toughness of test samples is better with induction hardening without tempering than that after conventional full carburizing process. However, since that is yet to be fully understood and implemented, a tempering through low power induction is included in this comparison. This is a station parallel to the high powered hardening line. Both lines can be fed with parts by the same robot.
2. The total working time per year is given by 22 h/day, 280 days and 3 shifts, sums to 6300 hours per year.

The carburizing process

The carburizing is assumed to be an integrated pre-heating, carburizing, quenching and tempering equipment of low pressure type, see Figure 125. Palettes of 80 gears each are loaded into the furnace. The input data has been acquired and by experience and estimations, see Table 24. The process time of the entire carburizing process is estimated to 8,5 hours. This can be considered a short process time of carburizing. It is a result of the integrated furnace system considered.

The total estimation of carburizing with respect to costs, energy consumption and staff costs are summarized in Table 25. The cost of heat treatment through carburising is estimated to **2,41 € per gear**.



Figure 125. The new low pressure carburizing line of Fiat Powertrain. (a) Photo and (b) schematic of the furnace charging.

The induction hardening process

The induction hardening system is a robotized in-line system. There is a high cost of this system associated with the requirement of extremely fast heating of the gear, meaning that the power supply must deliver extremely high power, though in the time of about 1 second. This is taken into account for in comparison.

An issue not dealt with in the project is the tempering process. All carburized gears are tempered for about 1-1.5 h at 180-200°. This is done as a final step of the batch carburizing in dedicated furnace. The toughness obtained on induction hardened components and the need of subsequent tempering is not fully understood. Consequently, we must include a tempering step after the induction hardening. This can be done in a batch process after the induction hardening. However, this is undesired since we lose the in-line feature of induction hardening. Such a batch tempering would increase the process time from about 1 minute for the induction hardening itself to about 3 hours (!!). Therefore, to fully explore the possibilities of induction hardening it was chosen to include tempering by induction heating, cp. Table 24. This is done in a parallel station that is fed with gears by a robot. The tempering power is only about 17 kW, as compared to that of the induction hardening of 1278 kW. Such a station is at significantly lower cost (about 30 000 €). The time of induction tempering is typically 1 minute and the temperature is about 230°C.

The total estimation of induction hardening with respect to costs, energy consumption and staff costs are summarized in Table 26. Two bottom lines are given, one with the induction hardening process itself and the other with a batch based tempering included. The cost of heat treatment through induction hardening is estimated to **0.64 € per gear**. It becomes clear that the question of tempering subsequent to induction hardening is extremely important for the production economy of gear hardening through induction hardening.

Table 24. Input data of the hardening routes compared.

Carburizing Input:				Induction hardening Input:	
Investment and associated equipment kEUR	2500				1500
Life time of equipment Years	10				10
Electrical cost, EUR/kWh	0,11				0,11
Preheating Power kW	70				178
Preheating time [h]	1		[seconds]		3,6
Heating Power kW	255				1278
Carburizing time [h]	2,5		Induction hardening [seconds]		0,15
Gas quench power kW	100		Quench power (water spray) [kW]		5
Quenching time [h]	0,5		[seconds]		25
Working hours one shift/year	1500		Working hours one shift/year		1500
Number of shifts	4		Number of shifts		4
Power for handling kW	40		Power for handling and robot kW		5
Power for tempering furnace kW	70		Induction tempering power kW		17
Manual labour hourly rate	60				60
No. gears per batch (cell)	80				1
			Process time of hardening [s]		40
Standstill before carburizing [h]	0,5				
Standstill after carburizing [h]	0,5				
			Power for handling tempering furnace kW		10
Tempering preheating time	1				1
Tempering time [h]	2		Induction tempering [s]		60
Gas quenching time	0,2				
			Investment tempering furnace [k€]		250
Process time carburizing total [min]	510		Process time induction hardening & tempering total [min]		2

Table 25. Summation of costs, times and energy of carburizing of the demonstrator gear.

	Cost EUR/gear	Cost total/year EUR	Energy Per gear [kWh]	Energy Total/year	Space [m * m]	Cycle time [sec]	Process time [min]
Investment and associated equipment	0,45	250000					
Energy consumption total	0,64	353100	5,8	3210000			
Maintenance	0,090909	50000					
Space requirement carburizing					12x30 m		
Energy consumption carburizing & process time	0,972813					180	240
Space requirement tempering					10x5		
Energy consumption tempering & process time						142	190
Loading & unloading of pallettes, transportation & standstill	0,25					105	30
SUM	2,41	653100	5,8	3210000	400	427	570

Table 26. Summation of costs, times and energy of induction hardening of the demonstrator gear.

	Cost EUR/gear	Cost total/year EUR	Energy Per gear [kWh]	Energy Total/year	Space [m * m]	Cycle time [sec]	Process time [min]
Investment and associated equipment	0,27	150000					
In-line process						39	1
Energy consumption hardening process	0,025	14000	0,23	127000			
Energy consumption handling and robot	0,20	108000	0,05	30000			
Maintenance	0,018	10000					
Space requirement					8 * 8		
Tempering energy	0,084	46200	0,76	420000			
Tempering & time	0,045	25000			5 * 10	100	1
SUM	0,64	353200	1,05	577000	115	2	2

MACHINING PROCESSES

The machining processes included in the gear production of today are: green turning (several steps), hob milling, drilling, chamfering and grinding. The two steels that are to be compared with respect to machinability are the reference 18CrMo4 and the 50CrMo4 quench-and-tempered to 350 HB (QH-T1), since the latter was agreed and used for the demonstrator manufacturing.

In WP3 the machinability in rough turning and hob milling are obtained. The cutting speed comparison and tool life numbers are compared in Table 27. The engagement times of the cutting processes of the C635 gear at Fiat powertrain is given in Table 28. The entire machining steps is given in ANNEX 6 Figure 149.

Table 27. Summary of data used in the calculation of machining costs.

Steel	Rough turning		Gear hobbing	
	Cutting speed	Tool life [min]	Cutting speed	Tool life [GTM]
18CrMo4 (C-IA)	424	15	200	3
50CrMo4 (QH-T1)	214	15	80	1.5

Table 28. Engagement time for each operation of the machining process of the C635 gear.

Operation	Time [s]
Internal facing	13
External facing	13
Finishing facing	8
Turning and facing	13
Turning and finishing facing	23
Finishing facing	13
Finishing facing	8
Hob milling	116
Chamfering	15
Snagging	15
Drilling	11
Boring	7
Hard part turning	26
Tooth grinding	125

A semi-automatic machining production was assumed. Each machine is assumed to need about 40% man time of a hourly cost of 50€ meaning that the actual staff cost at each machine is 20€. The machine time itself was divided in machining time, cp. Table 28 and an additional set-up time. The set-up time means the time of loading, unloading, clamping, unclamping of components, as well as exchange of cutting tools. Furthermore, the costs of cutting tools were estimated. The consumption of cutting tools was estimated given the tool life tests of WP3 in rough turning and in hob milling. The number of PCBN tools in hard part turning was roughly estimated given the tool life tests of WP4. The numbers of tools for drilling and chamfering were estimated. Given the in-data from WP3 and WP4 the total cost of the complete machining sequence of the C635 gear using the 18CrMo4 steel was calculated to **9 €** each, see Table 29.

The machining sequence using the 50CrMo4 steel through the induction hardening route introduced the following changes:

- **Green turning:** Almost 50% of cutting speed (214/424) and a doubled consumption of turning inserts.
- **Hob milling:** More than 50% reduction in cutting speed (80/200), a doubled consumption of hobbing tools with respect to both new tools (1000 €) and services (200 €).
- **Chamfering** is not studied in this project. However, the optimisation of the induction hardening process at the end of the project stresses the importance. Probably an improved chamfering process must be introduced. The chamfering cost is doubled as compared to the 18CrMo4 steel.

- **Drilling** is not studied either. The same change as in green turning is assumed.
- **Hard part turning of faces:** Induction hardening introduces significantly less distortion on a macro scale of a component as compared with carburizing, linked to the localised heating and quenching. Consequently, the major part of the hard part turning is eliminated. Only one operation remains as post in the table.
- **Tooth grinding:** The tooth grinding is assumed to be easier with induction hardened steel, primarily due to less material to remove thanks to the less distortion risks associated with induction hardening.

Based on the above assumptions and changes from the reference machining sequence of the 18CrMo4 steel, the total cost of machining operations of the C635 gear made of 50CrMo4 and induction hardened is **12 €.**, see Table 30.

The following comments can be made:

- The tooling cost is extremely small in these machining processes in comparison to the costs of machines and staff. This is relatively established as argument in marketing of cutting tools. The tooling cost is small in comparison to the potential cost saving in a production with higher throughput, meaning less machine time per produced part.
- The machine cost is roughly double to that of the staff cost.
- Almost three machines are locked up the full year in just the production of this C635 gear in green turning. (16130 hours of machine time compared with the 6300 hours available of the year.

Table 29. Summary of costs associated to machining processes of the demonstrator gear (18CrMo4) made through carburizing.

Operation	Tools [#]	Staff cost [€/h]	Tooling cost (€/tool)	Machine cost [€/h]	Sharpening [€]	Time in machine [h]	Set-up time [s]	Machining time [s/pc]	Cost (€)/year
Green turning	Tooling	1000	10						10 000
	Machine			40		16130	15	90,6	645 200
	Staff					16130	15	90,6	322 600
Hobbing	Tooling new hobs	45	1000						45 000
	Tooling sharpening Machine	360			200				72 000
	Staff			40		20070	15	116,4	802 800
Chamfering	Tooling	50	500						25 000
	Machine			40		4580	15	15	183 200
	Staff					4580	15	15	91 600
Drilling	Tooling	200	50						10 000
	Machine			40		7850	40	11,4	314 000
	Staff					7850	40	11,4	157 000
Finishing	Tooling	550	100						55 000
	Machine			40		6230	15	25,8	249 200
	Staff					6230	15	25,8	124 600
Tooth grinding	Tooling	50	200						10 000
	Machine			40		22120	20	124,8	884 800
	Staff					22120	20	124,8	442 400
Total cost/year (€)									4 846 k€
Total cost/pc									9 €

Table 30. Summary of costs associated to machining of the demonstrator gear (50CrMo4) made through induction hardening.

	Operation	Tools [#]	Staff cost [€/h]	Tooling cost (€/tool)	Machine cost [€/h]	Sharpening [€]	Time in machine [h]	Set-up time [s]	Machining time [s/pc]	Cost (€)/year
Green turning	Tooling	2000		10						20 000
	Machine				40		29790	15	180	1 191 600
	Staff		20				29790	15	180	595 800
Hobbing	Tooling new hobs	90		1000						90 000
	Tooling sharpening Machine	720			40	200	46750	15	291	1 870 000
	Staff		20				46750	15	291	935 000
	Tooling	75		500						37 500
Chamfering	Machine				40		6880	15	30	275 200
	Staff		20				6880	15	30	137 600
	Tooling	400		50						20 000
Drilling	Machine				40		9630	40	23	385 200
	Staff		20				9630	40	23	192 600
	Tooling	100		100						10 000
Finishing turn	Machine				40		3510	15	8	140 400
	Staff		20				3510	15	8	70 200
	Tooling	50		200						10 000
Tooth grinding	Machine				40		12530	20	62	501 200
	Staff		20				12530	20	62	250 600
	Total cost/year (€)									6 877 k€
	Total cost/pc									12 €

The costs per category of machining operation are summarized in Figure 126.

The following comments can be made:

- The cost per machining process ranges from about 0.8-5 €.
- Hobbing and tooth grinding appear to be most costly operations.
- The highest cost foreseen is the hob milling of the 345 HB 50CrMo4 steel.
- The cost of green turning and hob milling are roughly doubled from using the 18CrMo4 to the 50CrMo4.
- Some saving is foreseen in the minimized hard part turning and possibly in less need of tooth grinding.
- A number of solutions can be made to reduce the extra costs associated with the introduction of a new steel. The green turning performance would be very much improved by using harder carbide grades, e.g. Coromant GC4205. These are more heat resistant than the tested GC4215. That would improve the tool life of the 345 HB 50CrMo4 by perhaps 30% from the current results.
- The solution to high productivity in gear hobbing is currently being introduced. It is based on new concepts of hobs and skyving cutters made of cemented carbides. Today there are hobs with both solid carbide tools and with indexable inserts. This development has taken huge steps in the past year. The new tool materials and composites for gear cutting enable a new field of steels with higher hardness as compared to conventional carburizing steels.

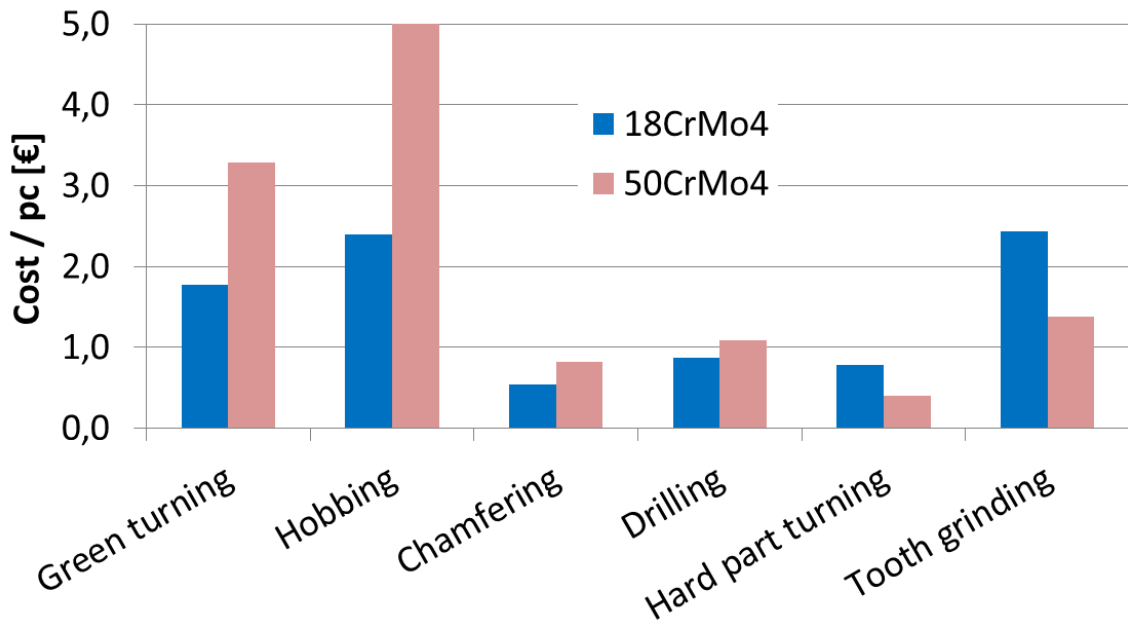


Figure 126. Summary of costs for each machining step of the C635 gear made through 18CrMo4 carburized and 50CrMo4 as induction hardened.

EXPLOITATION AND IMPACT OF THE RESEARCH RESULTS

The MAC D project enables a comprehensive comparison today's manufacturing route of a transmission gear through carburizing and a possible future manufacturing route through induction hardening. The following aspects are dealt with in the project:

- The selection of a steel that is suited for induction hardening of the demonstrator gear. The 50CrMo4 was chosen. This steel has a carbon content high enough to ensure a sufficient hardness uptake in the induction hardening process.
- Microstructures of the as-delivered work piece material has been dealt with in the machinability tests.
- The optimization of the induction hardening process throughout the project. Most attention and effort was spent on the process optimization for the demonstrator gear. In addition samples aimed at mechanical tests has also been induction hardened and compared with the corresponding carburized samples.
- Fatigue and mechanical properties of test samples and gears.
- The entire manufacturing route of the demonstrator gear, including the steel specification, forging process, machining processes and the current heat treatment through carburizing.
- The comparison of manufacturing costs associated with the reference gear made through carburizing and the possible gear made of 50CrMo4 through the induction hardening route.

Actual applications

Induction hardening is used today in a number of applications. Shafts is the primary component group:

- The cams of cam shafts are induction hardened in some combustion engine plants, with great success.
- Crank shafts have been subject to significantly increased torque in recent years as lined to the increase in engine torque of modern turbo charged engines. Induction hardening is therefore introduced in the radii surrounding the bearing positions to locally increase the fatigue strength of the crank shaft.
- Most drive shafts are induction hardened.

TECHNICAL POTENTIAL OF INDUCTION HARDENING OF GEARS

The project has shown a realistic technical possibility to replace carburizing of gears by induction hardening. Several aspects of this have been elucidated, the steel selection, the as-delivered microstructure, the development of the induction hardening process and the tailoring to a dedicated gear geometry and how to succeed with the fatigue strength of an induction hardened gear. These aspects are described in more detail below.

The project have given a good idea what kind of steel that is most suitable for induction hardening of gears. The steel should be of C50, 50CrMo4 or similar. By experience it is established that the hardenability should be kept within relatively tight tolerance from batch to batch in a mass production of such a component.

Furthermore a preferred microstructure of the as-delivered condition from the forging stage has also been established. Given the extremely short time of heating before quenching of this gear the rule of thumb is as dissolved carbon structure as possible the better for the hardness uptake after induction hardening. The project investigated a quench-and-tempered microstructure of 345 HB that was found suitable.

Induction hardening of helical gears will always be difficult, due to the inherent angles at the tooth edges. One side (flank) of the tooth will be more heated than the other. The effort and success of the project was to tailor an induction hardening process that generated a beneficial case of hardened steel in the root position. That was obtained also very close to the tooth edges. However, one of the tooth flanks on the respective side of the gear showed uneven hardening. It will probably not affect the root fatigue strength. However, it should be investigated more in detail with respect to the actual loads and possibility of contact fatigue of the tooth flanks.

Note that induction hardening of spur gears is much more straightforward. A large number of such applications exist today.

Fatigue tests were made using test sample geometries. The biaxial fatigue tests indicated that it is possible to increase the fatigue strength using induction hardening as compared with carburized

steel. Note however that induction hardening is an extremely geometry dependent technique. Fatigue tests aiming at actual industrial introduction of a certain transmission part must be made on that particular component.

ECONOMIC POTENTIAL OF INDUCTION HARDENING OF GEARS

The direct costs of heat treating the demonstrator gear by low pressure carburizing has been compared with a robotised cell with induction hardening followed by short time tempering through induction. The investment cost, the energy costs, staff costs and maintenance costs have been included. The costs are as follows:

Carburizing: 2.41 € per gear

Induction hardening: 0.64 € per gear.

Two important cost aspects have not been possible to conclude, (I). The aspect of in-line process vs batch process in the line of manufacturing steps and (II). The value of locked and unlocked values in the plant, aiming at the process time of carburizing of 8.5 h, as compared to that of induction hardening of only 2 minutes (!).

The costs associated with machining steps are described in detail. They are primarily based on data from the production of the Verrone plant of Fiat Powertrain. Some parts are described in detail, some are more or less assumed, as not being part of the work of the project, e.g. costs of drilling. Induction hardening is much less prone to distortion as compared with carburizing. An important possible saving is elimination or minimization of hard part turning steps.

The preliminary cost of the complete machining process of the C635 demonstrator gear made of 18CrMo4 and carburized is **9 €**. The corresponding cost of the 50CrMo4 being induction hardened is **12 €**.

One can note the general difference in cost estimation between the hardening processes and the machining processes. Given the fact that the heat treatment is one process itself, albeit complex, and the machining steps are multiple, the difference in costs between the two groups of manufacturing steps is realistic.

Any possible patent filing;

To the authors best knowledge no patent is to be filed from the project. The know-how that would maybe be possible and interesting to patent could be the know how and details of the successful induction hardening of the helical gear.

Publications / conference presentations resulting from the project;

This is up to discussion after the final report has been published.

LIST OF FIGURES

Figure 1. Examples of induction hardening of components. (a) A spur gear and (b) a shaft.....	5
Figure 2. Toughness values recorded with Charpy V testing. NOTE: The C-H was carburized at Fiat. The QL-H1, QH-H1 and B-H were induction treated at EFD Induction.	8
Figure 3. Cutting speed that corresponds to tool life of 15 minutes.	9
Figure 4. Configuration of the cutting tests. Face milling of bars made of the workpiece materials of the project.	10
Figure 5. The milling cutter. (a) overview in the tool holder and (b) typical wear of the cutting edge after a cutting test.....	10
Figure 6. Tool life tests in gear hobbing simulation. The volume of removed chip transformed to corresponding gear tooth metres.....	10
Figure 7. Bar chart of tool life tests in hard part turning. Bars from tests with carbide tools are given with black edges.	11
Figure 8. Combined tension-compression and torsional fatigue tests.	12
Figure 9. Fatigue limit results with confidence interval of 95%.	13
Figure 10. The model gear for component fatigue testing at Gerdau. (a) Mounted in the fatigue testing rig and (b) detail of the gear tooth geometry.	13
Figure 11. The primary demonstrator, a helical gear in a Fiat manual gear box for a small car.	14
Figure 12. Photo of an ongoing induction hardening cycle of the demonstrator gear.....	15
Figure 13. Etched cross sections of the induction hardened gear, positioned (a) 1.5 mm from the left hand edge, (b) middle and (c) 1.5 mm from the right hand edge.	15
Figure 14. Summary of costs for each machining step of the C635 gear made through 18CrMo4 carburized and 50CrMo4 as induction hardened.....	16
Figure 15. TTA diagram of 50CrMo4 with three realistic starting microstructures.	17
Figure 16. Blanks prepared for hard turning in the Hardinge lathe at CRF.	19
Figure 17. Schematic of the induction designed and manufactured for the toughness tests of 35CrMo4 and 50CrMo4.....	21
Figure 18. Cross section (etched) of an induction hardened Charpy sample. The approximate zones of hardening are given in orange lines.	21
Figure 19. Charpy samples prior to test. As-delivered (top), and heat treated (bottom).	22
Figure 20. (a) Configuration of induction hardening of tensile test samples. (b) The induction coil.	22
Figure 21. Hardness depth profiles of the induction hardened samples for tensile test made of 35CrMo4.	23
Figure 22. Hardness depth profiles of the induction hardened samples for tensile test made of 50CrMo4.	23
Figure 23. Automatic measure analyzer by LOM at GERDAU I+D laboratory.	24
Figure 24. Results of oxide analysis for (a) 18CrMo4 (C-IA), (b) 35CrMo4 (QL-T1, QL-T2) (c) 50CrMo4 (QH-T1 & QH-T2) and (d) 100Cr6 (B-SA).	25
Figure 25. Results of sulphide analysis for (a) 18CrMo4 (C-IA), (b) 35CrMo4 (QL-T1, QL-T2) (c) 50CrMo4 (QH-T1 & QH-T2) and (d) 100Cr6 (B-SA).	26
Figure 26. Bar charts of inclusionary characteristics recorded with PDA-OES. (a) Sulphides, (b) oxides and (c) complex inclusions.	27
Figure 27. Representative optical micrographs of the C-IA steel. (LOM).....	28
Figure 28. Hardness depth profiles of the work piece materials delivered from the steel manufacturing.	29
Figure 29. Hardness depth profiles of the work piece materials after secondary heat treatment....	30
Figure 30. Toughness values recorded with Charpy V testing. NOTE: The C-H was carburized at Fiat. The QL-H1, QH-H1 and B-H were induction treated at EFD Induction.	31
Figure 31. Taylor curves for the tested materials. $a_p=2$ mm and $f=0.4$ mm.	34
Figure 32. Cutting speed that corresponds to tool life of 15 minutes.	34
Figure 33. Preliminary comparison of ultimate strength and cutting speed at tool life 15 minutes (V15) of the tested steels.	35
Figure 34. Configuration of the cutting tests. Face milling of bars made of the workpiece materials of the project.	36
Figure 35. The milling cutter. (a) overview in the tool holder and (b) typical wear of the cutting edge after a cutting test.	36
Figure 36. Tool life tests in gear hobbing simulation. No. of passes vs. cutting speed.	37
Figure 37. Schematic of the gear tooth volume calculation for the concept of gear tooth meters comparison in tool life tests.	38
Figure 38. Tool life tests in gear hobbing simulation. The volume of removed chip transformed to corresponding gear tooth metres.....	38

Figure 39. Side views of the (a) primary cutting edge and (b) the secondary cutting edge of the turning cutting tool CNMG120408 PM GC2015. (SEM-BS)	39
Figure 40. Method of flank wear measurement.	39
Figure 41. Micrographs from tool life tests with 18CrMo4 (C-IA) at (a) 350 m min ⁻¹ , (b) 400 m min ⁻¹ , (c) 450 m min ⁻¹ and (d) 500 m min ⁻¹ . $a_p=2$ mm, $f=0.4$ mm/rev. (SEM-BS)	40
Figure 42. Micrographs from tool life tests with 35CrMo4 (QL-T2) at (a) 150 m min ⁻¹ , (b) 175 m min ⁻¹ , (c) 200 m min ⁻¹ and (d) 250 m min ⁻¹ . $a_p=2$ mm, $f=0.4$ mm/rev. (SEM-BS)	40
Figure 43. Flank wear after 2 minutes and after 6 minutes @ 225 m/min with tested steels.	41
Figure 44. Test setup of the chip map tests.	43
Figure 45. Test procedure to identify zones of controlled chip breakage	43
Figure 46. Chip map for QH-T1 at a cutting speed of $v_c = 225$ m/min	44
Figure 47. Limits for controlled chip breakage at a cutting speed of $v_c = 225$ m/min	44
Figure 48. Example of a work piece and a chip root of a quick stop test according to the method of Buda [BUDA68].....	45
Figure 49. Shear angle Φ and chip thickness ratio λ_h	45
Figure 50. Experimental setup of fundamental cutting test in finishing turning.	47
Figure 51. Workpiece specimen for interrupted orthogonal cutting in steel without heat treatment and cutting tool inserts.	48
Figure 52. Temperature measurement for two of performed test. (a) 10° and 75 m min ⁻¹ and (b) 34° and 100 m min ⁻¹	49
Figure 53. Radiation Temperature depending on the angle of material cut (for C-IA steel) and the Temperature depending on the steel for a given angle for material cut (34°). Cutting Speed: 75 m/min; $f = 0.2$ mm/rev	50
Figure 54. RT vs Material in hardness decrease in order.	50
Figure 55. T vs Vc for two different materials C-IA and QH-T1	51
Figure 56. Specific Forces vs interrupted angle.....	51
Figure 57. Specific Forces vs cutting speed.	52
Figure 58. Specific Forces vs material.	52
Figure 59. Qualitative comparison of results between the tested steels in the fundamental cutting tests.	53
Figure 60. Cutting tools of tool life tests in WP4. (a) Cemented carbide GC3205 grade and (b) PCBN tool of grade CB7014 with mechanically locked edge of PCBN.	55
Figure 61. Representation of the machinable length of the billet and the positions of the point of the reliefs.....	56
Figure 62. Photo from tool life test in hard part turning with CBN cutting tool in the Hardinge lathe.	57
Figure 63. Micrographs of the flank side of used cutting tools from tool life tests of the QL-H1 steel. (a) CC cutting tool and (b) CBN cutting tool. (LOM)	58
Figure 64. Summary of the tool life tests in hard part turning of the QH-H1 and QH-H2 materials.....	58
Figure 65. Bar chart of tool life tests in hard part turning. Bars from tests with carbide tools are given with black edges.....	58
Figure 66. Chart of SEM micrographs of the used CBN cutting tools in the tool wear study.	61
Figure 67. Test setup for rime zone analysis	62
Figure 68. Tool life graph for QH-H1 (50CrMo4) 58 HRC.	63
Figure 69. Roughness (Rz) after fine machining QH-H1 (50CrMo4) @ 58 HRC.	63
Figure 70. Fundamental investigations in tailored machining tests. The PCBN cutting tool rake face (a) as-received and (b) with EDM machined hole for optical fibre passage.	64
Figure 71. Temperature measurement signals.....	64
Figure 72. Temperature measurement signals.....	64
Figure 73. Temperature measurement signals at position P1 (Blind hole rake face)	65
Figure 74. Development of white layer formation, QH-H1 (50CrMo4)	66
Figure 75. Development of white layer formation, QH-H1 (50CrMo4).	66
Figure 76. Development of white layer formation, B-H1 (100Cr6).....	67
Figure 77. Residual stress profile, QH-H1 (50CrMo4, HRC59). (a) after the 16 th cut and (b) stress on the surface.....	67
Figure 78. Residual stress profiles, QH-H1 (50CrMo4, HRC59). (a) after the 16 th cut and (b) stress on the surface.....	68
Figure 79. Workpiece specimen for continuous orthogonal cutting of hardened steels and cutting tool inserts.	69
Figure 80. Workpiece specimens already prepared for different hardened steels.....	69
Figure 81. Test planning of the fundamental cutting tests in finishing.	70
Figure 82. Cutting edge geometry	70
Figure 83. Failed of the cutting edge at feedrate of 0.15mm	71
Figure 84. RT vs Cutting speed for different materials and feed rate	71

Figure 85. RT vs hardness for two different feed-rates	72
Figure 86. Cutting force vs Cutting speed	72
Figure 87. Specific cutting force vs Cutting speed	73
Figure 88. Feed force vs Cutting speed.....	73
Figure 89. Specific Feed force vs Cutting speed	74
Figure 90. Specific forces vs Material's hardness.....	75
Figure 91. C-H (18CrMo4) samples manufacturing process.	77
Figure 92. QH-H2 (50CrMo4) fine machined after the induction hardening manufacturing process.	77
Figure 93. Manufacturing process for the QL-H1 (35CrMo4) and QH-H2 (50CrMo4) specimens fine machined before the induction hardening.	77
Figure 94. Drawing of multiaxial test sample.....	78
Figure 95. Drawing of the rotating beam test samples.	78
Figure 96. Hardness profiles and etched cross sections of (a) C-H carburized, (b) QL-H1(35CrMo4) IH, (c) QH-H2 (50CrMo4) IF FMB and (d) QH-H2 (50CrMo4) IH FMA of the rotating beam test samples	80
Figure 97. Display of the position of X-ray analysis of the actual samples.	80
Figure 98. The model gear for component fatigue testing at Gerdau. (a) Mounted in the fatigue testing rig and (b) detail of the gear tooth geometry.	81
Figure 99. Summary of fatigue limit results in T-C tests.	83
Figure 100. Summary of fatigue limit results in torsional tests.	83
Figure 101. Summary of fatigue limit results in biaxial tests.	84
Figure 102. AMSLER four point bending test machine.....	85
Figure 103. Fatigue limit results with confidence interval of 95%.	85
Figure 104. S-N diagram for the different test series.....	86
Figure 105. SEM-micrographs of fracture surfaces (a) C-H carburized, (b) QL-H1, (c) QH-H2 FMB, (d) QH-H2 FMA.	86
Figure 106. Hardness depth and typical positions, marked with ●, ■ and ▲, of fracture initiation for the fatigue tested samples.....	87
Figure 107. Manufacturing process followed with the 18CrMo4 case hardened gears.	88
Figure 108. Manufacturing process followed with the QH-H2 treated gears.	88
Figure 109. Points of the gear tooth where the hardness was measured at different depths transversally to the surface (following the discontinuous lines).....	88
Figure 110. Fatigue test performed over gears in the RUMUL machine.	89
Figure 111. The primary demonstrator, a helical gear in a Fiat manual gear box for a small car. ..	92
Figure 112. The secondary demonstrator, a secondary gear shaft in a Fiat manual gear box for a small car.	93
Figure 113 (a) The machine set up and (b) the hob milling tool.....	94
Figure 114. Soft machining of the demonstrator part. (a) As-forged, (b) turned and (c) gear hobbled.	94
Figure 115. Fiat hardness specification and gear manufacturing piloting.	96
Figure 116. Micrographs of used cutting edges of the gear hob (a) as new, (b) after 4 gears and (c) after 34 gears.	98
Figure 117. (a) As-hobbed gear teeth and (b) the chamfering tool at Fiat Powertrain.	98
Figure 118. The induction hardening machine at EFD Induction in Germany. (a) Overview and (b) detail of the induction coil and the water spray devices for quenching.	99
Figure 119. Photo of an ongoing induction hardening cycle of the demonstrator gear.	99
Figure 120. The project consortium in front of the induction hardening device at EFD Induction.	100
Figure 121. Cross section from the middle of a gear after a successful induction hardening treatment.....	100
Figure 122. Cross sections of gear teeth. 8a) A tooth with the conventional chamfering process and (b) a gear tooth with a 1.5 mm chamfer manually ground at EFD.....	101
Figure 123. Schematic of a gear with chamfering of the entire tooth profiles.....	101
Figure 124. Cross sections of the optimized hardened gear tooth obtained.	102
Figure 125. The new low pressure carburizing line of Fiat Powertrain. (a) Photo and (b) schematic of the furnace charging.	104
Figure 126. Summary of costs for each machining step of the C635 gear made through 18CrMo4 carburized and 50CrMo4 as induction hardened.....	111
Figure 127. Micrographs at the periphery, middle and centre of steel bars, from the 35CrMo4 steel in the T1 condition. (LOM)	120
Figure 128. Micrographs at the periphery, middle and centre of steel bars, from the 35CrMo4 steel in the T2 condition. (LOM)	120

Figure 129. Micrographs at the periphery, middle and centre of steel bars, from the 50CrMo4 steel in (a) T1 condition and (b) T2 condition. (LOM)	121
Figure 130. Micrographs at the periphery, middle and centre of steel bars, from the 100Cr6 steel in the B-SA condition. (LOM)	121
Figure 131. Micrographs at the periphery, middle and centre of steel bars, from the 18CrMo4 steel in the C-H1 condition. (LOM)	121
Figure 132. Micrographs at the periphery, middle and centre of steel bars, from the 35CrMo4 steel in the QL H1 condition. (LOM)	122
Figure 133. Micrographs at the periphery, middle and centre of steel bars, from the 35CrMo4 steel in the QL H2 condition. (LOM)	122
Figure 134. Micrographs at the periphery, middle and centre of steel bars, from the 50CrMo4 steel in (a) H1 condition and (b) H2 condition. (LOM)	123
Figure 135. Micrographs at the periphery, middle and centre of steel bars, from the 100Cr6 steel in the H (through hardened) condition. (LOM).....	123
Figure 136. Micrographs of cutting edges used in tool life tests with 35CrMo4 (QL-T1). $a_p=2$ mm, $f=0.4$ mm/rev.....	125
Figure 137. Micrographs of cutting edges used in tool life tests with 50CrMo4 (QH-T1). $a_p=2$ mm, $f=0.4$ mm/rev.....	125
Figure 138. Micrographs of cutting edges used in tool life tests with 50CrMo4 (QH-T2). $a_p=2$ mm, $f=0.4$ mm/rev.....	126
Figure 139. Chip roots for all steel variants for a feed of $f = 0.3$ mm and a cutting speed of $v_c = 300$ m/min	126
Figure 140. Un-deformed chip thickness h and chip thickness h_{ch}	127
Figure 141. Cutting force measurement signals	128
Figure 142. Development of white layer formation, QH-H2 (50CrMo4)	128
Figure 143. Development of white layer formation, QH-H2 (50CrMo4)	129
Figure 144. Development of white layer formation, QL-H2 (35CrMo4)	129
Figure 145. Development of white layer formation, QL-H2 (35CrMo4)	130
Figure 146. Development of white layer formation, B-H1 (100Cr6)	130
Figure 147. A theoretical approach of fatigue load distribution of multiaxial T-C and torsional load tests. Representative hardness depth profiles are included to demonstrate how the test conditions can be modified to suit the tested heat treatment characteristics.	131
Figure 148. Drawing of the gear with measures and tolerances after machining operations.....	132
Figure 149. All relevant machining details of the demonstrator gear manufacturing.	133
Figure 150. Forging details. (I). Punching, (II). Piercing and (III). Orbital lamination (rolling)...	134

LIST OF TABLES

Table 1. Steel variants and denominations for the rough soft machining part of the project.	6
Table 2. Steel variants and denominations for the hard fine machining part of the project.	6
Table 3. Chemical composition from the heat in the steel plant. This is a selection of the most important elements.	7
Table 4. Numerical summary of tensile tests. Hardness values included.	8
Table 5. Steel grades selected in the project.	17
Table 6. Steel variants and denominations for the rough soft machining part of the project.	18
Table 7. Hardness values for the rough soft machining part of the project. The requested numbers are given on top and the actual numbers are given with bold text below.	18
Table 8. Steel variants and denominations for the hard fine machining part of the project.	19
Table 9. Requested target hardness values for the fine hard machining part of the project.	19
Table 10. Chemical composition from the heat in the steel plant.	24
Table 11. Microstructure study summary.	27
Table 12. Numerical summary of tensile tests.	30
Table 13. <i>Test conditions used for the screening test</i>	42
Table 14. <i>Testing matrix of the screening parameters</i>	42
Table 15 : Summary of more relevant results (engagement angle 34 °, Cutting speed of 75 m/min, feed rate of 0.2 mm).	53
Table 16. Summary of the tool life tests in hard part turning at CRF.	57
Table 17. Properties summary of the multiaxial fatigue test samples	78
Table 18. Summary of the different fatigue samples heat treatments and test conditions.	79
Table 19. Residual stress measurements of samples for fatigue tests.	80
Table 20. Hardened layer properties.	83
Table 21. Hardness profiles on different points of a gear tooth.	89
Table 22. Machining parameters of the helical gear. Rough facing, finishing facing and gear hobbing are given.	95
Table 23. Machining parameters of the 2nd gear shaft. Two roughing operations are given.	95
Table 24. Input data of the hardening routes compared.	104
Table 25. Summation of costs, times and energy of carburizing of the demonstrator gear.	105
Table 26. Summation of costs, times and energy of induction hardening of the demonstrator gear.	106
Table 27. Summary of data used in the calculation of machining costs.	107
Table 28. Engagement time for each operation of the machining process of the C635 gear.	107
Table 29. Summary of costs associated to machining processes of the demonstrator gear (18CrMo4) made through carburizing.	109
Table 30. Summary of costs associated to machining of the demonstrator gear (50CrMo4) made through induction hardening.	110

ANNEX WP1

ANNEX WP2

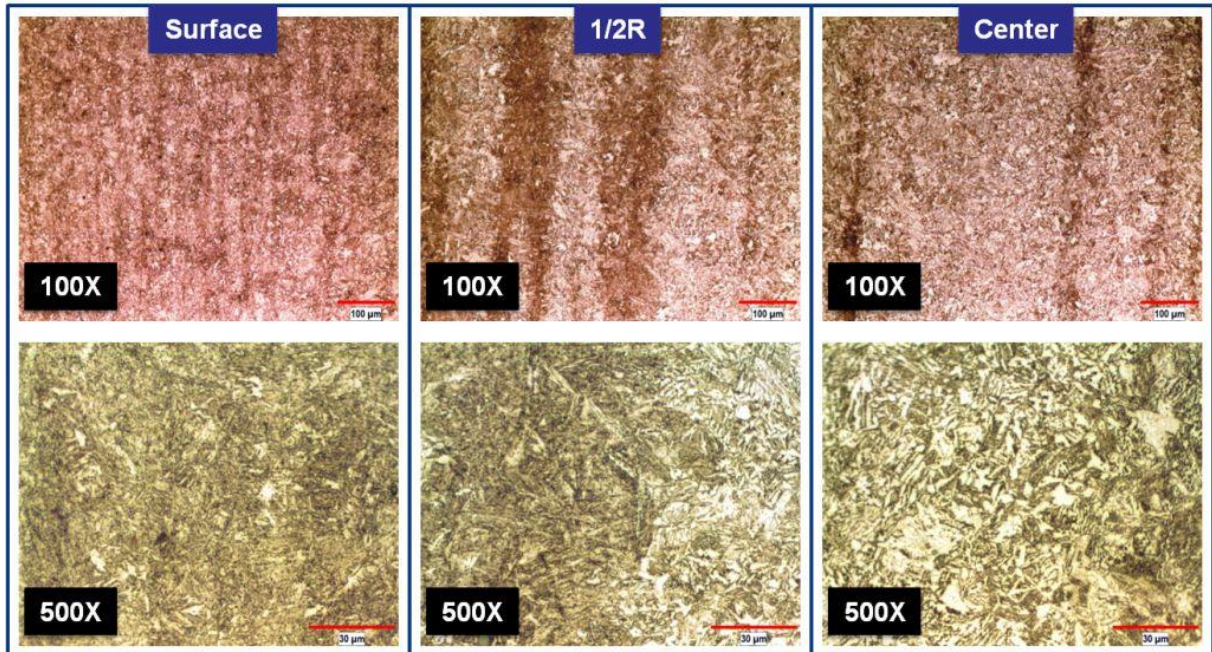


Figure 127. Micrographs at the periphery, middle and centre of steel bars, from the 35CrMo4 steel in the T1 condition. (LOM)

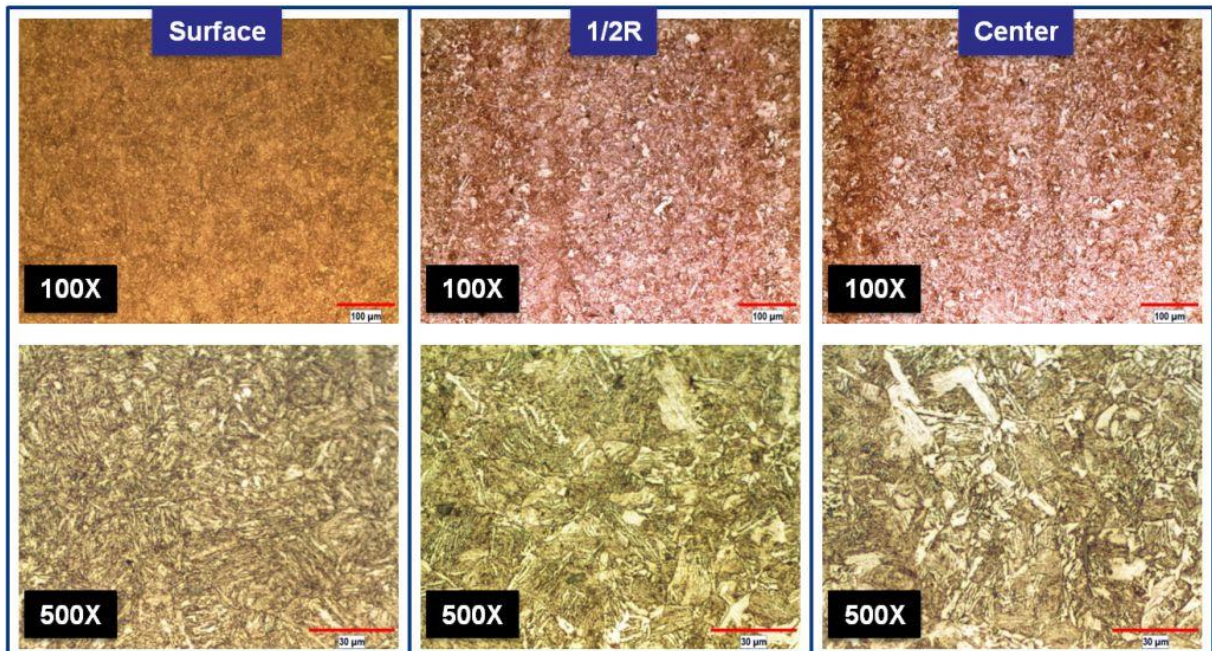


Figure 128. Micrographs at the periphery, middle and centre of steel bars, from the 35CrMo4 steel in the T2 condition. (LOM)

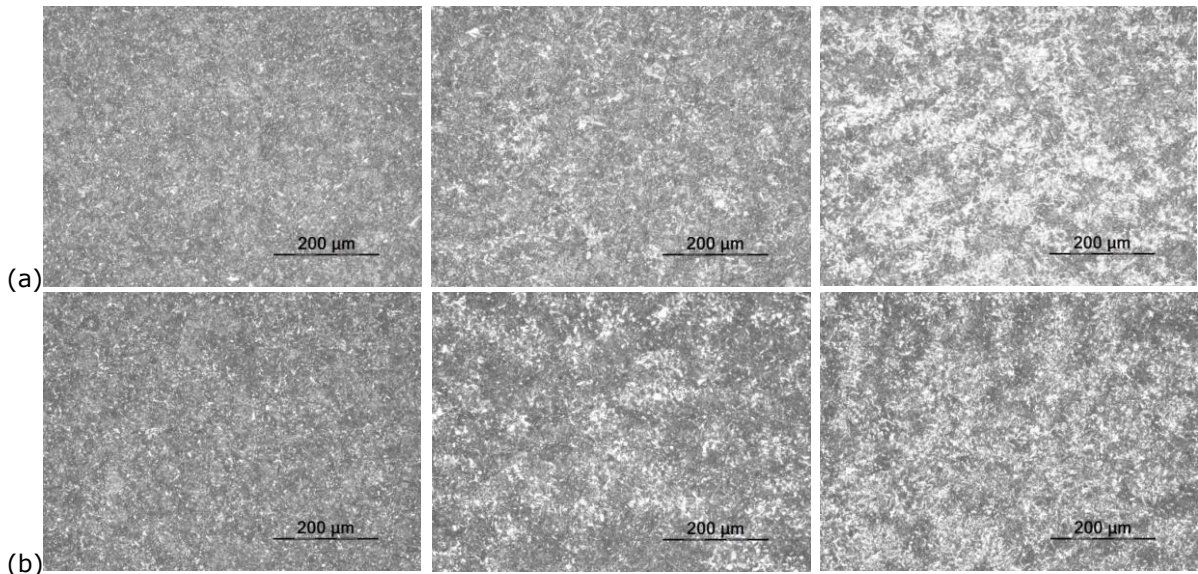


Figure 129. Micrographs at the periphery, middle and centre of steel bars, from the **50CrMo4** steel in (a) **T1** condition and (b) **T2** condition. (LOM)

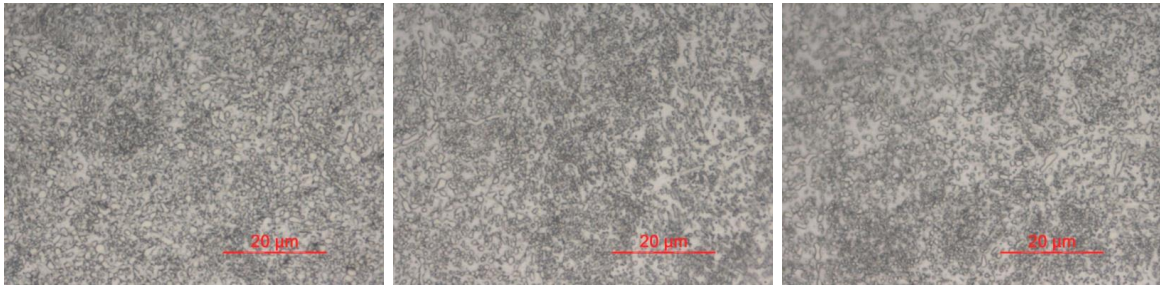


Figure 130. Micrographs at the periphery, middle and centre of steel bars, from the 100Cr6 steel in the B-SA condition. (LOM)

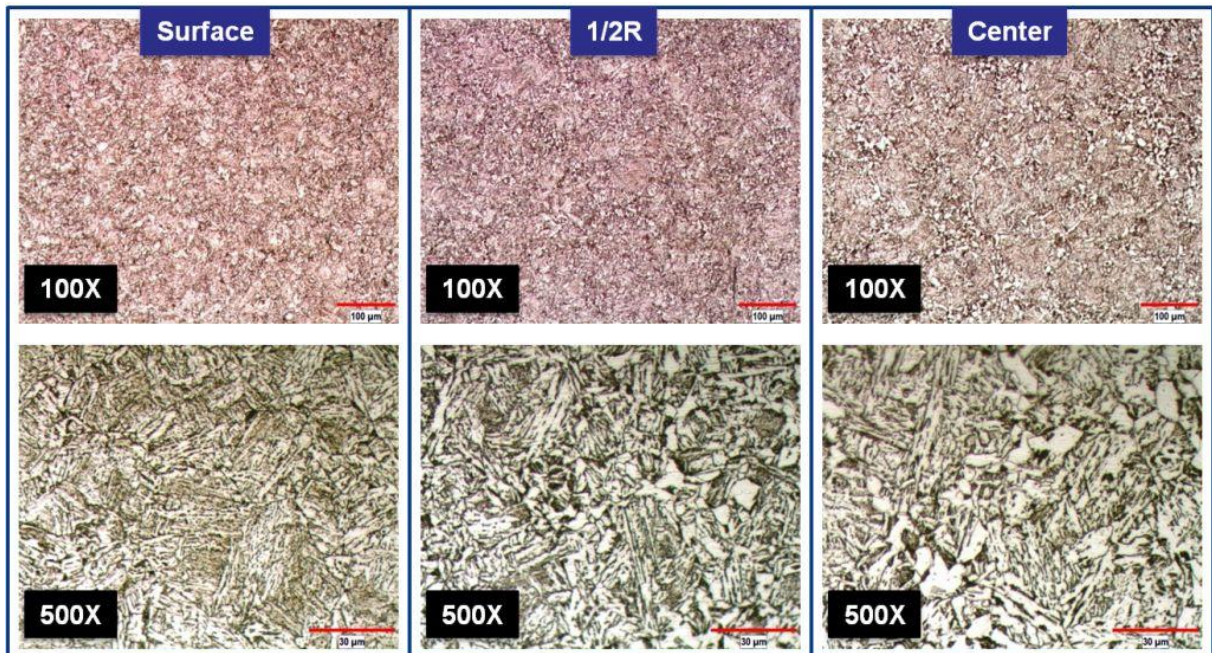


Figure 131. Micrographs at the periphery, middle and centre of steel bars, from the 18CrMo4 steel in the C-H1 condition. (LOM)

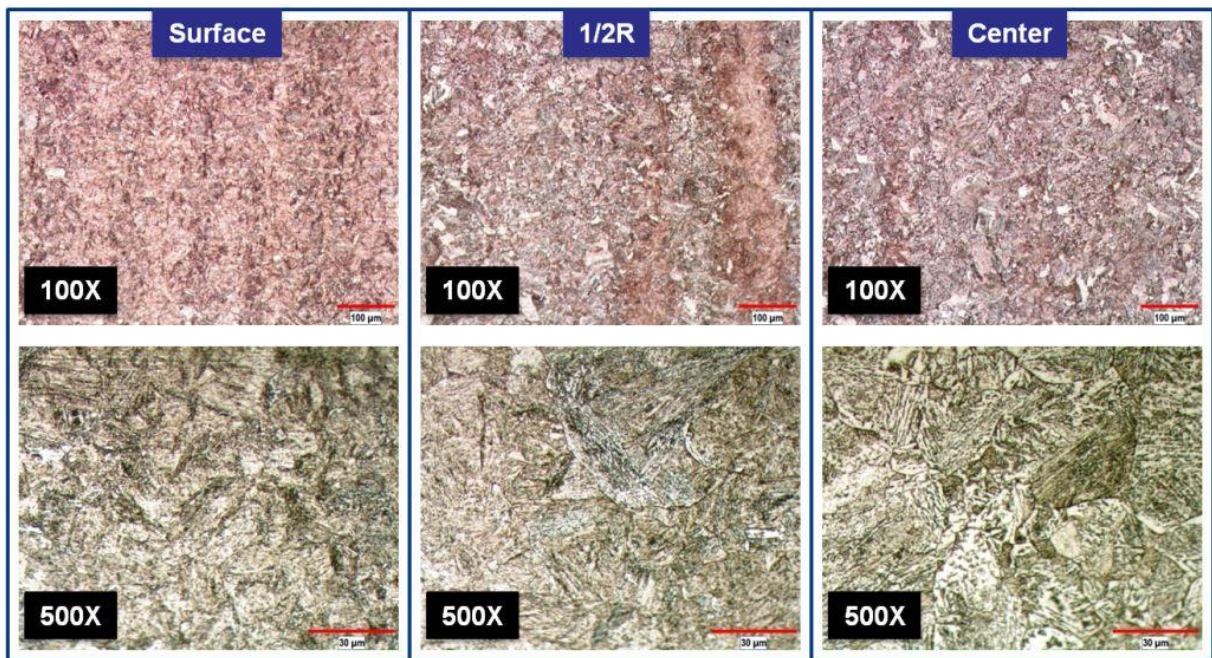


Figure 132. Micrographs at the periphery, middle and centre of steel bars, from the 35CrMo4 steel in the QL H1 condition. (LOM)

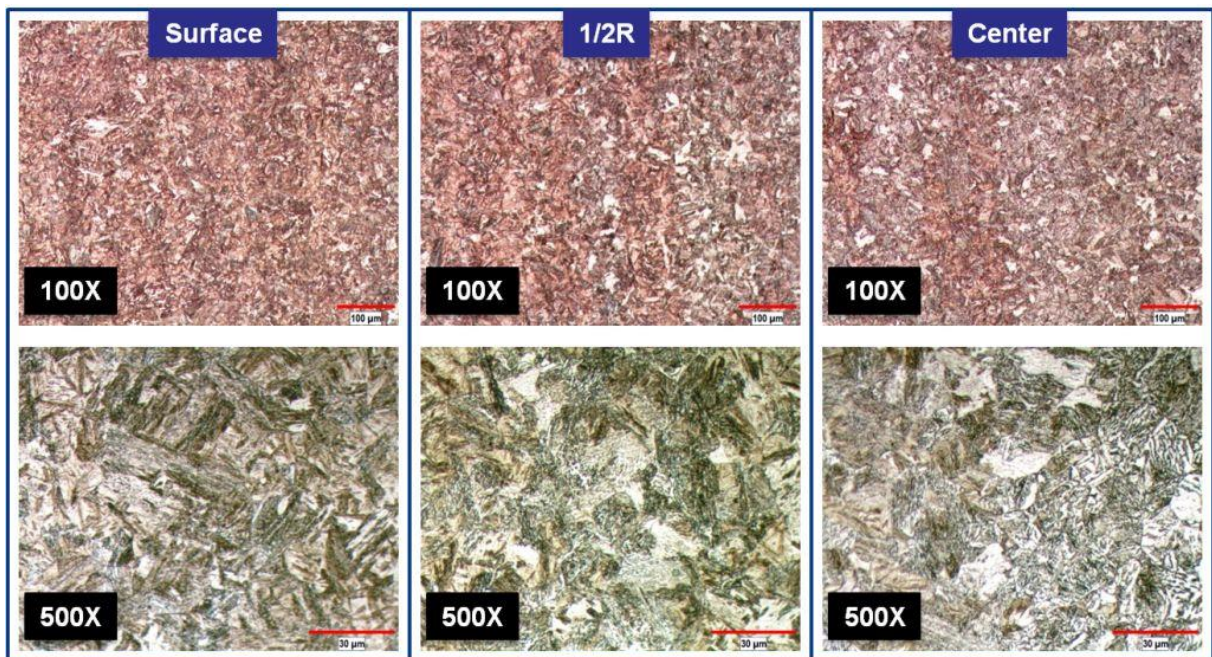


Figure 133. Micrographs at the periphery, middle and centre of steel bars, from the 35CrMo4 steel in the QL H2 condition. (LOM)

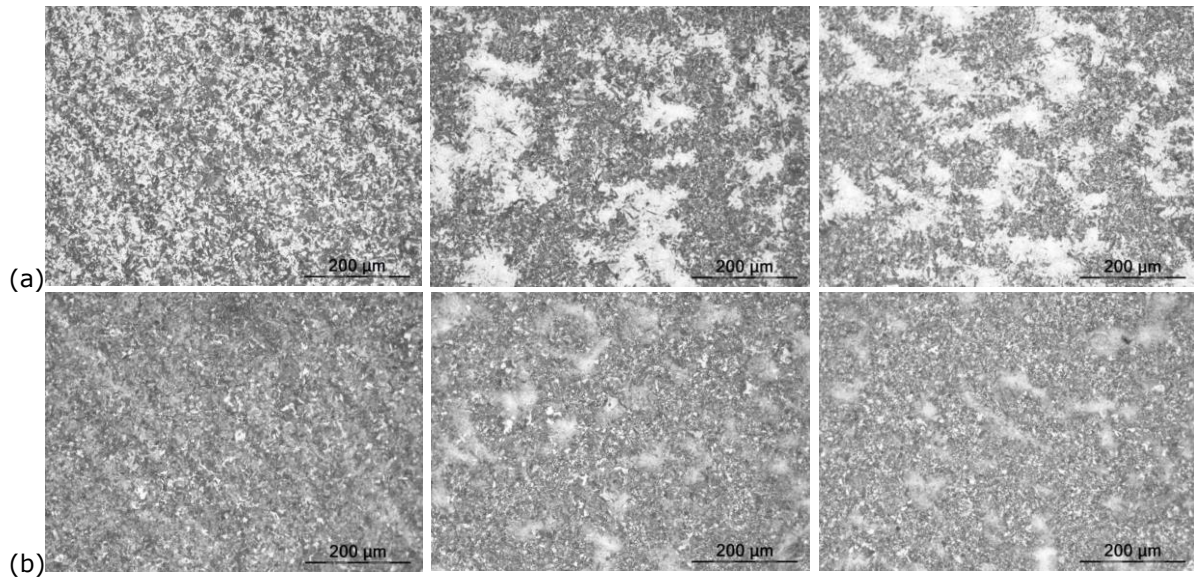


Figure 134. Micrographs at the periphery, middle and centre of steel bars, from the **50CrMo4** steel in (a) **H1** condition and (b) **H2** condition. (LOM)

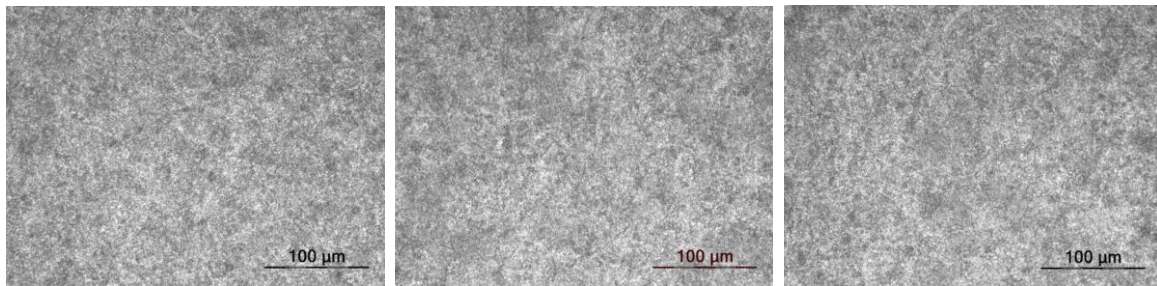
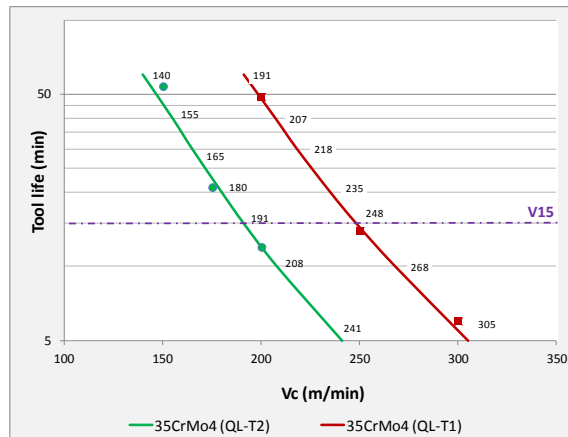
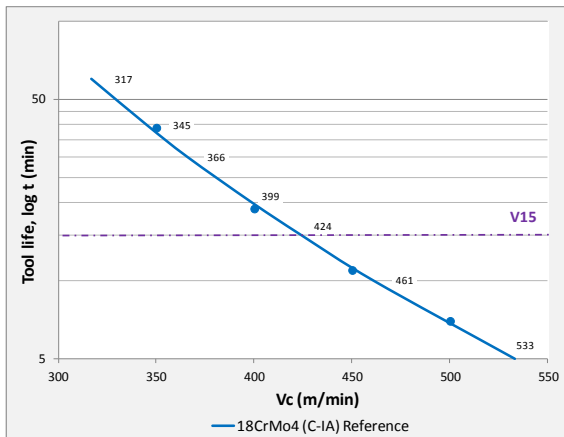


Figure 135. Micrographs at the periphery, middle and centre of steel bars, from the **100Cr6** steel in the **H** (through hardened) condition. (LOM)

ANNEX WP3

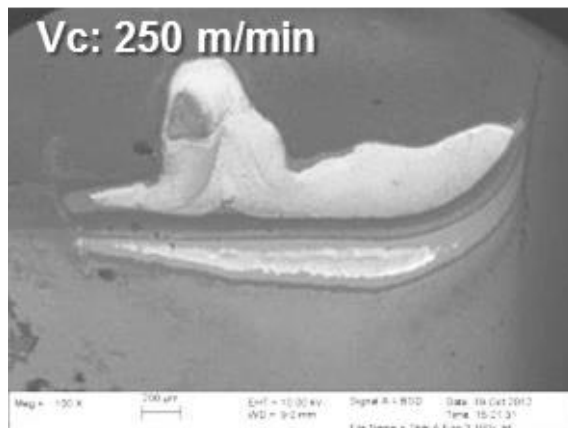
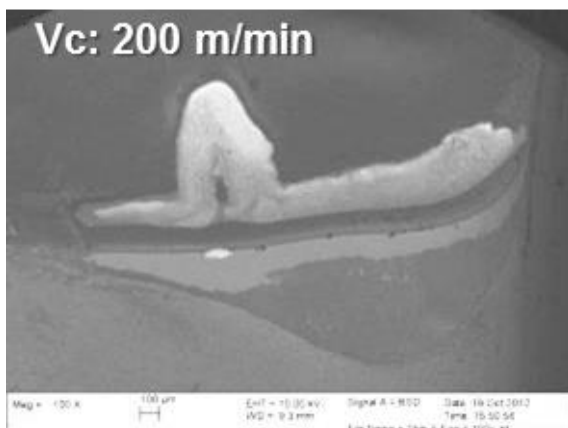


Hardness results for the materials after the secondary heat treatment.

		Hardness at different distances from the surface (HRC)							
Steel grade	Reference	5mm	10mm	15mm	20mm	25mm	30mm	35mm	40mm
18CrMo4	C-H1	24,3	24,2	23,5	22,2	23,1	22,4	20,3	22,2
35CrMo4	QL-H1	39,0	41,2	36,8	36,8	36,1	33,3	32,2	32,5
35CrMo4	QL-H2	45,7	45,6	43,8	44,1	39,8	38,9	37,0	37,2
50CrMo4	QH-H1								
50CrMo4	QH-H2								
100Cr6	B-H1								

Hardness results for the materials in the as-delivered conditions.

		Hardness at different distances from the surface (HB)							
Steel grade	Reference	5mm	10mm	15mm	20mm	25mm	30mm	35mm	40mm
18CrMo4	C-IA	160	161	161	157	147	147	145	145
35CrMo4	QL-T1	276	259	247	240	229	233	220	219
35CrMo4	QL-T2	304	306	306	287	283	280	275	261
50CrMo4	QH-T1								
50CrMo4	QH-T2								
100Cr6	B-SA								



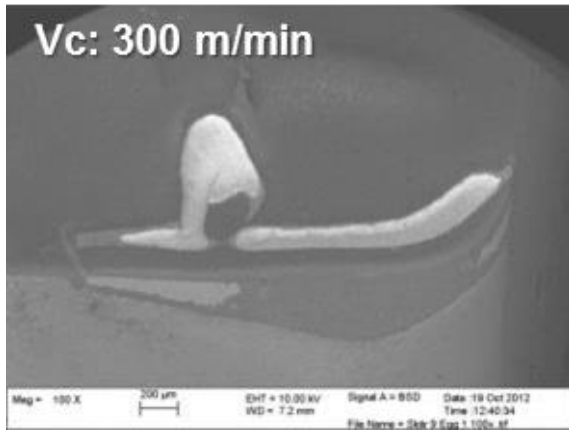


Figure 136. Micrographs of cutting edges used in tool life tests with 35CrMo4 (QL-T1). $a_p=2$ mm, $f=0.4$ mm/rev.

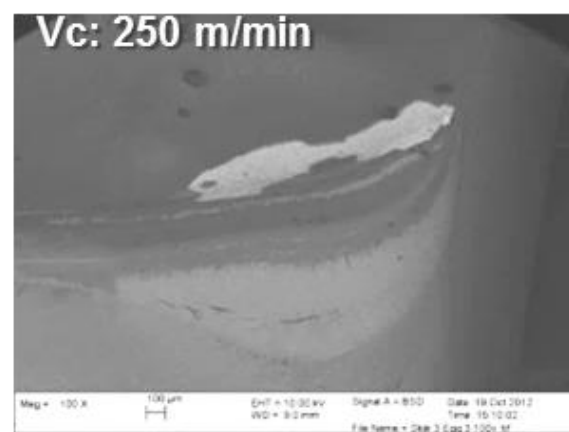
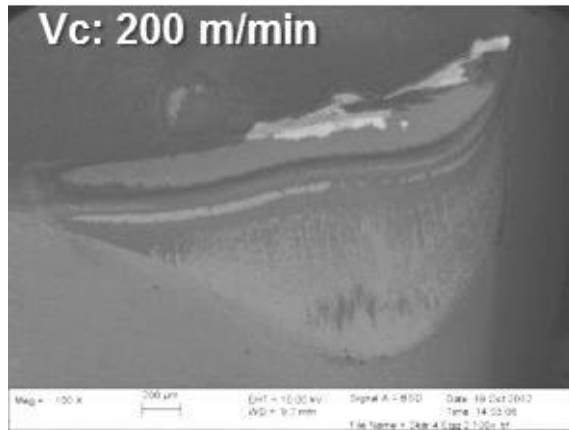
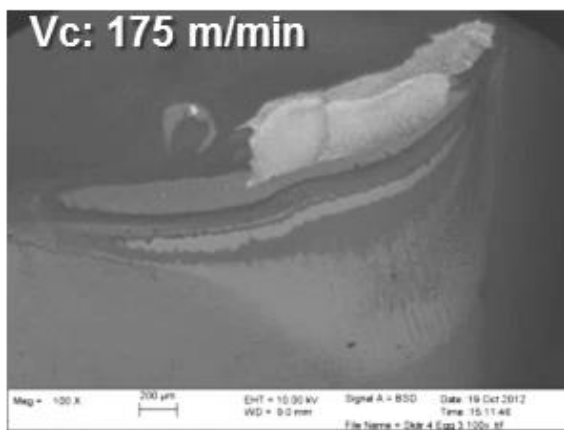


Figure 137. Micrographs of cutting edges used in tool life tests with 50CrMo4 (QH-T1). $a_p=2$ mm, $f=0.4$ mm/rev.

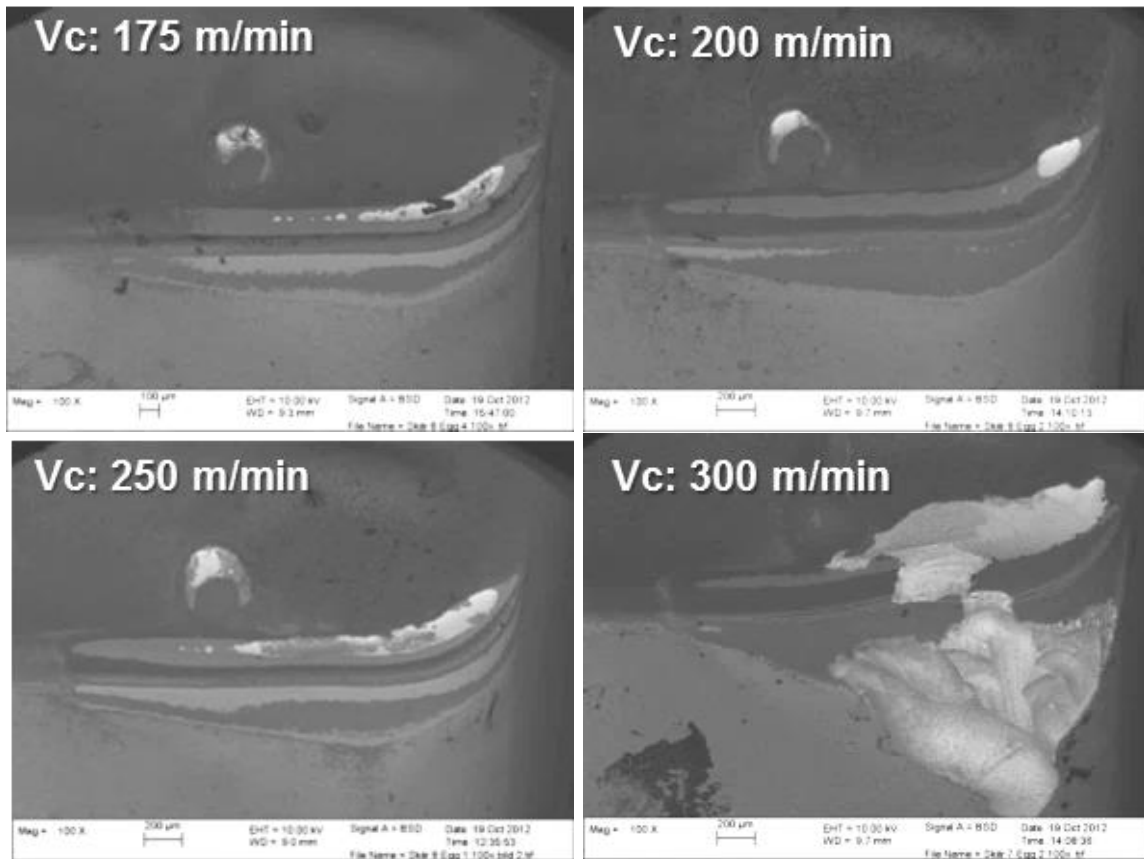


Figure 138. Micrographs of cutting edges used in tool life tests with 50CrMo4 (QH-T2). $a_p=2$ mm, $f=0.4$ mm/rev.

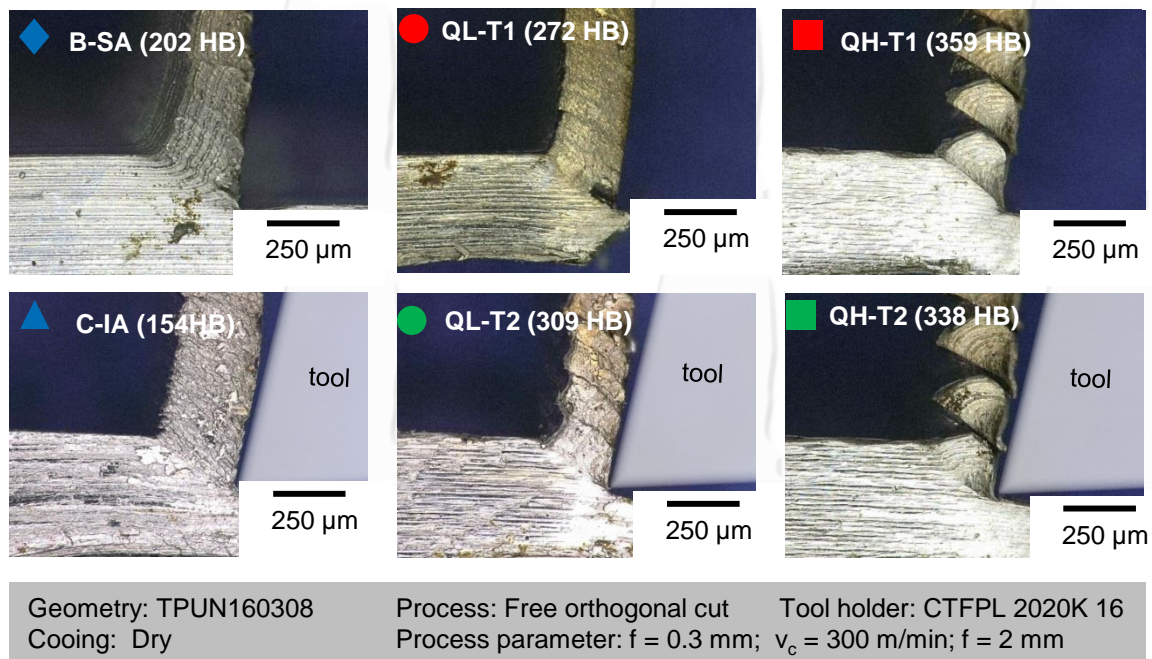


Figure 139. Chip roots for all steel variants for a feed of $f = 0.3$ mm and a cutting speed of $v_c = 300$ m/min

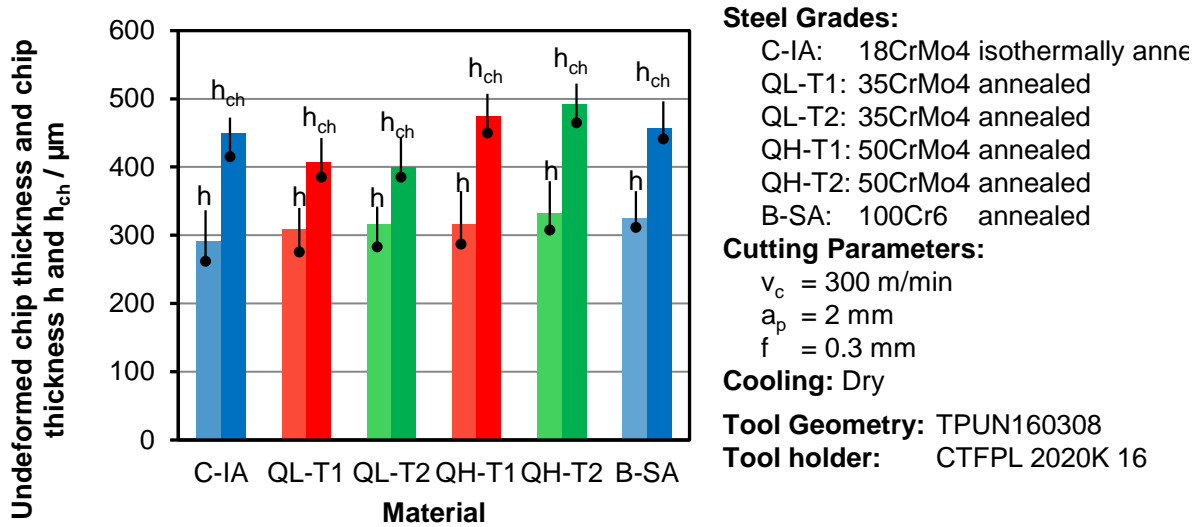
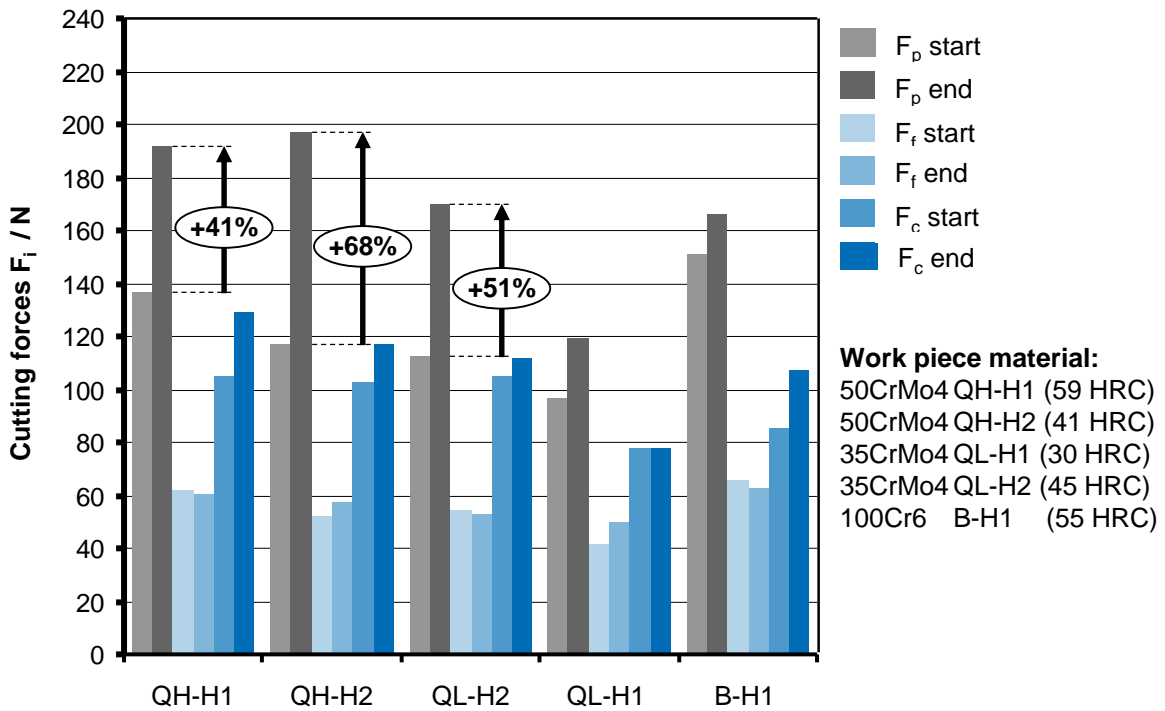


Figure 140. Un-deformed chip thickness h and chip thickness h_{ch}

ANNEX WP4



Process parameters: $v_c = 160$ m/min; $f = 0.08$ mm; $a_p = 0.2$ mm Tool: CNGA120408S
 Cutting material: PCBN CB7014

Figure 141. Cutting force measurement signals

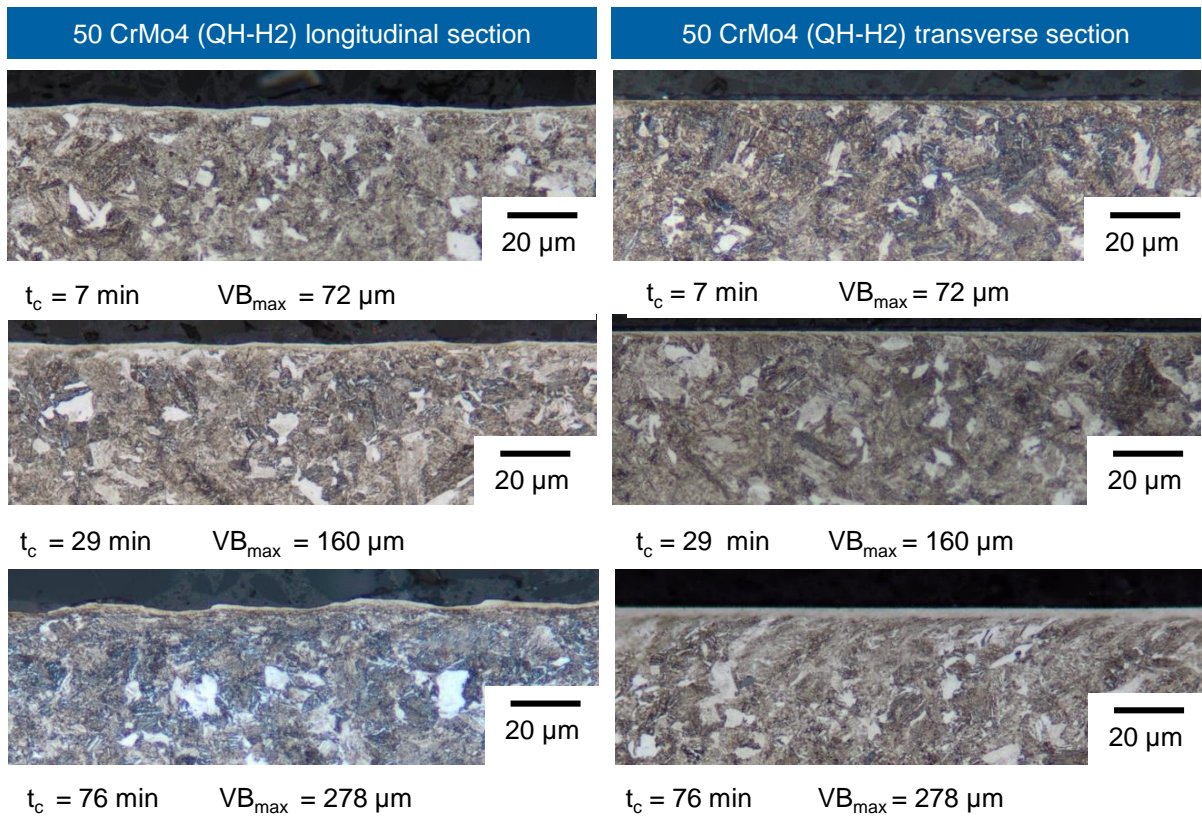


Figure 142. Development of white layer formation, QH-H2 (50CrMo4)

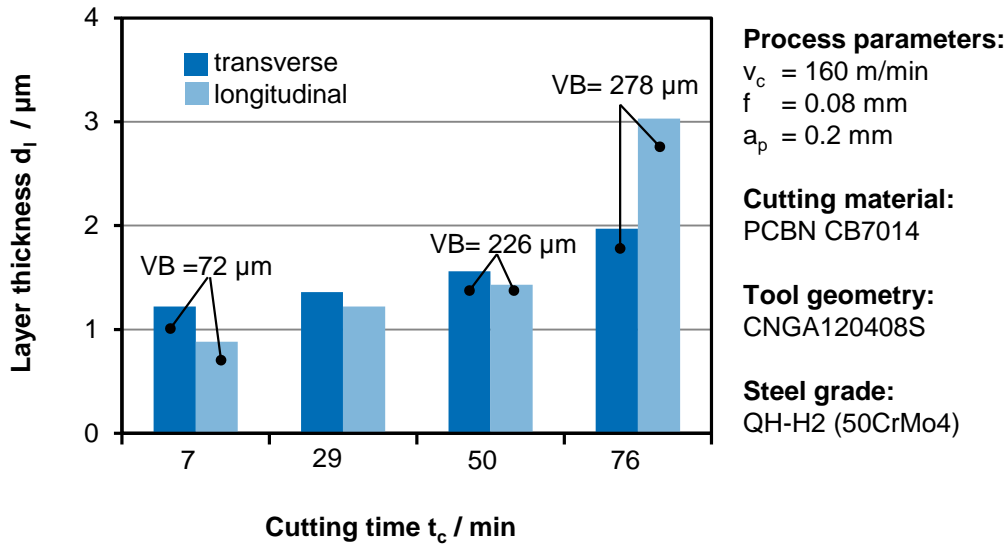


Figure 143. Development of white layer formation, QH-H2 (50CrMo4)

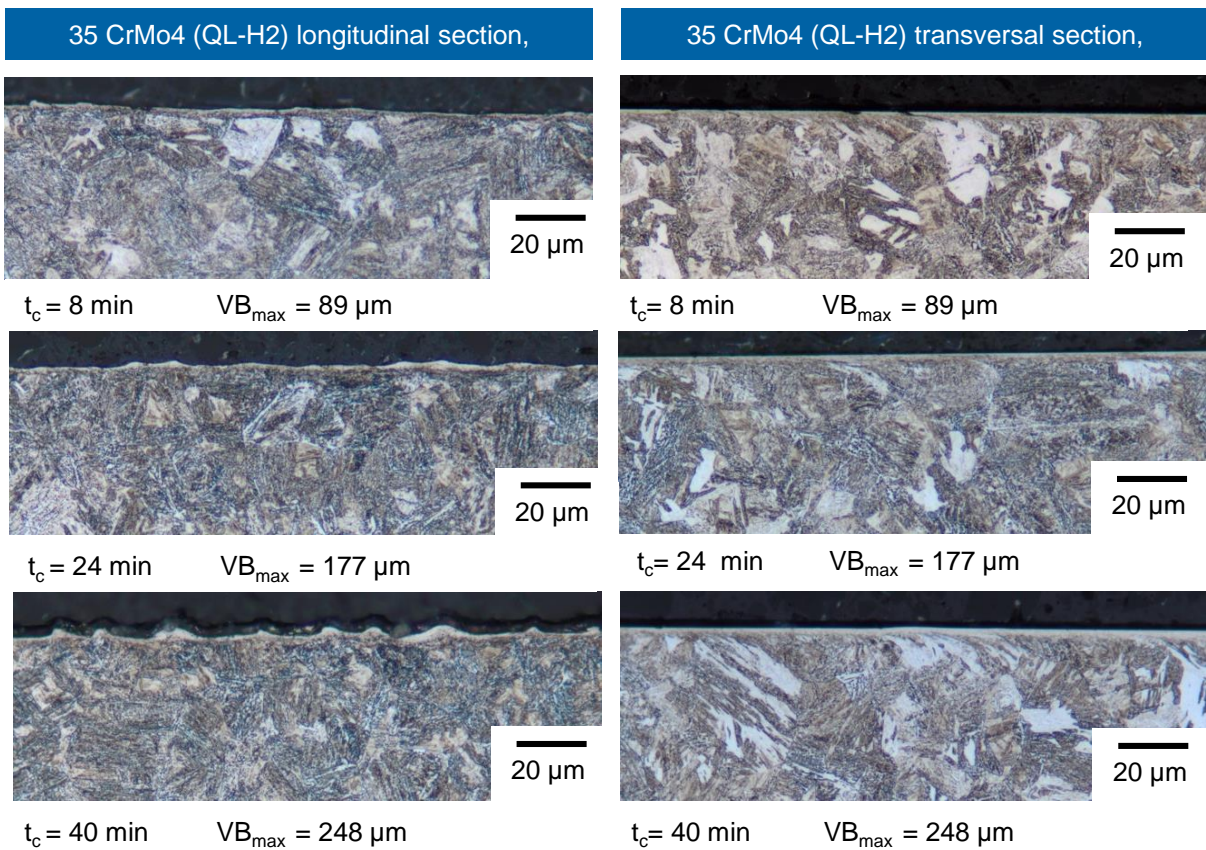


Figure 144. Development of white layer formation, QL-H2 (35CrMo4)

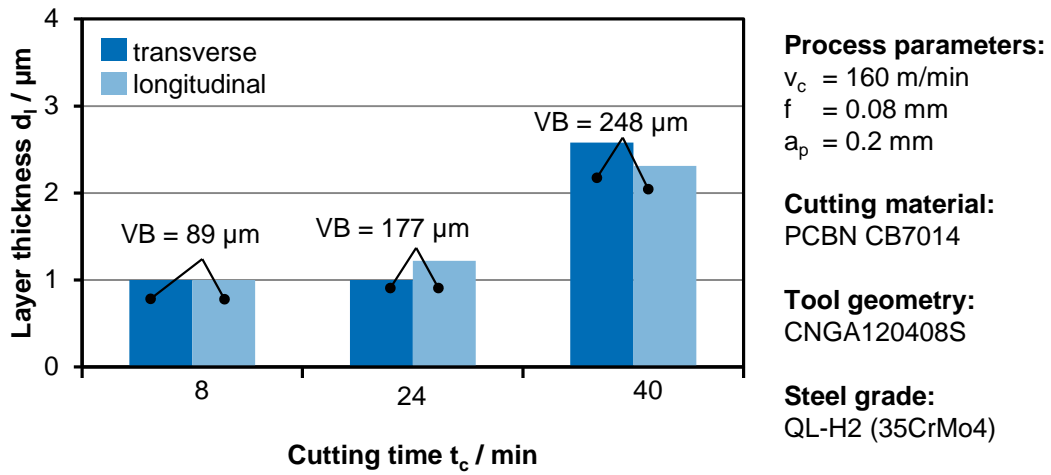


Figure 145. Development of white layer formation, QL-H2 (35CrMo4)

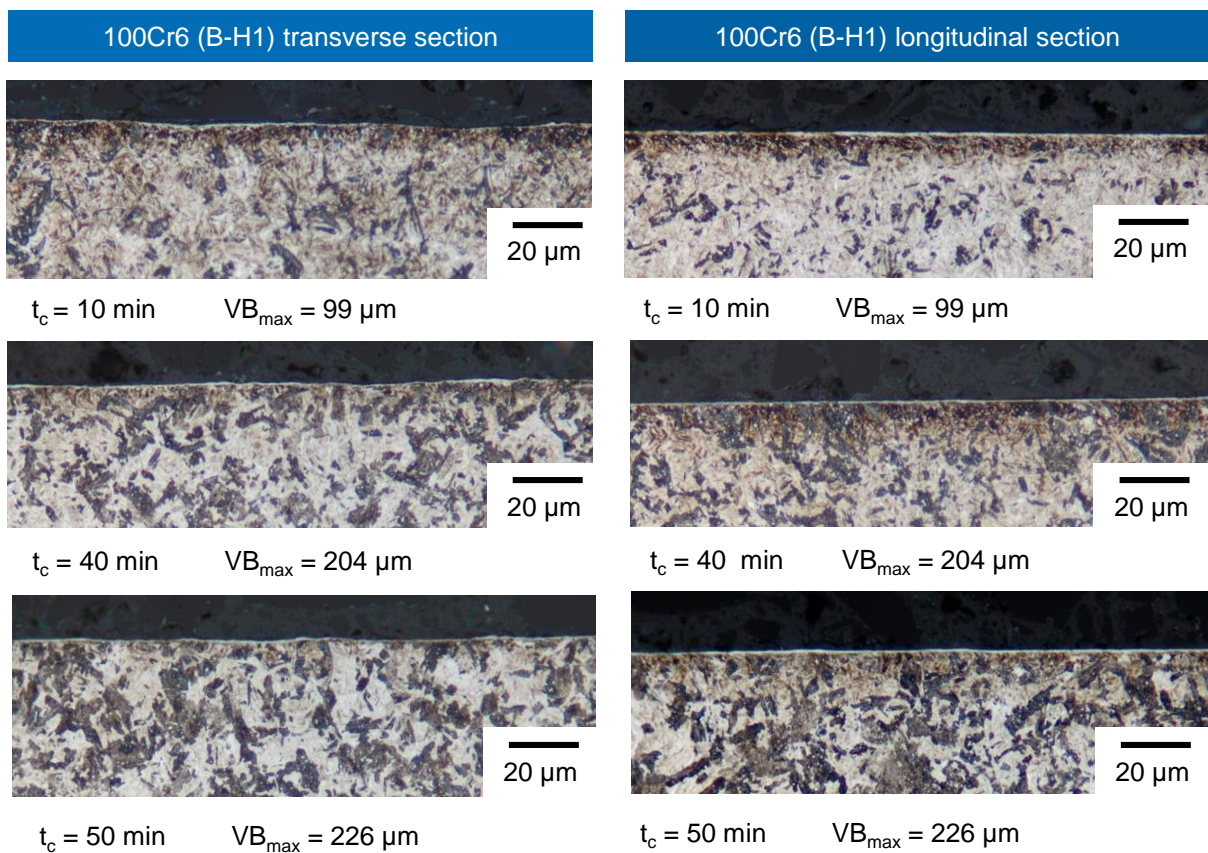


Figure 146. Development of white layer formation, B-H1 (100Cr6)

ANNEX WP5

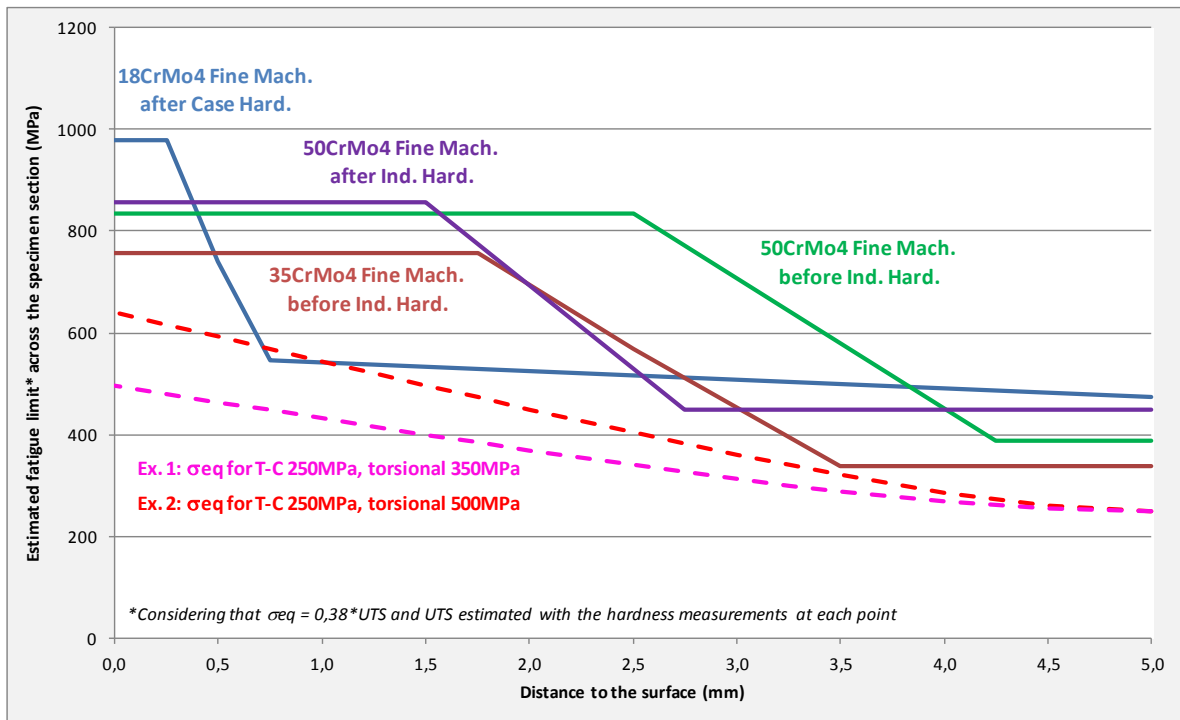


Figure 147. A theoretical approach of fatigue load distribution of multiaxial T-C and torsional load tests. Representative hardness depth profiles are included to demonstrate how the test conditions can be modified to suit the tested heat treatment characteristics.

OP	Operation detail	Stock (micron)	Working stroke (mm)	Number of uses	Total stroke (calculated) (mm)	Working time (centsec)	N. Revolution (rev/min)	N. cutting edge	Cutting speed (m/min)	Feed per revolution (mm/rev)	Feed per tooth (mm)	Feed per min (mm)
							n	z	vc	f	fz	vf
10	Internal facing	1.100	60	1	60	22,00	850	1	250 cost	0,39	0,39	330
10	External facing	1.400	37	1	37	21,00	550	1	300 cost	0,36	0,36	200
10	Finishing facing	800	30	1	30	14,00	812	1	300 cost	0,27	0,27	220
10	Turning and facing	900	53	1	53	21,00	700	1	250 cost	0,40	0,40	280
10	Turning and finishing facing	700	40	1	40	38,00	1000	1	300 cost	0,33	0,33	330
10	Finishing facing	800	34	1	34	21,00	600	1	300 cost	0,28	0,28	167
10	Finishing facing	800	21	1	21	14,00	610	1	300 cost	0,25	0,25	150
30	Hob milling	500	50	1	50	194,00	305	19	105	2,10	0,11	
40	Chamfering					25,00		52				
40	Snagging					25,00		1				
60	Drilling		14	5	70	19,00	1962	2	65	0,18	0,092	360
60	Chamfering	700	2	1	2	3,00	396	1	15	0,15	0,15	60
80	Shotblasting											0
100	Boring after Heat Treatment	280	9	1	9	12,00	570	1	170	0,13	0,13	74
100	Interrupted facing	150	20	1	20	43,00	304	1	110	0,15	0,15	46
110	Grinding	70/flank		1		208,00	1900		2089	0,00		

Figure 149. All relevant machining details of the demonstrator gear manufacturing.

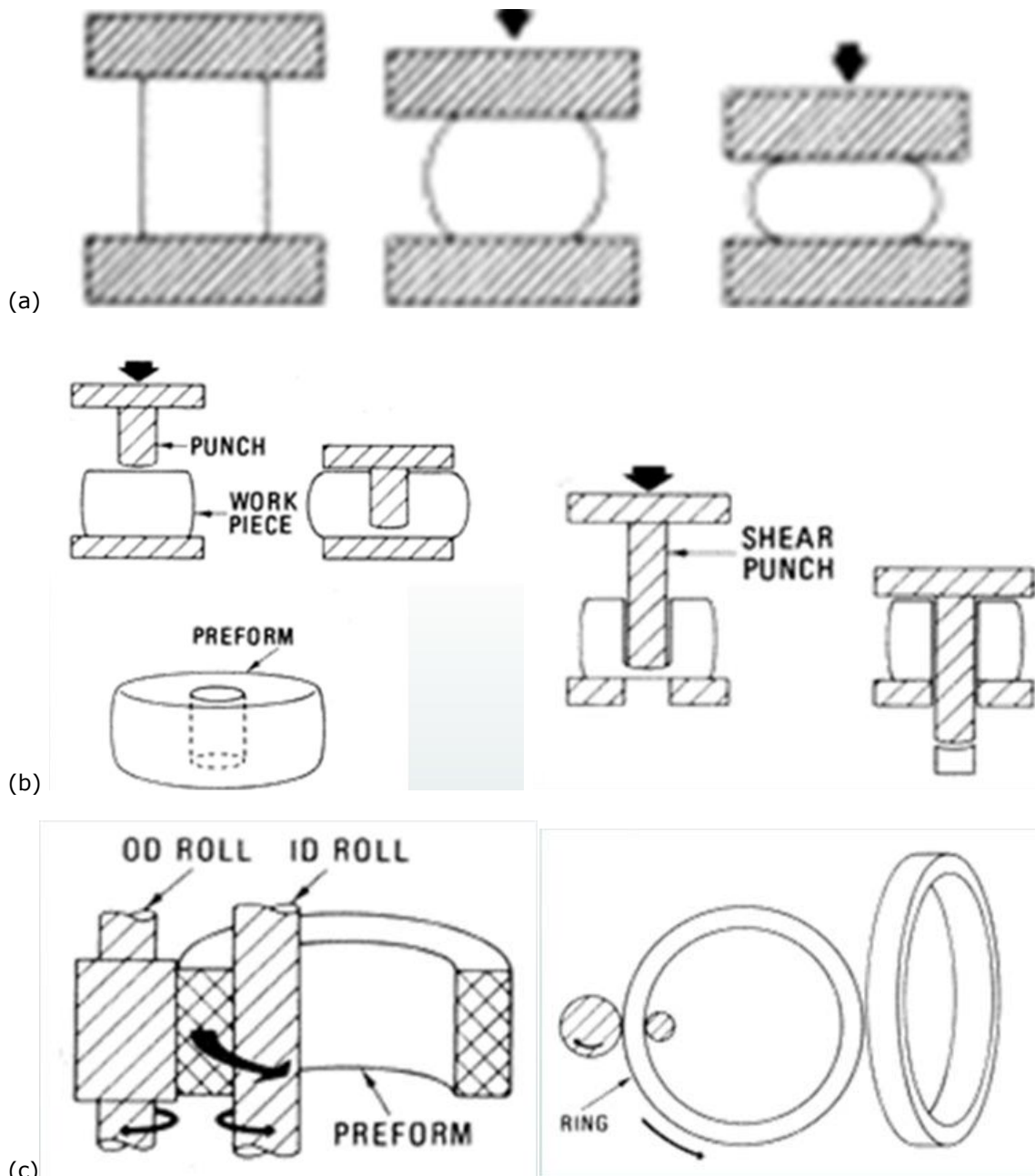


Figure 150. Forging details. (I). Punching, (II). Piercing and (III). Orbital lamination (rolling).

HOW TO OBTAIN EU PUBLICATIONS

Free publications:

- one copy:
via EU Bookshop (<http://bookshop.europa.eu>);
- more than one copy or posters/maps:
from the European Union's representations (http://ec.europa.eu/represent_en.htm);
from the delegations in non-EU countries (http://eeas.europa.eu/delegations/index_en.htm);
by contacting the Europe Direct service (http://europa.eu/eurodirect/index_en.htm) or
calling 00 800 6 7 8 9 10 11 (freephone number from anywhere in the EU) (*).

(*) The information given is free, as are most calls (though some operators, phone boxes or hotels may charge you).

Priced publications:

- via EU Bookshop (<http://bookshop.europa.eu>).

The MAC D project has shown a realistic potential to replace today's carburizing route in the manufacturing of a helical gear with an induction hardening route. The transition includes evaluation and choice of a new suitable steel and as delivered microstructure from the forging, data of machinability in the vital machining processes, a comparison of fatigue strength and a complete comparison of manufacturing costs.

A comparison of direct costs of heat treatment was made including investment, maintenance, energy requirement and staff. The costs are as follows:

- **Carburizing: 2.41 € per gear**
- **Induction hardening: 0.64 € per gear.**

The total costs of the machining processes were obtained from machinability data of the project and production data of Fiat Powertrain.

- The cost of the carburizing route using 18CrMo4 was **9 €** per gear.
- The cost of the induction hardening route using 50CrMo4 was **12 €** per gear.

The fatigue strength of an induction hardened gear has a full potential to rival the strength of a carburized gear. More detailed studies are recommended before the industrial introduction of an induction hardened gear application.

Green machining of a 50CrMo4 steel at 345 HB in both rough turning and a simulated hob milling test showed roughly a 50% reduction in performance as compared with the reference 18CrMo4 steel at 160 HB. That extra cost is to some extent compensated by reduced costs in hard part turning and tooth grinding. The primary cost associated with lower performance is the extended machine time and more staff costs.